The role of non-coding RNAs in vascular damage in hypertension and CKD

Ku-Geng Huo

Division of Experimental Medicine

McGill University

Final thesis submission in November 2017

(A thesis submitted to McGill University in partial fulfillment of the requirements of the degree of PhD Experimental Medicine – Thesis)

Table of Contents

Table of Contents i

Abstract v

Résumé vii

Abbreviations ix

List of tables xi

List of figures xii

Preface and contribution of authors xv

Acknowledgements xviii

CHAPTER I: Introduction 1

1. Hypertension 2

1.1 BP measurement, diagnosis and assessment 2

1.2 Hypertension pathophysiology 3

1.2.1 The kidneys 3

1.2.2 The brain and the sympathetic nervous system 4

1.2.3 The heart 4

1.2.4 The vasculature 5

1.2.5 Genetic and environmental factors 6

2. Chronic kidney disease (CKD) 6

3. The arterial wall 7

3.1 Structure and composition 8

3.1.1 Intima 8

3.1.2 Media 9

3.1.3 Adventitia 9

3.2 Vascular damage in hypertension and CKD 10

3.2.1 Vascular remodeling 10

3.2.2 Vascular stiffening 11

3.2.3 Endothelial dysfunction 14

4. Ang II in hypertension and vascular damage 15
5. Non-coding RNAs (ncRNAs) 18
5.1 miRNAs 19
5.1.1 miRNA biogenesis 19
5.1.2 miRNA-mediated gene regulation 21
5.1.3 miRNAs as potential therapeutic targets 23
5.2 lncRNAs 24
5.2.1 lincRNAs 24
5.2.2 circRNAs 25
5.2.3 Antisense RNAs 26
5.2.4 Pesudogenes 26
5.2.5 Coding lncRNAs 27
5.2.6 Methods to target lncRNAs 28
5.3 Circulating ncRNAs 29
5.3.1 The origin of circulating ncRNAs 29
5.3.2 Roles of circulating ncRNAs 30
5.3.3 Circulating ncRNAs as biomarkers and the challenges of studying circulating ncRNAs 30
6. ncRNAs and cardiovascular disease 32
6.1 ncRNAs and hypertension 33
6.1.1 miRNAs and hypertension 33
6.1.2 lncRNAs and hypertension 35
6.2 ncRNAs and CKD 35
6.2.1 miRNAs and CKD 36
6.2.2 lncRNAs and CKD 36
6.3 ncRNAs and vascular damage 37
6.3.1 miRNAs and vascular damage 37
6.3.2 lncRNAs and vascular damage 40
6.4 ncRNAs involved in hypertension, CKD and vascular damage 41
7. ncRNAs as biomarkers or therapeutic targets in the clinic 44
7.1 ncRNA profiling 44
7.2 ncRNAs as biomarkers 48

7.3 ncRNAs as therapeutic targets 50
8. Experimental design, hypothesis and objectives 51
8.1 Experimental design 51
8.2 Hypothesis and objectives 53
8.3 Methodology 53
8.3.1 RNA extraction 54
8.3.2 Library construction and RNA sequencing 54
8.3.3 Bioinformatic pipeline 54
8.3.4 Measurement of miRNA and mRNA expression by RT-qPCR 55
8.3.5 Validating miRNA-mRNA pairs 55
CHAPTER II: Vascular ncRNA profiling in Ang II-induced vascular damage and hypertension 56
CHAPTER III: Vascular ncRNA profiling in essential hypertension with or without CKD 119
CHAPTER IV: Circulating ncRNA profiling in essential hypertension with or without CKD 148
CHAPTER V: Discussion 168
9. miRNAs and vascular damage in hypertension and CKD 169
9.1 *Dlk1-Dio3* region 169
9.1.1 DLK1-DIO3 miRNAs in cell proliferation and migration 170
9.1.2 DLK1-DIO3 region in cardiovascular disease 171
9.1.3 DNA methylation in DLK1-DIO3 miRNA expression 172
9.2 miR-431-5p and Ets homologous factor (Ehf) 173
9.2.1 miR-431-5p 174
9.2.1 EHF 175
9.2.3 The interaction between miR-431-5p and Ehf in Ang II-induced vascular injury and hypertension 175
9.3 miR-145-3p 177
10. Circulating miRNAs in hypertension and CKD 178
10.1 let-7g-5p 179
10.2 Circulating miRNAs and vascular damage 179

11. Limitations and challenges 180
12. Perspectives 182
References 184

Abstract

Hypertension and chronic kidney disease (CKD) are two of the most prevalent global health concerns that account for millions of deaths per year. They are both associated with vascular damage that is characterized by vascular remodeling and stiffening, as well as endothelial dysfunction, which contribute to further development of the disease and lead to end organ damage. MicroRNAs (miRNAs) are important non-coding RNA regulators of gene expression that cause translational repression and transcript degradation upon binding to their target mRNAs. miRNAs have been demonstrated to be associated with hypertension and CKD, and play a critical role in vascular cell development and function. However, their role in vascular damage is still poorly studied. We hypothesized that vascular and circulating miRNAs are dysregulated in hypertension and CKD; the dysregulation of vascular miRNAs is a key driving force of pathological gene expression changes that contribute to vascular damage; key dysregulated vascular miRNAs are potential therapeutic targets and key dysregulated circulating miRNAs are potential biomarkers for vascular damage in hypertension and CKD. The thesis contains 3 studies testing our hypotheses.

In the first study, we profiled miRNAs using RNA sequencing in mesenteric arteries of mice infused or not with angiotensin (Ang) II for 7 or 14 days. We observed that both 7-day and 14-day Ang II infusion induced blood pressure (BP) elevation, oxidative stress and vascular stiffening, whereas only 14-day Ang II-infusion caused endothelial dysfunction and vascular remodeling. Using a candidate approach, we have identified miR-431-5p and its target Ets Homologous Factor (*Ehf*) as key regulators in Ang II-induced hypertension and vascular damage. miR-431-5p and *Ehf* were up- and down-regulated by 14-day Ang II-infusion, respectively, and were both correlated with BP. We demonstrated that miR-431-5p targets *EHF* in human aortic vascular smooth muscle cells, where EHF down-regulates collagen type I alpha 1 chain (*Col1a1*), and miR-382-5p. Intravenous injection of miR-431-5p inhibitors down-regulated miR-431-5p, *Col1a1* and miR-382-5p, and up-regulated *Ehf* in mesenteric arteries, delayed BP elevation and reduced vascular damage in mice infused with Ang II for 14 days.

In the second study, we profiled miRNAs as above but this time in small arteries dissected from subcutaneous gluteal biopsies performed in normotensive, hypertensive and CKD subjects to identify differentially expressed vascular miRNAs. Combined with the data from the first study, we found a common miRNA, miR-145-3p, that was down-regulated in both 7-day Ang II-infused mice and CKD patients. Whether miR-145-3p mediates vascular damage in Ang II-induced hypertension model and CKD remains to be elucidated.

In the third study, we profiled circulating miRNAs from plasma of the same cohort of normotensive hypertensive and CKD subjects as in the second study. We identified and validated 4 differentially expressed miRNAs, let-7g-5p, miR-26a-5p, miR-191-5p and let-7b-5p, among which let-7g-5p was correlated with estimated glomerular filtration rate. We also found a correlation between circulating let-7g-5p and genes that were differentially expressed in small arteries of CKD patients.

To summarize, miR-431-5p and its target *Ehf* are potential important regulators in the pathophysiology of vascular damage in hypertension, and may serve as novel therapeutic targets in the clinic. miR-145-3p may play a role in the development of Ang II-induced and CKD-associated vascular injury. Let-7g-5p has potential clinical value to serve as a biomarker for vascular damage in CKD.

Résumé

L'hypertension et l'insuffisance rénale chronique (IRC) sont des problèmes de santé mondiale les plus répandus et responsables de millions de décès annuellement. L'hypertension et l'IRC sont associés aux dommages vasculaires caractérisés par du remodelage et du durcissement vasculaire et de la dysfonction endothéliale, qui contribuent à la progression de la maladie et aux lésions des organes cibles. Les microARN (miARN) sont des ARN non codants qui régulent l'expression génique par répression de la traduction ou dégradation des ARN messager (ARNm). Il a été démontré que les miARN sont associés à l'hypertension et à l'IRC et jouent un rôle essentiel dans le développement et la fonction des cellules vasculaires. Cependant, leurs rôles dans les dommages vasculaires sont inconnus. Nous avons émis l'hypothèse que les miARN vasculaires et circulants sont dérégulés dans l'hypertension et l'IRC. La dérégulation des miARN est un moteur clef des changements pathologiques de l'expression génique conduisant aux dommages vasculaires, qui pourrait être une cible thérapeutique. Les miARN circulant pourraient servir de biomarqueurs des dommages vasculaires dans l'hypertension et l'IRC. La thèse contient trois études testant nos hypothèses.

Dans la première étude, nous avons profilé les miARN et ARNm par séquençage des ARN des artères mésentériques (AM) de souris infusées ou non avec l'angiotensine (Ang) II pendant 7 ou 14 jours. Nous avons observé une élévation de la pression artérielle (PA), du stress oxydatif et du durcissement des AM dans les souris infusées avec l'Ang II pour 7 ou 14 jours, et une dysfonction endothéliale et du remodelage des MAs dans les souris infusées avec l'Ang II pendant 14 jours. Nous avons identifié avec une approche candidate miR-431-5p et sa cible, le facteur homologue ETS (*Ehf*), comme des régulateurs clefs dans l'hypertension et les dommages vasculaires induits par l'Ang II. miR-431-5p et *Ehf* étaient respectivement augmenté et réduit par 14 jours d'infusion d'Ang II. Tous les deux étaient corrélés avec la PA. Nous avons démontré dans des cellules vasculaires lisses aortiques humaines que miR-431-5p cible *EHF*, alors que EHF régule à la baisse la chaine de collagène de type I alpha 1 (*Col1a1*) et le miR-382-5p. L'injection intraveineuse d'inhibiteurs de miR-431-5p a diminué miR-431-5p, *Col1a1* et

miR-382-5p, et a augmenté *Ehf* dans les AM, et a retardé l'élévation de la PA et réduit les dommages vasculaires chez les souris infusées avec l'Ang II pendant 14 jours.

Dans la deuxième étude, nous avons profilé les miARN comme plus haut dans les petites artères de biopsies sous-cutanées de la fesse de sujets non hypertendus, hypertendus ou atteints d'IRC. En combinant les données de cette étude avec celles de la première étude, nous avons trouvé un miARN commun, miR-145-3p, qui était diminué dans les souris infusées avec l'Ang II pendant 7 jours et les patients avec IRC. Cependant, il reste à préciser si miR-145-3p agit sur les dommages vasculaires dans le modèle d'hypertension induit par l'Ang II et dans l'IRC.

Dans la troisième étude, nous avons profilé les miARN circulant dans le plasma de la cohorte de sujets de l'étude précédente. Nous avons identifié 4 miARN exprimés différentiellement, let-7g-5p, miR-26a-5p, miR-191-5p et let-7b-5p. let-7g-5p était corrélé avec le taux de filtration glomérulaire estimé. Nous avons également trouvé une corrélation entre let-7g-5p et les gènes exprimés de façon différentielle dans les petites artères de patients avec IRC.

En résumé, miR-431-5p et sa cible *Ehf* pourraient agir comme des régulateurs maîtres des dommages vasculaires dans l'hypertension. miR-431-5p a le potentiel de servir comme cible thérapeutique pour contrer les dommages vasculaires et l'hypertension. miR-145-3p pourrait jouer un rôle dans le développement des dommages vasculaires induits par l'Ang II et l'IRC. Let-7g-5p a un potentiel clinique pour servir comme biomarqueur des dommages vasculaires dans l'IRC.

Abbreviations

ACE	Angiotensin-converting enzyme
AI	Augmentation index
Ang	Angiotensin
AP	Augmented pressure
ARB	Angiotensin receptor blocker
BGN	Biglycan
BP	Blood pressure
ceRNA	Competing endogenous RNA
CKD	Chronic kidney disease
COL1A1	Collagen type I alpha 1 chain
CTGF	Connective tissue growth factor
Dlk1-Dio3	Delta-like homolog 1-Type III iodothyronine deiodinase
ECM	Extracellular matrix
eGFR	Estimated glomerular filtration rate
EGFR	Epidermal growth factor receptor
EHF	Ets homologous factor
ERK	Extracellular signal-regulated kinase
FDM	Flow-mediated dilatation
FDR	False discovery rate
GO	Gene ontology
GPCR	G protein-coupled receptor
GWAS	Genome-wide association study

MCSA	Media cross-sectional area
lncRNA	Long non-coding RNA
miRNA	microRNA
MLC	Myosin light chain
MMP	Matrix metalloprotease
ncRNA	Non-coding RNA
NGS	Next-generation sequencing
NO	Nitric oxide
ORF	Open reading frame
PP	Pulse pressure
PWV	Pulse wave velocity
RAAS	Renin-angiotensin-aldosterone system
RISC	RNA-induced silencing complex
ROS	Reactive oxygen species
RT-qPCR	Real-rime quantitative reverse transcription polymerase chain reaction
shRNA	Small hairpin RNA
siRNA	Small interfering RNA
SMC	Smooth muscle cells
SNP	Single nucleotide polymorphisms
TGF-β	Transforming growth factor beta
TF	Transcription factor
UTR	Untranslated region

List of tables

Chapter II

Table I-1. List of ncRNAs involved in hypertension, CKD and vascular damage..... 41

Chapter II

Table II-1. The expression of 9 up-regulated microRNAs and ETS homologous factor (*Ehf*) mRNA correlates with systolic blood pressure (SBP) or diastolic blood pressure (DBP) 83

Supplemental table II-S1. Oligonucleotide primers for mouse mRNA quantitative PCR 101
Supplemental table II-S2. Oligonucleotide primers for human mRNA quantitative PCR 102
Supplemental table II-S3. Oligonuclotide containing the *EHF* 3' untranslated region with the wild-type or mutated miR-431-5p target region 103
Supplemental table II-S4. Quantity and quality of RNA extracted from mesenteric arteries (MAs) of sham-operated and angiotensin II-infused mice 104
Supplemental table II-S5. List of differentially expressed microRNA in mesenteric arteries of 7 and 14 days angiotensin II-infused mice 105
Supplemental table II-S6. List of differentially expressed mRNA in mesenteric arteries of 7 days angiotensin II-infused mice (Not provided in this thesis) 106
Supplemental table II-S7. List of differentially expressed mRNA in mesenteric arteries of 14 days angiotensin II-infused mice (Not provided in this thesis) 106
Supplemental Table II-S8. Gene ontology term enrichment for differentially expressed mRNAs in mesenteric arteries of 7 days angiotensin II infused mice 107
Supplemental Table II-S9. Gene ontology term enrichment for differentially expressed miRNA-targeted differentially expressed mRNAs in mesenteric arteries of 7 days infused angiotensin II mice..... 108
Supplemental Table II-S10. Gene ontology (GO) term enrichment for differentially expressed mRNAs in mesenteric arteries of 14 days infused angiotensin II mice 109
Supplemental Table II-S11. Gene ontology term enrichment for differentially expressed miRNA-targeted differentially expressed mRNAs in mesenteric arteries of 14 days angiotensin II-infused mice..... 112
Supplemental Table II-S12. KEGG and REACTOME signaling pathway enrichment for differentially expressed mRNAs in mesenteric arteries of 7- and 14 days angiotensin II-infused mice 114

Supplemental table II-S13. Gene ontology (GO) term enrichment in EHF-targeting DE mRNAs in mesenteric arteries of 14 days angiotensin II-infused mice..... 115
Supplemental table II-S14. *In vivo* miR-431-5p inhibition did not alter the organ weights corrected by tibia length in angiotensin (Ang) II infused mice..... 118

Chapter III

Table III-1. Demographic characteristics 133
Table III-2. Hemodynamic and mechanical parameters..... 134

Chapter IV

Table IV-1. Correlations between circulating DE miRNA and vascular gene expression. 160

List of figures

Chapter I

Figure I-1. Schematic view of an arterial wall in cross-section. (Adapted from: Expert Reviews in Molecular Medicine. 2002. Cambridge University Press. http://journals.cambridge.org/fulltext_content/ERM/ERM4_01/S1462399402004039sup006.htm. Accessed on Apr 21st, 2017)..... 8
Figure I-2. Large and small artery remodeling in hypertension. Adapted from Schiffrin, 2004 (*26*)..... 11
Figure I-3. Formation of augmented pressure (AP) due to interference of the forward wave with the reflected wave. Adapted from Kum *et al.* (*70*)..... 12
Figure I-4. Schematic mechanism of endothelium-dependent relaxation. 14
Figure I-5. Ang II signaling pathways in hypertension and vascular damage..... 18
Figure I-6. miRNA biogenesis and function..... 20
Figure I-7. Mechanisms of miRNA targeting gene regulation. 22
Figure I-8. lncRNA-mediated transcriptional and post-transcriptional regulation..... 28
Figure I-9. Bioinformatic pipelines for ncRNA profiling..... 48

Chapter II

Figure II-1. Angiotensin (Ang) II infusion induced blood pressure elevation, endothelial dysfunction, vascular remodeling, stiffening and oxidative stress. 76

Figure II-2. Heat maps and molecular network for miRNA and mRNA expression profiles. 77
Figure II-3. miR-431-5p directly targets ETS homologous factor (*EHF*) in human aortic vascular smooth muscle cells. 79
Figure II-4. ETS homologous factor (EHF) negatively regulates collagen type I alpha 1 chain (*COL1A1*), miR-431-5p and miR-382-5p in human aortic vascular smooth muscle cells. 80
Figure II-5. *In vivo* miR-431-5p inhibition increased ETS homologous factor (*Ehf*) mRNA expression and decreased collagen type I alpha 1 chain (*Col1a1*) and miR-382-5p levels in mesenteric arteries of angiotensin (Ang) II infused mice. 81
Figure II-6. *In vivo* miR-431-5p inhibition protected against angiotensin (Ang) II-induced blood pressure elevation, endothelial dysfunction, vascular remodeling, stiffening and oxidative stress. 82

Supplemental Figure II-S1. Angiotensin (Ang) II infusion did not affect mesenteric artery vasoconstriction responses to norepinephrine (NE), relaxation responses to acetylcholine (Ach) in the presence of the nitric oxide synthase inhibitor N^{ω}-nitro-L-arginine methyl ester (L-NAME), endothelium-independent relaxation responses to sodium nitroprusside (SNP) or media cross-sectional area (MCSA). 96
Supplemental Figure II-S2. Seventeen out of 23 up-regulated miRNAs are located in the conserved Delta-like homolog 1-Type III iodothyronine deiodinase (*Dlk1-Dio3*) genomic region (highlighted in gray or red). 97
Supplemental Figure II-S3. miR-431-5p is expressed in mouse and human vascular smooth muscle cells. 97
Supplemental Figure II-S4. *EHF* does not regulate mRNA expression of biglycan (*BGN*, **A**), fibronectin 1 (*FN1*, **B**) and connective tissue growth factor (*CTGF*, **C**) in human vascular smooth muscle cells. 98
Supplemental Figure II-S5. *In vivo* miR-431-5p inhibition did not alter mRNA expression of biglycan (*Bgn*, **A**), fibronectin 1 (*Fn1*, **B**) and connective tissue growth factor (*Ctgf*, **C**) in mesenteric arteries of angiotensin (Ang) II infused mice. 99
Supplemental Figure II-S6. *In vivo* miR-431-5p inhibition did not affect mesenteric artery vasoconstriction responses to norepinephrine (NE), endothelium-dependent relaxation responses to acetylcholine (Ach) in the presence of the nitric oxide synthase inhibitor N^{ω}-nitro-L-arginine methyl ester (L-NAME), endothelium-independent relaxation responses to sodium nitroprusside (SNP) or media cross-sectional area (MCSA) in angiotensin (Ang) II-infused mice. 100

Chapter III

Figure III-1. Venn diagrams are presenting the number of differentially expressed miRNAs (upper panel) and differentially expressed mRNAs (lower panel) in small resistance arteries uniquely associated with the hypertensive (HTN), uniquely associated with the chronic kidney disease (CKD) patients and in both groups, compared to normotensive subjects (P<0.05). 136
Figure III-2. The figure represents a molecular network integrating differentially expressed microRNA (miR) and gene data, the predicted interactions between miRs and mRNAs (black lines), transcription factors and genes (purple arrow lines), and top 3 enriched gene ontology (GO) terms in small arteries of hypertensive patients compared to normotensive subjects (q<0.01). 137
Figure III-3. The figure represents a molecular network integrating differentially expressed microRNA (miR) and gene data, the predicted interactions between miRs and mRNAs (black lines) and transcription factors and genes (purple arrow lines), and top 3 enriched gene ontology (GO) terms in small arteries of chronic kidney disease patients compared to normotensive subjects (q<0.001). 138
Figure III-4. Determination of the quality of small artery RNA using an Agilent 2100 bioanalyzer.. 139

Chapter IV

Figure IV-1. Venn diagrams represent the number of differentially expressed miRNAs in platelet-free plasma uniquely associated with the hypertensive subjects (HTN), uniquely associated with chronic kidney disease patients (CKD), compared to normotensive subjects (P<0.01 & q<0.1). 158
Figure IV-2. Correlations between RNA sequencing (RNA-seq) results and real-rime quantitative reverse transcription polymerase chain reaction (RT-qPCR) results on let-7g-5p, miR-26a-5p, miR-191-5p and let-7b-5p. 159

Chapter V

Figure V-1. Interactions between differentially expressed TFs and differentially expressed *Dlk1-Dio3* miRNAs. 173

Preface and contribution of authors

In accordance with the guidelines of the Faculty of Graduate and Postdoctoral Studies of McGill University, the contribution of authors for 3 manuscripts included in this thesis is listed below. All 5 chapters of this thesis were written by Ku-Geng Huo and revised by Ernesto L. Schiffrin. All elements in this thesis represent original scholarship and a distinct contribution to knowledge.

First study (Chapter II) - miR-431-5p inhibition protects against angiotensin II-induced hypertension and vascular injury

Ku-Geng Huo: Designed experiments, collected samples, conducted most experiments, analyzed data from most experiments and wrote the manuscript.
Julio C. Fraulob-Aquino: Collected samples, conducted myography experiments.
Tlili Barhoumi: Collected samples, conducted myography experiments.

Chantal Richer: Prepared libraries for microRNA and mRNA sequencing.

Suellen C. Coelho: Conducted myography experiments.

Sofiane Ouerd: Conducted DHE staining and analyzed results.

Mathieu Lajoie: Provided bioinformatic advices.

Daniel Sinnett: Supervised the profiling study.

Pierre Paradis: Designed experiments, supervised the whole study, reviewed data analysis and revised the manuscript.

Ernesto L. Schiffrin: Designed experiments, supervised the whole study and revised the manuscript.

Second study (Chapter III) - microRNA profiling in small resistance arteries of hypertensive patients with or without chronic kidney disease

Ku-Geng Huo: Collected samples, extracted RNA, analyzed profiling and clinical data, and wrote the manuscript.

Julio C. Fraulob-Aquino: Collected samples, conducted large artery evaluation experiments and analyzed clinical data.

Chantal Richer: Prepared libraries for microRNA and mRNA sequencing.

Asia Rehman: Collected samples.

Marie Briet: Designed experiments, provided statistical advices for clinical data analysis.

Mark L. Lipman: Recruited patients.

Daniel Sinnett: Supervised the profiling study.

Pierre Paradis: Designed experiments, conducted large artery evaluation experiments, supervised the whole study, reviewed data analysis and revised the manuscript.

Ernesto L. Schiffrin: Designed experiments, supervised the whole study and revised the manuscript.

Third study (Chapter IV) - Circulating let-7g-5p as potential biomarkers for vascular damage in chronic kidney disease

Olga Berillo*: Extracted RNA and analyzed profiling data.

Ku-Geng Huo*: Collected samples, extracted RNA, analyzed profiling and clinical data, and wrote the manuscript.

Julio C. Fraulob-Aquino: Collected samples, conducted large artery evaluation experiments and analyzed clinical data.

Chantal Richer: Prepared libraries for microRNA and mRNA sequencing.

Marie Briet: Designed experiments, provided statistical advices for clinical data analysis.

Mark L. Lipman: Recruited patients.

Daniel Sinnett: Supervised the profiling study.

Pierre Paradis: Designed experiments, conducted large artery evaluation experiments, supervised the whole study, reviewed data analysis and revised the manuscript.

Ernesto L. Schiffrin: Designed experiments, supervised the whole study and revised the manuscript.

*These authors contributed equally

Acknowledgements

I would like to express my sincerest thanks to:

My family and relatives for supporting my pursuit of graduate study aboard, and my friends who are proud of my career choice as a scientist;

Dr. Ernesto L. Schiffrin for giving me an opportunity to work in his lab, providing scientific knowledge and supervising my graduate projects;

Dr. Pierre Paradis for providing scientific knowledge and supervising my graduate projects;

All my colleagues in Dr. Schiffrin's lab for their help and friendship;

Adriana Cristina Ene, Veronique Michaud, Heather Mlynarski, Guillem Colell Dinarès and Isabelle Miguel for their excellent technical support;

The members of my thesis committees (Dr. Jamie Engert, Dr. Mark Servant, Dr. Johanne Tremblay and Dr. Miltiadis Paliouras) for their helpful comments;

The Division of Experimental Medicine of McGill University for their financial support.

CHAPTER I: Introduction

Review of Literature and Objectives

1. Hypertension

Hypertension, or high blood pressure (BP), is one of the most prevalent and costly global health disorders and the leading risk factor for death and disability worldwide. In 2010, it affected 31.1 % (1.39 billion) of adults worldwide, with 28.5% (0.35 billion) in high income countries and 31.5% (1.04 billion) in low- and middle-income countries (*1*). Hypertension is the most expensive part of cardiovascular disease cost. In 2011, only in the United States, the estimated direct and indirect cost of hypertension is $46.4 billion (*2*), which was projected to increase to $200.3 billion and $389.0 billion when taking sequelae treatment into consideration by 2030 (*3*). Moreover, hypertension was ranked the number one (compared to 4th in 1990) risk factor for global disease burden, accounting for 9.4 million deaths and 7.0% disability-adjusted life years (DALYs, sum of years lived with disability and years of life lost) in 2010 (*4*).

1.1 BP measurement, diagnosis and assessment

Circulating blood exerts a force against the walls of the arteries. This force is the BP. During ventricular systole, the heart pumps blood into the aorta, from where it flows to peripheral arteries, and exerts a higher pressure called systolic BP. During ventricular diastole, the blood stops flowing from the left ventricle into the aorta while it continues to flow to peripheral arteries, and accordingly the pressure against the arterial walls becomes lower up to a nadir that is called diastolic BP.

In the 2016 Hypertension Canada guideline for BP measurement, diagnosis and assessment, 4 approaches were introduced for BP assessment (*5*).

1. In non-automated office BP measurement (non-AOBP) using electronic (oscillometric) upper arm devices, a mean systolic BP $\geq$ 140 mm Hg or diastolic BP $\geq$ 90 mm Hg is considered high. A mean systolic BP between 130-139 mm Hg or diastolic BP between 85-89 mm Hg is considered high-normal.

2. In automated office BP measurement (AOBP) using automated devices such as BPtru, a mean systolic BP ≥ 135 mm Hg or diastolic BP ≥ 85 mm Hg is considered high.

3. In ambulatory BP measurement (ABPM), a mean awake systolic BP ≥ 135 mm Hg or diastolic BP ≥ 85 mm Hg, or a mean 24-hour systolic BP ≥ 130 mm Hg or diastolic BP ≥ 80 mm Hg is considered high.

4. In home BP monitoring (HBPM), a mean systolic BP ≥ 135 mm Hg or diastolic BP ≥ 85 mm Hg is considered high.

1.2 Hypertension pathophysiology

Hypertension is a complex multifactorial disease that involves multiple interrelated mechanisms at both the physiological level and the molecular level. In 95% of cases, hypertension has no identifiable cause and is classified as essential, or primary hypertension (*6*). Multiple organs including the kidneys, the brain, the heart and the vasculature, as well as the crosstalk between different organs, are involved in the pathophysiology of hypertension. Genetic and environmental factors contribute to the development of hypertension.

1.2.1 The kidneys

The kidneys play a dominant role in long-term BP regulation by controlling water and sodium balance, and mediating the activation of the renin-angiotensin-aldosterone system (RAAS), which is a central hormone system for BP regulation (*7*). For example, when BP drops, the kidneys release an enzyme called renin that catalyzes the cleavage of angiotensinogen to generate angiotensin I, which is further converted by angiotensin-converting enzyme (ACE) to yield an octapeptide hormone called angiotensin (Ang) II that is able to raise blood pressure by constricting vessels and increasing aldosterone secretion. The latter acts on sodium reabsorption in the kidneys retaining sodium and accordingly water. Compromised renal function in kidney disease leads to impaired BP regulation, and has been linked to hypertension (*8, 9*). There is an epidemiological

association between hypertension and chronic kidney disease (See Section 2 in this chapter). Dysregulation of the RAAS is a key factor in the crosstalk between kidney disease and hypertension, given that RAAS blockade can efficiently lower BP and is renoproctective (*9-12*). Furthermore, Ang II infusion has been shown to induce BP elevation and sodium reabsorption in mice (*13*) and dogs (*14*).

1.2.2 The brain and the sympathetic nervous system

As opposed to the kidneys' long-term dominant role in BP regulation, the brain primarily acts as a short-term BP regulator via the sympathetic nervous system (*15*). Sympathetic nervous excitation stimulates the fight-or-flight response that leads to increased heart rate and therefore cardiac output, as well as release of catecholamines by the adrenal medulla, resulting in BP elevation. Heightened sympathetic activity has been linked to reduced renal excretory capability by increasing sodium reabsorption (*16, 17*), demonstrating the crosstalk between the sympathetic nervous system and the kidneys in hypertension. The RAAS also plays a part in the brain effects on BP regulation. Ang II infusion in rodents has been reported to increase reactive oxygen species (ROS) production in the subfornical organ (SFO) of the brain (*18*). Ang II injection into the brain was also able to increase BP (*19*). Overexpression of different types of SFO superoxide dismutases, which convert superoxide into hydrogen peroxide, by targeted adenovirus vectors abolished Ang II-induced hypertension (*18, 19*).

1.2.3 The heart

Increased heart rate and cardiac output raise BP, and are fundamental elements to maintain BP. In the case of hypertension with increased peripheral vascular resistance, left ventricular (LV) mass increases as a form of maladaptation in order to maintain cardiac output, resulting in pathological LV hypertrophy. Many studies have reported the association between hypertension and LV hypertrophy (*20, 21*). LV hypertrophy is a manifestation of target-organ damage in essential hypertension and an independent risk factor for cardiovascular events and mortality in hypertensive subjects. It has been

demonstrated that hypertensive subjects with LV hypertrophy exhibit increased cardiac sympathetic activity (*22*), showing the crosstalk between the sympathetic nervous system and the heart in hypertension. The RAAS also plays an important role in hypertensive LV hypertrophy, given that Ang II induces cardiac myocyte hypertrophy and cardiac fibroblast division *in vitro* (*23*), and clinical trials have shown that RAAS blockade by losartan, an Ang II receptor antagonist (*24*), or by ACE inhibitors (*25*) results in regression of LV hypertrophy in patients with essential hypertension.

1.2.4 The vasculature

The contraction and relaxation of the walls of arteries play a critical role in BP maintenance. High BP is accompanied by increased peripheral vascular resistance that is mainly attributed to vasoconstriction, vascular remodeling, stiffening and endothelial dysfunction. Vascular remodeling is a form of maladaptative increase in vascular wall thickness or decrease in lumen diameter that maintains wall tension upon BP elevation in hypertension, according to the Law of LaPlace (*26*). Vascular stiffening is largely the result of dysregulation of extracellular matrix (ECM) turnover, which leads to increased collagen and fibronectin deposition and higher collagen:elastin ratio (*27-29*). The remodeling and stiffening of the arterial walls result in increased pulse pressure (PP), and therefore a greater pulsatile energy transmitted to the periphery, resulting in injury to small arteries and arterioles, alteration in tissue perfusion, and organ damage (*30-32*). This damage to arteries can lead to dysfunction of the endothelium. Moreover, endothelial dysfunction may be caused by local inflammation in the arterial wall, which generally is associated with increased ROS production (*33-35*). The RAAS also plays a critical role in vascular physiology and pathophysiology. A deeper description of the arterial wall structure, vascular remodeling, vascular stiffening, endothelial dysfunction and the effect of the RAAS's major effector Ang II on vascular physiology and pathophysiology will be presented in Section 3 and Section 4 of this chapter.

1.2.5 Genetic and environmental factors

Genetic and environmental factors play an important role in the development of hypertension. Multiple genome-wide association studies (GWAS) have identified genetic variants associated with BP (*36-38*). Differential gene expression was observed in whole blood of hypertensive subjects in expression profiling studies, suggesting the importance of gene regulation at the level of transcription in the pathophysiology of hypertension (*39*). Common single nucleotide polymorphisms (SNPs) in the microRNA binding sites of the RAAS-related genes have been found to associate with BP, suggesting that post-transcriptional gene regulation by non-coding RNAs also plays a role (*40*). A trans-ancestry genome-wide association and replication study identified BP-associated variants that are linked to DNA methylation, showing the implication of epigenetics in hypertension (*41*). Environmental factors such as chronic social stress, smoking, alcohol consumption, sodium intake and unhealthy diets, and physical inactivity are also risk factors for hypertension (*42, 43*).

2. Chronic kidney disease (CKD)

Chronic kidney disease (CKD) is a global health concern with a worldwide prevalence of 13.4% for stages 1-5 and 10.6% for stages 3-5 (*5*). According to the National Kidney Foundation, the United States spent more than $48 billion on CKD treatment per year, and China is expected to lose US$ 558 billion over the next 10 years on death and disability attributable to heart and kidney disease (https://www.kidney.org/kidneydisease/global-facts-about-kidney-disease#_ENREF_1, accessed on Apr 18th, 2017).

CKD is an independent risk factor for cardiovascular disease including hypertension. There is an epidemiological association between hypertension and CKD. The prevalence of high BP has been reported to be over 85% in stage 3 and over 90% in stages 4-5 CKD patients (*44*). Vascular stiffening and calcification are strongly linked to abnormal mineral metabolism in CKD (*45*). Like vascular remodeling in hypertension, vascular

calcification in CKD, where vascular smooth muscle cells acquire osteoblastic function, also involves inflammation, oxidative stress and the RAAS. Blockade of the RAAS has efficiently reduced kidney disease progression (*9-12*). Dual RAAS blockade by ACE an inhibitor and an angiotensin receptor blocker (ARB) in CKD patients improved arterial stiffness, as shown by reduced pulse wave velocity and augmentation index (*46*).

The definition and classification of CKD are based on estimated glomerular filtration rate (eGFR) and albumin-creatinine ratio (ACR) (*44*). Stage 1 CKD is defined as eGFR > 90 ml/min/1.73 m^2 with other evidence of kidney damage; stage 2 is defined as eGFR between 60 and 89 ml/min/1.73 m^2 with with other evidence of kidney damage; stage 3 is defined as eGFR between 30 and 59 ml/min/1.73 m^2; stage 4 is defined as eGFR between 15 and 29 ml/min/1.73 m^2; and stage 5 is defined as eGFR between < 15 ml/min/1.73 m^2. Although eGFR is currently the primary diagnosis and evaluation marker for CKD, it is an estimated value calculated from serum creatinine corrected for age and sex. Considering that the true GFR is difficult and time-consuming to measure in most current clinical settings (*47*), there is demand for novel biomarkers that provide greater convenience and higher accuracy. Over the last decade, circulating microRNAs have emerged as potential novel biomarkers for cancers (*48*) and cardiovascular disease (*49*). microRNAs have been implicated in kidney disease in some studies (*50*). Serum microRNAs was shown to vary in different CKD stages (*51*). Those studies suggest a promising future direction in utilizing microRNAs as novel diagnostic or prognostic predictors in CKD. The association between microRNAs and CKD, as well as details in circulating microRNAs as biomarkers in CKD will be further addressed in Section 6.2.1 and Section 5.3 of this chapter.

3. The arterial wall

Arteries are blood vessels that carry blood from the heart to organs and tissues throughout the body. Abnormalities in arterial structure, composition or function are a fundamental manifestation of cardiovascular disease that contribute to target-organ damage. This

section will cover the description of the basic arterial structure and current findings on vascular injury in hypertension and CKD.

3.1 Structure and composition

The arterial wall is composed of three distinct layers: the intima, the media and the adventitia (Figure I-1). Each layer consists of different cell types that have different roles in the maintenance of arterial structure and function.

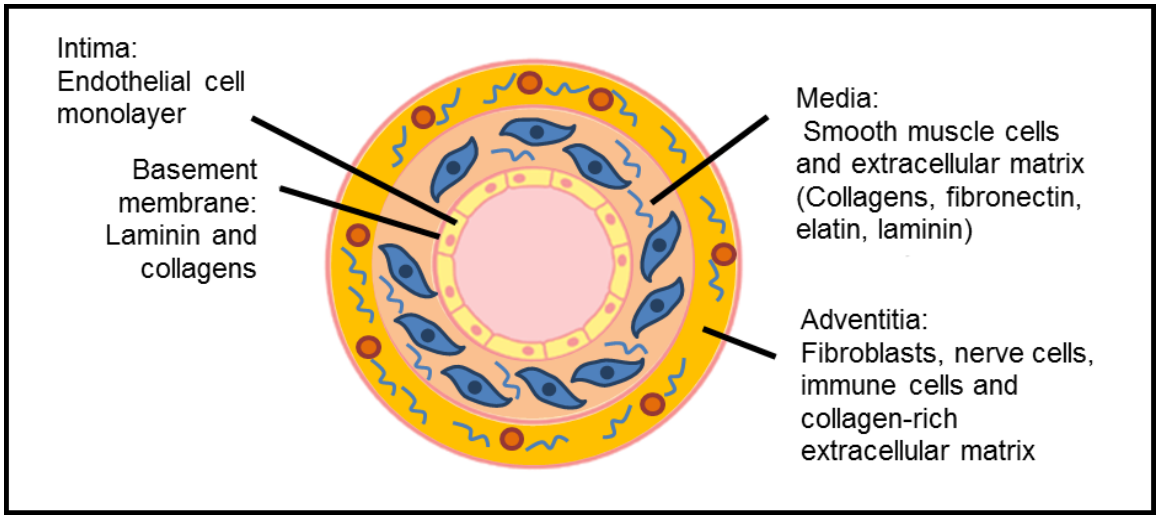

Figure I-1. Schematic view of an arterial wall in cross-section. (Adapted from: Expert Reviews in Molecular Medicine. 2002. Cambridge University Press. http://journals.cambridge.org/fulltext_content/ERM/ERM4_01/S1462399402004039sup006.htm. Accessed on Apr 21st, 2017)

3.1.1 Intima

The Intima is the innermost layer of the arterial wall consisting of a monolayer of endothelial cells that form an interface between circulating blood and the rest of the arterial wall. What separates the endothelial cells from the media is the basement membrane that is composed of laminin and different types of collagens, which carry out a supportive and barrier function. Endothelial cells are separated from the blood by the

glycocalix, which is a few nanometers thick, and a 0.5 μm endothelial surface lining constituted by different types of membranous glycoproteins, proteoglycans, glycosaminoglycans and other macromolecules (*52*). These surface components contribute to sense the mechanical forces generated by the circulating blood, in response to which the endothelial cells release factors into the blood as well as abluminally toward the underlying vascular smooth muscle cells (SMCs) to regulate vascular tone. (See Section 3.2.3 in this chapter for details)

3.1.2 Media

The middle layer of an arterial wall is made up of SMCs surrounded by ECM including elastic membranes between the different layers of SMCs. The composition of the ECM includes collagen type I and III, fibronectin, elastin and laminin that have a supportive role. The level of collagen and fibronectin deposition, as well as the collagen:elastin ratio in the media are the main determinants of arterial stiffness. Signals received from the endothelial cells mediate phosphorylation and dephosphorylation of the myosin light chain (MLC), which regulate the myosin-actin cross-bridging activity in the SMCs, directly leading to vasoconstriction and vasorelaxation, respectively (*53*). (See Section 3.2.3 in this chapter for details)

3.1.3 Adventitia

The adventitia is the outermost layer of an arterial wall that is composed predominantly of fibroblasts, nerve cells, immune cells and the surrounding collagen-rich ECM. It is also a site where microvessels called vasa vasorum penetrate into the wall to carry nutrients and oxygen for arterial cells (*54*). The adventitia anchors the arteries to the neighboring tissues. It serves to mediate communication between the neighboring tissues and the vascular endothelial and smooth muscle cells (*55*). Upon vascular injury, the adventitia is able to produce factors to stimulate cell growth and migration for vascular cell repair, which may in turn contribute to vascular remodeling (*56*). Studies also show

that the adventitia is involved in local inflammation and ROS production, which is largely attributable to the adventitial immune cells (*57, 58*).

3.2 Vascular damage in hypertension and CKD

Hypertension and CKD are characterized by vascular damage that includes vascular remodeling, vascular stiffening and endothelial dysfunction. Both large and small artery injury has been reported in essential hypertension and CKD, as well as in different animal models.

3.2.1 Vascular remodeling

Vascular remodeling in hypertension is referred to as structural changes in the vascular wall that contribute to increased peripheral resistance. Both large arteries and small resistance arteries undergo vascular remodeling in hypertension (*26, 29*). In essential hypertensive patients, large elastic arteries such as the aorta and the carotid arteries undergo outward remodeling, which means increased outer diameter, and growth and proliferation of vascular SMCs that results in increased media thickness, while lumen diameter may be enlarged or decreased (Figure I-2) (*26, 59*). Small resistance arteries with lumen diameter of approximately 100 to 400 microns (*60*), such as subcutaneous arteries in humans and mesenteric arteries in mice, were primarily reported to undergo eutrophic remodeling, meaning an increase in media/lumen ratio without changes in media cross-sectional area (MCSA). Eutrophic remodeling was also found in small resistance arteries of Ang II-treated animal hypertension models (Figure I-2) (*61*). The mechanism of eutrophic remodeling is still poorly understood, but it is likely due to the combination of inward growth and outward apoptosis in the arterial wall (*62*). It has been shown that Ang II stimulates growth factor production and protein synthesis in vascular SMCs that lead to cell growth and proliferation (*63, 64*). At the same time, Ang II could also be a trigger of cell apoptosis both *in vitro* (*65*) and *in vivo* in the aorta of spontaneously hypertensive rats (*66*) via Ang II type 2 receptors. In secondary hypertensive patients and animal models, some of which may involve activation of the

endothelin (ET) system (*35, 67*), small resistance arteries undergo hypertrophic remodeling, with an increase in both media/lumen ratio and MCSA (Figure I-2). Small artery remodeling may be the earliest manifestation of target-organ damage in hypertension, given that one study reported small artery remodeling in 100% cases of mild hypertensive patients, while endothelial dysfunction was present in 60% and LV hypertrophy was present in only 45% of cases (*68*).

Vascular remodeling is believed to be maladaptative in order to maintain wall tension upon BP elevation in hypertension, according to the Law of LaPlace (*26*), as T = P x D / (4 x t), where T = wall tension, P = pressure, D = lumen diameter, t = wall thickness. As indicated in the equation, to maintain a specific wall tension upon increase in BP, the wall has to go through a decrease in lumen diameter and/or an increase in wall thickness. Remodeling and increased stiffness of aorta increases the pulsatility, leading to greater transmission of pulsatile energy downstream into the periphery contributing to target-organ damage (*30-32*).

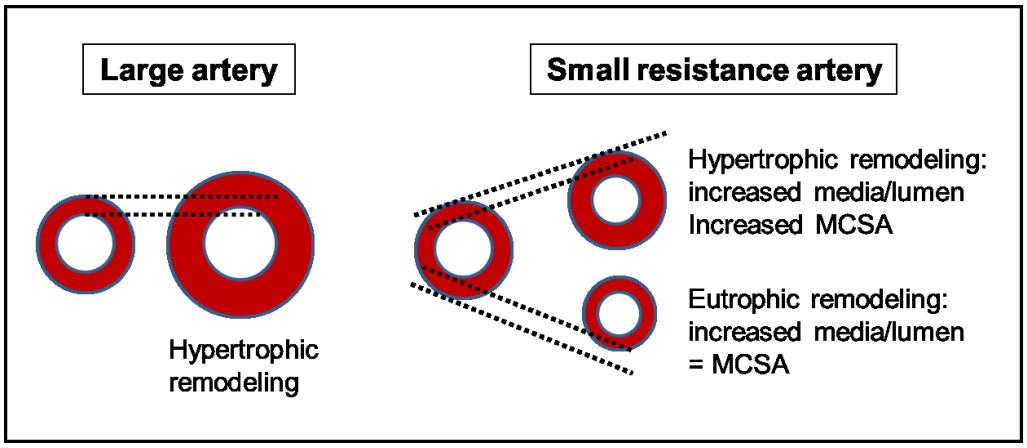

Figure I-2. Large and small artery remodeling in hypertension. Adapted from Schiffrin, 2004 (*26*).

3.2.2 Vascular stiffening

Besides structural remodeling, the arterial wall also displays stiffening in hypertension, which is contributed largely by increased collagen and fibronectin deposition, as well as

collagen:elastin ratio in both human essential hypertension and rodent hypertensive models (*27-29*). Collagen fibers, mostly collagen type I and III in arteries, and fibronectin provide skeletal support and rigidity strength to the arteries. As a consequence, increases in collagen and fibronectin deposition result in increased stiffness. Elastin on the contrary, is responsible for the elasticity of the arteries, conferring arteries compliance and the ability to distend with high BP. Increases in the collagen:elastin ratio characterize vascular stiffening. Vascular stiffening increases the propagation speed of the pulse wave in the arteries, i.e. pulse wave velocity (PWV). In the situation of increased PWV, when the reflected pulse wave coming from the periphery meets with the incident (forward) wave coming from the heart earlier and results in augmented systolic pressure (AP) (Figure I-3). When central pressure is elevated, it generates a higher PP, which is transformed to greater pulsatile energy that injures the peripheral small resistance arteries in the brain and kidneys, leading to target organ damage (*32, 69, 70*). Thus, PWV and augmentation index (AI, meaning the AP to PP ratio) are common parameters for large artery stiffness evaluation. Small artery stiffness on the other hand, is commonly measured by pressurized myography, and presented in a stress-strain curve, in which the strain refers to the level of deformation of the arterial walls upon changes in BP, whereas the stress indicates the tension applied to the arterial walls. A leftward shift of the curve suggests increased small artery stiffness (*33, 71*).

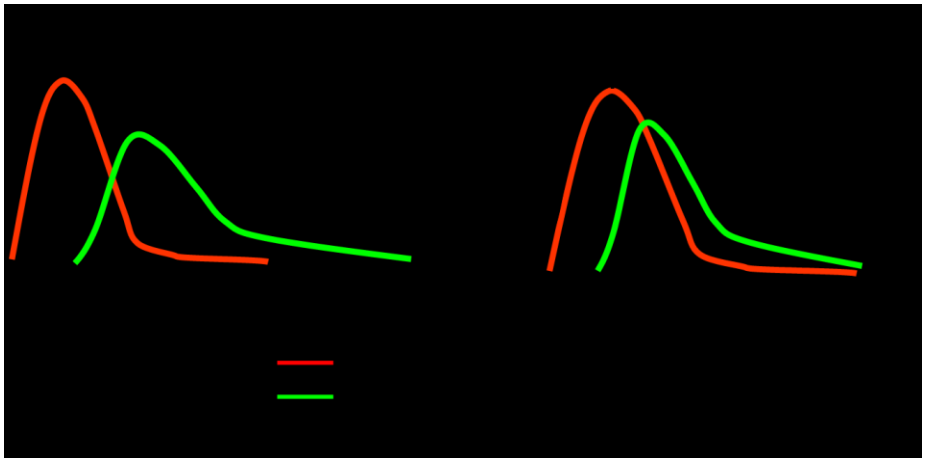

Figure I-3. Formation of augmented pressure (AP) due to interference of the forward wave with the reflected wave. Adapted from Kum *et al.* (*70*).

The RAAS is also involved in vascular stiffening in hypertension. It has been shown that Ang II stimulates collagen synthesis in human vascular SMCs via the Ang II type 1 receptor (*72*). The Ang II-induced collagen overexpression at the transcriptional level was found to be transforming growth factor beta (TGF-β)-dependent. Ang II treatment was also able to increase fibronectin (*73*) and inhibit elastin (*74*) expression at the transcriptional level in vascular SMCs. Aldosterone infusion, which increased ET-1 expression, also induced vascular remodeling and deposition of collagen type I and III and fibronectin (*75*). Matrix metalloproteases (MMPs), who are able to regulate the turnover of ECM proteins such as collagens and elastin, have been implicated in vascular remodeling and stiffening (*76, 77*). Ang II treatment was shown to up-regulate MMP-2 expression at both mRNA and protein levels via the Ang II type 1 receptor. This effect was mediated by the activation of the extracellular signal-regulated kinase (ERK) ½ signaling pathway (*78*). Expression levels of other ECM proteins such as biglycan (BGN) (*79, 80*) and connective tissue growth factor (CTGF) (*81, 82*) have also been reported to increase in various tissues by Ang II treatment. A selective Ang II type 2 receptor agonist was able to lower aortic collagen and fibronectin levels, and reduce small artery stiffening in spontaneously hypertensive rats (*71*).

Small artery remodeling causes increases in resistance to blood flow and therefore mean BP. This leads to arterial stiffening in large arteries that through enhanced pulsatility will impact on small arteries, stiffening the former and the latter through ECM protein deposition. This cross-talk between large and small arteries forms a feed-forward vicious circle that exaggerates the hemodynamic phenotype (*32, 83, 84*).

Vascular stiffening in CKD is not as well studied as in hypertension. It has been reported that CKD patients undergo arterial calcification that causes increased vascular stiffness (*85, 86*). A strong inverse relationship between eGFR and coronary artery calcification was found in CKD patients (*87*). The molecular mechanisms underlying vascular calcification are still poorly understood, but it is believed to involve the RAAS, oxidative stress and inflammation (*45*).

3.2.3 Endothelial dysfunction

Endothelial cells, which are in contact with the circulating blood separated only by the glycocalix and endothelial surface lining, release factors that act on SMCs in the media to regulate vascular tone upon exposure to stimuli from the circulation such as shear stress (*53, 88, 89*). A main vasodilator released by endothelial cells is nitric oxide (NO), which is diffused to the neighboring SMCs where it binds to soluble guanylate cyclase (sGC). This binding leads to the conversion from GTP to cyclic GMP (cGMP), which activates the cGMP-dependent protein kinase (PKG). The activated PKG inhibits Ca^{2+} influx into the cells, activates K^+ efflux and dephosphorylates MLC by stimulation of MLC phosphatase. These changes lead to membrane hyperpolarization and vessel relaxation. On the other hand, MLC kinase-mediated MLC phosphorylation leads to vessel contraction (Figure I-4).

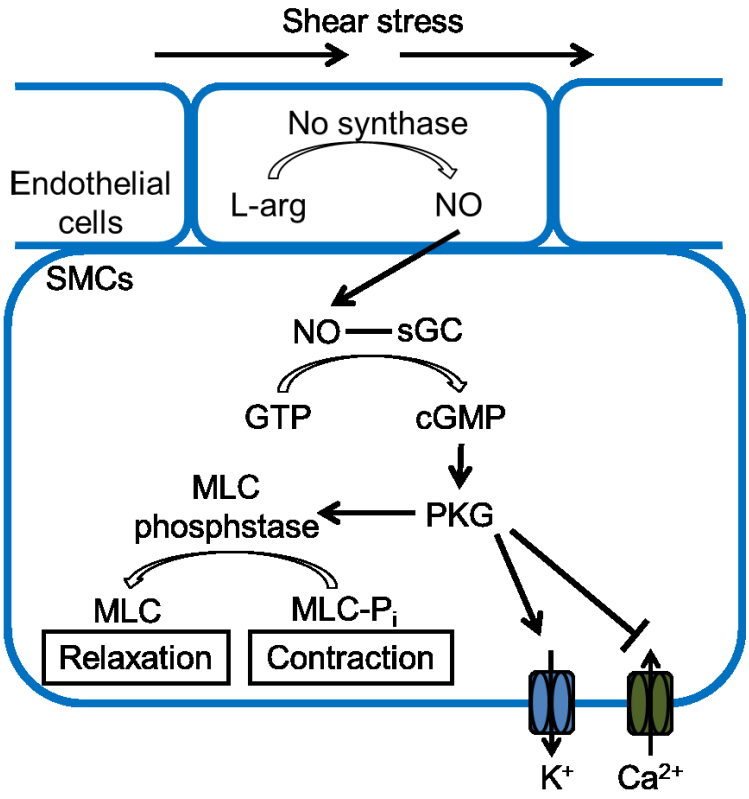

Figure I-4. Schematic mechanism of endothelium-dependent relaxation.

Over the last few decades, endothelial dysfunction has been shown to associate with hypertension (*90, 91*). Essential hypertension is characterized by defective NO bioavailability caused by ROS-induced NO oxidation and/or NO synthase uncoupling (*92, 93*). In large arteries, endothelium-dependent flow-mediated dilatation (FMD) has been shown to inversely correlate with both systolic and diastolic BP in humans (*94*). Essential hypertensive patients were reported in another study to display reduced FMD (*95*). In small resistance arteries of essential hypertensive patients, a marginally decreased endothelial function was demonstrated by an impaired endothelium-dependent relaxation to acetylcholine (*68*). CKD patients also showed decreased FMD, which was inversely correlated with inflammatory marker C-reactive protein (*96*), and endothelial dysfunction in small resistance arteries (*97, 98*). Animal models infused with Ang II have also been shown to increase ROS production, decrease NO bioavailability and induce endothelial dysfunction (*33-35*). Blockade of the RAAS by the Ang II type I receptor blocker valsartan was able to reduce ROS production, improve endothelial function and lower BP (*99*).

4. Ang II in hypertension and vascular damage

As mentioned previously, Ang II is the primary effector of the RAAS. It increases BP mainly through contraction of vessels, vascular remodeling, endothelial dysfunction and aldosterone-mediated sodium retention in the kidneys. Numerous studies have shown the Ang II is also able to induce vascular remodeling and stiffening. This section will cover some of the main Ang II-induced signaling pathways involved in hypertension and vascular damage.

In mammals, there are 2 known high-affinity Ang II plasma membrane receptors, namely AT_1R and AT_2R. To date, most well-studied physiological effects of Ang II act through AT_1Rs, which are expressed in a variety of organs including the brain, the lungs, the kidneys, the heart and the vasculature (*100, 101*). The Ang II action through AT_2Rs is

much less studied, and essentially induces effects opposite to AT_1R. The AT_1R is a 359-amino-acid protein that is highly conserved between species. It belongs to the seven-membrane G protein-coupled receptor (GPCR) superfamily, with G protein interaction taking place in the NH_2 terminal transmembrane domain and the first and third extracellular loops.

The binding of Ang II to AT_1Rs triggers a series of signaling cascades that lead to vasoconstriction, protein synthesis, cell division and ROS production (Figure I-5). Given that AT_1Rs have no intrinsic kinase activity, non-receptor tyrosine kinases play an important part to initiate signaling events by phosphorylating intracellular proteins. Among those non-receptor tyrosine kinases, Src, which is one of the earliest activated (within seconds) enzymes by Ang II, acts as a central player in the Ang II-induced pathways that include the Ras-Raf-MEK-ERK cascade, the PI3K-Akt pathway and the JAK-STAT pathway. Src is also able to trigger the epidermal growth factor receptor (EGFR) pathway that contributes to induce other signaling pathways such as the PI3K-Akt and the Ras-Raf-MEK-ERK pathways. Phospholipase C (PLC), which is another early Ang II-activated (also within seconds) enzyme, plays a predominant role in Ang II-induced vessel contraction (*102*). Phosphorylation and activation of PLC, which is at least partially dependent on Src, leads to the formation of inositol-1,4,5-triphosphate (IP_3) and diacylglycerol (DAG). IP_3 binds to receptors on the sarcoplasmic reticulum of vascular SMCs and increases calcium efflux from the sarcoplasmic reticulum into the cytoplasm. The calcium ions then bind to calmodulin and activate myosin light chain kinase (MLCK), which leads to the phosphorylation of the MLC and enhanced myosin-actin cross-bridging, finally resulting in vessel contraction. DAG on the other hand, activates protein kinase C (PKC), which in turn phosphorylates and activates the Na^+/H^+ pump. This results in increased intracellular pH and alkalinization, which is important for myosin-actin cross-bridging and vessel contraction (*103*). Moreover, DAG is also able to trigger the Ras-Raf-MEK-ERK cascade that activates c-fos and other transcription factors. c-fos then dimerizes with c-jun, which is activated through the JNK pathways, to form the transcription factor AP-1. These transcription factors activated through different pathways (including Ras-Raf-MEK-ERK, PI3K-Akt, JAK-STAT and JNK) induce the expression of their target genes, which are responsible for protein synthesis and cell

division, and lead to vascular remodeling and ECM formation that contributes to vascular stiffening. The NAD(P)H oxidases (NOXs) are activated through some of the above pathways and are responsible for the ROS (such as superoxide and hydrogen peroxide) production and local inflammation in the vessels (*100, 101, 104, 105*). ROS in turn contributes to stimulate Src-initiated pathways and forms a feed-forward vicious circle (*106-108*). It also induces the activation of nuclear factor kappa-light-chain-enhancer of activated B cells (NF-κB), which increases the expression of vascular cell adhesion molecule 1 (VCAM-1) and intercellular adhesion molecule 1 (ICAM-1), and finally leads to vascular inflammation and endothelial dysfunction (*107, 109, 110*). Besides PLC, Ang II also induces activation of phospholipase D (PLD) and phospholipase A_2 (PLA_2). The activated PLD catalyzes the hydrolysis of phosphatidylcholine (PC) to produce choline and phsophatidic acid (PA). PA is then converted into DAG, which activates PKC and the downstream pathways as mentioned above (*111*). The activation of PLA_2 leads to the generation of arachidonic acid (AA) and other metabolites, which together contribute to induce the Ras-Raf-MEK-ERK pathway and NOX activation (*104, 112*).

As many other ligand-receptor interactions, the Ang II-AT_1R binding is also transient. Within minutes upon simulation by Ang II, AT_1Rs undergo internalization, a process in which AT_1Rs get endocytosed into endosomes. The cells therefore become desensitized to further Ang II simulation. Approximately 25% of the endosomal AT_1Rs will be recycled back to the plasma membrane, with the remainder degraded by lysosomes (*113, 114*). Phosphorylation of the threonine and serine residues of the AT_1R cytoplasmic tail, which leads to uncoupling of AT_1Rs from the associated G proteins, has been shown to play a role in its internalization and desensitization (*115, 116*).

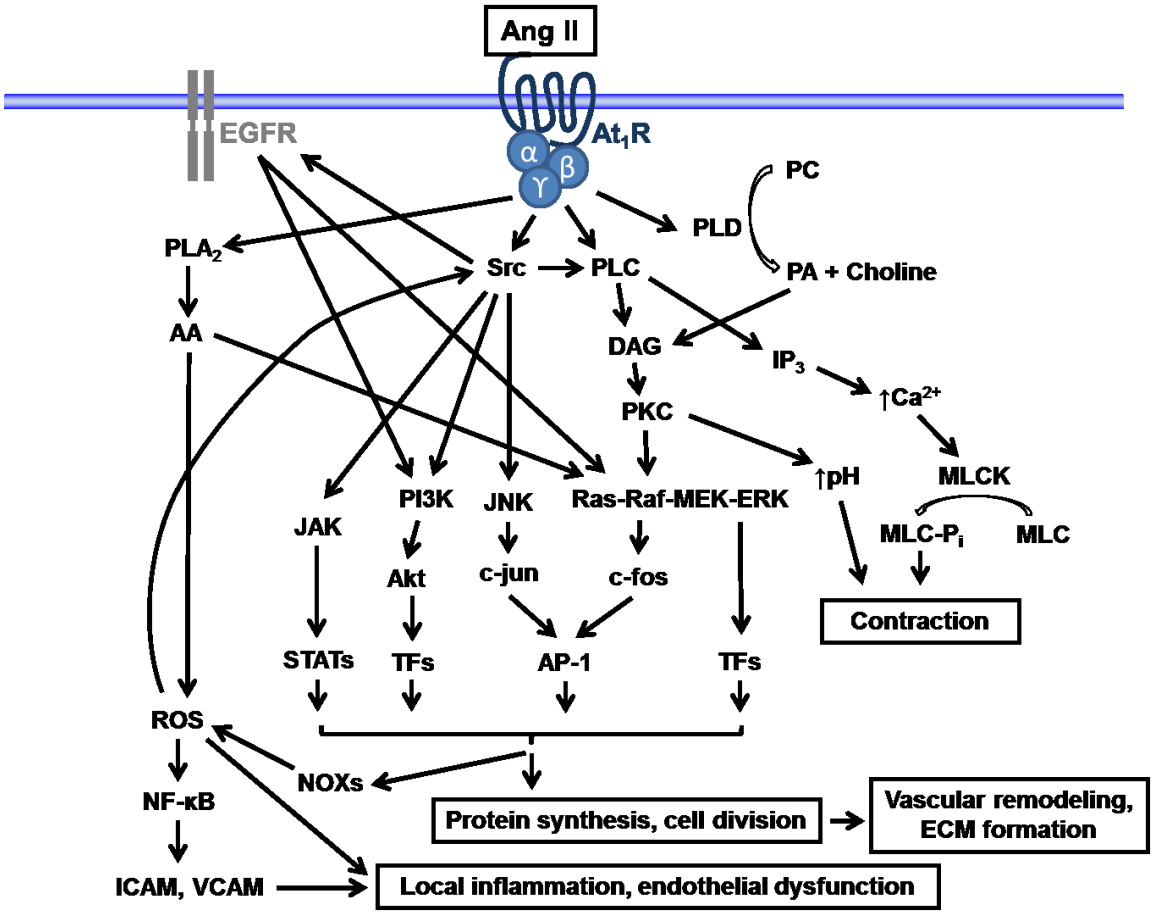

Figure I-5. Ang II signaling pathways in hypertension and vascular damage.

5. Non-coding RNAs (ncRNAs)

About two-thirds of the mammalian genome is transcribed into RNAs, but only less than 2% encode for proteins. The remaining majority of RNAs are classified as non-coding RNAs (ncRNAs) (*117*). These ncRNAs, once thought to be junk in the genome, have been shown by accumulating studies over the past two decades to play critical regulatory roles in gene expression at both transcriptional and post-transcriptional levels, during developmental and differentiation processes, as well as in disease development. ncRNAs can be divided into two main categories: 1, small ncRNAs that include microRNAs (miRNAs), small nuclear RNAs (snRNA) and small nucleolar RNAs (snoRNAs); 2, long

ncRNAs (lncRNAs) that include long intergenic ncRNAs (lincRNAs), circular RNAs (circRNAs), antisense RNAs and pseudogenes. This section will cover the biogenesis of ncRNAs, the molecular mechanisms of ncRNA-mediated gene regulation, the potential of ncRNAs being therapeutic targets, as well as the role of circulating ncRNAs and their value in clinical applications.

5.1 miRNAs

5.1.1 miRNA biogenesis

miRNAs are a class of small ncRNAs about 22 nt long that regulate gene expression post-transcriptionally by causing mRNA degradation and translation repression (*118, 119*). The precursor of a miRNA, a 60- to 80-nt pri-miRNA, is either transcribed directly from a miRNA gene in the genome, or spliced out from an intron of an mRNA (Figure I-6) (*120, 121*). In the case of direct transcription, a pri-miRNA forms a stem-loop secondary structure that contains a 5' cap and a 3' poly-A tail. It is then further processed by an RNase III enzyme Drosha and an RNA-binding protein DGCR8 to produce a precursor called pre-miRNA that contains a ~22-nt stem and a loop without the 5' cap and 3' poly-A tail. When a miRNA is originating from an mRNA, it is spliced out from an intron, and goes through debranching and re-folding to form a stem-loop pre-miRNA called a mitron. Pre-miRNAs are then exported by Exportin 5 from the nucleus to the cytoplasm, where they are further processed by another RNase III enzyme, Dicer, and an RNA-binding protein TRBP. Dicer cleaves out the loop of the pre-miRNA to yield a ~22 nt miRNA duplex, which is unwound by an unidentified ATP-dependent helicase to generate 2 single-stranded mature miRNAs. It was once thought that only one strand of the mature miRNA, namely the guide strand, was incorporated into an argonaute protein Ago2 to form an RNA-induced silencing complex (RISC), while the complementary strand, namely the star strand, will be degraded. Later studies have shown that both strands can be packed into the RISC, with the thermodynamic properties of the miRNA duplex playing a critical role in strand selection (*122, 123*). The ATP-dependent helicase

unwinds the miRNA duplex from both ends. In each case, the strand whose 5' end is the unwinding start end will be incorporated into the RISC, while the complementary strand is degraded. As a result, either strand can be packed into the RISC, depending at which end the unwinding starts. However, evolution makes the ATP-dependent helicases favor unwinding the miRNA duplex from the less internally stable end, which would cost less energy. As a consequence, there is a bias in strand selection during the formation of mature miRNAs, with the guide strand being the major RISC-bound form, and the star strand being the minority. There are two official ways for miRNA nomenclature. The first is miR-XYZ and miR-XYZ*, with the miR-XYZ* being the minority, and the second is miR-XYZ-5p and miR-XYZ-3p, without specifying which is the majority.

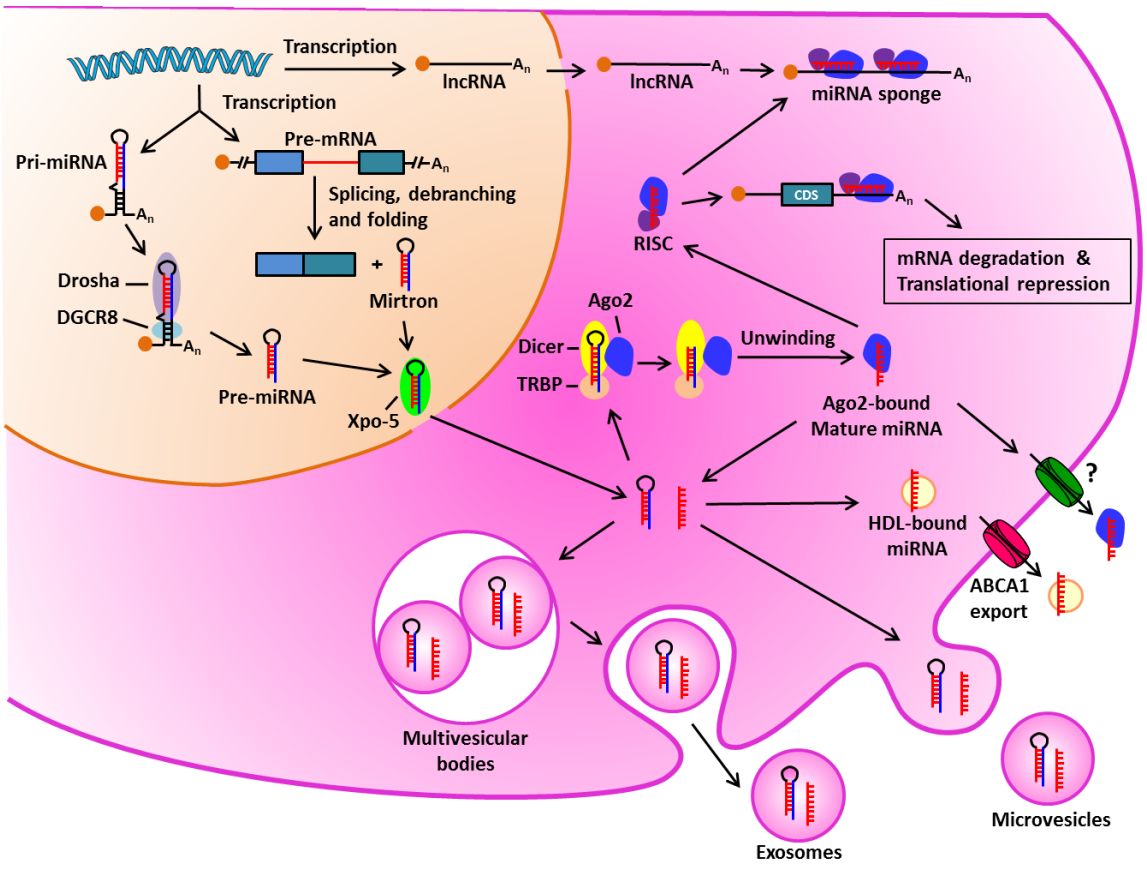

Figure I-6. miRNA biogenesis and function.

5.1.2 miRNA-mediated gene regulation

The single-stranded mature miRNA in the RISC serves as a guide to target mRNAs. In the canonical fashion, it binds to the 3' untranslated region (UTR) of the target mRNA in a perfect-pairing fashion in the seed region, in position 2-7 (6mer) or 2-8 (7mer) from the 5' end of the miRNA, with or without a 3' supplementary base pairing (*120, 121, 124*). The strength of the miRNA targeting effect varies between different types of miRNA-mRNA binding. A 6mer pairing has weaker effects than a 7mer pairing, and an 8mer pairing (7mer with an adenine at position 1 of the miRNA) has a stronger effect than 7mer (*125, 126*). The presence of 3' supplementary binding increases miRNA targeting efficiency. Some studies have shown that a strong 3' supplementary pairing with imperfect seed matching, or with a less-than-6mer seed matching, could also be sufficient to confer miRNA function (*124, 127, 128*).

The miRNA-mRNA binding could lead to mRNA degradation and/or translation repression. The original theory was that a perfectly matched miRNA-mRNA pair leads to mRNA cleavage, whereas an imperfectly matching would normally result in translational repression. However, later studies have shown that even imperfect base-pairing miRNA-mRNA duplex could cause mRNA degradation (*129*), and most of the time, mRNA degradation and translation repression occur together (*118, 119*). Upon binding to the target mRNA, the RISC localizes to P bodies, which are cytoplasmic foci enriched for de-adenylating and de-capping enzymes that destabilize mRNAs (*130*). Ago2 in the RISC plays a central role in the miRNA silencing mechanism. It possesses endonuclease activity and is responsible for cleaving the miRNA-mRNA duplex. During miRNA-mediated translational repression, the 5' cap-binding and 3' poly-A tail functions of the target mRNA are inhibited, which may also involve de-capping and de-adenylation that occur in the P bodies (*131-133*). Studies have demonstrated that replacing the 5'cap with a non-functional ApppN cap, or introducing an internal ribosome entry site was able to prevent miRNA-mediated translation repression.

miRNAs can also bind to their targets in non-canonical fashions, which may yield variable outcomes in terms of gene regulation. One example is the 3' supplementary binding with imperfect seed match that was mentioned earlier in this section. Such

binding decreases miRNA targeting efficiency. Besides binding to the 3' UTRs of the target mRNAs, miRNAs can also bind to the 5' UTR or the coding region (Figure I-7). Jopling *et al.* found an interaction between miR-122 and the 5' UTR of the hepatitis C virus RNA, which may facilitate RNA replication (*134*). A phase 2a clinical trial using a miR-122 inhibitor called Miravirsen to treat hepatitis C virus infection received promising results in reducing viral RNA levels (*135*). On the contrary, in another study it was demonstrated *in vitro* that exogenous miRNA let-7a bound to the 5' UTR of the luciferase reporter gene and decreased gene expression (*136*). When a miRNA binds to the coding region of the target mRNA, it also causes mRNA degradation and translational repression, but the targeting efficiency is lower compared to a 3' UTR binding (*137*). miRNAs can also regulate gene expression at the transcriptional level. A few studies have reported that miRNAs were found in the nuclei and could target the genome at the promoter region (Figure I-7) (*138-140*). However, results varied between studies. Robert *et al.* showed that transfection of miR-373 mimics induced target gene expression upon binding to the promoter (*139*), while Younger *et al.* found a repressor effect with the transfection of miR-423-5p mimics, which also bound to the promoter of the target DNA (*140*).

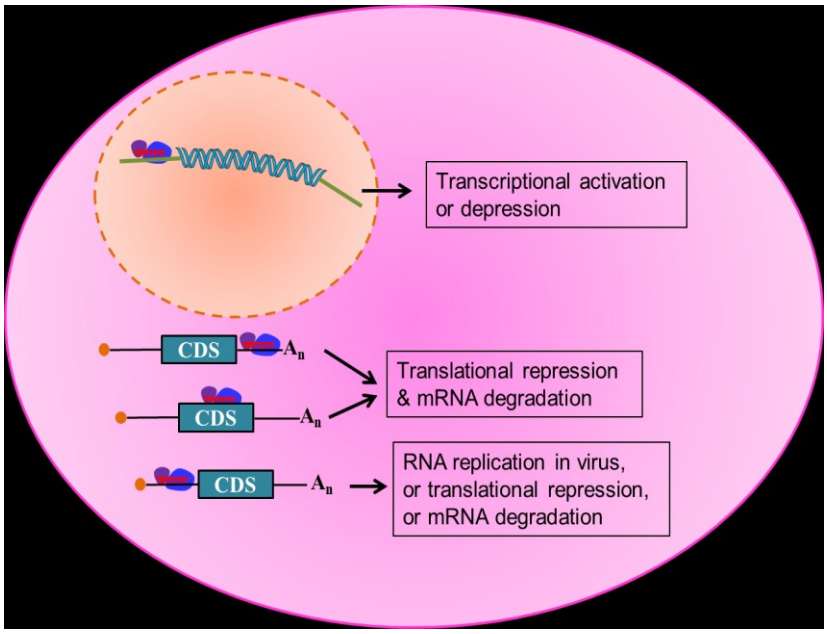

Figure I-7. Mechanisms of miRNA targeting gene regulation.

5.1.3 miRNAs as potential therapeutic targets

Alterations of miRNA genes in the genome would result in changes of target gene expression. For example, amplification or duplication of a miRNA gene would cause down-regulation of the target genes, and deletion of a miRNA gene would result in up-regulation of the target genes. Mutations in the seed region of a miRNA gene could lead to a change of targets. Mutations or variants of miRNA genes or miRNA binding sites, as well as dysregulation of miRNA expression have been associated with different pathologies. Current findings on the implication of miRNAs in cardiovascular diseases including hypertension, CKD and vascular damage will be described in Section 6 of this chapter. One miRNA can target multiple mRNAs and one mRNA can be targeted by multiple miRNAs. It has been reported that there are more than 45000 conserved miRNA-binding sites in human 3' UTR. On average, there are more than 500 predicted targets per miRNA family (*126*). The ability to regulate expression of a large amount of genes allows miRNAs to act as master regulators in complicated gene networks involved in development or different physiological pathways. Alterations of a single miRNA could have a large effect on normal body functions by affecting hundreds of other genes. At the same time, this confers miRNAs the potential to become potent therapeutic targets in clinical applications.

Current methods used to target miRNAs include the gain-of-function approach by miRNA mimics or viral miRNA expression vectors, and the loss-of-function approach by miRNA inhibitors or viral small interfering RNA (siRNA) expression vectors. Delivery of miRNA mimics, miRNA inhibitors or viral expression vectors could be done by injection or infusion intravenously (*141-143*), subcutaneously (*135, 144*), intra-arterially (*145*) or intra-peritoneally (*146*). Although various delivery methods are feasible, there are still many challenges such as poor targeting delivery to the tissue of interest, fast degradation of miRNA mimics and inhibitors and risk of immunotoxicity (*147*). Moreover, considering that one miRNA could target hundreds of mRNAs, off-target effects remain a big concern. *In vivo* gain-of-function approaches are technically more difficult compared to loss-of-function approaches and usually involve using viral

expression vectors that may induce stronger immune-toxicity, while the use of miRNA mimics should be more cautious since they bypass the endogenous miRNA biogenesis and targeting machinery and may cause greater non-specific targeting effects (*148*). There are much less successful *in vivo* miRNA mimic gain-of-function examples than successful *in vivo* knockdown by miRNA inhibitors, suggesting a greater technical difficulty in miRNA mimic delivery or efficacy *in vivo*. The only clinical trial using miRNA mimics as targeting therapy was ended prematurely after observing multiple immune-related severe adverse events (See Section 7.3 ncRNAs as therapeutic targets for details).

5.2 lncRNAs

lncRNAs are ncRNAs with longer than 200 nt. Compared to small ncRNAs, lncRNAs are able to form high order structures that provide them greater capability to bind small molecule or protein ligands (*117, 149*). The high order structure also adds complexity and versatility to target recognition, with or without the help of DNA- or RNA-binding protein ligands. lncRNA-mediated gene regulation is therefore more miscellaneous than miRNA-mediated gene regulation. There are different types of lncRNAs including lincRNAs, circRNAs, antisenses and pseudogenes. Each type may regulate gene expression in one or multiple ways, at the transcriptional level and/or post-transcriptional level.

5.2.1 lincRNAs

lincRNAs are transcribed from non-coding genome regions between protein-coding genes, as the "i" in lincRNA stands for "intergenic". The length of lincRNAs can reach up to tens of thousands of nucleotides, giving them great potential to fold into high order structures and interact with small molecule and/or protein ligands (*150*). They can bind to promoter and/or enhancer regions in the genome to regulate gene expression at the transcriptional level (Figure I-8) (*117, 149, 151*). Upon binding, lincRNAs together with their ligands can recruit other transcription factors or repressors to regulate RNA

transcription. It has been shown that lincRNA binding was also able to change DNA and chromatin methylation status by affecting recruitment of DNA methyltransferase 3 that methylates DNA and histone lysine *N*-methyltransferase EHMT2 that methylates histones (*152*). The lincRNA-mediated post-transcriptional gene regulation is still poorly studied, but their ability of base-pairing and interacting with RNA-binding proteins suggests that lincRNAs may also bind to mRNAs, regulating protein translation or mRNA turnover. lincRNAs can also act as a miRNA sponge, or by competing with endogenous RNAs (ceRNAs) to repress miRNA activity by base-pairing with and sequestering miRNAs (Figure I-8) (*128, 153*). The ceRNA-miRNA binding may induce miRNA degradation, provided that siRNA knockdown of the ceRNA leads to increased target miRNA levels (*128*).

5.2.2 circRNAs

circRNAs are covalently closed ncRNAs derived from precursor mRNAs. Current data suggest that they are generated from back-splicing events driven by the spliceosomal machinery, which could be facilitated by internal intron base-paring or other RNA-binding proteins (*154, 155*). circRNAs generally have low expression compared to other ncRNAs, suggesting that they may be merely a type of by-product generated during post-transcriptional processing. However, recently studies have reported that these by-products could also possess regulatory potency on gene expression. Like lincRNAs, they can act as ceRNAs to compete with mRNAs for miRNA binding and repress miRNA activity (Figure I-8). Memczak *et al*. showed that circRNA *CDR1as* was densely bound to the miRNA effector protein AGO and had tens of conserved miR-7 binding sites. Expression vector-induced gain-of-function displayed similar effect as miR-7 knockdown (*156*). On the same issue of the journal, another research group published a similar finding on a circRNA *ciRS-7* that also interacted with AGO and could serve as a miR-7 sponge (*157*). Li *et al*. identified a circRNA *cir-ITCH* that competed with the E3 ubiquitin protein ligase *ITCH* to interact with miR-7, miR-17 and miR-214. A positive correlation between *cir-ITCH* and *ITCH* suggests that the presence of *cir-ITCH* may up-regulate *ITCH* expression (*158*).

5.2.3 Antisense RNAs

Antisense RNAs are transcribed from the complementary strand of a protein-coding gene. An antisense RNA could come from an antisense gene that localizes in the position of the opposite strand that overlaps the sense mRNA, or could result from an aberrant extension of a neighbor gene in the opposite strand that causes overlapping (*159*). As a complementary sequence, antisense RNAs are able to bind to their sense mRNAs, mediating gene expression at the post-transcriptional level (Figure I-8). Unlike the RNA interference effect by antisense oligonucleotides, the sense-antisense RNA duplex formation could also increase mRNA stability and protect mRNA from miRNA-induced or RNase E-induced degradation by masking the miRNA or RNase E recognition sites (*160-162*). Carrieri *et al.* demonstrated that Uchl1 antisense increased UCHL1 protein translation by interacting with the 5' end of the *Uchl1* mRNA (*163*). Such antisense activity depended on the presence of a SINEB2 repeat element in the Uchl1 antisense RNA. However, another study by Darfeuille *et al*. reported that IstR-1 was an antisense RNA bound to tisAB mRNA and led to RNase III-induced cleavage of the sense-antisense RNA duplex and translational repression by competing with standby ribosomes (*164*).

5.2.4 Pesudogenes

A pseudogene is a non-coding gene that shares a high degree of similarity with a protein-coding gene (*165, 166*). They are believed to be derived from functional protein-coding genes but have lost their coding capability. Based on their origin, pesudogenes can be classified into unitary pseudogenes, duplicated pseudogenes or processed pseudogenes. Unitary pseudogenes are resulted from spontaneous mutations of originally functional protein-coding genes that introduce premature stop codons or impaired regulatory sequences, leading to the production of non-functional or dysfunctional proteins to be degraded. Duplicated pseudogenes are duplicated from a protein-coding gene into another genomic region. Some duplicated pseudogenes have lost their coding ability due

to a partial duplication in the coding regions or the loss of key regulatory regions during duplication, while others were once functional, but became silenced during evolution (*167, 168*). Processed pseudogenes are derived from mRNAs that are reversely transcribed to cDNA, and then integrated into the genome. They are characterized by the lack of introns, promoters and enhancers with the presence of poly-A tails.

These pseudogenes that were once thought to be "junk" emerged during evolution, have been recently shown to play a key regulatory role in gene expression. The ncRNAs transcribed from the pseudogenes share highly similar sequences with their protein-coding counterparts, which allows them to bind to similar proteins or other ncRNAs. Poliseno *et al*. demonstrated that the *PTENP1* pseudogene of the tumor suppressor gene *PTEN* could act as a miRNA sponge to compete with the *PTEN* mRNA for miRNA binding. The 3' UTR of *PTENP1*, which binds to miRNAs that target *PTEN*, has tumor suppressive activity (*169*). Moreover, it has been reported that a pseudogene *Lethe* could bind to the subunit RelA of the nuclear factor complex NF-κB and inhibit RelA's DNA binding, thereby suppressing its target gene activation (*170*).

5.2.5 Coding lncRNAs

By definition, ncRNAs have no open reading frames (ORFs), and therefore do not code for proteins. However, recent findings on the identification of small ORFs in lncRNAs suggest that many lncRNAs may actually code for small peptides (Figure I-8) (*171, 172*). The small ORFs of coding and non-coding RNAs identified by ribosome profiling have been uploaded in a database in www.sorfs.org. As early as 1995, Chen *et al*. reported that eukaryotic ribosomes could initiate translation on circRNAs (*173*). After that, more studies have identified small peptides encoded by other lncRNAs. These small peptides are not just abnormal or incomplete proteins that are non-functional. Anderson *et al*. found a small peptide MLN encoded by a putative lncRNA that could regulate skeletal muscle performance. MLN has a transmembrane alpha helix and was found to be embedded in the sarcoplasmic reticulum membrane, where it regulated Ca^{2+} uptake by inhibiting SERCA pump activity (*174*). Kondo *et al.* revealed small peptides from 11 to 32 amino acids encoded by a *Drosophila* ncRNA *polished rice* (*pri*). These small

peptides were able to change the transcription factor Svb from a repressor to an activator by N-terminal truncation (*175*).

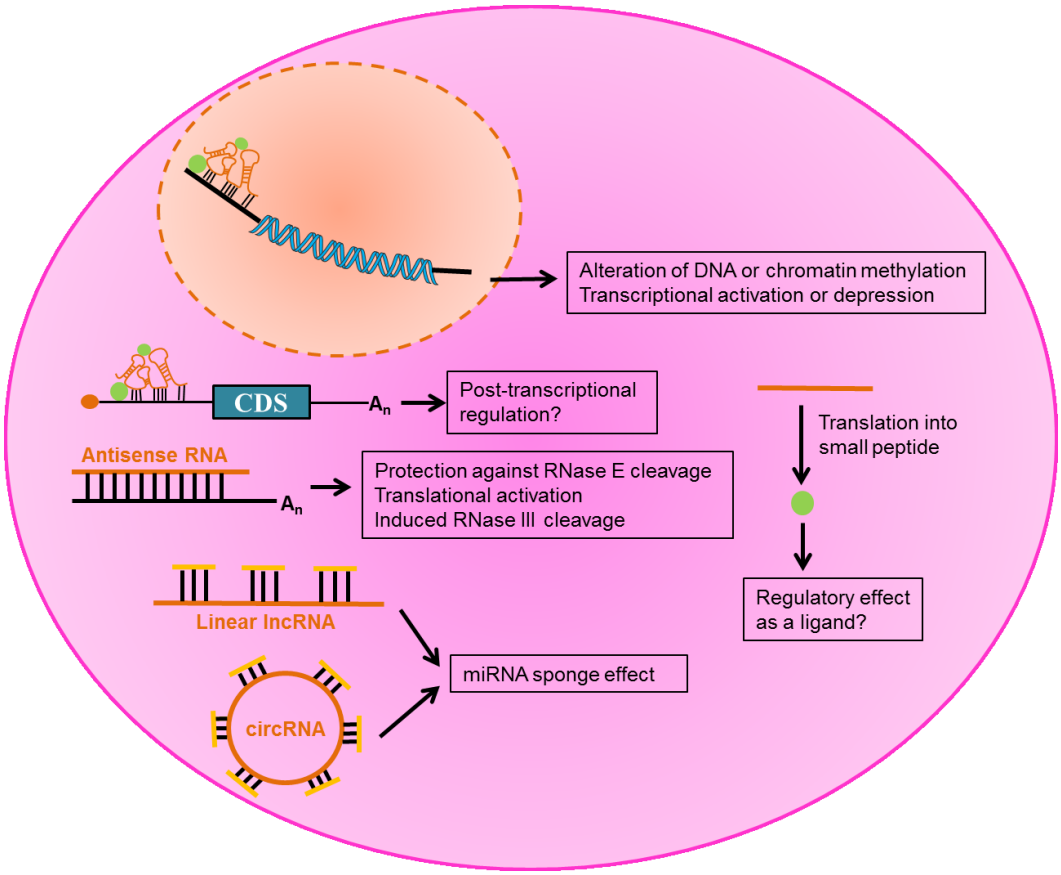

Figure I-8. lncRNA-mediated transcriptional and post-transcriptional regulation.

5.2.6 Methods to target lncRNAs

lncRNAa have been linked to different pathologies. Current findings on the implication of lncRNAs in cardiovascular disease including hypertension, CKD and vascular disease will be described in Section 6 of this chapter. lncRNAs generally have relatively low expression levels compared to mRNAs. This may be due to a tissue-specific expression pattern (*176*). This makes lncRNAs interesting therapeutic targets for disease. There are several approaches to target lncRNAs that may be adapted to clinical use. One approach is siRNA knockdown. Although numerous studies have shown successful lncRNA

knockdown by siRNA *in vitro* (*177, 178*), *in vivo* knockdown seems to be technically more difficult, which therefore limits its potential in clinical applications. Another approach is antisense oligonucleotide silencing by the RNase H machinery. Wheeler *et al*. were able to effectively knockdown the lncRNA *Malat-1* in skeletal muscle by systemic administration of antisense oligonucleotides in mice, without evidence of renal or liver toxicity (*179*). However, lncRNAs, especially those who have long sequence, tend to fold into high order structures, which may significantly decrease siRNA- and antisense-targeting efficacy with reduced accessibility. An alternative approach using ribozymes has been proposed (*180*). A ribozyme that recognizes a specific target RNA sequence and catalyzes target RNA cleavage may possess advantages over siRNAs and antisense oligonucleotides when acting on complex lncRNAs. Nevertheless, targeting lncRNAs in clinical applications is still in its infancy. More research needs to be done in animal models before these techniques are applied in clinical trials.

5.3 Circulating ncRNAs

5.3.1 The origin of circulating ncRNAs

Recent studies have found that ncRNAs are also present as a cell-free extracellular form in biological fluids such as circulating blood and urine. These cell-free circulating miRNAs were actually cell-derived miRNAs produced by the canonical intracellular miRNA biogenesis pathways described in the last section. They are released into the extracellular space either as a vesicle-associated form or as a non-vesicle-associated form (Figure I-6) (*48, 49, 181*). Vesicle-associated circulating miRNAs can either by packed into intracellular membrane-bound compartments called endosomes (50-100 nm), and then released out of the cells through fusion with plasma membrane as exosomes, or they can be released directly within microvesicles (100-1000 nm) through outward budding. Non-vesicle-associated circulating miRNAs on the contrary, are usually bound with high-density lipoproteins (HDL) or AGO2. The HDL-bound miRNAs are then released into the extracellular space by the ATP-binding cassette transporter A1 (ABCA1). HDL-

bound miRNA delivery has been shown to be dependent on scavenger receptor class B type I (SR-BI) (*182*). The transport mechanisms of AGO2-bound miRNAs are still unclear. Besides being released from cells, circulating miRNAs can also be found in apoptotic bodies, which are fragmented vesicles resulting from cells that have broken apart during apoptosis. There have been studies showing the presence of circulating lncRNAs in exosomes (*183*). However, whether they can be released as protein-bound non-vesicle-associated circulating lncRNAs remains to be elucidated.

5.3.2 Roles of circulating ncRNAs

One major function of exosomes and microvesicles is to promote communication with neighboring and far away cells. The existence of circulating forms may allow long-distance ncRNA-mediated gene regulation. Zhao *et al*. demonstrated that miR-150 was packed into microvesicles, released from acute myelomonocytic leukemia cells and taken up by the co-cultured vascular endothelial cells, where it targeted *c-Myb* and reduced c-Myb protein levels (*184*). Similarly, Umezu *et al*. observed that the exosome-associated miR-92a was released from chronic myeloid leukemia cells and targeted integrin a5 (*ITGA5*) in the co-cultured recipient vascular endothelial cells (*185*). Zernecke *et al*. showed that miR-126 in the apoptotic bodies of serum-starved apoptotic vascular endothelial cells were taken up by the cultured endothelial cells, where it targeted regulator of G protein signaling 16 (*RGS16*) and thereby induced chemokine CXCL12 production (*186*). HDL-bound miRNAs were also shown to be delivered to cultured recipient cells and target mRNA expression (*182*).

5.3.3 Circulating ncRNAs as biomarkers and the challenges of studying circulating ncRNAs

Circulating ncRNAs have been implicated in different pathologies including cancer and cardiovascular disease (*48, 183, 187, 188*). Moreover, circulating miRNAs show extraordinary stability and resistance to degradation even under harsh conditions such as extreme pH, high temperature, long-term storage, multiple freeze-thaw cycles or the

presence of RNases (*49, 189-191*). This is likely due to their association with vesicles or proteins, which protect them from degradation. Isolated circulating miRNAs or synthetic miRNAs added exogenously were much more vulnerable to degradation by RNase activity. Although it is unknown whether circulating lncRNAs are bound to proteins, exosomal lncRNAs were also shown to be remarkably stable under similar harsh conditions (*187, 192, 193*). This characteristic makes circulating ncRNAs interesting potential biomarkers that can be utilized as diagnostic tools or to give insight into cell-cell communication between injured and healthy tissues, or between tumor and normal cells. Current findings on circulating ncRNAs in hypertension, CKD and vascular damage will be covered in Section 6 of this chapter.

Circulating biological fluids may be easy to collect, but profiling circulating ncRNAs to identify biomarkers remains challenging (*48, 188, 194, 195*). Current methods to profile circulating ncRNAs include qPCR array, microarray, nanostring nCounter and next-generation sequencing (NGS). Detailed description of these methods will be covered in Section 7.1 of this chapter. The first challenge of profiling circulating ncRNAs we are facing is the extraction of circulating ncRNAs. Since they are present in a cell-free form, they tend to have very low expression levels. It is difficult to isolate enough RNAs for profiling experiments using traditional RNA extraction kits. Scale-up approaches could be an option. Although the ideal recommended input sample volumes for most commercially available kits are relatively low due to the limiting capacity of their columns to filter out residual contaminant substances like DNA and proteins, Mitchell *et al*. has demonstrated a successful modified protocol with up-scaled sample volume and up-scaled acid-phenol chloroform to remove DNA and proteins (*189*). Recently, new commercial kits that allow high sample volume have been developed. Another option is to work directly with low RNA amount, and use pre-amplification before profiling. But potential bias introduced during pre-amplification due to additional PCR cycles is still a concern. The second challenge is sample contamination. Red blood cells are vulnerable to rupture. Hemolysis has been shown to alter circulating miRNA patterns in plasma (*196*). Sample collection must be taken carefully and isolation of plasma should ideally start with low-speed centrifugation (1000 X g) to separate red blood cells without causing rupture. In order to obtain cell-free platelet-free circulating ncRNAs, a high-speed

centrifugation (10,000 X g) must follow. Without a high-speed centrifugation, one may falsely believe that enough circulating ncRNAs has been extracted. However, the extracted ncRNAs are likely coming from platelets, as demonstrated by the fact that platelet-rich plasma shows much higher miRNA levels than platelet-poor plasma (*197*). Although these platelet-derived circulating ncRNAs may still serve as biomarkers for diagnosis, they do not function in cell-cell communication and therefore do not provide information on injured tissue- or tumor-released ncRNAs. The third challenge is normalization for ncRNA levels. In a high-throughput profiling study, ncRNA levels can be normalized by total read counts, based on the presumption that the total RNA levels are similar between individuals. But in the case of real-rime quantitative reverse transcription polymerase chain reaction (RT-qPCR) quantification for only a few ncRNAs, this approach is not applicable. The U6 small nuclear RNA is commonly used as a housekeeping RNA to normalize miRNAs levels. However, there are studies reporting that U6 is unsuitable for circulating miRNA normalization because its levels vary between control and diseased subjects (*198, 199*). Moreover, there are no ideal housekeeping circulating ncRNAs identified, and synthetic spike-in RNAs can only correct for technical variability but not serve as internal controls. The best normalization approach today perhaps is to normalize by the geometric mean of multiple literature-suggested housekeeping ncRNAs or the least variable ncRNAs from previous profiling studies (*200*).

6. ncRNAs and cardiovascular disease

Over the last decade, accumulating evidence has indicated a strong association between ncRNAs and cardiovascular disease, implying ncRNAs' crucial regulatory role in the underlying molecular mechanisms of cardiovascular pathophysiology (*201-203*).

As early as 2007, Zhao *et al*. demonstrated the necessity of normal miRNA biogenesis in heart development using a mouse model with *Dicer* deletion specifically in cardiac progenitors (*204*). The embryos of the *Dicer* knockout mice exhibited pericardial edema

and poorly ventricular myocardium development, which eventually led to cardiac failure and lethality by embryonic day 12.5 (E12.5). After that, emerging studies have shown the involvement of miRNAs in different cardiovascular diseases including cardiac hypertrophy and failure (*205, 206*), atrial fibrillation (*207, 208*), metabolic syndrome (*209, 210*), atherosclerosis (*211, 212*), hypertension (*213, 214*) and CKD (*215, 216*).

The first link between lncRNAs and cardiovascular disease can be traced back to 2006, when Ishii *et al*. used linkage disequilibrium mapping to identify SNPs in a myocardial infarction-associated locus that encodes a lncRNA, later named myocardial infarction associated transcript (*MIAT*) by the authors (*217*). One year later, 2 large collaborative genome-wide association studies conducted on over 1000 subjects by the Wellcome Trust Case Control Consortium (WTCCC) (*218*) and deCODE genetics (*219*), respectively, identified SNPs on susceptibility locus *INK4* of chromosome 9p21 that is associated with myocardial infarction and coronary artery disease. The *INK4* locus encodes a lncRNA called *ANRIL* that has also been linked to coronary artery disease, atherosclerosis and diabetes (*220-222*). The interaction between lncRNAs and miNRAs has also been shown to play a role in cardiovascular disease. For example, Wang *et al*. demonstrated that the lncRNA *CHRF*, which acted as a ceRNA, competed with myeloid differentiation primary response gene 88 (*Myd88*) for miR-489 binding in cardiomyocytes, thereby modulating cardiac hypertrophy (*128*).

This section will present current findings on the roles of miRNAs and lncRNAs in hypertension, CKD and vascular damage.

6.1 ncRNAs and hypertension

6.1.1 miRNAs and hypertension

As mentioned previously in Section 1.2.5, BP-associated common SNPs were identified in the 3' UTR microRNA binding sites of the RAAS-related genes (*40*). A few years later, more studies have found other SNPs on different miRNA-binding sites that are linked to essential hypertension risk. For example, the rare SNP rs12731181 (A>G) located in the

3’ UTR of prostaglandin F2α receptor (*FP*) had been shown to associate with higher BP in a Han Chinese population. The presence of this rare SNP reduced the binding strength between miR-590-3p and *FP*, thereby causing an up-regulation of *FP* and enhancing *FP*-mediated vascular contractility (*223*). Yang *et al*. found that the expression level of Activating transcription factor 1 (*ATF1*), which was higher in essential hypertension patients compared to normotensive subjects in another gene expression profiling study, was higher in people with SNP rs11169571 (T>C), which is a miR-1283 binding site located in the 3’ UTR of *ATF1* (*224*).

Abnormal miRNA expression levels were observed in essential hypertensive patients. Li *et al*. used microarrays to profile miRNA expression in the plasma of essential hypertensive patients. These authors identified 27 differentially expressed miRNAs and for the first time showed a link between essential hypertension and cytomegalovirus (HCMV) infection, since HCMV-encoded miRNA hcmv-miR-UL112 was among one of the most significantly up-regulated miRNAs and increased HCMV seropositivity was found in the hypertensive patients studied (*214*). However, it is noteworthy that the researchers in this study did not perform a high-speed centrifugation to remove platelets in the plasma. Thus, their circulating miRNA profile could likely come from platelets or debris of immune cells that have uptaken HCMV RNAs during the immune response against HCMV infection.

Tissue miRNAs have also been shown to associate with hypertension. Marques *et al*. in microarray profiling studies identified 11 and 13 differentially expressed miRNAs in the kidney medulla and cortex, respectively, of hypertensive subjects (*213*). They also selected candidate miRNAs to validate their differential expression by RT-qPCR, as well as the interaction between candidate miRNAs and hypertension-associated genes by luciferase reporter assays. They found that in the medulla, down-regulated let-7c targeted up-regulated *NR4A2*; and in the cortex, down-regulated miR-663 targeted up-regulated *REN* and *APOE*, and down-regulated miR-181a targeted up-regulated *REN* and *AIFM1*. The involvement of the miR-132/miR-212 cluster in hypertension has been reported by multiple studies in different tissues and cell types. Ang II-infused rats exhibited increased expression of miR-132/miR-212 in the heart, kidneys, aorta and plasma. Patients treated with Ang II receptor blockade had significantly lower miR-132 levels and a trend to

reduced miR-212 levels in internal mammary artery tissue (*225*). Ang II treatment caused up-regulation of miR-132 and miR-212 in the human embryonic cell line HEK293N (*226*) and in vascular SMCs (*227*). Jin *et al*. further demonstrated that miR-132, which was also up-regulated by Ang II in vascular SMCs, induced monocyte chemoattractant protein-1 (*MCP-1*) by targeting *PTEN* (*227*). Interestingly, *PTEN* has long been known as a tumor suppressor gene that is able to inhibit cell proliferation (*228*) and play a role in cardiac hypertrophy (*229, 230*). The above findings together may indicate the involvement of miR-132 in vascular SMC proliferation that contributes to vascular remodeling in hypertension.

6.1.2 lncRNAs and hypertension

Compared to miRNAs, the role of lncRNAs in hypertension is less studied. Gopalakrishnan *et al.* for the first time used NGS to identify hundreds of differentially expressed lncRNA in Dahl salt-sensitive compared to Dahl salt-resistant rats, as well as between Dahl salt-sensitive and spontaneously hypertensive rats (*231*). Combining the analyses of mRNA expression profiling in the same animals and the co-expression between nearby (cis) differentially expressed lncRNAs and mRNAs, they provided prioritized lncRNAs for future functional studies. Leung *et al.* used a similar approach to identify hundreds of differentially expressed lncRNAs and mRNAs in Ang II-transfected vascular SMCs as well as their cis co-expression (*232*). Moreover, they also found a cis co-expression relationship between the lncRNA *lnc-Ang362* and the miR-221/miR-222 cluster, both of which were up-regulated by Ang II transfection. siRNA knockdown of *lnc-Ang362* decreased miR-221/miR-222 expression levels and proliferation of vascular SMCs, indicating that *lnc-Ang362* may promote miR-221/miR-222 transcription by an unknown mechanism.

6.2 ncRNAs and CKD

6.2.1 miRNAs and CKD

miRNAs have been implicated in kidney development and injury, and in CKD. Chu *et al*. showed that *Dicer* knockout in the metanephric mesenchyme that develops into nephron progenitors resulted in remarkably abnormal renal development. The metanephrons underwent complete regression at E14.5 with no identifiable renal structures (*233*). Wei *et al*. on the other hand, demonstrated a protective effect against ischemia reperfusion-induced kidney injury by deleting *Dicer* in proximal tubular cells. Mice with this *Dicer* deletion also exhibited better renal function and improved survival (*234*). A global decrease of circulating miRNA levels in the plasma of CKD patients was observed by Neal *et al*., who also identified several circulating miRNAs that were correlated with eGFR levels (*235*). However, they did not perform high-speed centrifugation to remove platelets in the plasma, which suggests that the findings were likely a result of decrease of platelet miRNA levels in CKD. Recently, Ulbing *et al*. conducted a miRNA profiling study on the plasma of CKD patients to identify differentially expressed miRNAs and their predicted targets that may bring some insight into the pathophysiology of CKD (*215*). These authors showed that miR-223-3p and miR-93-5p, both of which were down-regulated in stage 4 and stage 5 CKD patients, were correlated with eGFR and interleukin-6 (*IL-6*) levels. Both miR-222-3p and miR-93-5p were predicted to target *IL-6*. Compared to the previous study, the plasma in this study underwent high-speed centrifugation to achieve platelet-free circulating miRNA profiling.

6.2.2 lncRNAs and CKD

Research on the roles of lncRNAs in CKD is still in its infancy. In an early GWAS in 2007, Hanson *et al*. identified a SNP in the lncRNA *PVT1* that was associated with end-stage renal disease. There is an ongoing study looking at circulating lncRNAs and their relationship with nearby mRNAs in CKD (*236*). This study may provide candidate CKD-associated lncRNAs for future functional studies.

6.3 ncRNAs and vascular damage

6.3.1 miRNAs and vascular damage

Normal miRNA biogenesis is also critical for vascular development and function. Albinsson *et al.* showed that SMC-specific *Dicer* deletion at exons 20 and 21 reduced vascular SMC proliferation and differentiation, which resulted in decreased vessel wall thickness, contractile dysfunction and hemorrhage, finally leading to embryonic lethality at E16 to E17 (*237*). Similar outcome was observed by Pan *et al*. one year later using SMC-specific *Dicer* deletion at exons 1 and 2, which resulted in reduced vascular SMC proliferation, dilated vessels, hemorrhage and embryonic lethality between E14.5 to E15.5 (*238*). Numerous studies have reported the involvement of miRNAs in vascular SMC proliferation and differentiation. One of the most frequently reported miRNAs may be the miR-145/miR-143 cluster. miR-145 and miR-143 are co-transcribed miRNAs that are highly expressed in vascular SMCs. They are responsible for decreased vascular SMC proliferation and enhanced differentiation by targeting transcription factors including Kruppel-like factor 4 (*Klf4*), which activates SMC proliferation genes and represses SMC differentiation genes, myocardin (*Myocd*), which is able to induce SMC gene expression in fibroblasts and promote fibroblast-to-SMC conversion, and *Elk-1*, which is a *Myocd* competitor (*239*). Knockout of miR-145/miR-143 displayed structural changes in the SMC layers of the vessels, impeded neointima formation in response to injury, compromised vascular contractility and significantly reduced BP (*240-242*). miR-663, which was down-regulated in Platelet-Derived Growth Factor (PDGF)-induced proliferating vascular SMCs, was also shown to regulate vascular SMC differentiation by targeting the transcription factor *JunB*, which in turn down-regulated a downstream *JunB* target myosin light chain 9 (*MYL9*) (*243*). miR-133 on the other hand, was found to reduce vascular SMC proliferation by targeting the transcription factor *Sp-1*, which regulates SMC gene expression (*145*). Expression levels of miR-125b, miR-145 and miR-155 were decreased in CKD rats. Overexpression of miR-155 inhibited vascular SMC proliferation by targeting Ang II type I receptor (*AT1R*) (*216*). miR-221 and miR-222 were found to promote vascular SMC calcification, which is characteristically found

in CKD, potentially by modulating cellular inorganic phosphate and pyrophosphate levels (*244*).

Compared to vascular SMCs, *Dicer* knockdown by siRNAs in endothelial cells resulted in reduced proliferation and cord formation of endothelial cells, as well as increased eNOS activation *in vitro* (*245*). Surprisingly, *in vivo* endothelial cell-specific *Dicer* but not *Drosha* silencing by siRNA exhibited reduced angiogenesis, whereas *in vitro Drosha* knockdown displayed only minor antiangiogenic effects compared to *Dicer* knockdown (*246*). miR-126 has been demonstrated to be an endothelial cell-specific miRNA that regulates endothelial cell growth in response to vascular endothelial growth factor (VEGF), and is responsible for the integrity of blood vessel formation and angiogenesis (*247, 248*). The miR-221/miR-222 cluster, which promotes vascular SMC calcification was also shown to inhibit endothelial tube formation and migration by targeting KIT Proto-Oncogene Receptor Tyrosine Kinase (*c-Kit*) (*249*), whereas miR-92a could repress endothelial cell proliferation and migration by targeting endothelial homeostasis regulators *KLF4* and Mitogen-Activated Protein kinase kinase 4 (*MKK4*) (*250*). Inhibition of miR-92a increased phosphorylation of ERK1/2 and JNK/SAPK in endothelial cells, and promoted endothelial cell proliferation. miR-132 was able to induce inflammation on endothelial cells by targeting silent information regulator 1 (*SIRT1*), which modulates endothelial pro-inflammatory processes (*251*).

The vascular SMC differentiation modulators miR-143 and miR-145 may play a role in cell-cell communication between vascular SMCs and endothelial cells. Hergenreider *et al*. reported that shear stress induced the release of miR-143/miR-145-containing microvesicles from vascular endothelial cells. These microvesicles were then uptaken by the co-cultured vascular SMCs, where miR-143 and miR-145 regulated target gene expression (*252*).

Beyond in hypertension and CKD, miRNAs have also been implicated in vascular damage in other types of cardiovascular diseases such as coronary artery disease (CAD) and pulmonary hypertension. Expression of miR-145, which plays a role in controlling SMC proliferation, was also reported to be decreased in atherosclerotic lesions with neointimal hyperplasia (*239*). Dentelli *et al*. showed that miR-222 is down-regulated by

inflammatory stimuli such as interleukin (IL)-3 or basic fibroblast growth factor (bFGF) treatment in human endothelial cells from advanced neovascularized atherosclerotic lesions. They demonstrated that miR-222 expression decreases gradually from early lesions to advanced plaques, and that miR-222 targets Signal Transducer And Activator Of Transcription 5A (*STAT5A*), which is a transcription factor involved in cell proliferation, differentiation and survival, suggesting that miR-222 could be a regulator for inflammation-induced new vessel formation and atherosclerotic plague progression (*253*). On the contrary, Minami *et al*. reported that miR-222 is up-regulated in endothelial progenitor cells from CAD patients compared to those from non-CAD subjects. A 12-month lipid lowering therapy with atorvastatin but not pravastatin decreased miR-222 levels. They also observed a positive correlation between low-density lipoprotein and miR-222 levels in atorvastatin-treated patients (*254*). Fang *et al*. showed that endothelial miR-10a and its targets Homeobox A1 (*HOXA1*) have lower and higher expression levels, respectively, in the atherosclerosis-susceptible aortic arch compared to the atherosclerosis-protected descending thoracic aorta (*255*). Expression of miR-155 was demonstrated by Nazari-Jahantigh *et al*. to by up-regulated in both atherosclerotic lesions and inflammatory macrophages of *ApoE* knockout mice, where miR-155 targets the NF-κB repressor Silencing of B-Cell CLL/Lymphoma 6 (*Bcl6*), leading to enhanced atherosclerotic plaque formation and activated expression of chemokine C-C Motif Chemokine Ligand 2 (CCl2) (*256*). miR-204 expression levels were decreased in pulmonary artery smooth muscle cells (PASMCs) from patients with pulmonary arterial hypertension (PAH) and from rodent PAH models, and were negatively correlated with PAH severity (*257*). The authors also demonstrated that inhibition of miR-204 promotes PASMC proliferation and triggers antiapoptotic effects via the Src–STAT3–NFAT pathway. *In vivo* miR-204 mimic delivery to the lungs by nebulization significantly reduced PAH severity. TGF-β-superfamily growth factor treatment by TGF-β or bone morphogenetic protein (BMP4) increased miR-21 and SMC markers smooth muscle α-actin (*SMA*) expression in PASMCs. These induced SMA marker expression, effect that was enhanced by miR-21 mimic transfection and blunted by miR-21 inhibitor transfection. miR-21 modulated PASMC phenotype by targeting the tumour suppressor gene Programmed Cell Death 4 (*PDCD4*) (*258*). Caruso *et al*. observed an up-regulation

of miR-451 in lung tissues from both chronic hypoxia- and monocrotaline-induced PAH rats, and demonstrated that both TGF-β and BMP4 treatment are able to induced miR-451 in PASMCs (*259*). Interestingly, and opposite to the findings in many other types of cardiovascular pathologies including essential hypertension and CAD, miR-145 was shown to be up-regulated in PASMCs from hypoxia-induced PAH mice and patients with the PAH-associated BMPR2 mutations, as well as in the lungs of PAH patients. Both miR-145 knockout and miR-145 knockdown by anti-miRNAs protected mice from developing PAH in response to hypoxia (*260*). Bertero *et al*. observed an up-regulation of miR-130a, miR-130b, miR-301a and miR-301b in both hypoxia-exposed PASMCs and pulmonary artery endothelial cells, as well as in both the intima and the media of small pulmonary vessels from severe PAH patients (*261*). The authors also demonstrated that the PAH-induced up-regulation of the miR-130/301 family is dependent on HIF-2α and POU5F1/OCT4, and that the miR-130/301 family promotes PAH by targeting PPARγ.

6.3.2 lncRNAs and vascular damage

Several recent studies have identified lncRNAs that regulate vascular SMC and endothelial cell phenotype. Wu *et al*. demonstrated that lincRNA-p21, whose expression levels decreased in patients with coronary heart disease, inhibited vascular SMC proliferation by competing with p53 to interact with an E3 ubiquitin-protein ligase mouse double minute 2 (MDM2), releasing MDM2's repressor effect on p53, which allows p53 to regulate its target gene expression and modulate SMC apoptosis. *In vivo* knockdown of lincRNA-p21 by siRNAs induced vascular SMC proliferation and caused neointima hyperplasia (*262*). Ballantyne *et al*. used NGS to identify a novel lncRNA, which they called smooth muscle-induced lncRNA enhances replication (*SMILR*), that regulates vascular SMC proliferation, possibly through cis-regulation on proximal genes including *HAS2* and *HAS2-AS1* (*263*). They found that *SMILR* expression was induced in both the nucleus and cytoplasm of vascular SMCs by the treatment with interleukin-1α and platelet-derived growth factor. siRNA knockdown of *SMILR* remarkably reduced vascular SMC proliferation. As mentioned already, Leung *et al.* identified an Ang II-

induced lncRNA *lnc-Ang362* that may activate miR-221/miR-222 expression and promote vascular SMC proliferation (*232*).

The lncRNA *ANRIL*, which has also been linked to coronary artery disease, atherosclerosis and diabetes (*220-222*), was recently reported to be induced by pro-inflammatory factors TNF-α in endothelial cells. *ANRIL* was shown to be an essential element for TNF-α to regulate downstream inflammatory genes such as *IL6* and *IL8* in endothelial cells, possibly due to its ability to interact with transcription factor YY1 and facilitate its binding to the promoters of *IL6* and *IL8* (*264*). Michalik *et al.* revealed a role of the lncRNA *MALAT1* on endothelial cell function and vessel growth by demonstrating that knockdown of *MALAT1* by siRNAs inhibited endothelial cell proliferation, and that *MALAT1* knockout mice exhibited reduced endothelial cell proliferation and neonatal retina vascularization (*265*).

6.4 ncRNAs involved in hypertension, CKD and vascular damage

Table I-1. List of ncRNAs involved in hypertension, CKD and vascular damage

ncRNAs	Involvement	Reference
miR-590-3p	Targets *FP* and mediates vascular contractility.	(*223*)
miR-1283	Targets *ATF1* in essential hypertension.	(*224*)
let-7c	Down-regulated in the medulla of hypertensive patients, where it targets *NR4A2*.	(*213*)
miR-663	Down-regulated in the cortex of hypertensive patients, where it targets *REN* and *APOE*.	(*213*)
miR-181a	Down-regulated in the cortex of hypertensive patients, where it targets *REN* and *AIFM1*.	(*213*)

Table I-1. Cont.

ncRNAs	Involvement	Reference
miR-132/miR-212	Induced by Ang II in the heart, kidneys, aorta, plasma and vascular SMCs, induces *MCP-1* by targeting *PTEN* in vascular SMCs. miR-132 is able to induce inflammation on endothelial cells by targeting *SIRT1*.	(*225*), (*227*), (*251*)
lnc-Ang362	up-regulated by Ang II transfection. siRNA knockdown of *lnc-Ang362* decreased miR-221/miR-222 expression levels and proliferation of vascular SMCs.	(*232*)
miR-223-3p and miR-93-5p	Down-regulated in stage 4 and stage 5 CKD patients, correlated with eGFR and *IL-6*, and target *IL-6*.	(*215*)
PVT1	SNP was associated with end-stage renal disease.	(*236*)
miR-145/miR-143	Responsible for decreased vascular SMC proliferation and enhanced differentiation by targeting *Klf4*, *Myocd* and *Elk-1*. Required for vascular contractility and BP maintenance. miR-145 is decreased in CKD rats. Involved in cell-cell communication between vascular SMCs and endothelial cells. Down-regulated in atherosclerosis. Up-regulated in PAH.	(*239*), (*240-242*), (*216*), (*252*), (*260*)
miR-663	Down-regulated in PDGF-induced proliferating vascular SMCs. Regulates vascular SMC differentiation by targeting *JunB*.	(*243*)
miR-133	Reduce vascular SMC proliferation by targeting *Sp-1*	(*145*)

Table I-1. Cont.

ncRNAs	Involvement	Reference
miR-221 and miR-222	Promote vascular SMC calcification. Inhibit endothelial tube formation and migration by targeting *c-Kit*. miR-222 expression is decreased in atherosclerotic lesions. miR-222 is up-regulated in endothelial progenitor cells from CAD patients.	(*244*), (*249*), (*253*), (*254*)
miR-92a	Repress endothelial cell proliferation and migration by targeting *KLF4* and*MKK4*.	(*250*)
miR-125b and miR-155	Down-regulated in CKD rats. Overexpression of miR-155 inhibited vascular SMC proliferation by targeting *AT1R*. miR-155 is up-regulated in atherosclerotic lesions and targets the NF-κB repressor *Bcl6*, leading to enhanced plaque formation	(*216*), (*256*)
miR-204	Decreased in PASMCs from PAH patients and PAH rodent models, and is negatively correlated with PAH severity.	(*257*)
miR-21	Induced by TGF-β or BMP4 in PASMCs and modulated PASMC phenotype.	(*258*)
miR-451	Up-regulation of in PAH lung tissues. Induced by TGF-β or BMP4 in PASMCs.	(*259*)
miR-130/miR-301 family	Up-regulation in both hypoxia-exposed PASMCs and pulmonary artery endothelial cells, as well as in both the intima and the media of small pulmonary vessels from severe PAH patients. Promotes PAH by targeting PPARγ.	(*261*)

Table I-1. Cont.

ncRNAs	Involvement	Reference
lincRNA-p21	Down-regulated in coronary heart disease. Inhibited vascular SMC proliferation by competing with p53 to bind MDM2.	(*262*)
SMILR	Regulates vascular SMC proliferation, possibly through cis-regulation on *HAS2* and *HAS2-AS1*.	(*263*)
ANRIL	SNP associated with CAD, atherosclerosis and diabetes. Induced by TNF-α in endothelial cells. Interact with YY1 and facilitate its binding to the promoters of *IL6* and *IL8*.	(*220-222*), (*264*)
MALAT1	Promotes endothelial cell proliferation and neonatal retina vascularization.	(*265*)

7. ncRNAs as biomarkers or therapeutic targets in the clinic

7.1 ncRNA profiling

As mentioned in Section 5.3.3, current methods to profile ncRNAs include qPCR array, microarray, nanostring nCounter, and NGS.

Traditional RT-qPCR is not useful as a profiling approach due to its low throughput. However, once a candidate biomarker has been identified, RT-qPCR would be the best option since it is easy, fast and cheap to quantify ncRNAs. Compared to traditional qPCR, qPCR array is a derivative medium-throughput qPCR platform that has been recently developed. It allows simultaneous quantification of hundreds of genes that are pre-designed or custom-designed. This means it is not adequate for genome-wide profiling studies. However, if a pool of candidate genes has been previously selected based on

literature review or previous studies, qPCR array would be an ideal approach since it is relatively cheap and the results are easy to analyze. Microarray on the other hand allows us to simultaneously quantify expression of tens of thousands of genes whose probes were pre-coated on the microarray chips, where the cDNAs hybridize to the probes and give fluorescent signals. Although it has a higher output, it is less sensitive compared to Taqman qPCR arrays, and signal intensity of low-expressed genes can be heavily affected by background noise such as non-specific hybridization (*266*). The Nanostring nCounter platform allows direct counting of mRNA without reverse transcription or amplification (*267*). This method provides a sensitivity level better than microarray and similar to Taqman qPCR, and at the same time minimizes bias caused by enzymatic reactions. However, like qPCR array, Nanostring nCounter is a medium-throughput system that allows simultaneous quantification of up to 800 genes. These approaches limit studies only to known ncRNAs. There are still many unidentified ncNRAs, especially those who are located in intergenic or intronic regions. The emergence of NGS gives us the possibility to study all RNA species including the unannotated ones, since NGS uses degenerate primers to hybridize different combinations of base sequences. This allows us to detect even the previously unannotated RNA species, then map them to the genome, analyze their potential secondary structure, and accordingly categorize them into different ncRNA species. NGS also provides supreme sensitivity and specificity, even for low-expressed transcripts. In order to identify novel ncRNAs and ncRNAs with very low expression levels, deep sequencing is usually required. Different NGS platforms have different minimal requirement for discovery mode (usually ~10-20 million qualified mapped reads per sample) to identify novel RNA species. Coming along with all these advantages is a high financial cost. Although the price of NGS is getting lower and lower with improved technologies, it is still considerably more expensive than other profiling platforms, especially when deep sequencing is needed. Another challenge of NGS is the difficulty in data handling and analysis. The process of sequencing data analysis generates large amounts of raw and intermediate files that demand enough space (usually at the Terabyte level) for data processing and storage. Data analysis usually involves a series of bioinformatic tools, most of which require at least minimal bioinformatics and programming knowledge to work with, and many of which demand a computationally

powerful workstation to run. The necessity of bioinformatics training and high computational requirements also significantly increase the cost of NGS.

There are a variety of bioinformatic pipelines available to analyze gene expression sequencing data. The two most popular pipelines will be described here (Figure I-9). Before starting the pipelines, it is important to make sure that a good sequencing quality is achieved. One of the most popular tools for sequence quality control is FastQC (https://www.bioinformatics.babraham.ac.uk/projects/fastqc/), which visualizes the base quality from the sequencing data. Base quality (Q) is defined as $Q=-10 \times \log_{10}(P_E)$, where P_E means the probability of error. A minimal Q of 20, *i.e.* 1% error rate, is usually considered as good sequence quality, and Q>30, *i.e.* <0.1% error rate, is considered as ideal. One of the pipelines mostly used is the Tuxedo pipeline that uses a combination of bioinformatic tools named Bowtie, Tophat, Cufflinks and Cuffdiff. Bowtie 1 (*268*) and Bowtie 2 (*269*) are alignment tools that map sequences to the genome. Bowtie 1 was designed to work with shorter sequences (up to 50 bp), while Bowtie 2 works better for long sequences. However, both Bowtie 1 and 2 for designed for genomic DNA sequence alignment since they do not take intron splicing into consideration. For RNA sequence alignment, Tophat, which uses the Bowtie 1 algorithm for alignment (*270, 271*) or Tophat 2, which can use either the Bowtie 1 or Bowtie 2 algorithm (*272*), is generally used. In addition to the Bowtie 1 or Bowtie 2 alignment algorithm, Tophat and Tophat 2 also analyze splice junctions, which allows us to identify isoforms of transcripts that have resulted from alternative splicing. Cufflinks is then used to annotate, assemble and count the mapped sequence reads, followed by differential expression analysis by Cuffdiff (*273*). The other one of the most popular pipelines uses STAR for sequence alignment. It has been reported to be more precise and 50X faster than Tophat 2 (*274*). HTSeq-count is then used for annotation, assembly and counting of the mapped reads (*275*), followed by differential expression analysis by an R package EdgeR (*276*). The biggest advantage of EdgeR over Cuffdiff is that EdgeR allows multi-group comparisons whereas Cuffdiff allows only two-group comparisons. However, EdgeR is less user friendly, and requires intermediate R programming level. For miRNA sequencing specifically, miRdeep2 (*277*) is one of the mostly used tools. miRdeep2 can align RNA sequences by either Bowtie or STAR, then annotate, assemble and count mature miRNAs reads based on the miRBase

mature miRNA sequences. It is also able to analyze the potential stem-loop structures formed by the RNA sequences and their up- or down-stream genomic sequences, which allows the prediction of novel miRNAs that are previously unannotated in the miRBase. Differential expression analysis for miRDeep2 results can be done by EdgeR. In the case of circRNA profiling, as mentioned previously in Section 5.2.2, circRNAs are generated from back-splicing events, so their sequences may be mapped to regular mRNA or lncRNA regions. STAR and CIRI (*278*) can analyze non-canonical splicing events between nearby junctions using the unmapped sequences, enabling them to identify and quantify circRNAs.

After identifying ncRNAs of interest, the next step is to analyze the interactions between different RNA species. There are numerous tools available for miRNA target prediction, each with their own advantages. TargetScan (*126, 279*) takes into account the conservation among species and scores the miRNA targeting based on miRNA binding site features including seed match, 3' compensatory paring and site position. RNAhybrid (*280*) uses minimum free energy to score the miRNA-target pairing and allows the identification of non-seed binding. New approaches like miRANDA-mirSVR (*281*) and SVMicrO (*282*) use machine learning to build a miRNA target predictor that was trained on a large training dataset of previous miRNA experiments. They also take into account features like seed matching, minimum free energy and conservation. However, all these tools tend to predict too many targets, leading to a high false positive rate. In order to improve the results, one can use multiple tools for prediction and take the common targets as the ones with high confidence. Another way to improve prediction is to perform total RNA profiling, or total RNA profiling after miRNA mimic/inhibitor treatment, then compare the total RNA and miRNA profiles to analyze and validate the miRNA-target relationship. Predicting lncRNA-target pairs is more complicated since lncRNAs tend to fold into high order structures and proteins may be involved in target binding. Current methods to analyze lncRNAs targeting generally only look at the linear base pairing. A pull-down experiment such as Chip-Seq can be used to confirm the interaction between lncRNAs and their targets.

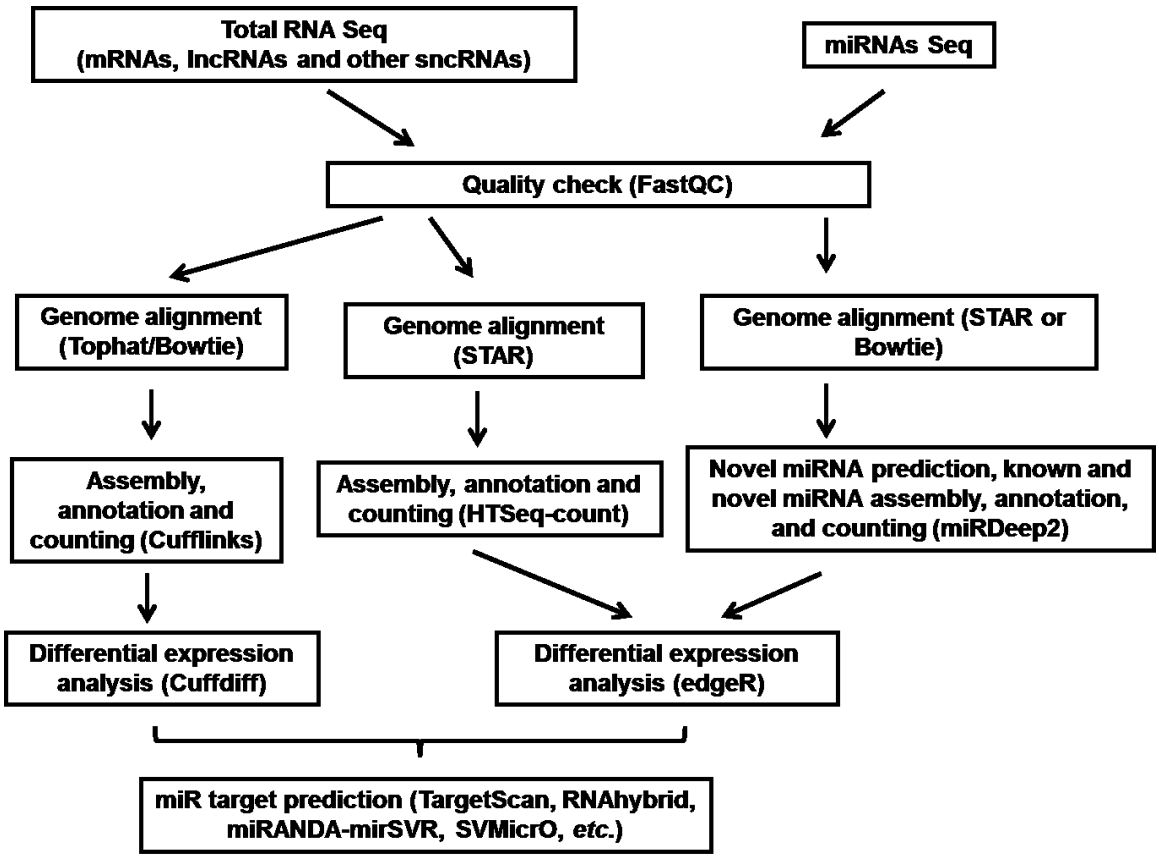

Figure I-9. Bioinformatic pipelines for ncRNA profiling.

7.2 ncRNAs as biomarkers

Many studies have shown the value of circulating ncRNAs as biomarkers for diagnosis or prognosis in the clinic. Two meta-analysis-based studies revealed the potential of circulating miR-21 as a diagnostic or prognostic biomarker for various cancers. The finding of Wu *et al.* suggests that circulating miR-21 may be used to predict early-stage cancers (*283*), whereas Wang *et al.* found that circulating miR-21 is not suitable for cancer diagnosis, but has a value to predict survival (*284*). Circulating miR-1 and miR-133a were reported to be up-regulated in patients with myocardial infarction (MI), and miR-133a was also associated with post-MI death, making it possible to serve as a prognostic biomarker for MI (*285, 286*). Kumarswamy *et al.* used microarray RNA profiling to identify a mitochondrial lncRNA, which they referred to as *LIPCAR*, that was

down-regulated in the plasma during an early stage of MI and can be used as a predictor for post-MI mortality (*287*).

However, in many cases of complex diseases such as cancer and cardiovascular disease, one candidate ncRNA usually does not yield enough power for early disease detection or prognosis prediction. The combination of multiple ncRNAs using a modeling approach has been reported to perform better. Lin *et al*. first used qPCR array to identify candidate circulating miRNAs that were differentially expressed in patients with hepatocellular carcinoma. Different combinations of these candidate miRNAs were put together in a logistic regression model to build a predictor for early hepatocellular carcinoma detection using a training cohort. By evaluating the prediction performance in independent validation cohorts, they found the best predictor using a combination of 7 miRNAs in the modeling (miR-29a, miR-29c, miR-133a, miR-143, miR-145, miR-192, and miR-505). Their predictor exhibited higher prediction accuracy than the conventional method using a cutoff α-fetoprotein of 20 ng/mL (AFP20) (*288*). Similarly, Kuo *et al*. used NGS to identify differentially expressed miRNAs in white blood cells from patients with Kawasaki disease, followed by a machine learning approach to build a predictor for Kawasaki disease diagnosis using 10 candidate miRNAs. Their predictor demonstrated robustness and reliability with a prediction sensitivity of 84.20% and a specificity of 81.8% (*289*).

Aside from the current findings that suggest the value of circulating ncRNAs as biomarkers, there is concern about the reproducibility of the results. Witwer in a review showed poor overlap in differentially expressed circulating miRNAs among different studies, and some miRNAs had too low fold change to be validated (*290*). Building a prediction model also has limitations. It generally requires a large dataset for data training and validation. This significantly increases the financial burden for the profiling studies to identify candidate ncNRAs. Compared to the conventional statistical comparisons between 2 groups (*T*-test) or multiple groups (analysis of variance, or ANOVA), the modeling approach also requires more statistical knowledge and in many cases some programming skills, as many modeling algorithms need to be optimized to obtain the best performance.

7.3 ncRNAs as therapeutic targets

There are so far 2 clinical trials utilizing miRNAs as targets to develop novel treatments. The very first miRNA-targeting drug to enter clinical trials is a locked nucleic acid (LNA)-based miR-122 inhibitor called Miravirsen that was used to treat hepatitis C virus (HCV) infection. A pre-clinical study was done on non-human primates to show improved HCV-induced liver pathology without evidence of viral resistance or side effects (*291*). The later phase IIa clinical trial on HCV patients showed a prolonged dose-dependent reduction in HCV RNA levels, also without evidence of viral resistance or side effects (*135*). The second one was developed by Mirna therapeutics, Inc. using gain-of-function liposomal miR-34a mimics (MRX34) to treat patients with advanced solid tumors. The Phase I study showed evidence of antitumor activity in a subset of patients (*143*). However, as mentioned previously in Section 5.1.3, *in vivo* mRNA mimic treatments tend to induce stronger immune-toxicity due to their bypass of the endogenous miRNA biogenesis and targeting machinery. In fact, after observing multiple immune-related severe adverse events, Mirna therapeutics, Inc. decided to stop the ongoing Phase I clinical trial and announced that they would not initiate an additional translational study of MRX34 that they had planned earlier (https://finance.yahoo.com/news/mirna-therapeutics-halts-phase-1-200500073.html). Inhibition of miR-33a and miR-33b has reached the pre-clinical stage, showing a successful increase in plasma high-density lipoprotein cholesterol and decrease of very-low-density lipoprotein cholesterol in non-human primates (*292*).

Using ncRNAs as therapeutic target in translation is in its infancy and still facing many challenges. The halting of the MRX34 clinical trial is a good example showing us the technical difficulties and safety concerns around developing novel ncRNA-targeting therapies. More studies still need to be done on the optimization of the drug design to improve targeting efficacy and delivery, and to overcome safety issues.

8. Experimental design, hypothesis and objectives

8.1 Experimental design

This thesis is part of our miRNA profiling project that includes multiple studies using different rodent medels of hypertension in combination with clinical studies on hypertensive patients with and without CKD. The goal of this project is directed toward identifying conserved miRNAs that play a key regulatory role on various components of the pathophysiolology of vascular damage associated with hypertension and CKD.

Various experimental models have been used to mimic human diseases in research to study the underlying pathophysiology and molecular mechanisms. The first hypertensive model we used in our miRNA profiling project is Ang II-infused C57BL/6 mice. We aimed to use this model to identify miRNA regulators in vascular damage associated with RAAS activation. The C57BL/6 mouse is one of the most popular animal models, largely due to its high genetic similarity with humans, easy breeding, robustness, etc. Moreover, the reference mouse genome assemblies in the UCSC and the NCBI databases also come from the C57BL/6 strain, although NCBI provides other mouse strain genome assemblies as well (https://genome.ucsc.edu/FAQ/FAQreleases#release3). This makes C57BL/6 the preferred mouse strain for genomic and genetic studies. As cited above in multiple sections of this chapter, many studies have demonstrated that Ang II is able to induce differential gene expression, BP elevation, vascular remodeling and stiffening, endothelial dysfunction and increased ROS production *in vivo*, as well as differential gene expression, increased growth factor production and cell proliferation of different cell types *in vitro*. The Ang II-infused mouse model is therefore frequently used to understand the pathophysiology and molecular mechanisms of human hypertension and the associated vascular damage that has been linked to RAAS activation. Ang II is generally administrated by injection to look at its acute effects or by infusion at a constant rate using mini-osmotic pumps to look at its chronic effects.

In the first study (Chapter II) of this thesis, the 7-day and 14-day Ang II-infused mouse models are used to look at effect of Ang II-induced vascular damage and gene expression

changes at different time points compared to the 7-day and 14-day sham groups. miRNA and total RNA expression profiling were performed using NGS in small resistance mesenteric arteries to identify differentially expressed miRNAs, mRNAs and lncRNAs. The combination of the RNA profiles was used to refine the prediction of miRNA targets in the mRNAs and lncRNAs whose expression levels changed in the opposite direction. From the differentially expressed genes, transcription factors were identified and transcription factor targets were also predicted. The interactions between different RNA species were integrated into molecular networks together with gene enrichment analyses. This allowed us to study the molecular mechanisms of Ang II-induced vascular damage and hypertension. It will provide insights allowing identification of potential key regulators that may be used as therapeutic targets in future clinical applications.

In the second study (Chapter III), normotensive, hypertensive (systolic BP > 135 mm Hg or diastolic BP of 85-115 mm Hg with BpTRU) and CKD subjects (eGFR < 60 mL/min/m^2) were recruited to evaluate vascular damage noninvasively in large arteries and gene expression changes in the small resistance arteries from subcutaneous gluteal biopsies. miRNA and total RNA expression profiling were done using NGS and data were analyzed as in the Ang II-infused mouse study above. The human and mouse results were then compared to find common differentially expressed genes.

In the third study (Chapter IV), cell-free platelet-free plasma was isolated from whole blood of the same cohort of human subjects as in the second study. Small RNA expression profiling was done using NGS to identify differentially expressed circulating miRNAs. Correlations between circulating miRNA expression levels and clinical parameters were performed to prioritize for candidate biomarker selection. Correlations between circulating miRNA levels and gene expression levels from the small resistance artery RNA profiles were performed to study potential cell-cell communication that involves vascular cells.

8.2 Hypothesis and objectives

There have been 69 drugs in 15 classes approved in the United States for hypertension treatments, many of which are used in combination. Yet a significant population (50%) of hypertensive patients have uncontrolled BP, many of them on ≥3 drugs of different classes (*293*). Current treatments for CKD primarily target the RAAS as in hypertension treatments (*294*). There is currently no cure for hypertension or CKD, but there is growing demand for better treatment.

Given that vascular damage is associated with hypertension and CKD, and is one of the earliest manifestation and a cause of target-organ damage, in the first and second studies we hypothesized that the RNA profiles in small resistance arteries differ in Ang II-infused mice and hypertensive patients with or without CKD compared to the control mice and normotensive subjects, respectively. By conducting these two studies, we aimed to identify conserved hypertension- and CKD-associated genes involved in RAAS activation to provide advanced knowledge on the pathological molecular networks of vascular damage in hypertension and CKD. The ultimate goal is to identify ncRNAs that play key regulatory roles in those pathological molecular networks and harness them in novel therapies to target vascular damage in hypertension and CKD.

In the third study, we hypothesized that the circulating ncRNA profiles differ in hypertensive patients with or without CKD compared to normotensive subjects. The first goal of this study was to gain further insight into the circulating ncRNA-related cell-cell communication that involves vascular cells by comparing the results from the second and third manuscripts. The second goal was to identify potential biomarkers for CKD diagnosis and/or prognosis, and for vascular damage in hypertension and CKD.

8.3 Methodology

8.3.1 RNA extraction

The dissected mouse mesenteric arteries (first study) or human small arteries (second study) were homogenized in 1 mL of mirVana miRNA lysis/binding buffer in a 5 mL tube for 1 min at maximum speed with a Polytron PT 1600 E homogenizer and processed for total RNA extraction using the mirVana miRNA isolation kit, followed by genomic DNA removal with the TURBO DNA-free kit according to the manufacturer's protocol. Circulating miRNAs were isolated from 6 ml of cell-free, platelet-free plasma (third study) with the QIAamp Circulating Nucleic Acid kit using the miRNA extraction protocol. Total RNA and small RNA quality were assessed with an Agilent 2100 bioanalyzer.

8.3.2 Library construction and RNA sequencing

Total RNA and small RNA libraries were constructed using the TruSeq stranded total RNA sample preparation kit and the TruSeq small RNA sample preparation kit, respecteiely. Total RNA was sequenced in a 2 x 101 bp pair-end high-output mode in the first study and in a 2 x 76 bp pair-end high-output mode in the second study. In all three studies, small RNA was sequenced in a 1 x 51 bp single-end rapid mode.

8.3.3 Bioinformatic pipeline

Sequence base-calling, adapter trimming, sample separation and bcl-to-fastq format conversion were done in Bcl2fastq, followed by sequence alignment STAR. HTSeq-count was used for total RNA gene assembly, annotation and counting. miRDeep2 was used for novel miRNA prediction, known and novel miRNA annotation and counting. Differential expression analysis was done in R (https://www.r-project.org) using the EdgeR package. Hierarchical clustering analyses in the first study were performed with the differentially expressed miRNAs and total RNAs and visculized in heat maps using R. TargetScan was used to predict targets of differentially expressed miRNAs in the inversely related differentially expressed mRNAs. TF binding site prediction in the promoters of differentially expressed genes was performed using the FIMO tool of Meme

Suite. Molecular network construction was conducted in Cytoscape. Gene enrichment analysis was performed using the ClueGO tool in Cytoscape.

8.3.4 Measurement of miRNA and mRNA expression by RT-qPCR

In the first study, for miRNAs quantification, reverse transcription was done using the TaqMan® MicroRNA Reverse Transcription Kit and qPCR was performed using the TaqMan Small RNA Assays. miRNA expression was normalized by U6 small nuclear RNA (snRNA). For mRNA quantification, reverse transcription was done using the Quantitect RT kit and qPCR was performed using SsoFast EvaGreen Supermix. mRNA expression was normalized by ribosomal protein S16 (*Rps16*) mRNA levels. In the third study, reversed transcription was done using the Qiagen miScript II RT Kit and qPCR was performed using the miScript Primer Assay with miScript SYBR Green PCR. The geometric mean of the 3 least variable miRNAs with at least 50 reads per million total mapped reads from the sequencing date was used for normalization.

8.3.5 Validating miRNA-mRNA pairs

Human aortic SMCs were transfected with miRNA mimics or inhibitors for 24 hours. RNA was extracted and used to measure miRNA and mRNA expression by RT-qPCR. Luciferase assays were conducted as follows. The oligonucleotides containing wild-type or mutated miRNA binding sites were annealed and sub-cloned into the multiple cloning site of the pmirGLO dual-luciferase miRNA target expression vector. Human aortic SMCs were co-transfected with mirVana miRNA mimics or inhibitors and the above vectors using Lipofectamine 3000 for 48 hours. Luciferase assays were performed using the Dual-Luciferase reporter assay system.

CHAPTER II: Vascular ncRNA profiling in Ang II-induced vascular damage and hypertension

miR-431-5p inhibition protects against angiotensin II-induced hypertension and vascular injury

Ku-Geng Huo[1], Julio C. Fraulob-Aquino[1], Tlili Barhoumi[1], Chantal Richer[3], Suellen C. Coelho[1], Sofiane Ouerd[1], Mathieu Lajoie[3], Daniel Sinnett[3,4], Pierre Paradis[1], Ernesto L. Schiffrin[1,2*]

[1]Vascular and Hypertension Research Unit, Lady Davis Institute for Medical Research, [2]Department of Medicine, Sir Mortimer B. Davis-Jewish General Hospital, McGill University; [3]Division of Hematology-Oncology, Research Center, CHU Ste-Justine, [4]Department of Pediatrics, Faculty of Medicine, Université de Montréal, Montréal, Canada.

Corresponding author:

Ernesto L. Schiffrin, MD, PhD, FRSC, FRCPC, FAHA

Sir Mortimer B. Davis-Jewish General Hospital, #B-127,

3755 Côte-Ste-Catherine Rd.,

Montreal, Quebec, Canada H3T 1E2

Fax: 514-340-7539

Phone: 514-340-7538

E-mail: ernesto.schiffrin@mcgill.ca

http://ladydavis.ca/en/ernestoschiffrin

Abstract

Background: Vascular injury is an early manifestation and a cause of end-organ damage in hypertension. microRNAs play an important role in cardiovascular disease, but their implication in vascular injury remains poorly studied. We aimed to use RNA sequencing and systems biology to identify key regulators that mediate gene expression changes in the course of vascular injury in angiotensin (Ang) II-induced hypertension.

Methods: Ten-week old male C57BL/6 mice were infused or not with Ang II for 7 or 14 days. Blood pressure (BP) was measured by telemetry, and mesenteric artery (MA) function and mechanical properties by pressurized myography. Total RNA was extracted from MAs for expression profiling by RNA sequencing to identify differentially expressed (DE) microRNAs and mRNAs. Gene ontology enrichment analyses were performed on DE mRNAs. The targets of DE microRNAs were predicted from the inversely related DE mRNAs. DE transcription factors were identified from DE mRNAs and their targets predicted from all the DE microRNAs and mRNAs.

Results: We identified DE microRNAs and mRNAs in both 7- and 14-day Ang II-infused mice. We found that 17 out of 23 up-regulated microRNAs in the 14-day Ang II group are located in a conserved microRNA cluster of the delta-like homolog 1-type III iodothyronine deiodinase (*Dlk1-Dio3*) region, 9 of which have expression levels that correlated with BP. Among those 9, we showed *in vitro* in human aortic vascular smooth muscle cells that miR-431-5p directly targets an Ang II-down-regulated BP-correlated transcription factor Ets homologous factor (EHF), leading to up-regulation of 2 EHF targets, collagen type I alpha 1 chain (*Col1a1*) and another *Dlk1-Dio3* microRNA miR-382-5p, both of which were up-regulated by Ang II. IV injection of miR-431-5p inhibitors decreased miR-431-5p, miR-382-5p, *Col1a1* and increased *Ehf* in MAs. *In vivo* miR-431-5p inhibition delayed Ang II-induced BP elevation, and reduced endothelial dysfunction, vascular stiffening and oxidative stress.

Conclusions: miR-431-5p and its target *Ehf* act as key regulators in the pathophysiology of vascular damage in hypertension. miR-431-5p inhibition has potential to serve as a novel target for therapy of vascular disease associated with hypertension.

Introduction

microRNAs (miRNAs) are a class of small non-coding RNA (ncRNA) about 22 nt long that play an important posttranscriptional gene regulatory role in developmental, physiological and pathophysiological processes in various organs including the cardiovascular system (1, 2). miRNAs regulate gene expression by binding to the 3' untranslated region (UTR) of their target mRNAs to induce mRNA degradation and translation repression. It has been shown that mammalian miRNAs predominantly act by decreasing target mRNA levels (3, 4). One miRNA can target multiple mRNAs (5), suggesting a master regulator potential of miRNAs in gene-gene interaction networks in various pathological conditions and a promising future as potential therapeutic targets.

Hypertension is a major cause of cardiovascular disease and the number one risk factor for global disease burden and death worldwide (6). Vascular injury, as a key pathological feature in hypertension, is accompanied by dysregulation in gene expression associated with vascular remodeling and dysfunction, which result in elevated peripheral resistance and finally lead to target-organ damage (7). Small artery remodeling in particular, may be the earliest manifestation of target-organ damage in mild essential hypertension (8, 9). Angiotensin (Ang) II is a major component of the renin-angiotensin-aldosterone system that participates in the development of hypertension (10). Ang II causes blood pressure (BP) elevation though vasoconstriction and its renal actions as well as by causing small artery injury that is characterized by endothelial dysfunction, vascular remodeling, oxidative stress and inflammation (7).

Differential miRNA expression profiles have been observed in essential hypertension and other cardiovascular diseases (11, 12). miRNAs have been shown to play an important role in BP regulation and vascular function (13), as well as in regulation of extracellular matrix genes and vascular smooth muscle cell (VSMC) proliferation that characterize vascular damage in hypertension (11). Ang II has been demonstrated in vitro to alter miRNA expression in human embryonic kidney cells, rat cardiac fibroblasts (14) and rat VSMCs (15). However, the role of miRNAs in vascular injury in hypertension remains poorly studied. We hypothesized that vascular miRNAs are dysregulated in Ang II-

infused mice, and that the dysregulation of vascular miRNAs is a key driving force of pathophysiological gene expression changes that contribute to vascular injury.

In the present study, we used next-generation sequencing (NGS) to identify differentially expressed (DE) vascular miRNAs and mRNAs in Ang II-infused mice, and then predicted targets of DE miRNAs from the inversely related DE mRNAs. We aimed to identify key miRNA-mRNA pairs that mediate Ang II-induced vascular injury. A large number of miRNAs in a conserved miRNA cluster located in the delta-like homolog 1-type III iodothyronine deiodinase (*Dlk1-Dio3*) region were found to be up-regulated by Ang II. Using an unbiased systems biology approach, we identified miR-431-5p and its target, ETS homologous factor (*Ehf*) as key regulators in a molecular network associated with Ang II-induced vascular injury. We showed by in vitro gain- and loss-of-function experiments that miR-431-5p directly targets *Ehf*, therefore leading to up-regulation of 2 downstream EHF targets, collagen type I alpha 1 chain (*Col1a1*) and another *Dlk1-Dio3* miRNA miR-382-5p. IV injection of miR-431-5p inhibitors decreased miR-431-5p levels in mesenteric arteries (MAs), resulting in increased expression of *Ehf* as well as decreased expression of *Col1a1* and miR-382-5p. In vivo miR-431-5p inhibition delayed Ang II-induced BP elevation, and protected against endothelial dysfunction, vascular stiffening and oxidative stress.

Methods

A detailed Methods section is provided in the Online Data Supplement.

Experimental design

The study was approved by the Animal Care Committee of the Lady Davis Institute for Medical Research and McGill University, and followed recommendations of the Canadian Council of Animal Care.

A group of 10 to 12-week-old male C57BL/6J WT (Harlan laboratories, Indianapolis, IN) mice (n = 10) infused or not SC with Ang II (1000 ng/kg/min) for 7 or 14 days with ALZET osmotic mini pumps (Model 1002, Durect Corporation, Cupertino,

CA) were used to determine changes of miRNA and mRNA expression in MAs by RNA sequencing. A systems biology approach was used to identify key miRNA regulators that mediate gene expression changes in the course of vascular injury. BP was determined by telemetry in a subset of the above mice (n = 6 for Ang II-infused and n=5 for sham) from two days before to the end of the 14-day treatment period as previously described (16).

A second group of 10 to 12-week-old male C57BL/6J WT mice (n = 7) infused or not with Ang II for 7 or 14 days were used to assess MA function and mechanical properties by pressurized myography as previously described (17).

Mouse VSMCs isolated from mesenteric arteries, endothelial cells (ECs) and fibroblasts from the lungs of a group of 10 to 12-week-old male C57BL/6J WT mice (n = 12), as well as human aorta smooth muscle cells (HASMCs) and ECs (HAECs) (ScienCell, Carlsbad, CA) were used to determine which vascular cell types express the candidate key miRNA regulator miR-431 by reverse transcription-quantitative PCR (RT-qPCR).

In order to determine whether human miR-431-5p targets EHF, the expression of *EHF* was measured by RT-qPCR in HASMCs transfected with miR-431-5p mimics or inhibitors.

A luciferase miRNA target expression vector assay (Promega, Madison, WI) was used to confirm whether miR-431-5p targets *EHF* in a canonical miRNA targeting machinery in HASMCs transfected with miR-431-5p mimics or inhibitors.

In order to determine whether *EHF* targets *COL1A1* and miR-382-5p, the expression of *COL1A1* and miR-382-5p was determined by RT-qPCR in HASMCs transfected with si*EHF*.

The effect of *in vivo* miR-431-5p inhibition on Ang II-induced BP elevation and vascular injury were tested using another group of 10 to 12-week-old male C57BL/6J WT mice (n=7) infused with Ang II (1000 ng/kg/min) for 14 days and injected IV via the tail vein with 20 mg/kg of locked nucleic acid (LNA) scrambled inhibitors or miR-431-5p inhibitors (Exiqon, Vedbaek, Denmark) on day 1 and day 7 of the treatment period. BP was determined as above in a subset of these mice (n=6). At the end of the study, MA

miRNA and mRNA expression was measured in by RT-qPCR. MA function and mechanical properties were determined as above in a fourth group of 10 to 12-week-old male C57BL/6J WT mice (n=7) infused with Ang II and injected IV with LNA scrambled inhitibors or miR-431-5p inhibitors as above.

Data analysis

Results are presented as means ± SEM. Comparisons in BP and concentration-response curve data were carried out using two-way analysis of variance (ANOVA) for repeated measures. Other comparisons between more than 2 groups were done using two-way ANOVA as indicated. All ANOVA tests were followed by a Student–Newman–Keuls *post-hoc* test. Comparisons between 2 groups were done using unpaired or paired Student *t*-test as indicated. Correlation between DE miRNA or DE mRNA and systolic or diastolic BP was obtained using a Pearson correlation conducted in R. ANOVA and *t*-tests were performed in SigmaPlot version 13 (Systat Software, San Jose, CA). $P<0.05$ was considered statistically significant. Differential expression analysis was performed using an ANOVA-like test in EdgeR based on generalized linear models. Differential expression was defined with a threshold of 1.5-fold change and false discovery rate (FDR) <0.05.

Results

Ang II infusion induced blood pressure elevation, endothelial dysfunction, vascular remodeling, stiffening and oxidative stress

A mouse model of Ang II infusion for 7 or 14 days was used to study vascular injury, hypertension and associated gene changes. Ang II infusion reached a plateau BP elevation of ~40 mmHg at day 5 compared to sham groups (Fig. II-1A), and remained elevated to a similar degree at 7 and 14 days of Ang II infusion. MA contractile responses to norepinephrine (NE) showed no difference between groups (Supplemental Fig. II-S1A). The 14-day Ang II group exhibited a 35% impairment of endothelium-dependent relaxation to acetylcholine (Ach) compared to the 14-day sham group, whereas the 7-day

Ang II group showed a 20% impairment that did not reach statistical significance (Fig. II-1B). Ach-induced vasodilatation was completely abrogated in the presence of the nitric oxide (NO) synthase inhibitor N^{ω}-nitro-L-arginine methyl ester (L-NAME) in all groups (Supplemental Fig. II-S1B). There was no difference between groups in endothelium-independent relaxation to the NO donor sodium nitroprusside (SNP) (Supplemental Fig. II-S1C). Eutrophic remodeling was observed only in the 14-day Ang II-infused mouse MAs, as indicated by a 32% increase in media/lumen ratio (M:L) (Fig. II-1C) without change in media cross-sectional area (MCSA) (Supplemental Fig. II-S1D). MA stiffening was observed in both 7- and 14-day Ang II groups, as shown by a leftward shift of the stress-strain curve and a 25% decrease in strain at 140 mmHg (Fig. II-1D). Both 7-day and 14-day Ang II infusion increased reactive oxidative species (ROS) production by ~2-fold in the MA wall and MA perivascular adipose tissue (PVAT) (Fig. II-1E&F)

Expression profiles of vascular miRNA, mRNA and other ncRNAs in MAs of Ang II-infused mice

To identify DE vascular miRNAs and mRNAs in early and late stages of Ang II-induced hypertension, we used NGS to profile miRNA and mRNAs from MAs from 7-day and 14-day Ang II-infused mice. The RNA samples showed excellent quality, as indicated by average RIN between 8.34 and 8.57 (Supplemental Table II-S4).

In small RNA sequencing, all the samples had base quality >25 at every position, indicating excellent sequencing quality. An average of 18.1±0.4 million qualified single-end reads were obtained from the small RNA sequences, 73.8±0.8% of which were mapped to single locus and 13.9±0.4% were mapped to multiple loci. Differential expression analysis identified 1 down-regulated miRNA in the 7-day Ang II group, while 23 up-regulated and 12 down-regulated miRNAs were found in the 14-day Ang II group (Supplemental Table II-S5). The DE miRNAs separate the 14-day but not the 7-day Ang II group in a hierarchical clustering analysis (Fig. II-2A).

In total RNA sequencing, all the samples had base quality >25 at every position, indicating excellent sequencing quality. An average of 35.6±0.7 million qualified paired-end reads were obtained from the total RNA sequences, 72.4±1.1% of which were

mapped to single locus and 16.5±0.6% were mapped to multiple loci. One sample in the 14-day Ang II group was excluded because of low mapping % (19.4% to single locus and 2.7% to multiple loci). Differential expression analysis identified 33 up-regulated mRNAs and 11 down-regulated mRNAs uniquely associated with the 7-day Ang II group, 440 up-regulated mRNAs and 250 down-regulated mRNAs uniquely associated with the 14-day Ang II group, while 109 up-regulated mRNAs and 6 down-regulated mRNAs in both groups (gene list not shown in this thesis). The DE mRNAs separated both the 7-day and 14-day Ang II groups from the Sham groups in a hierarchical clustering analysis (Fig. II-2B). Gene ontology (GO) term enrichment analysis showed that the 7-day DE genes were enriched for GO terms involved in extracellular matrix (ECM) and cell proliferation (Supplemental Table II-S8), whereas the 14-day DE genes were enriched for ECM, developmental processes, cell motility, growth factor signaling, inflammation, cell proliferation, protein transport, peptidase activity and apoptosis (Supplemental Table II-S10). In KEGG and REACTOME enrichment analysis, the 7-day DE genes were enriched for PI3K-Akt signaling pathway, whereas the 14-day DE genes were enriched for PI3K-Akt, PDGF, IGF1R, ERBB2, FGFR, Rap1, p53, DAP12 and EGFR signaling pathways (Supplemental Table II-S12).

The miRNA and total RNA sequencing data have been deposited in the Gene Expression Omnibus (GEO) database, www.ncbi.nlm.nih.gov/geo (accession no. GSE101711).

Next, we tried to identify targets of the DE miRNAs. To refine miRNA target prediction in this study, in addition to searching for miRNA binding sites in the 3' UTRs, we combined deep sequencing of miRNAs and mRNAs, then predicted miRNA targets only in the inversely related genes. This approach allowed us to focus on the miRNA-mRNA pairs that were both changed by Ang II infusion but in opposite directions. It is noteworthy that when we used all genes for miRNA target prediction without filtering by the mRNA sequencing data, an average of ~3800 targets per miRNA were predicted, as opposed to ~45 in this study (Supplemental Table II-S5). In GO term enrichment, the 7-day DE miRNAs-targeting DE genes were enriched for ECM and cell proliferation (Supplemental Table II-S9), whereas the 14-day DE miRNA-targeting DE genes were enriched for ECM, developmental processes, cell motility, growth factor signaling, cell

proliferation, protein transport and responses to wounding (Supplemental Table II-S11). In KEGG and REACTOME enrichment, the 14-day DE miRNA-targeting DE genes were enriched for PI3K-Akt, PDGF and ERBB2 signaling pathways (Supplemental Table II-S12). We also identified transcription factors (TFs) from the DE mRNAs and predicted their targets from all the DE miRNAs and mRNAs. A main molecular network that integrates the 14-day DE genes involved in the top 2 enriched GO term groups, namely ECM and developmental processes, as well as the interactions between 14-day DE miRNAs, DE TFs and their DE gene targets are presented in Fig. II-2C.

miRNAs in the *Dlk1-Dio3* region were up-regulated in MAs of 14-day Ang II-infused mice

The goal of this study was to identify key regulators that play a pivotal role on the Ang II-induced DE genes. Interestingly, 17 out of 23 14-day up-regulated miRNAs were located in a miRNA cluster of the conserved *Dlk1-Dio3* region on chromosome 12qF1, which corresponds to chromosome 14q32 in humans (18) (Supplemental Fig. II-S2). Correlations were found between systolic and diastolic BP and the expression levels of 9 out of 17 *Dlk1-Dio3* miRNAs (Table II-1).

Dysregulation of miRNAs in the *DLK1-DIO3* region (14q32) has been shown to be involved in cell proliferation and migration in multiple pathologies (18, 19), and reported to be associated with atherosclerosis (20) in humans. Genome-wide association studies (GWASs) showed risk single nucleotide polymorphisms (SNPs) in the *DLK1-DIO3* region associated with coronary artery disease (21) and type 1 diabetes (22). A linkage study with >6000 individuals revealed linkage evidence for hypertension, systolic BP and diastolic BP at 14q32 (23). Given the literature background on the *DLK1-DIO3* region and its potential link to hypertension, we focused on the 9 BP-correlated *Dlk1-Dio3* miRNAs for key regulator identification. Using a candidate approach, we selected miR-431-5p as a potential key regulator for further function studies for the following reasons: 1, FDR for differential expression was ranked 1st among all the DE miRNAs; 2, the number of predicted DE targets was ranked 1st among the 9 BP-correlated miRNAs; 3, its sequence is 100% conserved in human.

Next, we looked at the downstream targets of miR-431-5p and identified a TF EHF that was down-regulated by the 14-day Ang II infusion. It is noteworthy that the expression levels of *Ehf* were also inversely correlated with both systolic and diastolic BP (Table II-1), and the miR-431-5p binding site on the *Ehf* 3' UTR is highly conserved between human and mouse (Fig. II-3A). Moreover, EHF was predicted to regulate expression of 7 of the 9 BP-correlated miRNAs including miR-431-5p, as well as genes involved in ECM, developmental processes, growth factor signaling, responses to wounding, ossification, peptidase activity, cell proliferation and protein transport (Supplemental Table II-S13). It has been previously shown in prostate cancer that EHF negatively regulates *Col1a1* (24), which was up-regulated by Ang II in MAs in our study. Based on the aforementioned reasons, we selected miR-431-5p, *Ehf* and *Col1a1* for further gain- and loss-of-function experiments.

miR-431-5p targets *Ehf*, which in terms up-regulates *Col1a1*, miR-431-5p and miR-382-5p

Since MAs are composed of ECs, VSMCs and fibroblasts, it is important to determine where miR-431-5p is expressed. RT-qPCR showed that miR-431-5p was expressed at a much higher level in VSMCs compared to endothelial cells and fibroblasts in mouse MAs (Supplemental Fig. II-S3A). In human cells, miR-431-5p was expressed in VSMCs but not in endothelial cells (Supplemental Fig. II-S3B).

Considering that both the miR-431-5p sequence and the miR-431-5p binding site on the *Ehf* 3' UTR are conserved between human and mouse, we used human VSMCs for further functional experiments. Transfection of miR-431-5p mimics decreased *EHF* levels on human VSMCs (Fig. II-3B), while transfection of miR-431-5p inhibitors increased *EHF* levels (Fig. II-3C). To demonstrate if miR-431-5p directly targets *EHF* in a canonical miRNA targeting mechanism, we constructed luciferase reporter vectors that contain the conserved wild-type or mutated miR-431-5p binding site on the human *EHF* 3' UTR (Fig. II-3D) downstream of the luciferase coding region, namely WT-pmirGLO-*EHF* and mut-pmirGLO-*EHF*, respectively. Co-transfection of miR-431-5p mimics with WT-pmirGLO-*EHF* but not mut-pmirGLO-*EHF* caused a 50% decrease in luciferase

expression levels, while co-transfections of scrambled mimics with WT-pmirGLO-*EHF* and mut-pmirGLO-*EHF* showed no difference (Fig. II-3E).

Ehf was predicted to down-regulate ECM genes *Col1a1*, Biglycan (*Bgn*), fibronectin 1 (*Fn1*), connective tissue growth factor (*Ctgf*) that were up-regulated by 14-day Ang II infusion, as well as 7 out of 9 BP-correlated miRNAs. We used siRNAs to knockdown *EHF* (Fig. II-4A) in human VSMCs and showed up-regulation of *COL1A1* (Fig. II-4B), miR-431-5p (Fig. II-4C) and another BP-correlated miRNA miR-382-5p (Fig. II-4D), whose FDR of differential expression was ranked 2nd (just after miR-431-5p) and is also 100% conserved between human and mouse. However, expression levels of *BGN* (Supplemental Fig. II-S4A), *FN1* (Supplemental Fig. II-S4B) and *CTGF* (Supplemental Fig. II-S4C) did not change upon siEHF transfection. Given that miR-431-5p mimic and inhibitor transfections directly regulated *EHF* expression, we hypothesized that *COL1A1* and miR-382-5p would be indirectly regulated as well. As expected, miR-431-5p mimic transfection up-regulated *COL1A1* (Fig. II-4E) and miR-382-5p (Fig. II-4F). However, miR-431-5p inhibitor transfection down-regulated *COL1A1* (Fig. II-4G) but not miR-382-5p (Fig. II-4H).

In vivo injection of miR-431-5p inhibitors protected against Ang II-induced hypertension and vascular damage

Given the *in vitro* result, we proposed that in vivo inhibition of miR-431-5p could also increase *Ehf* levels and decrease *Col1a1* and miR-382-5p levels. We injected miR-431-5p inhibitors intravenously in mice at day 0 and day 7 of a 14-day Ang II infusion, and then looked at gene expression and vascular function and mechanics in MAs at day 14 after sacrifice. Intravenous injection of miR-431-5p inhibitors remarkably decreased miR-431-5p levels in MAs, compared to the control (Fig. II-5A). In agreement with the *in vitro* loss-of-function results, miR-431-5p inhibition in MAs led to increases in *Ehf* (Fig. II-5B) and decreases in *Col1a1* (Fig. II-5C) and miR-382-5p (Fig. II-5D) without changes in *Bgn* (Supplemental Fig. II-5A), *Fn1* (Supplemental Fig. II-5B) or *Ctgf* (Supplemental Fig. II-5C).

Mice injected with miR-431-5p inhibitors showed no difference in heart, kidney, spleen or liver weights compared to the control group (Supplemental Table II-S14). miR-431-5p inhibition in MAs resulted in delayed increase of systolic BP by Ang II infusion (Fig. II-6A), a 30% improvement in endothelium-dependent relaxation to Ach (Fig. II-6B) and reduced MA stiffness, as shown by a rightward shift of the stress-strain curve and a 15% increase in strain at 140 mmHg (Fig. II-6D). There were no differences between groups in MA contractile responses to NE (Supplemental Fig. II-6A), endothelium-dependent relaxation to Ach in the presence of L-NAME (Supplemental Fig. II-6B), endothelium-independent relaxation to SNP (Supplemental Fig. II-6C), M:L (Fig. II-6C) or MCSA (Supplemental Fig. II-6D). miR-431-5p inhibition also caused a decrease in ROS production of 65% in MA wall and of 50% in MA PVAT (Fig. II-6E&F).

Discussion

The present study demonstrated for the first time that a 14-day Ang II infusion up-regulated expression of a large number of *Dlk1-Dio3* miRNAs in MAs. A BP-correlated *Dlk1-Dio3* miRNA, miR-431-5p, directly targets *Ehf* in VSMCs and led to up-regulation of *Col1a1* and another *Dlk1-Dio3* miRNA, miR-382-5p. *In vivo* miR-431-5p inhibition in MAs of 14-day Ang II-infused mice up-regulated *Ehf*, down-regulated *Col1a1* and miR-382-5p, delayed Ang II-induced BP elevation and protected against vascular damage and oxidative stress.

Although both 7-day and 14-day Ang II infusion led to similar degree of BP elevation, there were significant differences in terms of gene expression changes in MAs. While the 7-day Ang II infusion caused down-regulation of only 1 miRNA and differential expression of genes involved in ECM and cell division, the 14-day Ang II infusion resulted in changes of a larger number of miRNAs that included 17 Dlk1-Dio3 miRNAs and >5 times more genes that are involved not only in ECM and cell proliferation, but also in developmental processes, cell motility, growth factor signaling, inflammation, etc. In the 14-day groups, the total DE genes and DE miRNA-targeting DE genes showed similar GO enrichment, suggesting that the DE miRNAs could be key regulators of the DE genes involved in the enriched molecular and physiological

processes. The difference between the 7-day and 14-day Ang II-induced DE genes may partially explain the vascular function and mechanics results, in which the 7-day Ang II-infused mice exhibited only MA stiffness, whereas the 14-day Ang II-infused mice showed endothelial dysfunction, eutrophic remodeling and stiffening of MAs.

The majority (17 out of 23) of 14-day Ang II-induced up-regulated miRNAs belong to the conserved *Dlk1-Dio3* region. Expression levels of more than half (9 out of 17) of up-regulated *Dlk1-Dio3* miRNAs were correlated with both systolic and diastolic BP. For these reasons and previous publications (18, 19, 23) that suggest a potential link between the *Dlk1-Dio3* miRNAs and hypertension, we focused on the BP-correlated *Dlk1-Dio3* miRNAs to identify key regulators. In order to find key genes that are associated with hypertension, we also performed correlation analysis between mRNA expression and BP. This approach finally led to the identification of the miR-431-5p-*Ehf* pair, whose expression levels were correlated with BP. Previous studies have showed that miR-431-5p is able to promote skeletal muscle differentiation, regeneration and dystrophy (25, 26). However, it is unclear whether it is able to affect smooth muscle phenotype. This study demonstrated for the first time that miR-431-5p contributes to ECM biogenesis in smooth muscle cells by targeting the transcription factor *Ehf*, which has been previously shown to negatively regulate *Col1a1* and reduce cell proliferation in human prostate cancer cells (24). In the *in vivo* study it was expected by our hypothesis that miR-431-5p inhibition in MAs would up-regulate *Col1a1* by targeting *Ehf*, thereby leading to reduced vascular stiffening. It was a fortuitous finding that it also decreased oxidative stress and improved endothelial function. The molecular mechanism by which miR-431-5p inhibition decreases ROS product remains to be elucidated by future experiments.

This is the first study to adopt a systems biology approach combining whole-genome coding and non-coding RNA expression profiling, bioinformatic analysis and wet-lab validation to identify key regulators in vascular injury. Taken together, our results suggest that miR-431-5p and its target *Ehf* act as key regulators in the pathophysiology of vascular injury in hypertension. miR-431-5p inhibition has potential to serve as a novel target for therapy in vascular disease associated with hypertension.

Acknowledgements

We are grateful to Adriana Cristina Ene, Guillem Colell Dinarès, Isabelle Miguel and Véronique Michaud for excellent technical support and Virginie Sailour for excellent bioinformatics support.

Disclosures

None.

Reference

1. He L, Hannon GJ. MicroRNAs: small RNAs with a big role in gene regulation. Nature reviews Genetics. 2004;5:522-531.

2. Sayed D, Abdellatif M. MicroRNAs in development and disease. Physiological reviews. 2011;91:827-887.

3. Guo H, Ingolia NT, Weissman JS, Bartel DP. Mammalian microRNAs predominantly act to decrease target mRNA levels. Nature. 2010;466:835-840.

4. Hu W, Coller J. What comes first: translational repression or mRNA degradation? The deepening mystery of microRNA function. Cell research. 2012;22:1322-1324.

5. Sun W, Julie Li YS, Huang HD, Shyy JY, Chien S. microRNA: a master regulator of cellular processes for bioengineering systems. Annual review of biomedical engineering. 2010;12:1-27.

6. Lim SS, Vos T, Flaxman AD, Danaei G, Shibuya K, Adair-Rohani H, Amann M, Anderson HR, Andrews KG, Aryee M, Atkinson C, Bacchus LJ, Bahalim AN, Balakrishnan K, Balmes J, Barker-Collo S, Baxter A, Bell ML, Blore JD, Blyth F, Bonner C, Borges G, Bourne R, Boussinesq M, Brauer M, Brooks P, Bruce NG, Brunekreef B, Bryan-Hancock C, Bucello C, Buchbinder R, Bull F, Burnett RT, Byers TE, Calabria B, Carapetis J, Carnahan E, Chafe Z, Charlson F, Chen H, Chen JS, Cheng AT, Child JC, Cohen A, Colson KE, Cowie BC, Darby S, Darling S, Davis A, Degenhardt L, Dentener F, Des Jarlais DC, Devries K, Dherani M, Ding EL, Dorsey ER, Driscoll T, Edmond K, Ali SE, Engell RE, Erwin PJ, Fahimi S, Falder G, Farzadfar F, Ferrari A, Finucane MM, Flaxman S, Fowkes FG, Freedman G, Freeman MK, Gakidou E, Ghosh S, Giovannucci E, Gmel G, Graham K, Grainger R, Grant B, Gunnell D, Gutierrez HR, Hall W, Hoek HW, Hogan A, Hosgood HD, 3rd, Hoy D, Hu H, Hubbell BJ, Hutchings SJ, Ibeanusi SE, Jacklyn GL, Jasrasaria R, Jonas JB, Kan H, Kanis JA, Kassebaum N, Kawakami N, Khang YH, Khatibzadeh S, Khoo JP, Kok C, Laden F, Lalloo R, Lan Q, Lathlean T, Leasher JL, Leigh J, Li Y, Lin JK, Lipshultz SE, London S, Lozano R, Lu Y, Mak J, Malekzadeh R, Mallinger L, Marcenes W, March L, Marks R, Martin R, McGale P, McGrath J, Mehta S, Mensah GA, Merriman TR, Micha R,

Michaud C, Mishra V, Mohd Hanafiah K, Mokdad AA, Morawska L, Mozaffarian D, Murphy T, Naghavi M, Neal B, Nelson PK, Nolla JM, Norman R, Olives C, Omer SB, Orchard J, Osborne R, Ostro B, Page A, Pandey KD, Parry CD, Passmore E, Patra J, Pearce N, Pelizzari PM, Petzold M, Phillips MR, Pope D, Pope CA, 3rd, Powles J, Rao M, Razavi H, Rehfuess EA, Rehm JT, Ritz B, Rivara FP, Roberts T, Robinson C, Rodriguez-Portales JA, Romieu I, Room R, Rosenfeld LC, Roy A, Rushton L, Salomon JA, Sampson U, Sanchez-Riera L, Sanman E, Sapkota A, Seedat S, Shi P, Shield K, Shivakoti R, Singh GM, Sleet DA, Smith E, Smith KR, Stapelberg NJ, Steenland K, Stockl H, Stovner LJ, Straif K, Straney L, Thurston GD, Tran JH, Van Dingenen R, van Donkelaar A, Veerman JL, Vijayakumar L, Weintraub R, Weissman MM, White RA, Whiteford H, Wiersma ST, Wilkinson JD, Williams HC, Williams W, Wilson N, Woolf AD, Yip P, Zielinski JM, Lopez AD, Murray CJ, Ezzati M, AlMazroa MA, Memish ZA. A comparative risk assessment of burden of disease and injury attributable to 67 risk factors and risk factor clusters in 21 regions, 1990-2010: a systematic analysis for the Global Burden of Disease Study 2010. Lancet (London, England). 2012;380:2224-2260.

7. Schiffrin EL. Vascular remodeling in hypertension: mechanisms and treatment. Hypertension (Dallas, Tex : 1979). 2012;59:367-374.

8. Park JB, Schiffrin EL. Small artery remodeling is the most prevalent (earliest?) form of target organ damage in mild essential hypertension. Journal of hypertension. 2001;19:921-930.

9. Rizzoni D, Porteri E, Boari GE, De Ciuceis C, Sleiman I, Muiesan ML, Castellano M, Miclini M, Agabiti-Rosei E. Prognostic significance of small-artery structure in hypertension. Circulation. 2003;108:2230-2235.

10. Paradis P, Schiffrin EL. Renin-angiotensin-aldosterone system and pathobiology of hypertension. In: DeMello WC, Frohlich ED, eds. Renin Angiotensin System and Cardiovascular Disease. New York, N.Y.: Humana Press; 2009:35-58.

11. Shi L, Liao J, Liu B, Zeng F, Zhang L. Mechanisms and therapeutic potential of microRNAs in hypertension. Drug discovery today. 2015;20:1188-1204.

12. Romaine SP, Tomaszewski M, Condorelli G, Samani NJ. MicroRNAs in cardiovascular disease: an introduction for clinicians. Heart (British Cardiac Society). 2015;101:921-928.

13. Albinsson S, Skoura A, Yu J, DiLorenzo A, Fernandez-Hernando C, Offermanns S, Miano JM, Sessa WC. Smooth muscle miRNAs are critical for post-natal regulation of blood pressure and vascular function. PLoS One. 2011;6:e18869.

14. Jeppesen PL, Christensen GL, Schneider M, Nossent AY, Jensen HB, Andersen DC, Eskildsen T, Gammeltoft S, Hansen JL, Sheikh SP. Angiotensin II type 1 receptor signalling regulates microRNA differentially in cardiac fibroblasts and myocytes. British journal of pharmacology. 2011;164:394-404.

15. Jin W, Reddy MA, Chen Z, Putta S, Lanting L, Kato M, Park JT, Chandra M, Wang C, Tangirala RK, Natarajan R. Small RNA sequencing reveals microRNAs that modulate angiotensin II effects in vascular smooth muscle cells. The Journal of biological chemistry. 2012;287:15672-15683.

16. Barhoumi T, Kasal DA, Li MW, Shbat L, Laurant P, Neves MF, Paradis P, Schiffrin EL. T regulatory lymphocytes prevent angiotensin II-induced hypertension and vascular injury. Hypertension (Dallas, Tex : 1979). 2011;57:469-476.

17. Barhoumi T, Fraulob-Aquino JC, Mian MOR, Ouerd S, Idris-Khodja N, Huo K-G, Rehman A, Caillon A, Dancose-Giambattisto B, Ebrahimian T, Lehoux S, Paradis P, Schiffrin EL. Matrix metalloproteinase-2 knockout prevents angiotensin II-induced vascular injury. Cardiovascular Research. 2017

18. Benetatos L, Hatzimichael E, Londin E, Vartholomatos G, Loher P, Rigoutsos I, Briasoulis E. The microRNAs within the DLK1-DIO3 genomic region: involvement in disease pathogenesis. Cellular and molecular life sciences : CMLS. 2013;70:795-814.

19. Nadal E, Zhong J, Lin J, Reddy RM, Ramnath N, Orringer MB, Chang AC, Beer DG, Chen G. A MicroRNA cluster at 14q32 drives aggressive lung adenocarcinoma. Clinical cancer research : an official journal of the American Association for Cancer Research. 2014;20:3107-3117.

20. Aavik E, Lumivuori H, Leppanen O, Wirth T, Hakkinen SK, Brasen JH, Beschorner U, Zeller T, Braspenning M, van Criekinge W, Makinen K, Yla-Herttuala S. Global DNA methylation analysis of human atherosclerotic plaques reveals extensive genomic hypomethylation and reactivation at imprinted locus 14q32 involving induction of a miRNA cluster. European heart journal. 2015;36:993-1000.

21. Schunkert H, Konig IR, Kathiresan S, Reilly MP, Assimes TL, Holm H, Preuss M, Stewart AF, Barbalic M, Gieger C, Absher D, Aherrahrou Z, Allayee H, Altshuler D, Anand SS, Andersen K, Anderson JL, Ardissino D, Ball SG, Balmforth AJ, Barnes TA, Becker DM, Becker LC, Berger K, Bis JC, Boekholdt SM, Boerwinkle E, Braund PS, Brown MJ, Burnett MS, Buysschaert I, Carlquist JF, Chen L, Cichon S, Codd V, Davies RW, Dedoussis G, Dehghan A, Demissie S, Devaney JM, Diemert P, Do R, Doering A, Eifert S, Mokhtari NE, Ellis SG, Elosua R, Engert JC, Epstein SE, de Faire U, Fischer M, Folsom AR, Freyer J, Gigante B, Girelli D, Gretarsdottir S, Gudnason V, Gulcher JR, Halperin E, Hammond N, Hazen SL, Hofman A, Horne BD, Illig T, Iribarren C, Jones GT, Jukema JW, Kaiser MA, Kaplan LM, Kastelein JJ, Khaw KT, Knowles JW, Kolovou G, Kong A, Laaksonen R, Lambrechts D, Leander K, Lettre G, Li M, Lieb W, Loley C, Lotery AJ, Mannucci PM, Maouche S, Martinelli N, McKeown PP, Meisinger C, Meitinger T, Melander O, Merlini PA, Mooser V, Morgan T, Muhleisen TW, Muhlestein JB, Munzel T, Musunuru K, Nahrstaedt J, Nelson CP, Nothen MM, Olivieri O, Patel RS, Patterson CC, Peters A, Peyvandi F, Qu L, Quyyumi AA, Rader DJ, Rallidis LS, Rice C, Rosendaal FR, Rubin D, Salomaa V, Sampietro ML, Sandhu MS, Schadt E, Schafer A, Schillert A, Schreiber S, Schrezenmeir J, Schwartz SM, Siscovick DS, Sivananthan M, Sivapalaratnam S, Smith A, Smith TB, Snoep JD, Soranzo N, Spertus JA, Stark K, Stirrups K, Stoll M, Tang WH, Tennstedt S, Thorgeirsson G, Thorleifsson G, Tomaszewski M, Uitterlinden AG, van Rij AM, Voight BF, Wareham NJ, Wells GA, Wichmann HE, Wild PS, Willenborg C, Witteman JC, Wright BJ, Ye S, Zeller T, Ziegler A, Cambien F, Goodall AH, Cupples LA, Quertermous T, Marz W, Hengstenberg C, Blankenberg S, Ouwehand WH, Hall AS, Deloukas P, Thompson JR, Stefansson K, Roberts R, Thorsteinsdottir U, O'Donnell CJ, McPherson R, Erdmann J, Samani NJ. Large-scale association analysis identifies 13 new susceptibility loci for coronary artery disease. Nature genetics. 2011;43:333-338.

22. Wallace C, Smyth DJ, Maisuria-Armer M, Walker NM, Todd JA, Clayton DG. The imprinted DLK1-MEG3 gene region on chromosome 14q32.2 alters susceptibility to type 1 diabetes. Nature genetics. 2010;42:68-71.

23. Wu X, Kan D, Province M, Quertermous T, Rao DC, Chang C, Mosley TH, Curb D, Boerwinkle E, Cooper RS. An updated meta-analysis of genome scans for hypertension and blood pressure in the NHLBI Family Blood Pressure Program (FBPP). American journal of hypertension. 2006;19:122-127.

24. Albino D, Longoni N, Curti L, Mello-Grand M, Pinton S, Civenni G, Thalmann G, D'Ambrosio G, Sarti M, Sessa F, Chiorino G, Catapano CV, Carbone GM. ESE3/EHF controls epithelial cell differentiation and its loss leads to prostate tumors with mesenchymal and stem-like features. Cancer research. 2012;72:2889-2900.

25. Lee KP, Shin YJ, Panda AC, Abdelmohsen K, Kim JY, Lee SM, Bahn YJ, Choi JY, Kwon ES, Baek SJ, Kim SY, Gorospe M, Kwon KS. miR-431 promotes differentiation and regeneration of old skeletal muscle by targeting Smad4. Genes & development. 2015;29:1605-1617.

26. Wu R, Li H, Zhai L, Zou X, Meng J, Zhong R, Li C, Wang H, Zhang Y, Zhu D. MicroRNA-431 accelerates muscle regeneration and ameliorates muscular dystrophy by targeting Pax7 in mice. Nature communications. 2015;6:7713.

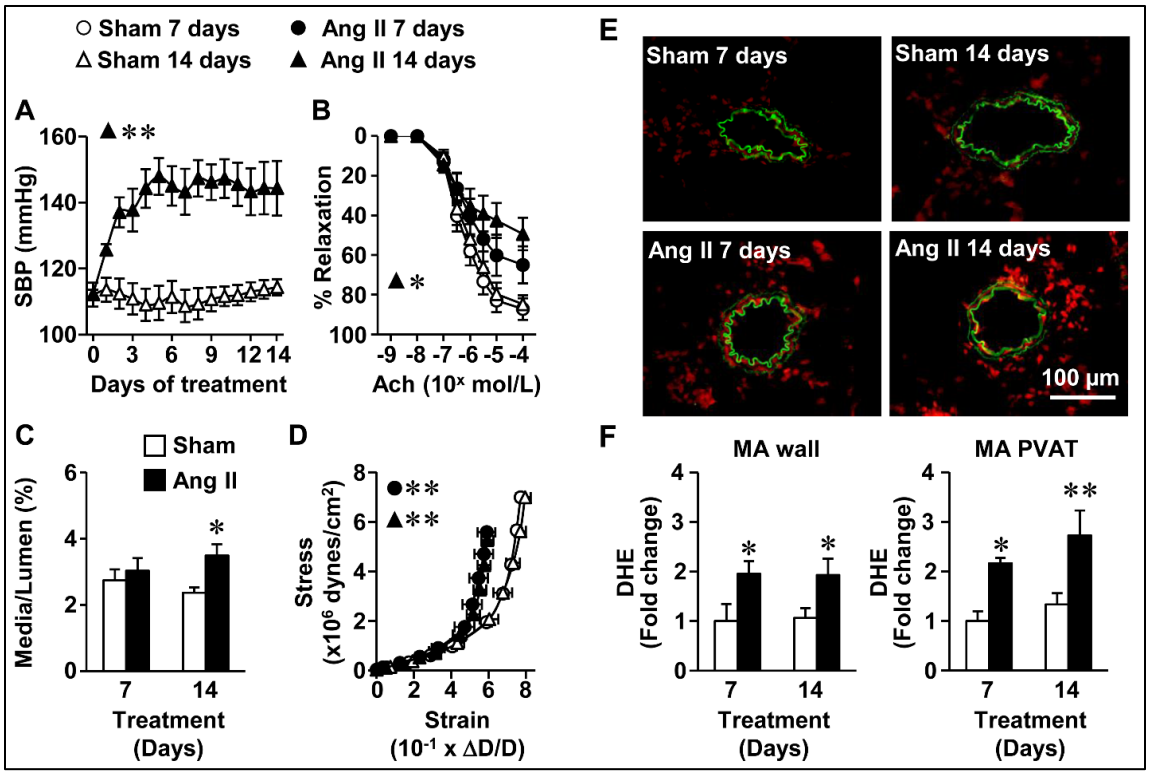

Figure II-1. Angiotensin (Ang) II infusion induced blood pressure elevation, endothelial dysfunction, vascular remodeling, stiffening and oxidative stress. Mean 24-hour systolic blood pressure (SBP, **A**) was measured by telemetry in mice infused with Ang II (1000 ng/kg/min) or not (sham) for 14 days. Vasodilatory responses to acetylcholine (Ach, **B**), media/lumen (**C**), vascular stiffness (**D**) of small mesenteric arteries using pressurized myography and reactive oxygen species generation by dihydroethidium (DHE) staining (**E** and **F**) in mesenteric artery media, adventitia and perivascular adipose tissue (PVAT) were determined in mice infused or not with Ang II for 7 or 14 days. Representative images of DHE staining are shown in **E**. Red and green fluorescence represent DHE fluorescence and elastin autofluorescence, respectively. Data are presented as means ± SEM, n = 5-7. Data were analyzed using two-way repeated measures ANOVA in **A** and **B** and two-way ANOVA in **C, D** and **F**, followed by a Student-Newman-Keuls *post hoc* test. In **D**, the strain values at 140 mmHg (the last points) were used for analysis. **P*<0.05 and ***P*<0.01 vs respective control.

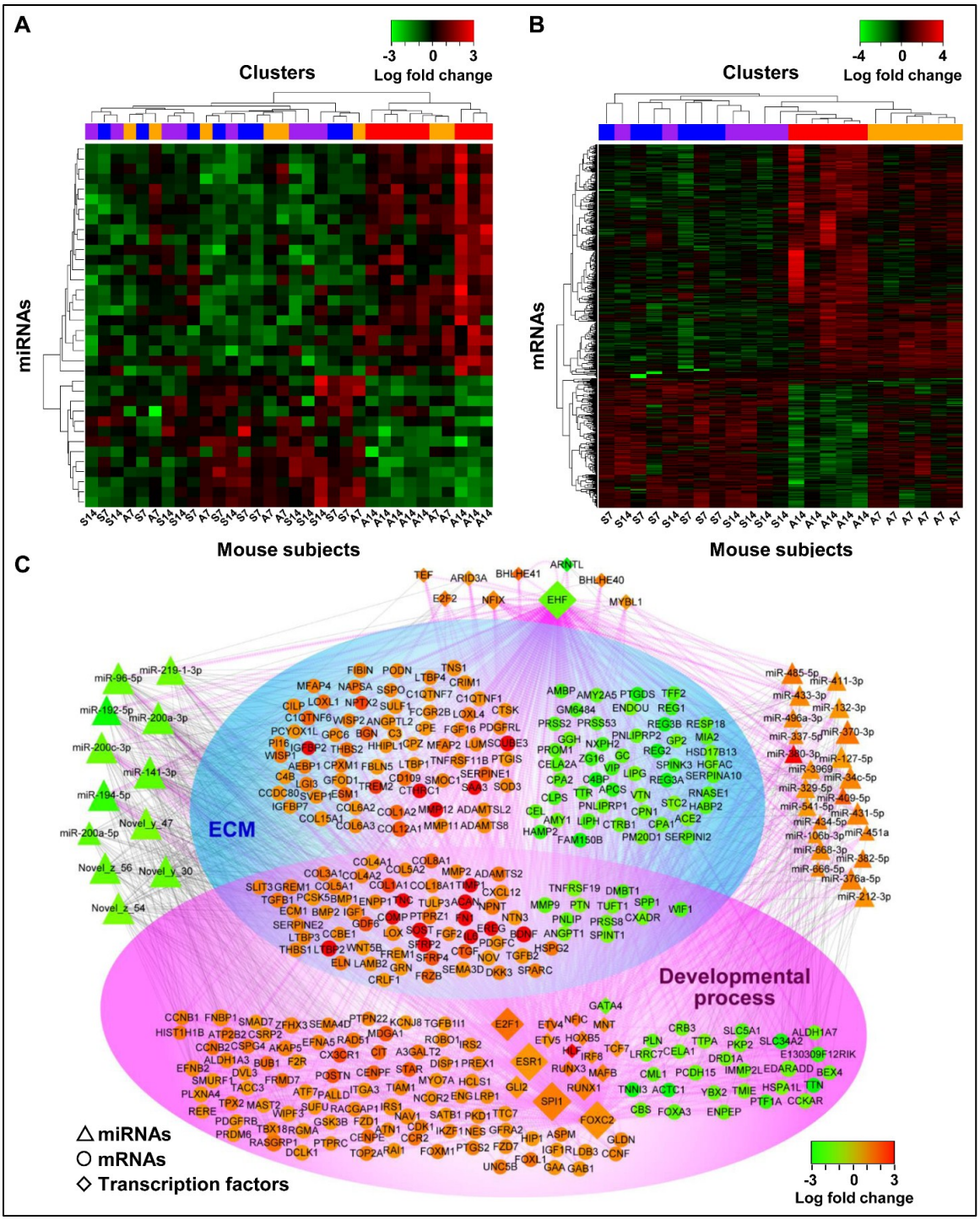

Figure II-2. **Heat maps and molecular network for miRNA and mRNA expression profiles.** Heat maps were generated using the differentially expressed (DE) miRNAs (**A**) and total RNAs (**B**) to present mouse subject grouping by hierarchical clustering analysis. Blue group: 7-day sham; orange group: 7-day Ang II; purple group: 14-day sham; red group: 14-day Ang II.

Figure II-2. (Cont.) C. A molecular network was constructed to present the 14-day DE genes involved in the top 2 enriched gene ontology term groups, and the interactions between 14-day DE miRNAs, DE transcription factors (TFs), and their DE gene targets. Black lines represent interactions between miRNAs and target genes, purple lines represent interactions between TFs and target genes. Node size is proportional to degree of connectivity. n = 8 in **A** and 5-6 in **B**.

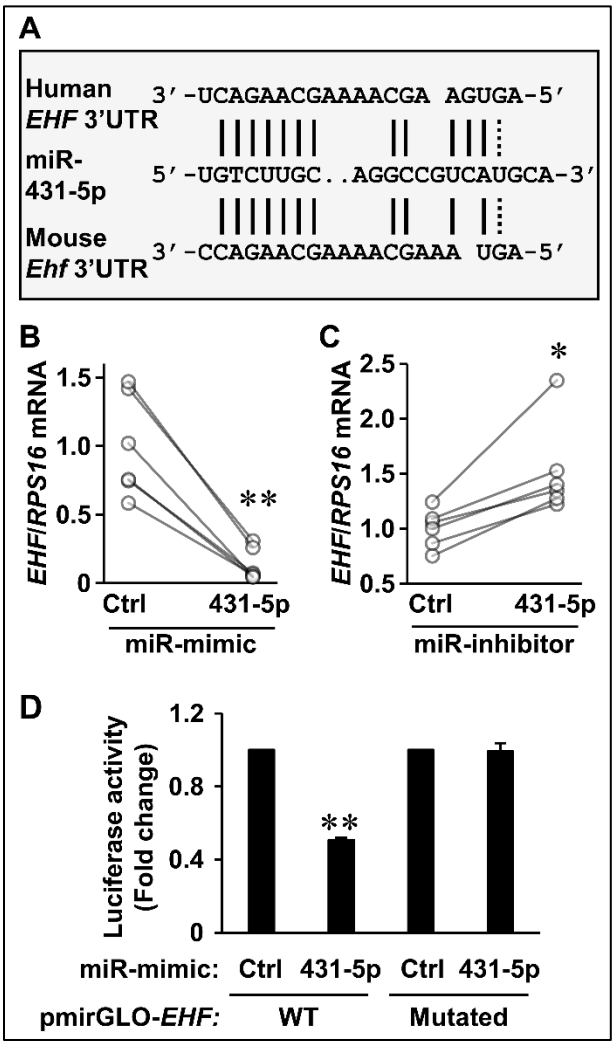

Figure II-3. miR-431-5p directly targets ETS homologous factor (*EHF*) in human aortic vascular smooth muscle cells. **A**. The conserved miR-431-5p binding sites in human *EHF* and mouse *Ehf* 3' untranslated region (UTR) are presented. mRNA expression of *EHF* and ribosomal protein S16 (*RPS16*) was determined by reverse transcription quantitative PCR in human aortic vascular smooth muscle cells transfected for 24 hours with control (Ctrl) or miR-431-5p microRNA (miR) mimics (**B**) or inhibitors (**C**). **D**. Luciferase activity was measured in human aortic vascular smooth muscle cells co-transfected for 48 hours with a pmirGLO reporter vector containing a *EHF* 3' UTR segment containing the wild-type (WT) or mutated (MUT) miR-431-5p binding site with control (Ctrl) or miR-431-5p mimics. Data are presented as means ± SEM, n = 6. Data were analyzed using paired *t*-test in **B** and **C**, and *t*-test in **E**. **P*<0.01 and ***P*<0.001 vs respective Crtl.

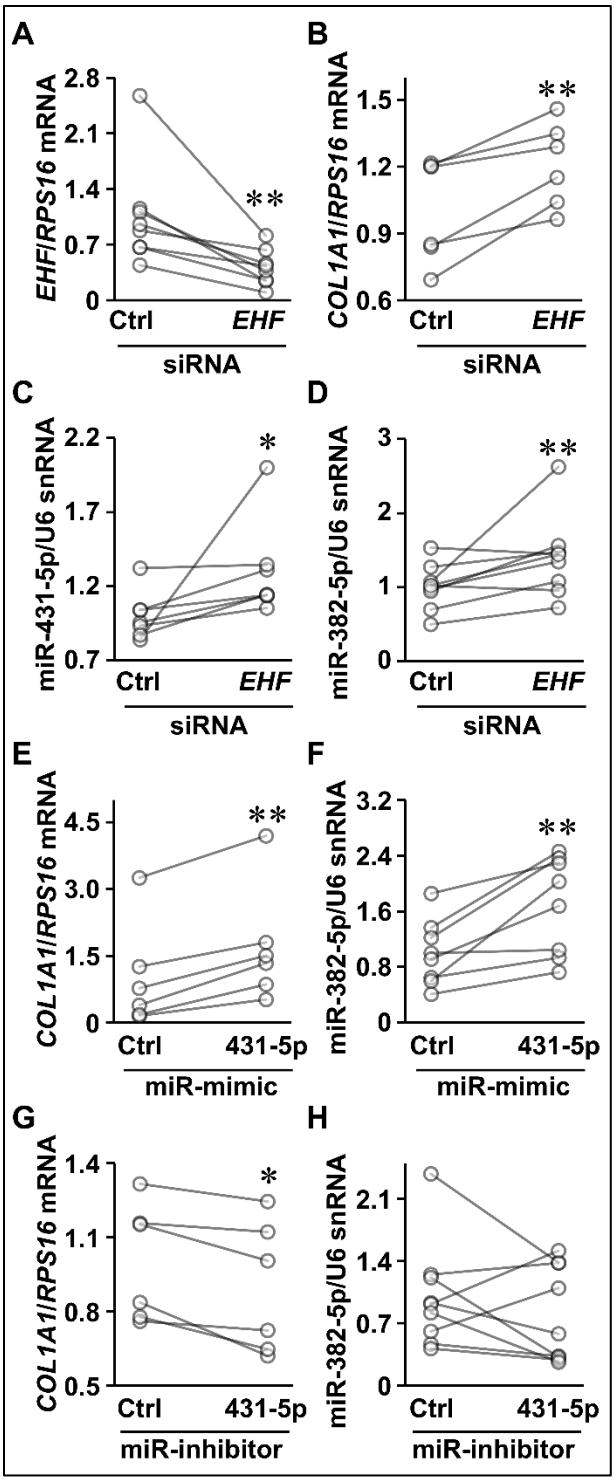

Figure II-4. ETS homologous factor (EHF) negatively regulates collagen type I alpha 1 chain (*COL1A1*), miR-431-5p and miR-382-5p in human aortic vascular smooth muscle cells. Expression of *EHF* (**A**), *COL1A1* (**B** and **G**), miR-431-5p (**C** and **F**) miR-382-5p (**D** and **H**) was determined by reverse transcription quantitative PCR in human aortic smooth muscle cells 24 hours after transfection of control (Ctrl) or *EHF* small interfering RNAs (siRNAs) (**A-D**), or Ctrl or miR-431-5p microRNA (miR) mimics (**E-F**) or inhibitors (**G-H**). Expression of Ribosomal protein S16 (*RPS16*) and U6 small nuclear RNA (snRNA) was used to normalize the expression of mRNA and microRNA, respectively. Data are presented as means ± SEM, n = 6-9. Data were analyzed using paired *t*-test. **P*<0.05 and ***P*<0.01 vs Ctrl.

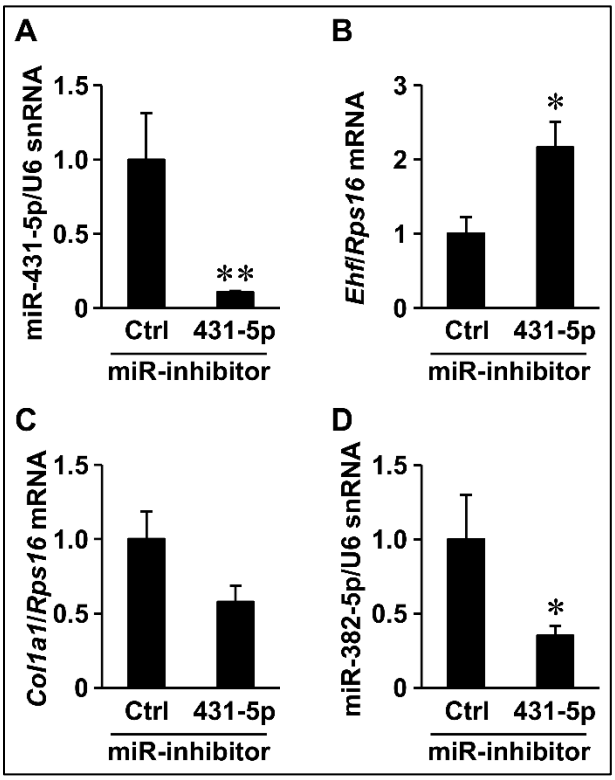

Figure II-5. *In vivo* miR-431-5p inhibition increased ETS homologous factor (*Ehf*) mRNA expression and decreased collagen type I alpha 1 chain (*Col1a1*) and miR-382-5p levels in mesenteric arteries of angiotensin (Ang) II infused mice. mRNA expression of miR-431-5p (**A**), *Ehf* (**B**), *Col1a1* (**C**) and miR-382-5p (**D**) was determined by reverse transcription quantitative PCR in mesenteric arteries of mice infused with Ang II (1000 ng/kg/min) for 14 days and injected IV with 20 mg/kg of control (Ctrl) or miR-431-5p microRNA (miR) inhibitors on day 1 and 7 of the treatment period. Data are presented as means ± SEM, n = 6-8. Data were analyzed using *t*-test. **P*<0.05 and ***P*<0.01 vs Ctrl.

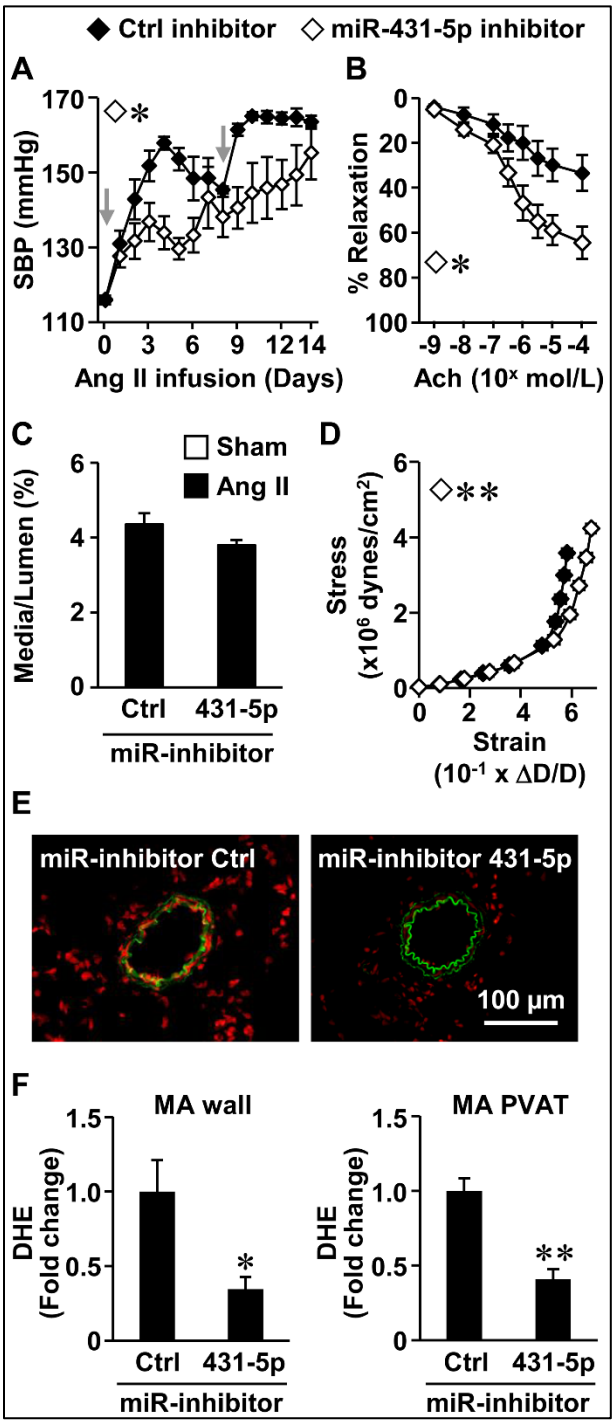

Figure II-6. *In vivo* miR-431-5p inhibition protected against angiotensin (Ang) II-induced blood pressure elevation, endothelial dysfunction, vascular remodeling, stiffening and oxidative stress. Mean 24-hour systolic blood pressure (SBP, **A**) was measured by telemetry, vasodilatory responses to acetylcholine (Ach, **B**), media/lumen (**C**), vascular stiffness (**D**) of small mesenteric arteries using pressurized myography and reactive oxygen species generation by dihydroethidium (DHE) staining (**E** and **F**) in mesenteric artery media, adventitia and perivascular adipose tissue (PVAT), all determined in mice infused with Ang II (1000 ng/kg/min) for 14 days and injected IV with 20 mg/kg of control (Ctrl) or miR-431-5p microRNA (miR)-inhibitors on day 1 and 7 of the treatment period. Grey arrows in **A** indicate days of miR-431-5p inhibitor injections. Representative images of DHE staining are shown in **E**. Red and green fluorescence represents DHE fluorescence and elastin autofluorescence, respectively. Data are presented as means ± SEM, n = 6-7. Data were analyzed using two-way repeated measures ANOVA followed by a Student-Newman-Keuls *post hoc* test in panels (**A** and **B**), and *t*-test in panels (**C**, **D** and **F**). In **D**, The strain values at 140 mmHg (the last points) were used for analysis. **P*<0.05 and ***P*<0.01 vs Ctrl.

Table II-1. The expression of 9 up-regulated microRNAs and ETS homologous factor (*Ehf*) mRNA correlates with systolic blood pressure (SBP) or diastolic blood pressure (DBP)

	Correlation with SBP		Correlation with DBP	
miRNAs/mRNA	**r**	***P***	**r**	***P***
miR-411-3p	0.91	0.001	0.89	0.001
miR-409-5p	0.85	0.004	0.79	0.012
miR-434-5p	0.78	0.012	0.82	0.006
miR-127-5p	0.77	0.014	0.78	0.014
miR-668-3p	0.74	0.020	0.82	0.007
miR-431-5p	0.74	0.024	0.81	0.008
miR-337-5p	0.71	0.033	0.79	0.011
miR-541-5p	0.68	0.042	0.84	0.004
miR-382-5p	0.68	0.043	0.76	0.017
Ehf	-0.88	0.009	-0.76	0.048

Correlations between microRNAs (miRNAs) and blood pressure, as well as between mRNAs and blood pressure of mice infused or not with Ang II (1000 ng/kg/min) for 14 days were done using Pearson correlation. r, correlation coefficient. n = 23.

SUPPLEMENTAL MATERIAL

miR-431-5p inhibition protects against angiotensin II-induced hypertension and vascular injury

Ku-Geng Huo[1], Julio C. Fraulob-Aquino[1], Tlili Barhoumi[1], Chantal Richer[3], Suellen C. Coelho[1], Sofiane Ouerd[1], Mathieu Lajoie[3], Daniel Sinnett[3,4], Pierre Paradis[1], Ernesto L. Schiffrin[1,2]*

[1]Vascular and Hypertension Research Unit, Lady Davis Institute for Medical Research, [2]Department of Medicine, Sir Mortimer B. Davis-Jewish General Hospital, McGill University; [3]Division of Hematology-Oncology, Research Center, CHU Ste-Justine, [4]Department of Pediatrics, Faculty of Medicine, Université de Montréal, Montréal, Canada.

Corresponding author:

Ernesto L. Schiffrin, MD, PhD, FRSC, FRCPC, FAHA

Sir Mortimer B. Davis-Jewish General Hospital, #B-127,

3755 Côte-Ste-Catherine Rd.,

Montreal, Quebec, Canada H3T 1E2

Fax: 514-340-7539

Phone: 514-340-7538

E-mail: ernesto.schiffrin@mcgill.ca

http://ladydavis.ca/en/ernestoschiffrin

Expanded Methods and Results

Experimental design

The study was approved by the Animal Care Committee of the Lady Davis Institute for medical research and McGill University, and followed recommendations of the Canadian Council of Animal Care.

A group of 10 to 12-week-old male C57BL/6J WT (Harlan laboratories, Indianapolis, IN) mice (n = 10) infused or not SC with angiotensin (Ang) II (1000 ng/kg/min) for 7 or 14 days with ALZET osmotic mini pumps (Model 1002, Durect Corporation, Cupertino, CA) were used to determine changes of microRNA (miRNA) and mRNA expression in mesenteric arteries (MAs) by RNA sequencing. A systems biology approach was used to identify key miRNA regulators that mediate gene expression changes in the course of vascular injury. Blood pressure (BP) was determined by telemetry in a subset of the above mice (n = 6 for Ang II-infused and n=5 for sham) from two days before to the end of the 14-day treatment period as previously described (1).

A second group of 10 to 12-week-old male C57BL/6J WT mice (n = 7) infused or not with Ang II for 7 or 14 days were used to assess MA function and mechanical properties by pressurized myography as previously described (2).

Mouse vascular smooth muscle cells (VSMCs), endothelial cells (ECs) and fibroblasts isolated from a group of 10 to 12-week-old male C57BL/6J WT mice (n = 12), as well as human aorta smooth muscle cells (HASMCs) and ECs (HAECs) (ScienCell, Carlsbad, CA) were used to determine which vascular cell types express the candidate key miRNA regulator miR-431 by reverse transcription-quantitative PCR (RT-qPCR).

In order to determine whether human miR-431-5p targets ETS homologous factor (*EHF*), the expression of *EHF* was determined by RT-qPCR in HASMCs transfected with miR-431-5p mimics or inhibitors.

A luciferase miRNA target expression vector assay (Promega, Madison, WI) was used to confirm whether miR-431-5p targets *EHF* in a canonical miRNA targeting machinery in HASMCs transfected with miR-431-5p mimics or inhibitors.

In order to determine whether EHF targets collagen type I alpha 1 chain (*COL1A1*) and miR-382-5p, the expression of *COL1A1* and miR-382-5p was determined by RT-qPCR in HASMCs transfected with si*EHF*.

The effect of in vivo miR-431-5p inhibition on Ang II-induced BP elevation and vascular injury were tested using a third group of 10 to 12-week-old male C57BL/6J WT mice (n=7) infused with Ang II (1000 ng/kg/min) for 14 days and injected IV via the tail vein with 20 mg/kg of locked nucleic acid (LNA) scrambled inhibitors or miR-431-5p inhibitors (Exiqon, Vedbaek, Denmark) on day 1 and day 7 of the treatment period. BP was determined as above in a subset of these mice (n=6). At the end of the study, MA miRNA and mRNA expression was measured in by RT-qPCR. MA function and mechanical properties were determined as above in a fourth group of 10 to 12-week-old male C57BL/6J WT mice (n=7) infused with Ang II and injected IV with LNA scrambled inhibitors or miR-431-5p inhibitors as above.

Ang II infusion

Mice were anesthetized with 3% isoflurane mixed with O2 at 1 L/min. The depth of anesthesia was confirmed by rear foot squeezing. The non-steroidal anti-inflammatory drug carprofen (20 mg/kg) was administered SC to minimize post-operation pain. Mice were then surgically implanted SC with ALZET osmotic mini pumps (model 1002, Durect Corporation) infusing angiotensin II (1000 ng/kg/min) for 14 days, as recommended by the manufacturer. Control mice underwent sham surgery.

Telemetry BP determination

BP was determined by telemetry as previously described (1). In brief, 9 to 11-week-old mice were anesthetized with isoflurane and injected with carprofen as above, surgically instrumented with PA-C10 telemetry transmitters as recommended by the manufacturer

(Data Sciences International, St. Paul, MN). Mice were allowed to recover for 7 to 10 days, during which carprofen was administered as above once a day for the first two days. BP was determined every 5 min for 10 sec from two days before to the end of the 14-day treatment period.

Collection of tissue

At the end of the protocol, mice were weighed and then anesthetized with isoflurane as above. For the first and third sets of mice, MAs were collected without the attached intestine under RNase-free condition and stored immediately in RNAlater (ThermoFisher Scientific, Waltham, MA) as previously described (3). The MAs were dissected from perivascular fat and veins in RNAlater and then used for RNA extraction. For the second and fourth sets of mice, the MA vascular bed attached to the intestine was harvested in 4 C oxygenated (95% air–5% CO2) Krebs solution (pH 7.4) containing (mmol/l): 120 NaCl, 25 NaHCO3, 4.7 KCl, 1.18 KH2PO4, 1.18 MgSO4, 2.5 CaCl2, 0.026 EDTA and 5.5 glucose.

Vascular function and mechanic studies

Second-order branches of mesenteric arteries (internal diameter between 150 and 250 μm) were dissected and mounted on a pressurized myograph. Endothelial function and mechanical properties were determined as previously described (2).

RNA extraction from MAs

The dissected MAs were homogenized in 1 mL of mirVana miRNA lysis/binding buffer (ThermoFisher Scientific) in a 5 mL tube for 1 min at maximum speed with a Polytron PT 1600 E homogenizer (Brinkmann Instruments, Mississauga, ON, Canada) equipped with a dispersing aggregate PT-DA 1607/2EC. The homogenate was centrifuged at 1500 x g for 2 minutes at 4 C to remove foam generated during homogenization, and processed for total RNA extraction using the mirVana miRNA isolation kit, followed by genomic DNA removal with the TURBO DNA-free kit according to the manufacturer's

protocol (ThermoFisher Scientific). The concentration and purity of the RNA were assessed with a NanoDrop ND-100 spectrophotometer (ThermoFisher Scientific). RNA quality was assessed with an Agilent 2100 bioanalyzer (Agilent Technologies, Santa Clara, CA). Samples with good RNA integrity number were used for small (n = 8) and total (n = 6) RNA library construction.

Small and total RNA library constructions and sequencing

One μg of total RNA was used for small RNA library construction using the TruSeq small RNA sample preparation kit (Illumina, San Diego, CA) and 500 ng of total RNA for total RNA library construction using the TruSeq stranded total RNA sample preparation kit (Illumina). Small RNA (1 x 51 bp single-end rapid mode in 4 lanes) and total RNA (2 x 101 bp pair-end high-output mode in 4 lanes) were sequenced using the HiSeq 2500 system (Illumina).

Bioinformatics data analysis and visualization

Sequence base-calling, adapter trimming, sample separation and bcl-to-fastq format conversion were done in Bcl2fastq (Illumina). FastQC (4) was used for sequence quality control. Only samples with >25 base quality at every position were included in the data analysis. The sequences were mapped to the mouse mm10 genome using STAR 2.3.1 (5). For small RNA sequence alignment specifically, the option *--outFilterMismatchNoverLmax 0.05* was used to allow maximal mismatch ratio of 0.05 (no mismatch allowed for reads <20nt and 1 mismatch allow per 20 nt). HTSeq-count 0.5.3p3 (6) was used for total RNA gene annotation and counting. miRDeep2 2.0.0.5 (7) was used for novel miRNA prediction, known and novel miRNA annotation and counting. Differential expression analysis was done in R 3.2.3 (https://www.r-project.org) using package EdgeR 3.6.8 (8). A trimmed mean of M-values (TMM) method in the EdgeR protocol was used for sequence read normalization. Only genes with expression level >1 read per million mapped reads in more than 8 (# of each group) samples were analyzed. Hierarchical clustering analyses and heatmap generation using differentially expressed

(DE) miRNAs and total RNAs were done in R. TargetScan 6.0 (9) was used to predict targets of DE miRNAs in the inversely related DE mRNAs. TF binding site prediction in the promoters (2000 bp upstream of the transcription initiation site) was performed with the FIMO tool of Meme Suite 4.10.0_2 (10). Molecular network construction was done in Cytoscape v3.2.0 (11). Gene enrichment analysis was performed using the ClueGO v2.1.5 tool in Cytoscape (12).

Determination of the vascular cell types expressing the candidate key miRNA regulator

Mouse VSMCs were isolated from MAs of 3 different batches of 10 to 12-week-old male C57BL/6J WT mice (n = 4 per batch) as previously described (2). Mouse VSMCs were grown in DMEM high glucose medium supplemented with 10 % heat inactivated FBS, 100 Units/mL of penicillin, 10 µg/mL of streptomycin and 2.8 mmol/L of L-glutamine (all from ThermoFisher Scientific). At passages 3-4 (P3-4), mouse VSMCs were passaged at a density of 20000 cells/cm2 into Corning Primaria 6-well cell culture plates (ThermoFisher Scientific), grown until they reached ~70-80% confluence. RNA was extracted and used to measure miRNA expression.

Mouse ECs were isolated from the lungs of a subset of the above mice using magnetic beads conjugated with anti–ICAM-2 antibodies as previously described (13), and grown in media constituted of 50% DMEM/F12 (ThermoFisher Scientific) and 50% Endothelial Cell Growth Medium (Lonza Group, Basel, Switzerland) that was supplemented with 100 Units/mL of penicillin, 100 µg/mL of streptomycin and 10% FBS. At P3, mouse ECs were passaged at a density of 20000 cells/cm2 into Corning Primaria 6-well cell culture plates, grown until they reached ~70-80% confluence. RNA was extracted and used to measure miRNA expression.

Fibroblasts were isolated from the lungs as follows. The cells that were not bound to magnetic beads conjugated with anti–ICAM-2 antibodies were plated into 75 cm2 Corning Primaria tissue culture flasks (ThermoFisher Scientific) and incubated for 30 minutes at 37°C in a humidified incubator with 5% CO2. Non-adherent cells were removed by washing with Gibco™ HBSS with Calcium and Magnesium (ThermoFisher

Scientific). The attached fibroblasts were grown in the same media as mouse VSMCs until they reached ~70-80% confluence. The fibroblasts were then passaged at a density of 20000 cells/cm2 into Corning Primaria 6-well cell culture plates, grown until they reached ~70-80% confluence. RNA was extracted and used to measure miRNA expression.

HASMCs were grown in Smooth Muscle Cell Medium supplemented with Smooth Muscle Cell Growth Supplement, 2% FBS, 100 units/mL of penicillin and 100 μg/mL of streptomycin (all from ScienCell) at 37°C in a humidified incubator with 5% CO2. HAECs were grown in Endothelial Cell Medium supplemented with Endothelial Cell Growth Supplement, 5% FBS, 100 units/mL of penicillin and 100 μg/mL of streptomycin (all from ScienCell) at 37°C in a humidified incubator with 5% CO2. Culture medium was changed every 2 days. When reached ~70-80% confluence, cells were passaged at a density of 6500 cells/cm2 into 75 cm2 Corning Primaria tissue culture flasks. At P3-5, cells were passaged at a density of 5200 cells/cm2 into Corning Primaria 6-well cell culture plates (ThermoFisher Scientific), grown until they reached ~70-80% confluence. RNA was extracted and used to measure miRNA expression.

Validation of predicted miR-431-5p and EHF targets

miR-431-5p mimic/inhibitor and siEHF transfections were performed in HASMCs at P4-6 that were seeded at a density of 5200 cells/cm2 into Corning Primaria 6-well cell culture plates. When HASMCs reached ~70-80% confluence, they were transfected with 10 mM of mirVana miR-431-5p mimics or inhibitors, or Silencer Select siEHF using Lipofectamine 3000 (all from ThermoFisher Scientific) for 24 hours. mirVana scrambled mimics/inhibitors and Silencer Select negative control siRNAs were used as controls. RNA was extracted and used to measure the expression of miR-431-5p targets and EHF targets.

RNA extraction from vascular cells

RNA was extracted from vascular cells with mirVana miRNA isolation kit using 500 μl

of mirVana miRNA lysis/binding buffer per well of 6-well cell culture plates.

Determination miRNA and mRNA expression evaluation by RT-qPCR

For miRNAs quantification, RT was done with 500 ng of total RNA using the TaqMan® MicroRNA Reverse Transcription Kit (ThermoFisher Scientific). For mouse miR-431-5p, qPCRs was performed using the Custom TaqMan Small RNA Assays (ThermoFisher Scientific) since majority of the reads mapped to miR-431-5p have one extra adenine (A) in 3' compared to the miRBase (http://www.mirbase.org/). For all the other miRNAs and U6 small nuclear RNA (snRNA), qPCR was performed using the TaqMan Small RNA Assays (ThermoFisher Scientific). All qPCR were run in an Applied Biosystems® 7500 Real-Time PCR System (ThermoFisher Scientific) according to the manufacturer's protocol. Oligonucleotide primers were validated to have PCR efficiency between 95% and 105% with single amplicon in the qPCR dissociation curve. miRNA expression was normalized by U6 small nuclear RNA (snRNA) and expressed as fold change over control.

For mRNA quantification, RT was done with 500 ng of total RNA using the Quantitect RT kit (Qiagen, Foster City, CA, USA). qPCR was performed using SsoFast EvaGreen Supermix (Bio-Rad Laboratories., Mississauga, ON, Canada) in an Mx3005P real-time PCR cycler (Agilent Technologies, Mississauga, ON, Canada). Oligonucleotide primers were designed to have a melting temperature (Tm) of 60°C and a 3' GC clamp using Primer3 (14). Oligonucleotide primers for mouse and human mRNA qPCR are listed in Supplemental table S1 and S2, respectively. Oligonucleotide primers were validated to have PCR efficiency between 95% and 105% and single amplicon with a Tm >80°C in the qPCR dissociation curve. The qPCR conditions were 2 min at 96 °C, followed by 40 cycles of 5 sec at 96°C and 30 sec at 58°C. mRNA expression was normalized by ribosomal protein S16 (Rps16) mRNA levels and expressed as fold change over control.

Luciferase reporter vector construction and assay

Sense and intense oligonucleotides were designed to contain a segment of the *EHF* 3' untranslated region with the wild-type (WT) or mutated (MUT) miR-431-5p binding site flanked by *SacI* and *XbaI* restriction sites, and an internal *NotI* restriction site used to confirm sub-cloning (Supplemental Table S3). The oligonucleotides were obtained phosphorylated from Integrated DNA Technologies (Coralville, IA, USA) to facilitate the sub-cloning. Sense and intense oligonucleotides were annealed and sub-cloned into the multiple cloning site of the pmirGLO dual-luciferase miRNA target expression vector (Promega) using the *SacI* and *XbaI* restriction sites according to the manufacturer's protocol. Clones of pmirGLO-WT-*EHF* or pmirGLO-MUT-*EHF* vectors were sequenced by Sanger sequencing to confirm the correct oligonucleotides subcloning.

The luciferase miRNA target expression vector assays were performed in HASMCs at P4-6 that were seeded at a density of 5208 cells/cm2 into Corning Primaria 6-well cell culture plates. When HASMCs reached ~70% confluence, they were co-transfected with 10 mM of mirVana miR-431-5p mimics or inhibitors and 800 ng of pmirGLO-WT-*EHF* or pmirGLO-MUT-*EHF* vectors using Lipofectamine 3000 (ThermoFisher Scientific) for 48 hours. Luciferase assays were performed using the Dual-Luciferase reporter assay system according to the manufacturer's protocol (Promega). Luciferase activity was determined using an Orion II microplate luminometer (Berthold detection systems Gmbh, Pforzheim, Germany).

Dihydroethidium (DHE) staining

Reactive oxygen species (ROS) production was measured in the media and perivascular adipose tissue (PVAT) of MAs using the ROS-sensitive fluorescent dye dihydroethidium as previously described (2).

Data Analysis

Results are presented as means ± SEM. Comparisons in BP and concentration-response curve data were carried out using two-way analysis of variance (ANOVA) for repeated

measures. Other comparisons between more than 2 groups were performed using two-way ANOVA as indicated. All ANOVA tests were followed by a Student–Newman–Keuls *post-hoc* test. Comparisons between 2 groups were done using unpaired or paired Student *t*-test as indicated. Correlation between DE miRNA or DE mRNA and systolic or diastolic BP was obtained using a Pearson correlation conducted in R. ANOVA and *t*-tests were done in SigmaPlot version 13 (Systat Software, San Jose, CA). $P<0.05$ was considered statistically significant. Differential expression analysis was performed using an ANOVA-like test in EdgeR based on generalized linear models. Differential expression was defined with a threshold of 1.5-fold change and false discovery rate (FDR) <0.05.

References

1. Barhoumi T, Kasal DA, Li MW, Shbat L, Laurant P, Neves MF, Paradis P, Schiffrin EL. T regulatory lymphocytes prevent angiotensin II-induced hypertension and vascular injury. Hypertension (Dallas, Tex : 1979). 2011;57:469-476.

2. Barhoumi T, Fraulob-Aquino JC, Mian MOR, Ouerd S, Idris-Khodja N, Huo K-G, Rehman A, Caillon A, Dancose-Giambattisto B, Ebrahimian T, Lehoux S, Paradis P, Schiffrin EL. Matrix metalloproteinase-2 knockout prevents angiotensin II-induced vascular injury. Cardiovascular Research. 2017

3. Simeone SM, Li MW, Paradis P, Schiffrin EL. Vascular gene expression in mice overexpressing human endothelin-1 targeted to the endothelium. Physiological genomics. 2011;43:148-160.

4. Andrews S. FastQC: A quality control tool for high throughput sequence data. 2014,

5. Dobin A, Davis CA, Schlesinger F, Drenkow J, Zaleski C, Jha S, Batut P, Chaisson M, Gingeras TR. STAR: ultrafast universal RNA-seq aligner. Bioinformatics (Oxford, England). 2013;29:15-21.

6. Anders S, Pyl PT, Huber W. HTSeq--a Python framework to work with high-throughput sequencing data. Bioinformatics (Oxford, England). 2015;31:166-169.

7. Friedlander MR, Mackowiak SD, Li N, Chen W, Rajewsky N. miRDeep2 accurately identifies known and hundreds of novel microRNA genes in seven animal clades. Nucleic acids research. 2012;40:37-52.

8. Robinson MD, McCarthy DJ, Smyth GK. edgeR: a Bioconductor package for differential expression analysis of digital gene expression data. Bioinformatics (Oxford, England). 2010;26:139-140.

9. Garcia DM, Baek D, Shin C, Bell GW, Grimson A, Bartel DP. Weak seed-pairing stability and high target-site abundance decrease the proficiency of lsy-6 and other microRNAs. Nature structural & molecular biology. 2011;18:1139-1146.

10. Grant CE, Bailey TL, Noble WS. FIMO: scanning for occurrences of a given motif. Bioinformatics (Oxford, England). 2011;27:1017-1018.

11. Shannon P, Markiel A, Ozier O, Baliga NS, Wang JT, Ramage D, Amin N, Schwikowski B, Ideker T. Cytoscape: a software environment for integrated models of biomolecular interaction networks. Genome research. 2003;13:2498-2504.

12. Bindea G, Mlecnik B, Hackl H, Charoentong P, Tosolini M, Kirilovsky A, Fridman WH, Pages F, Trajanoski Z, Galon J. ClueGO: a Cytoscape plug-in to decipher functionally grouped gene ontology and pathway annotation networks. Bioinformatics (Oxford, England). 2009;25:1091-1093.

13. Robins RS, Lemarie CA, Laurance S, Aghourian MN, Wu J, Blostein MD. Vascular Gas6 contributes to thrombogenesis and promotes tissue factor up-regulation after vessel injury in mice. Blood. 2013;121:692-699.

14. Rozen S, Skaletsky H. Primer3 on the WWW for general users and for biologist programmers. Methods in molecular biology. 2000;132:365-386.

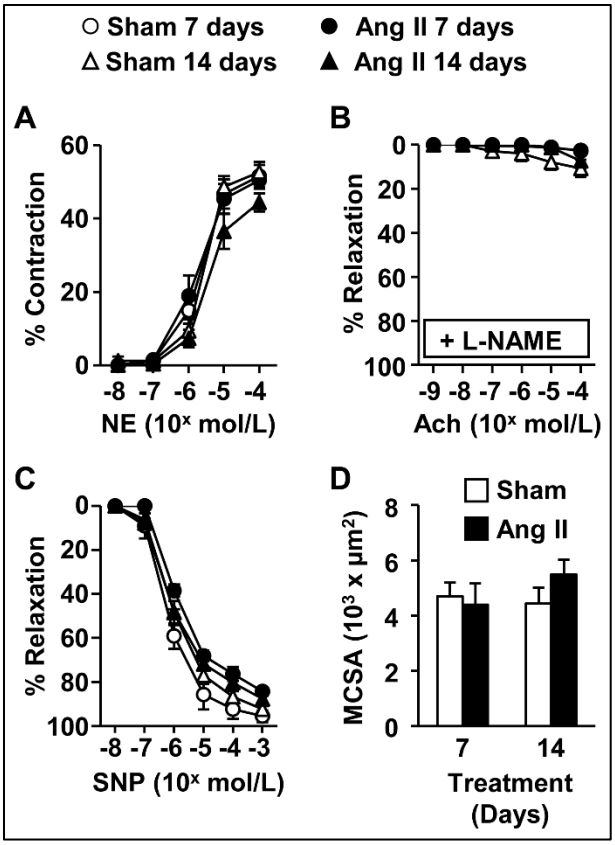

Supplemental Figure II-S1. Angiotensin (Ang) II infusion did not affect mesenteric artery vasoconstriction responses to norepinephrine (NE), relaxation responses to acetylcholine (Ach) in the presence of the nitric oxide synthase inhibitor N^{ω}-nitro-L-arginine methyl ester (L-NAME), endothelium-independent relaxation responses to sodium nitroprusside (SNP) or media cross-sectional area (MCSA). These parameters were determined by pressurized myography in mesenteric arteries of mice infused or not with Ang II (1000 ng/kg/min) for 7 and 14 days. Data are presented as means ± SEM, n = 6-7. Data were analyzed using two-way repeated measures analysis of variance (ANOVA) in (**A**-**C**) and two-way ANOVA in (**D**), both followed by a Student-Newman-Keuls *post hoc* test.

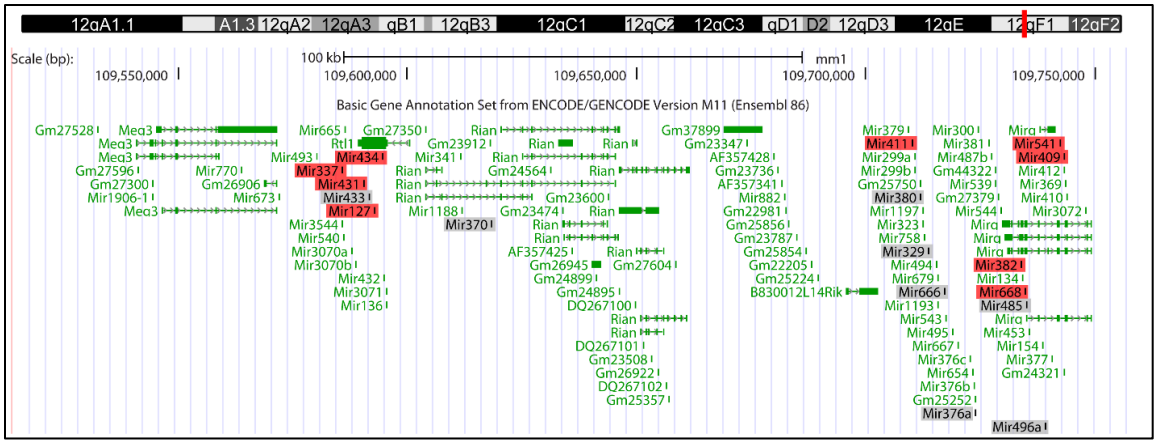

Supplemental Figure II-S2. Seventeen out of 23 up-regulated miRNAs are located in the conserved Delta-like homolog 1-Type III iodothyronine deiodinase (*Dlk1-Dio3*) genomic region (highlighted in gray or red). The expression of 9 of these miRNAs is correlated with blood pressure (highlighted in red). *Dlk1-Dio3* genomic map was downloaded from the University of California Santa Cruz (UCSC) Genome Browser (http://genome.ucsc.edu, last accessed on 12 July 2017).

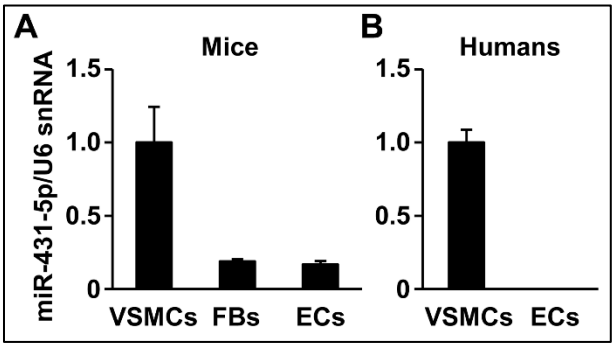

Supplemental Figure II-S3. miR-431-5p is expressed in mouse and human vascular smooth muscle cells. Expression of miR-431-5p and U6 small nuclear RNA (snRNA) was determined in (**A**) mouse mesenteric artery smooth muscle cells (VSMCs) and lung fibroblasts (FBs) and endothelial cells (ECs) , as well as in (**B**) human aortic VSMCs and ECs by reverse transcription quantitative PCR. The expression of miR-431-5p was normalized by U6 snRNA. Data are presented as means ± SEM, n = 3-5.

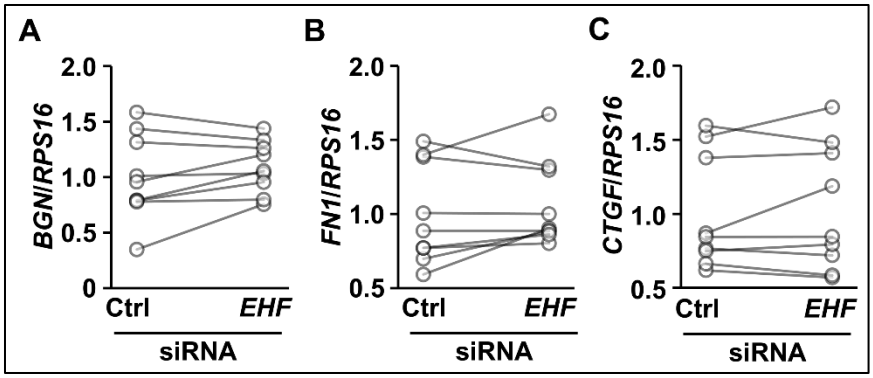

Supplemental Figure II-S4. *EHF* does not regulate mRNA expression of biglycan (*BGN*, **A**), fibronectin 1 (*FN1*, **B**) and connective tissue growth factor (*CTGF*, **C**) in human vascular smooth muscle cells. mRNA expression of *BGN*, *FN1*, *CTGF* and ribosomal protein S16 (*RPS16*) was determined by reverse transcription quantitative PCR in human aortic vascular smooth muscle cells transfected for 24 hours with control (Ctrl) or *EHF* small interfering RNA (siRNA). Data are presented as means ± SEM, n = 9. mRNA expression was normalized by *RPS16*. Data were analyzed using paired Student *t*-test.

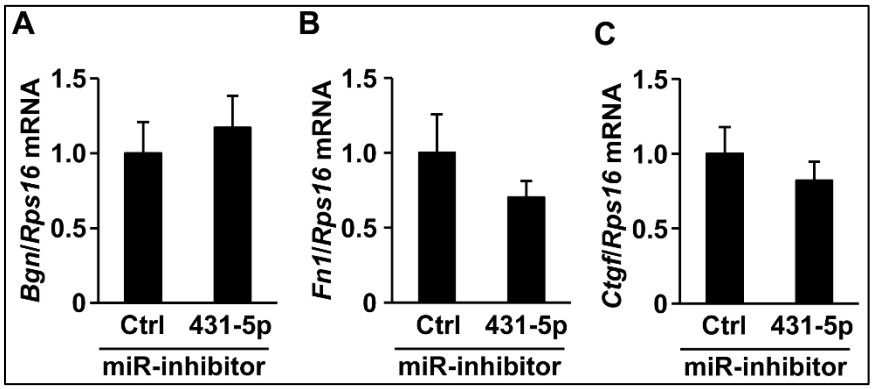

Supplemental Figure II-S5. *In vivo* miR-431-5p inhibition did not alter mRNA expression of biglycan (*Bgn*, **A**), fibronectin 1 (*Fn1*, **B**) and connective tissue growth factor (*Ctgf*, **C**) in mesenteric arteries of angiotensin (Ang) II infused mice. mRNA expression of *Bgn*, *Fn1*, *Ctgf* and ribosomal protein S16 (*Rps16*) was determined by reverse transcription quantitative PCR in mesenteric arteries of mice infused with Ang II (1000 ng/kg/min) for 14 days and injected IV with 20 mg/kg of control (Ctrl) or miR-431-5p microRNA (miR) inhibitors on day 1 and 7 of the treatment period. Data are presented as means ± SEM, n = 6-8. Data were analyzed using a Student *t*-test.

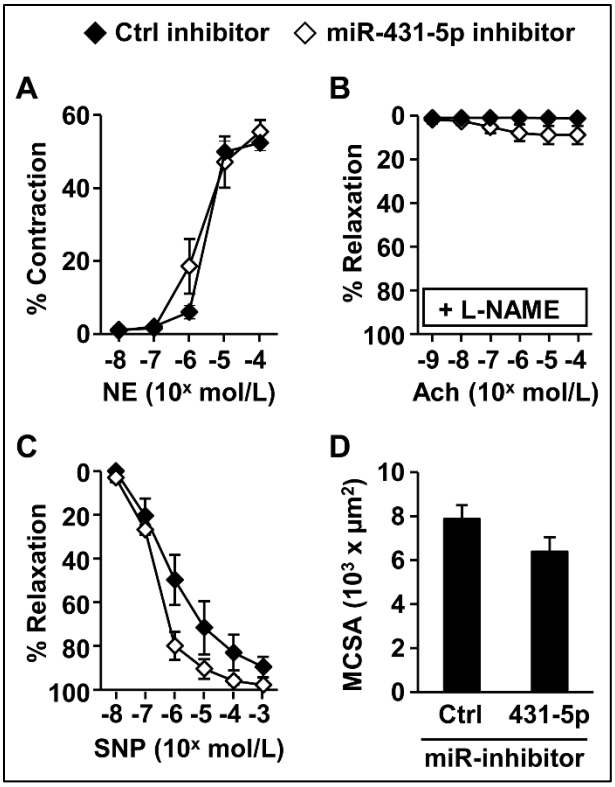

Supplemental Figure II-S6. *In vivo* miR-431-5p inhibition did not affect mesenteric artery vasoconstriction responses to norepinephrine (NE), endothelium-dependent relaxation responses to acetylcholine (Ach) in the presence of the nitric oxide synthase inhibitor N^{ω}-nitro-L-arginine methyl ester (L-NAME), endothelium-independent relaxation responses to sodium nitroprusside (SNP) or media cross-sectional area (MCSA) in angiotensin (Ang) II-infused mice. These parameters were determined by pressurized myography in mesenteric arteries of mice infused with Ang II (1000 ng/kg/min) for 14 days and injected IV with 20 mg/kg of control (Ctrl) or miR-431-5p microRNA (miR) inhibitors on day 1 and 7 of the treatment period. Data are presented as means ± SEM, n = 7. Data were analyzed using two-way repeated measures analysis of variance (ANOVA) in (**A**-**C**) and two-way ANOVA in (**D**), both followed by a Student-Newman-Keuls *post hoc* test.

Supplemental table II-S1. Oligonucleotide primers for mouse mRNA quantitative PCR

mRNA	Primers	Product size (bp)
Ehf	F: 5′-CCGATCCTTCCATCATGAAC-3′ R: 5′-GGTTCTTGTCTGGGCTCAAG-3′	267
Col1a1	F: 5'-GGTGAGACTGGTCCTGCTG-3' R: 5′-GACCGTTGAGTCCGTCTTTG-3'	274
Bgn	F: 5′-CAGCCTGACAACCTAGTCCAC-3′ R: 5′-TGGCACTGAAGGTAGGTGTG-3′	259
Fn1	F: 5′-TGTCCAGGAGTTCACTGTGC-3′ R: 5′-TGGTCATTTCTGTTTGATCTGG-3′	326
Ctgf	F: 5'-CCTAGCTGCCTACCGACTG-3' R: 5′-GACAGGCTTGGCGATTTTAG-3'	265
Rps16	F: 5′-ATCTCAAAGGCCCTGGTAGC-3′ R: 5′-ACAAAGGTAAACCCCGATCC-3′	211

The forward (F) and reverse (R) oligonucleotide primers used for quantitative PCR of mouse transcription factor ETS homologous factor (*Ehf)*, alpha-1 type I collagen (*Col1a1*), Biglycan (*Bgn*), fibronectin 1 (*Fn1*), connective tissue growth factor (*Ctgf*) and ribosomal protein S16 (*Rps16*) and their product sizes are displayed.

Supplemental table II-S2. Oligonucleotide primers for human mRNA quantitative PCR

mRNA	Primers	Product size (bp)
EHF	F: 5'-CAAAAAGCACAACCCGAGAG-3' R: 5′-GAGCCACTGCCTCTGATTTC-3'	143
COL1A1	F: 5'-TGATGATGCCAATGTGGTTC-3' R: 5′-AATCCATCGGTCATGCTCTC-3'	348
BGN	F: 5′-ATCTCAGAGGCCAAGCTGAC-3′ R: 5′-CACCCACTTTGGTGATGTTG-3′	307
FN1	F: 5′-AAAATGGCCAGATGATGAGC-3′ R: 5′-CGGGAATCTTCTCTGTCAGC-3′	349
CTGF	F: 5'-AAATGCTGCGAGGAGTGG-3' R: 5′-GCACTTTTTGCCCTTCTTAATG-3'	294
RPS16	F: 5′-TGGTCTCATCAAGGTGAACG-3′ R: 5′-ACCACCCTTTACACGGACAC-3′	139

The forward (F) and reverse (R) oligonucleotide primers used for quantitative PCR of human transcription factor ETS homologous factor (*EHF)*, alpha-1 type I collagen (*COL1A1*), Biglycan (*BGN*), fibronectin 1 (*FN1*), connective tissue growth factor (*CTGF*) and ribosomal protein S16 (*RPS16/Rps16*) and their product sizes are displayed.

Supplemental table II-S3. Oligonucleotide containing the *EHF* 3' untranslated region with the wild-type or mutated miR-431-5p target region

Oligonucleotides	Sequences
miR-431-5p binding site (sense)	5'-PO_4-CTAGCGGCCGCTCCTTAGAG**TGA**A**GC**AAAA**GCAAGAC**TTCAACCTCAACT- 3' *SacI* *NotI* 3' supplementary pairing Seed *XbaI*
miR-431-5p binding site (antisense)	5'-PO_4-CTAGAGTTGAGGTTGAA**GTCTTGC**TTTT**GC**T**TCA**CTCTAAGGAGCGGCCGCTAGAGCT-3' *XbaI* Seed 3' supplementary pairing *NotI* *SacI*
Mutated miR-431-5p binding site (sense)	5'-PO_4-CTAGCGGCCGCTCCTTAGAG**TCA**A**GC**AAAA**GGTAGTC**TTCAACCTCAACT-3' *SacI* *NotI* 3' supplementary pairing Seed *XbaI*
Mutated miR-431-5p binding site (antisense)	5'-PO_4-CTAGAGTTGAGGTTGAA**GACTACC**TTTT**GC**T**TGA**CTCTAAGGAGCGGCCGCTAGAGCT-3' *XbaI* Seed 3' supplementary pairing *NotI* *SacI*

The oligonucleotides were designed to contain the *EHF* 3' untranslated region with wild-type or mutated miR-431-5p binding site flanked by *SacI* and *XbaI* restriction sites, and an internal *NotI* restriction site used to confirm sub-cloning. The oligonucleotides were phosphorylated (PO_4-) to facilitate the sub-cloning. Restriction sites are indicated by underlined nucleotides. The 3' supplementary and seed binding regions are indicated by bold underlined nucleotides. Mutated nucleotides affecting the 3' supplementary pairing and seed regions are indicated by bold red nucleotides.

Supplemental table II-S4. Quantity and quality of RNA extracted from mesenteric arteries (MAs) of sham-operated and angiotensin II-infused mice

Groups	Number	RNA yield (µg)	RIN
Sham 7 days	10	6.8 ± 0.6	8.35 ± 0.11
Ang II 7 days	10	8.4 ± 0.6	8.57 ± 0.04
Sham 14 days	10	5.9 ± 0.5	8.34 ± 0.09
Ang II 14 days	12	6.7 ± 0.7	8.52 ± 0.10

Total RNA was extracted from mesenteric arteries of control (Sham) mice and mice infused with angiotensin (Ang) II-for 7 and 14 days. The concentration and purity of the RNA were assessed with a NanoDrop ND-100 spectrophotometer (ThermoFisher Scientific). RIN, RNA integrity number. Data are presented as means ± SEM.

Supplemental table II-S5. List of differentially expressed microRNA in mesenteric arteries of 7 and 14 days angiotensin II-infused mice

Changes	microRNA names	Fold change	P value	FDR	# of DE targets
		7 days angiotensin II infused mice			
Down	miR-145a-3p	0.67	4.75E-05	2.74E-02	37
		14 days angiotensin II infused mice			
Up	miR-431-5p	1.84	4.56E-07	2.63E-04	38
	miR-382-5p	1.92	3.61E-06	1.04E-03	22
	miR-541-5p	1.51	5.60E-06	1.07E-03	21
	miR-434-5p	1.85	7.59E-06	1.09E-03	2
	miR-337-5p	1.80	1.15E-05	1.33E-03	1
	miR-411-3p	1.67	3.33E-05	3.20E-03	25
	miR-132-3p	1.56	7.65E-05	5.81E-03	30
	miR-668-3p	1.70	1.23E-04	7.87E-03	25
	miR-106b-3p	1.59	3.63E-04	1.43E-02	3
	miR-329-5p	1.61	3.43E-04	1.43E-02	26
	miR-212-3p	1.62	5.45E-04	1.85E-02	30
	miR-127-5p	1.49	7.64E-04	1.99E-02	33
	miR-380-3p	3.17	7.55E-04	1.99E-02	22
	miR-496a-3p	1.77	7.66E-04	1.99E-02	21
	miR-433-3p	1.77	1.18E-03	2.43E-02	30
	miR-3969	1.65	1.41E-03	2.63E-02	25
	miR-666-5p	1.79	1.66E-03	2.89E-02	1
	miR-370-3p	2.05	1.89E-03	3.10E-02	46
	miR-409-5p	2.38	2.00E-03	3.20E-02	15
	miR-485-5p	2.03	2.28E-03	3.45E-02	40
	miR-376a-5p	1.85	3.28E-03	4.39E-02	39
	miR-451a	1.78	4.00E-03	4.93E-02	8
	miR-34c-5p	1.79	4.22E-03	4.96E-02	41
Down	miR-96-5p	0.56	8.07E-05	5.81E-03	101
	miR-141-3p	0.51	4.48E-04	1.61E-02	104
	miR-192-5p	0.34	6.90E-04	1.99E-02	73
	miR-200a-3p	0.53	8.99E-04	1.99E-02	104
	miR-200a-5p	0.52	9.34E-04	1.99E-02	46
	Novel_y_47	0.63	8.61E-04	1.99E-02	86
	Novel_z_56	0.55	9.24E-04	1.99E-02	79
	miR-200c-3p	0.57	1.24E-03	2.46E-02	89
	miR-194-5p	0.41	1.58E-03	2.84E-02	82
	Novel_y_30	0.55	2.51E-03	3.62E-02	93
	miR-219-1-3p	0.59	2.71E-03	3.72E-02	71
	Novel_z_54	0.64	4.05E-03	4.93E-02	98

IDs, identifications; FDR, false discovery rate; #, number.

Supplemental table II-S6. List of differentially expressed mRNA in mesenteric arteries of 7 days angiotensin II-infused mice (Not provided in this thesis)

Supplemental table II-S7. List of differentially expressed mRNA in mesenteric arteries of 14 days angiotensin II-infused mice (Not provided in this thesis)

Supplemental Table II-S8. Gene ontology term enrichment for differentially expressed mRNAs in mesenteric arteries of 7 days angiotensin II infused mice

GO groups	GO IDs	GO terms	FDR	# of genes
Extracellular matrix	GO:0005578	Proteinaceous extracellular matrix	3.60E-31	32
	GO:0044420	Extracellular matrix component	3.40E-18	16
	GO:0030198	Extracellular matrix organization	1.60E-16	18
	GO:0030199	Collagen fibril organization	1.20E-14	10
	GO:0032963	Collagen metabolic process	2.90E-09	8
	GO:0005604	Basement membrane	2.10E-08	8
Cell proliferation	GO:1903047	Mitotic cell cycle process	8.70E-22	32
	GO:0007067	Mitotic nuclear division	6.70E-21	26
	GO:0000280	Nuclear division	5.30E-20	28
	GO:0098813	Nuclear chromosome segregation	9.70E-13	15
	GO:0000819	Sister chromatid segregation	1.20E-12	13
	GO:0008608	Attachment of spindle microtubules to kinetochore	1.40E-12	8
	GO:0000776	Kinetochore	1.70E-12	12
	GO:0000793	Condensed chromosome	3.10E-12	14
	GO:0000070	Mitotic sister chromatid segregation	3.40E-11	11
	GO:0098687	Chromosomal region	3.40E-11	15

The top 10 gene ontology (GO) identifications (IDs) and terms are shown for the GO group cell proliferation. FDR, false discovery rate; #, number.

Supplemental Table II-S9. Gene ontology term enrichment for differentially expressed miRNA-targeted differentially expressed mRNAs in mesenteric arteries of 7 days infused angiotensin II mice

GO groups	GO IDs	GO terms	FDR	# of genes
Extracellular matrix	GO:0005578	Proteinaceous extracellular matrix	4.80E-17	15
	GO:0044420	Extracellular matrix component	6.30E-09	7
	GO:0043206	Extracellular fibril organization	1.10E-06	3
	GO:0005583	Fibrillar collagen trimer	1.20E-06	3
	GO:0005604	Basement membrane	1.20E-06	5
Cell proliferation	GO:0000819	Sister chromatid segregation	2.00E-08	7
	GO:0035371	Microtubule plus-end	4.80E-06	3

GO, Gene ontology; IDs, identifications; FDR, false discovery rate; #, number.

Supplemental Table II-S10. Gene ontology (GO) term enrichment for differentially expressed mRNAs in mesenteric arteries of 14 days infused angiotensin II mice

GO groups	GO IDs	GO terms	FDR	# of genes
Extracellular matrix	GO:0005578	Proteinaceous extracellular matrix	1.00E-34	76
	GO:0044420	Extracellular matrix component	2.10E-20	36
	GO:0030198	Extracellular matrix organization	1.40E-14	40
	GO:1903561	Extracellular vesicle	2.40E-13	173
	GO:0005604	Basement membrane	1.30E-12	24
	GO:0030199	Collagen fibril organization	1.60E-09	14
	GO:0032963	Collagen metabolic process	7.10E-08	16
Developmental processes	GO:0048731	System development	6.60E-24	287
	GO:0048513	Animal organ development	5.80E-20	228
	GO:0072359	Circulatory system development	3.60E-16	97
	GO:2000026	Regulation of multicellular organismal development	1.90E-15	135
	GO:0051270	Regulation of cellular component movement	3.40E-14	78
	GO:0001944	Vasculature development	3.80E-14	70
	GO:0001568	Blood vessel development	5.00E-14	68
	GO:2000145	Regulation of cell motility	1.20E-13	73
	GO:0048646	Anatomical structure formation involved in morphogenesis	3.70E-13	92
	GO:0051240	Positive regulation of multicellular organismal process	9.20E-13	113
Cell motility	GO:0016477	Cell migration	3.90E-18	111
	GO:0048870	Cell motility	5.30E-16	113
	GO:2000026	Regulation of multicellular organismal development	1.90E-15	135
	GO:0051270	Regulation of cellular component movement	3.40E-14	78
	GO:0030335	Positive regulation of cell migration	6.50E-14	52
	GO:2000145	Regulation of cell motility	1.20E-13	73
	GO:0071310	Cellular response to organic substance	7.20E-13	139
	GO:0051240	Positive regulation of multicellular organismal process	9.20E-13	113
	GO:0048514	Blood vessel morphogenesis	2.20E-11	56
	GO:0051094	Positive regulation of developmental process	3.40E-11	96

Supplemental Table II-S10. (Cont.)

GO groups	GO IDs	GO terms	FDR	# of genes
Growth factor signaling	GO:0007166	Cell surface receptor signaling pathway	7.80E-17	170
	GO:0010646	Regulation of cell communication	1.50E-13	178
	GO:0071310	Cellular response to organic substance	7.20E-13	139
	GO:0051240	Positive regulation of multicellular organismal process	9.20E-13	113
	GO:0009966	Regulation of signal transduction	2.50E-12	160
	GO:0070848	Response to growth factor	3.00E-11	60
	GO:0071559	Response to transforming growth factor beta	1.00E-10	31
	GO:0048584	Positive regulation of response to stimulus	1.10E-10	124
	GO:0071363	Cellular response to growth factor stimulus	4.30E-10	56
	GO:0007167	Enzyme linked receptor protein signaling pathway	1.10E-09	71
Inflammation	GO:0051240	Positive regulation of multicellular organismal process	9.20E-13	113
	GO:0042060	Wound healing	1.20E-12	49
	GO:0048584	Positive regulation of response to stimulus	1.10E-10	124
	GO:0022603	Regulation of anatomical structure morphogenesis	3.70E-09	73
	GO:0006954	Inflammatory response	5.50E-09	56
	GO:0032101	Regulation of response to external stimulus	1.50E-07	58
	GO:0001817	Regulation of cytokine production	3.50E-07	47
	GO:0080134	Regulation of response to stress	3.90E-07	78
	GO:0001819	Positive regulation of cytokine production	4.30E-06	33
	GO:0006935	Chemotaxis	8.00E-06	42
Cell proliferation	GO:2000026	Regulation of multicellular organismal development	1.90E-15	135
	GO:0045595	Regulation of cell differentiation	5.20E-11	116
	GO:0008284	Positive regulation of cell proliferation	9.80E-11	75
	GO:0042127	Regulation of cell proliferation	5.30E-10	108
	GO:0007067	Mitotic nuclear division	8.60E-10	46
	GO:0051241	Negative regulation of multicellular organismal process	2.90E-09	81
	GO:0022603	Regulation of anatomical structure morphogenesis	3.70E-09	73
	GO:0000280	Nuclear division	8.30E-09	53
	GO:0048285	Organelle fission	1.10E-08	55
	GO:0051093	Negative regulation of developmental process	2.00E-08	71

Supplemental Table II-S10. (Cont.)

GO groups	GO IDs	GO terms	FDR	# of genes
Protein transport	GO:0046903	Secretion	1.30E-07	73
	GO:0051049	Regulation of transport	2.30E-07	107
	GO:0001817	Regulation of cytokine production	3.50E-07	47
	GO:0032940	Secretion by cell	8.90E-07	63
	GO:0070201	Regulation of establishment of protein localization	1.90E-06	58
	GO:0046822	Regulation of nucleocytoplasmic transport	3.20E-06	24
	GO:0032880	Regulation of protein localization	3.30E-06	65
	GO:0051223	Regulation of protein transport	8.40E-06	53
	GO:0051050	Positive regulation of transport	8.60E-06	61
	GO:0042306	Regulation of protein import into nucleus	9.80E-06	20
Peptidase activity	GO:0008236	Serine-type peptidase activity	1.30E-08	31
	GO:0006508	Proteolysis	1.40E-08	110
	GO:0070011	Peptidase activity, acting on L-amino acid peptides	1.60E-07	55
	GO:0008237	Metallopeptidase activity	3.50E-07	25
	GO:0004252	Serine-type endopeptidase activity	1.80E-06	25
	GO:0004175	Endopeptidase activity	5.90E-06	40
	GO:0008235	Metalloexopeptidase activity	1.20E-05	11
Apoptosis	GO:0010941	Regulation of cell death	4.10E-07	95
	GO:0043067	Regulation of programmed cell death	1.70E-06	88
	GO:0060548	Negative regulation of cell death	1.80E-05	62

The top 10 gene ontology (GO) identifications (IDs) and terms are shown for the GO groups including developmental processes, cell motility, growth factor cell signalling, inflammation, cell proliferation, and protein transport. FDR, false discovery rate; #, number.

Supplemental Table II-S11. Gene ontology term enrichment for differentially expressed miRNA-targeted differentially expressed mRNAs in mesenteric arteries of 14 days angiotensin II-infused mice

GO groups	GO IDs	GO terms	FDR	# of genes
Extracellular matrix	GO:0005578	Proteinaceous extracellular matrix	4.80E-19	46
	GO:0030198	Extracellular matrix organization	9.70E-13	30
	GO:0044420	Extracellular matrix component	3.10E-12	22
	GO:0005604	Basement membrane	7.60E-09	16
	GO:0030199	Collagen fibril organization	1.60E-08	11
	GO:0032963	Collagen metabolic process	6.00E-07	12
Developmental processes	GO:0072359	Circulatory system development	1.80E-17	77
	GO:0001944	Vasculature development	1.70E-15	57
	GO:0001568	Blood vessel development	3.70E-15	55
	GO:0048646	Anatomical structure formation involved in morphogenesis	7.40E-13	69
	GO:0048514	Blood vessel morphogenesis	2.70E-12	45
	GO:0009887	Animal organ morphogenesis	7.20E-12	65
	GO:0001525	Angiogenesis	1.80E-11	39
	GO:0048729	Tissue morphogenesis	2.30E-09	45
	GO:0007507	Heart development	6.20E-09	41
	GO:0090092	Regulation of transmembrane receptor protein serine/threonine kinase signaling pathway	8.00E-09	23
Cell motility	GO:0030335	Positive regulation of cell migration	4.80E-15	43
	GO:0051270	Regulation of cellular component movement	9.30E-15	61
	GO:0030334	Regulation of cell migration	1.90E-14	56
	GO:0048870	Cell motility	4.80E-14	81
	GO:0002040	Sprouting angiogenesis	1.20E-07	13
	GO:0090287	Regulation of cellular response to growth factor stimulus	2.10E-07	22
	GO:0050920	Regulation of chemotaxis	4.80E-07	19
	GO:0001667	Ameboidal-type cell migration	4.90E-05	22
	GO:0010631	Epithelial cell migration	5.60E-05	17

Supplemental Table II-S11. (Cont.)

GO groups	GO IDs	GO terms	FDR	# of genes
Growth factor signaling	GO:0007167	Enzyme linked receptor protein signaling pathway	7.60E-12	58
	GO:0045597	Positive regulation of cell differentiation	7.50E-11	57
	GO:0070848	Response to growth factor	3.80E-10	44
	GO:0042327	Positive regulation of phosphorylation	1.30E-09	55
	GO:0001934	Positive regulation of protein phosphorylation	5.50E-09	52
	GO:0090092	Regulation of transmembrane receptor protein serine/threonine kinase signaling pathway	8.00E-09	23
	GO:0071559	Response to transforming growth factor beta	1.30E-08	22
	GO:0007169	Transmembrane receptor protein tyrosine kinase signaling pathway	3.70E-08	38
	GO:1905207	Regulation of cardiocyte differentiation	4.50E-08	10
	GO:0045785	Positive regulation of cell adhesion	4.50E-08	29
Cell proliferation	GO:0007067	Mitotic nuclear division	7.00E-08	32
	GO:0048285	Organelle fission	4.00E-07	38
	GO:0000280	Nuclear division	6.00E-07	36
	GO:0050678	Regulation of epithelial cell proliferation	4.50E-05	21
Protein transport	GO:0046822	Regulation of nucleocytoplasmic transport	7.40E-06	18
	GO:0006606	Protein import into nucleus	1.80E-05	20
	GO:0042306	Regulation of protein import into nucleus	2.00E-05	15
	GO:1900180	Regulation of protein localization to nucleus	2.40E-05	17
	GO:0034504	Protein localization to nucleus	3.30E-05	23
Response to wounding	GO:0042060	Wound healing	2.10E-10	35

The top 10 gene ontology (GO) identifications (IDs) and terms are shown for the GO groups including developmental processes, and growth factor cell signalling. FDR, false discovery rate; #, number.

Supplemental Table II-S12. KEGG and REACTOME signaling pathway enrichment for differentially expressed mRNAs in mesenteric arteries of 7- and 14 days angiotensin II-infused mice

Signaling pathways	7 days Ang II-infused mice		14 days Ang II-infused mice	
	All DE mRNAs	**DE miRNA-targeted DE mRNAs**	**All DE mRNAs**	**DE miRNA-targeted DE mRNAs**
	FDR (# of gene)	FDR (# of gene)	FDR (# of gene)	FDR (# of gene)
PI3K-Akt	3.22E-05 (13)		7.77E-08 (41)	2.27E-05 (26)
PDGF			8.14E-06 (23)	2.40E-05 (17)
IGF			1.81E-03 (11)	
ERBB2			6.83E-03 (15)	7.17E-03 (11)
FGFR			7.41E-03 (14)	
Rap1			7.99E-03 (19)	
p53			8.38E-03 (9)	
DAP12			8.42E-03 (15)	
EGFR			1.45E-02 (15)	

Ang, angiotensin; DE, differentially expressed; FDR, false discovery rate; #, number.

Supplemental table II-S13. Gene ontology (GO) term enrichment in EHF-targeting DE mRNAs in mesenteric arteries of 14 days angiotensin II-infused mice

GO groups	GO IDs	GO terms	FDR	# of genes
Extracellular matrix	GO:0030198	Extracellular matrix organization	1.20E-27	63
	GO:0005578	Proteinaceous extracellular matrix	2.00E-27	20
	GO:0031012	Extracellular matrix	3.40E-26	65
	GO:0044420	Extracellular matrix component	5.40E-18	32
	GO:0044259	Multicellular organismal macromolecule metabolic process	1.60E-13	24
	GO:0044243	Multicellular organism catabolic process	3.60E-13	19
	GO:0032963	Collagen metabolic process	2.40E-12	13
	GO:0030574	Collagen catabolic process	5.60E-12	26
	GO:0005604	Basement membrane	3.10E-10	76
	GO:0030199	Collagen fibril organization	6.10E-10	21
Developmental processes	GO:0001944	Vasculature development	1.90E-11	12
	GO:0030334	Regulation of cell migration	1.30E-10	43
	GO:0001525	Angiogenesis	1.50E-09	47
	GO:0030335	Positive regulation of cell migration	1.50E-09	21
	GO:0048514	Blood vessel morphogenesis	2.70E-09	29
	GO:1901342	Regulation of vasculature development	2.00E-08	13
	GO:0001501	Skeletal system development	3.00E-08	43
	GO:1904018	Positive regulation of vasculature development	5.70E-08	41
	GO:0007517	Muscle organ development	8.90E-08	35
	GO:0001655	Urogenital system development	6.00E-06	29
Growth factor signaling	GO:0005539	Glycosaminoglycan binding	4.20E-13	27
	GO:0032403	Protein complex binding	1.80E-12	22
	GO:0008201	Heparin binding	6.80E-11	34
	GO:0070848	Response to growth factor	1.00E-10	12
	GO:0005178	Integrin binding	1.20E-10	66
	GO:0071363	Cellular response to growth factor stimulus	3.80E-10	16
	GO:0090092	Regulation of transmembrane receptor protein serine/threonine kinase signaling pathway	7.30E-10	12
	GO:0005518	Collagen binding	9.50E-10	16
	GO:0090287	Regulation of cellular response to growth factor stimulus	2.70E-09	21
	GO:0071559	Response to transforming growth factor beta	5.10E-09	15

Supplemental Table II-S13. (Cont.)

GO groups	GO IDs	GO terms	FDR	# of genes
Response to wounding	GO:0009611	Response to wounding	6.40E-10	56
	GO:0042060	Wound healing	3.60E-09	48
	GO:1903035	Negative regulation of response to wounding	5.30E-05	11
	GO:1903034	Regulation of response to wounding	9.40E-05	16
	GO:0061041	Regulation of wound healing	2.10E-04	14
Ossification	GO:0001501	Skeletal system development	3.00E-08	43
	GO:0001503	Ossification	4.40E-08	36
	GO:0051216	Cartilage development	6.30E-07	22
	GO:0061448	Connective tissue development	1.20E-06	25
	GO:0002062	Chondrocyte differentiation	3.80E-05	13
	GO:0030278	Regulation of ossification	2.20E-04	17
	GO:0060348	Bone development	8.20E-04	15
Peptidase activity	GO:0008237	Metallopeptidase activity	3.60E-07	23
	GO:0008236	Serine-type peptidase activity	2.30E-06	29
	GO:0010466	Negative regulation of peptidase activity	1.10E-05	24
	GO:0061134	Peptidase regulator activity	8.80E-05	20
	GO:0010951	Negative regulation of endopeptidase activity	1.10E-04	21
	GO:0004222	Metalloendopeptidase activity	1.20E-04	13
	GO:0030414	Peptidase inhibitor activity	5.30E-04	16
Cell proliferation	GO:0007067	Mitotic nuclear division	5.30E-09	42
	GO:0000070	Mitotic sister chromatid segregation	2.40E-08	21
	GO:0000819	Sister chromatid segregation	9.00E-08	26
	GO:0051983	Regulation of chromosome segregation	2.00E-06	14
	GO:0000922	Spindle pole	2.10E-06	17
	GO:0050673	Epithelial cell proliferation	6.10E-06	31
	GO:0007059	Chromosome segregation	1.40E-05	28
	GO:0005819	Spindle	1.50E-05	26
	GO:0050678	Regulation of epithelial cell proliferation	2.90E-05	26
	GO:0051303	Establishment of chromosome localization	3.80E-05	11

Supplemental Table II-S13. (Cont.)

GO groups	GO IDs	GO terms	FDR	# of genes
Protein transport	GO:0046822	Regulation of nucleocytoplasmic transport	8.30E-05	20
	GO:1900180	Regulation of protein localization to nucleus	9.50E-05	20
	GO:0042306	Regulation of protein import into nucleus	1.30E-04	17
	GO:0046824	Positive regulation of nucleocytoplasmic transport	7.10E-04	12

FDR, false discovery rate; #, number.

Supplemental table II-S14. *In vivo* miR-431-5p inhibition did not alter the organ weights corrected by tibia length in angiotensin (Ang) II infused mice.

miR-inhibitors	Number	HW/TL (mg/mm)	KW/TL (mg/mm)	LW/TL (mg/mm)	SW/TL (mg/mm)
Ctrl	7	8.7 ± 0.2	18.0 ± 0.7	79.3 ± 3.4	3.8 ± 0.3
miR-431-5p	7	8.5 ± 0.3	18.5 ± 0.5	84.9 ± 1.8	3.3 ± 0.2

The heart (HW), kidneys (KW), liver (LW) and spleen (SW) weights and tibia length (TL) were determined in wild-type mice infused with angiotensin II (1000 ng/kg/min) for 14 days and injected IV with 20 mg/kg of control (Ctrl) or miR-431-5p microRNA (miR) inhibitors on day 1 and 7 of the treatment period. Data are presented as means ± SEM.

CHAPTER III: Vascular ncRNA profiling in essential hypertension with or without CKD

microRNA profiling in small resistance arteries of hypertensive patients with or without chronic kidney disease

Ku-Geng Huo[1], Júlio C. Fraulob-Aquino[1], Chantal Richer[3], Asia Rehman[1], Marie Briet[1,5], Mark L. Lipman[1,2], Daniel Sinnett[3,4], Pierre Paradis[1], Ernesto L. Schiffrin[1,2]

[1]Vascular and Hypertension Research Unit, Lady Davis Institute for Medical Research, [2]Department of Medicine, Sir Mortimer B. Davis-Jewish General Hospital, McGill University,

[3]Division of Hematology-Oncology, Research Center, CHU Ste-Justine,

[4]Department of Pediatrics, Faculty of Medicine, Université de Montréal, Montréal, Canada;

[5]INSERM U1083, CNRS UMR 6214, Centre Hospitalo-Universitaire d'Angers, Université d'Angers, Angers, France.

Disclosure:

This work was supported by the Canadian Institutes of Health Research (CIHR) grants MOP123465, a First Pilot Foundation Grant 143348, and a Discovery Grant from Servier France.

Abstract

Background: Hypertension and chronic kidney disease (CKD) are global health disorders that are epidemiologically associated. Vascular injury is an early manifestation in HTN and contributes to CKD. MicroRNAs (miRs) are important non-coding RNA regulators of gene expression. Dysregulation of miRs has been shown in HTN and CKD, but their implication in vascular injury remains unclear. We aimed to identify differentially expressed (DE) miRs in small arteries of HTN and CKD human subjects to get further insight into the pathophysiology of vascular injury in HTN and CKD.

Methods and results: Normotensive, hypertensive and CKD subjects (n=15-16) were studied. Total RNA was extracted from small arteries dissected from subcutaneous gluteal biopsies. The RNA was used for total and small RNA sequencing by Illumina HiSeq 2500. DE miRs and DE mRNAs (P<0.05) were identified using EdgeR, which demonstrated 3 up- and 6 down-regulated miRs, as well as 134 up- and 149 down-regulated mRNAs uniquely associated with hypertension, 42 up- and 39 down-regulated miRs, as well as 743 up- and 348 down-regulated mRNAs uniquely associated with CKD, while 2 up-regulated miRs and 101 up- and 75 down-regulated mRNAs were found in both groups. Target Scan was used to predict DE miR targets in the DE mRNAs. Enrichment analysis showed that the hypertension-associated DE miR-targeting DE mRNAs were highly enriched in gene ontology (GO) terms involved in peptidase activity, mitochondrial activity and immune responses (q<0.01), whereas the CKD-associated DE miR-targeting DE genes were highly enriched in GO terms involved in tube formation, fibroblast proliferation and EGF responses (q<0.001).

Conclusions: DE miRs were identified in small arteries of hypertensive and CKD patients. Enrichment analysis in DE miR-targeting DE mRNAs revealed GO terms that could be linked to different degrees of vascular changes in hypertension and CKD.

Introduction

Hypertension is one of the most prevalent global health disorders and is ranked the number one risk factor for death and disability worldwide, accounting for 9.4 million deaths and 7.0% disability-adjusted life in 2010 (1). Chronic kidney disease (CKD) is a global health burden with a worldwide prevalence of 13.4% for stages 1-5 and 10.6% for stages 3-5, according to a meta-analysis in 2016 (2). There is an epidemiological association between hypertension and CKD. The prevalence of high blood pressure has been reported in the 2000-2006 Kidney Early Evaluation Program to be over 85% in stage 3 and over 90% in stages 4-5 CKD patients (3). Hypertension and CKD are associated with vascular injury that is characterized by vascular remodeling (4, 5), stiffening (6, 7) and endothelial dysfunction (8-11), which contribute to further development of the disease and lead to end organ damage. Small resistance artery remodeling in particular may be the first manifestation of target-organ damage in hypertension (9). Large artery stiffness on the other hand, has a strong predictive value for mortality (12) and primary coronary events (13) in hypertensive patients. The molecular mechanisms underlying vascular injury are complex and still remain to be elucidated.

microRNAs (miRNAs) are small non-coding RNAs that act as master regulators on gene expression during normal cellular processes. In a canonical fashion, they bind to the 3' untranslated regions (UTRs) of their target mRNAs and cause mRNA degradation and translational repression (14-16). Aberrant miRNA expression has been linked to cardiovascular disease by studies over the last decade (17-21). Differentially expressed (DE) miRNAs have been identified in plasma of essential hypertensive patients (22) and CKD patients (23, 24) in profiling studies. Hypertension-associated single nucleotide polymorphisms (SNPs) were identified on miRNA-binding sites of genes that are related to the renin-angiotensin-aldosterone system (RAAS) (25) and vascular contractility (26).

Nevertheless, the role of miRNAs in vascular injury in essential hypertension and CKD is still unclear. We hypothesized that in patients with hypertension with or without CKD, miRNA and mRNA expression profiling in the wall of subcutaneous small resistance arteries would reveal miRNAs that regulate expression of mRNAs involved in

vascular injury. In the present study, we used an unbiased approach that combines miRNA and mRNA profiling by next generation sequencing, miRNA and transcription factor target prediction, gene enrichment analysis and wet lab validation to identify DE vascular miRNAs and mRNAs, as well as their interactions. In the first study of this thesis (Chapter II), we have performed gene expression profiling in small mesenteric arteries of angiotensin (Ang) II-infused mice. Combining the findings of the human and mouse studies allowed us to identify conserved vascular injury-associated genes involved in RAAS activation. The ultimate goal is to identify miRNAs master regulators and harness them as biomarkers or as novel therapeutic targets for clinical application.

Methods

Subject recruitment

The study protocol was approved by the Human Research Ethics Review Committee of the Jewish General Hospital, where the study was carried out. All the subjects included in the study provided written informed consent to participate. A complete physical examination was performed. Body weight and height were determined. Brachial blood pressure (BP) was measured with an automated device, BpTRU BPM-300 (VSM MedTech Devices, Coquitlam, BC, Canada) in a quiet room with controlled temperature of 22°C dedicated to BP determination after 5 min of rest in a sitting position in the absence of observers 6 times at 1 min intervals, and the mean of the last 5 measurements was used.

From June 25, 2013 to April 25, 2016, 16 hypertensive subjects were recruited in the study on the basis of systolic BP >135 mmHg or diastolic BP of 85-115 mmHg with BpTRU BPM-300 or treatment with anti-hypertensive medication for at least 6 months; 15 hypertensive subjects with nephroangiosclerosis (CKD group) on the basis of hypertension as above complicated with nephropathy defined as alteration of glomerular filtration rate (eGFR) below 60 mL/min/1.73 m2, after exclusion of other causes of CKD; and 15 normotensive subjects without hypertension or kidney disease. Subjects enrolled were 33 to 78 years old. The patients were followed in the Kidney Treatment Center and

in the Cardiovascular Prevention Center located on the first floor of Pavilion H of the Jewish General Hospital.

Subjects meeting any one of the following criteria were excluded: myocardial infarction within the 6 months; percutaneous coronary angioplasty or coronary artery bypass surgery within last 6 months; clinically significant atrioventricular (AV) conduction disturbances or arrhythmias (e.g. second- or third-degree AV block, sick-sinus syndrome or clinically significant bradycardia- resting heart rate <45 beats/minute); tachyarrhythmias; clinically significant arrhythmias; presence of an accessory bypass tract (e.g. Wolff-Parkinson-White syndrome); unstable angina pectoris; current or prior history of heart failure or known left ventricular ejection fraction ≤40%. In addition; smoking of 10 cigarettes or more, diabetes; co-existent conditions which could independently affect resistance vessels (e.g. any disease which may be associated with vasculitides: collagen-vascular diseases, chronic hepatitis B antigenemia, circulating immune complexes, complement disorders, amyloidosis, scleroderma, etc.); other concurrent severe disease which could preclude participation or survival, such as neoplasms or Acquired Immunodeficiency Syndrome (AIDS), or patients known to be human immunodeficiency virus (HIV) positive; any known bleeding or platelet disorder; mentally or legally incapacitated patients; or inability or unwillingness on the part of the patient to sign the Patient Informed Consent Form.

Biological sample collection

On the day of subject inclusion, blood and urine were sampled in the morning under fasting conditions. Blood was collected in BD Vacutainer EDTA or Vacutainer Plus serum tubes for blood biochemistry and urine analysis determined in the department of Diagnostic Medicine at the Jewish General Hospital according to routine methods. eGFR was determined by the Modification of Diet in Renal Disease formula (27).

Large artery evaluation

All patients were studied in a supine position in a quiet room with controlled temperature of 22 ± 1°C dedicated to vascular study. BP was measured with a BpTRU BPM-300 6 times at 2 min intervals, and the mean of the last 5 measurements was used. End-diastolic internal diameter, stroke change in diameter, and intima-media thickness (IMT) were measured on the right common carotid artery 2 cm before the bifurcation with a high-precision echotracking device (ArtLab®, Esaote, Maastricht, The Netherlands), as previously described and validated (28-30). Right radial artery and common carotid artery pressure waveforms were recorded non-invasively by aplanation tonometry (Sphygmocor®, Atcor Medical, Sydney, Australia), as previously validated (28, 30, 31). Circumferential wall stress ($\sigma\theta$, kPa) was calculated according to Lame´s equation as $\sigma\theta$ = (DBP x Dd)/2 x hd, where DBP is diastolic BP, and Dd and hd are the diastolic values of internal diameter and wall thickness during the cardiac cycle, respectively (32, 33). Carotid distensibility was determined from systolic–diastolic variations in arterial cross-sectional area (ΔA) and carotid pulse pressure (ΔP), assuming the lumen to be circular. The cross-sectional distensibility coefficient (DC) was calculated as $\Delta A/A \times \Delta P$. Carotid stiffness was calculated as DC½ as previously described (30). Incremental Young's elastic modulus was calculated as [3(1 + A/wall cross-sectional area)]/DC, where A is the diastolic lumen area (34, 35). Aortic stiffness was measured through the carotid to femoral pulse wave velocity (PWV) between the two sites by the foot-to-foot velocity method (Sphygmocor®, Atcor Medical, Sydney, Australia). Pulse transit time (seconds) between the carotid and femoral sites was multiplied by 0.8 and then divided by the distance (m) to obtain carotid-femoral PWV (30, 36). The 0.8 scaling factor was used to correct for the overestimation of the real carotid-femoral distance (37).

Subcutaneous biopsy

Gluteal biopsies of skin/subcutaneous tissue of the buttock were done at 8 am under sterile conditions and under local anesthesia with 2% lidocaine as previously described (38, 39). The skin/subcutaneous tissue sample was immediately placed in ice cold sterile PBS. Small arteries of about 150 to 300 μm were dissected and stored in RNAlater (ThermoFisher Scientific, Waltham, MA) and used immediately for total RNA isolation.

RNA extraction

Total RNA was isolated from small arteries using the mirVana miRNA isolation kit (ThermoFisher Scientific) as follows. In brief, small arteries were homogenized in 1 ml of Lysis/Binding Buffer using a Polytron PT 1600 E homogenizer (Brinkmann Instruments, Mississauga, ON, Canada) equipped with a dispersing aggregate PT-DA 1607/2EC at maximum speed for 1 min. The foam generated during the homogenization was removed by centrifuging at 1,500 g for 3 min at 4°C. The homogenate was then processed as recommended by the manufacturer to isolate total RNA containing miRNAs. The concentration and purity of the RNA were assessed with a NanoDrop spectrophotometer ND-100 V3.1.2 (Thermo Fisher Scientific). Quality of the total and small RNA was assessed with an Agilent RNA 600 Nano kit and an Agilent Small RNA kit, respectively, using an Agilent 2100 bioanalyzer (Agilent Technologies, Santa Clara, CA). RNA samples were separated into 3 tubes: 200-1000 ng for small RNA library preparation, 100 ng for total RNA library preparation, and the remaining RNA for reverse transcription-quantitative PCR (RT-qPCR) validation of selected genes. The tubes were stored at -80°C until used.

Small RNA and total RNA library construction

Total RNA (amounts indicated above) was used for small RNA library construction using the TruSeq small RNA sample preparation kit (Illumina, San Diego, CA) as indicated by the manufacturer with minor modification, as all the libraries were amplified using 15 cycles of PCR. Purification of amplified cDNA using 6% Novex TBE gel (ThermoFisher Scientific, Waltham, MA) was modified as follows, 160 µL of each pool of amplified cDNA libraries was concentrated using Agencourt AMPure XP PCR purification system (Beckman Coulter, Beverly, MA). In 1.5 mL tubes, each 160 µL of each pool of amplified cDNA libraries was mixed with 320 µL of AMPure XP paramagnetic bead mixture in a 1.5 mL tube, and incubated for 90 min at room temperature to ensure maximum binding of the small cDNA fragments. The tubes were inserted in a DynaMag-2 magnet (ThermoFisher Scientific) and incubated for 30 min at room temperature to

allow optimal separation of the small cDNA fragments bound to the magnetic beads from the contaminants. The small cDNA fragments bound to the magnetic beads were washed twice with 80% ethanol, and suspended in a large volume of water (100 µL) to ensure optimal elution. The volume of the eluate was reduced to 18 µL using a SpeedVac system, 4 µL of DNA loading dye was added, and loaded in one lane of a 6% Novex TBE gel. At the end of the electrophoresis, the gel was view on a UV transilluminator FOTO/PrepII (Fotodyne, Hartland, WI) and the 147 nt band primarily containing mature miRNA generated from ~22 nt small RNA fragment was isolated and processed as indicated in the manufacturer protocol.

One hundred ng of total RNA was used for total RNA library construction using the TruSeq stranded total RNA sample preparation kit as indicated by the manufacturer (Illumina).

RNA sequencing and data analysis

Small (miRNA) and total RNA libraries were sequenced was with an Illumina HiSeq 2500 system following the manufacturer's protocol at the platform of Integrated Centre for Pediatric Clinical Genomics of the Research Center of the Sainte-Justine University Hospital. The miRNA sequencing was done in the 1 x 50 bp high-output mode and total RNA sequencing in the 2 x 75 bp high-output mode.

Sequence data were first examined for base quality using FastQC (https://www.bioinformatics.babraham.ac.uk/projects/fastqc/). Sequences were mapped to the human genome hg38 with STAR (40). Small RNA sequences were mapped using the option *--outFilterMismatchNoverLmax 0.05* that allows a maximal mismatch ratio of 0.05 (no mismatch allowed for reads <20 nt and 1 mismatch allow per 20 nt). HTSeq-count (41) was used for total RNA gene annotation and counting. miRDeep2 was used for novel miRNA prediction, known and novel miRNA annotation and counting (42). EdgeR was used for differential expression analysis (43). A trimmed mean of M-values (TMM) method in the EdgeR protocol was used for sequence read normalization. Only genes with expression level ≥2 reads per million mapped reads in ≥14 samples (lowest subject # in any group) were analyzed. TargetScan was used to predict DE miRNA

targets in the DE mRNAs (44). Only predicted targets with context score percentile >50% were included in further analyses. TF binding site prediction in the promoter (1000 bp upstream of exon 1) was perform with the FIMO tool of Meme Suite (45). Molecular network construction was done in Cytoscape (46). Gene enrichment analysis was performed using the ClueGO tool in Cytoscape (47).

Statistical analysis

Results are presented as means ± SD. Comparisons between multiple groups were analyzed by one-way analysis of variance (ANOVA) followed by a Student–Newman–Keuls *post-hoc* test or Kruskal-Wallis one-way ANOVA on ranks, as needed. For RNA sequencing data analysis, an ANOVA-like test in EdgeR based on generalized linear models was used for differential expression analysis. Differential expression was defined as $P<0.05$.

Results

Clinical characteristics and large artery evaluation

The demographic parameters are presented in Table III-1. Fifteen normotensive subjects, 16 hypertensive patients and 15 CKD patients were recruited for this study from June 25, 2013 to April 25, 2016. The CKD patients were slightly older than normotensive subjects. The CKD group contained more male than female compared to the other groups that presented only slightly more male than female. Both hypertensive and CKD patients had higher systolic and diastolic blood pressure compared to normotensive subjects. High-density lipoprotein (HDL) was lower in CKD patients compared to normotensive subjects. Triglycerides and fasting blood glucose were similar in all groups. As expected, eGFR was lower in CKD patients compared to both normotensive subjects and hypertensive patients. It is noteworthy that eGFR was slightly lower in hypertensive patients compared to normotensive subjects, but >60 ml/min/1.73 m^2.

The hemodynamic characteristics are presented in Table III-2. As expected, hypertensive and CKD patients presented higher systolic, mean and diastolic BP. Carotid

internal diameter, IMT, wall/lumen, and wall cross-sectional area were similar in all groups. The carotid circumferential wall stress was greater in hypertensive and tended to be higher in CKD compared to normotensive subjects. The carotid distensibility was lower, and carotid Young elastic modulus and carotid stiffness were higher in hypertensive and CKD patients compared to normotensive subjects. The aorta was stiffer in hypertensive and CKD patients compared to normotensive subjects, as demonstrated by a greater carotid-femoral PWV.

Vascular small and total RNA profiling

Variable numbers and sizes of small arteries were dissected from gluteal biopsies of skin/subcutaneous tissue of the buttock. Total RNA was extracted successfully in all the samples except for one CKD patient due to the lack of arteries in the biopsies. On average, 1.5 μg (0.3-4.5 μg) of total RNA was extracted from the small arteries per subject. Due to the low RNA concentration in several samples, the RNA integrity numbers (RINs) were determined only in a subgroup of samples (19 out of 46) using the Agilent 2100 bioanalyzer. On average, a RIN of 7.9 was obtained, which indicate a good RNA quality. Despite the fact that a RIN could not be measured, the remaining samples with relatively low RNA concentration presented good RNA electrophoretic profiles (Fig. III-4), as the proportions of 18S and 28S RNA are similar as the samples with high RNA concentration and good RINs. All the samples were used to construct the small and total RNA libraries.

An average of 24.1 million qualified single-end reads per sample was obtained in the small RNA sequencing data, of which 78.3% and 15.3% were mapped to a unique locus and multiple loci of the human genome hg38 by STAR, respectively. As for the total RNA sequencing, an average of 27.9 million qualified pair-end reads per samples was obtained, of which 86.6% and 7.8% were mapped to a unique locus and multiple loci of the human genome hg38, respectively.

We identified 3 up-regulated and 6 down-regulated miRNAs, as well as 134 up-regulated and 149 down-regulated mRNAs uniquely associated with the hypertensive group, while 42 up-regulated and 39 down-regulated miRNAs, as well as 743 up-

regulated and 348 down-regulated mRNAs were found uniquely associated with the CKD group (Fig. III-1). Meanwhile, 2 up-regulated miRNAs, as well as 101 up-regulated and 75 down-regulated mRNAs were found in both groups.

We generated molecular networks to integrate predicted interactions between DE miRNAs and inversely expressed DE mRNAs and between DE TF and DE genes, and the 3 top enriched gene ontology (GO) terms for the hypertensive and CKD groups. The molecular networks showed that the hypertension-associated DE miRNA-targeting DE mRNAs were highly enriched in gene ontology (GO) terms involved in peptidase activity, mitochondrial activity and immune response (Fig. III-2), while the CKD-associated DE miRNA-targeting DE genes were highly enriched in GO terms involved in tube formation, fibroblast proliferation and EGF response (Fig. III-3).

Common gene changes between Ang II-infused mouse models and hypertensive patients with and without CKD

Comparing all the DE miRNAs and mRNAs found in the 7-day and 14-day Ang II-infused mice, essential hypertensive patients and CKD patients, we aimed to identify conserved vascular injury-associated genes involved in RAAS activation. One common DE miRNA, miR-145-3p, was down-regulated in both 7-day Ang II-infused mice and CKD patients. In terms of common DE mRNAs, 6 mRNAs (*Zfp36l2, Mafb, Ttyh3, Slc16a3, Kdm6b, Pld4*) were up-regulated, and 3 mRNAs (*Nucb2, Slc38a4, Ptn*) were down-regulated in the 14-day Ang II-infused mice, hypertensive patients and CKD patients. *KCTD12* and *C3* were up-regulated, whereas *Leo1* and *Ybx2* were down-regulated in both 14-day Ang II-infused mice and hypertensive patients. There were 42 up-regulated (not listed here) and 2 down-regulated (*Enpep* and *Tuft1*) mRNAs in both 14-day Ang II-infused mice and CKD patients.

Discussion

DE miRNAs and mRNAs were identified in small resistance arteries of hypertensive and CKD patients compared to those in vessels from normotensive subjects. Although similar

degrees of BP elevation and large artery (carotid and aortic) stiffness were observed between hypertensive patients and CKD patients, enrichment analysis in DE miRNA-targeting DE mRNAs revealed GO terms that could be linked to different degrees and types of small arterial changes between hypertension and CKD. It is noteworthy that the hypertensive subjects have lower eGFR compared to the normotensive subjects, which suggests that a subset of these subjects, although not classified as CKD, may display an early stage of impaired renal function.

This is still an ongoing study with additional analyses and experiments to be performed. Future experiments will include validating differential expression of selected DE miRNAs and their DE mRNA targets by real-rime quantitative reverse transcription polymerase chain (RT-qPCR), confirming miRNA-mRNA interactions by luciferase reporter assays and gain- or loss-of-function studies by miRNA mimic or inhibitor transfection, respectively. Candidate miRNAs and mRNAs selection will take into account the results from the degree of differential expression (*P* value and fold change), expression levels, gene enrichment analyses, RNA interactions and conserved gene changes between our Ang II-infused mouse model and patients.

The sole common DE miRNA between the Ang II-infused mouse model and patients, namely miR-145-3p, will be one of our main focuses in future experiments. miR-145-3p has recently been shown to be down-regulated in different cancers (48, 49), and we also observed down-regulation in the 7-day Ang II-infused mice and CKD patients. Chen *et al*. demonstrated that miR-145-3p was down-regulated in lung cancer and was able to inhibit cell migration and invasion by targeting Phosphoinositide-Dependent Protein Kinase-1 (*PDK1*) and suppressing mTOR activation (48). Goto *et al*. reported that miR-145-3p was also down-regulated in prostate cancer, where it targeted *MELK, NCAPG, BUB1*, and *CDK1*, all of which were up-regulated in prostate cancer and allowed prediction of patients' survival (49). Our mouse data showed that Ang II infusion caused up-regulation of genes involved in cell migration and proliferation. The CKD-associated DE genes we found in the present study also revealed enrichment for cell growth and proliferation. These genes may contribute significantly to vascular remodeling and stiffening. The possibility to inhibit cell migration and proliferation

makes miR-145-3p an interesting target for future clinical applications and to understand the pathophysiological molecular mechanisms of vascular injury.

Among the 9 conserved DE mRNAs in the Ang II-infused mouse model, hypertensive patients and CKD patients, some have been associated with cardiovascular disease. The AA and GA genotypes of single nucleotide polymorphism (SNP) rs2902940 of MAF BZIP Transcription Factor B (*MAFB*) have been shown to associate with increased risk of coronary artery disease and ischemic stroke, compared to the GG genotype (50). Interestingly, the association was found only in patients with higher body mass index, hypertension or diabetes. The C genotype of SNP rs12601558 of Solute Carrier Family 16 Member 3 (*SLC16A3*) has been linked to CKD in children (51) and chronic hypoxia-induced pulmonary hypertension (52). Lysine Demethylase 6B (*Kdm6b*) was shown to be up-regulated in the aortas of Ang II-infused rats, and was believed to cause demethylation of H3K27me3, therefore activating the transcription of Na+-K+-2Cl− Cotransporter 1 (*NKCC1*), which plays a role in maintenance of vascular tone and BP regulation (53). Phospholipase D Family Member 4 (*PLD4*) was reported to be a susceptibility gene for systemic sclerosis (54), a connective tissue autoimmune disease characterized by increased extracellular matrix protein production that is associated with systemic and renal artery injury (55). Pleiotrophin (PTN) has been known to be a heparin-binding cytokine that induces angiogenesis under normal and pathological conditions (56). PTN treatment activates expression of Vascular Endothelial Growth Factor (*VEGF*) in endothelial cells, improving cell migration (57). It was also able to reduce Prostaglandin-Endoperoxide Synthase 2 (*COX-2*) expression and induce Interleukin-10 (*IL-10*) and Transforming Growth Factor Beta (*TGFβ*) expression in macrophages, demonstrating an anti-inflammatory property. However, the relationship between vascular damage and these conserved DE mRNAs and the underlying pathophysiological molecular mechanisms are still unclear. Although preliminary analyses indicate that miR-145-3p does not target any of these conserved DE miRNAs in the canonical fashion, it does not rule out the possibility of non-canonical non-seed binding or indirect targeting. Deeper analyses and further experiments are required to investigate their potential interactions.

Table III-1. Demographic characteristics

Parameters	Normotensive subjects	Hypertensive patients	CKD patients
Number od subjects	15	16	16
Age (years)	52.5 ± 11.3	59.0 ± 10.3	65.7 ± 7.4*
Sex (male/female)	8/7	9/7	13/3
Body mass index (kg/m^2)	25.9 ± 4.1	26.3 ± 3.0	28.9 ± 5.2
Waist circumference (cm)	91.1 ± 11.7	90.9 ± 9.5	100.1 ± 15.9
SBP (mmHg)	116 ± 11	129 ± 15*	135 ± 21**
DBP (mmHg)	78 ± 6	81 ± 2*	79 ± 9*
Triglycerides (mmol/L)	1.0 ± 0.6	1.1 ± 0.5	1.4 ± 0.8
HDL (mmol/L)	1.8 ± 0.6	1.7 ± 0.5	1.4 ± 0.3*
Fasting blood glucose (mmol/L)	4.7 ± 0.5	4.8 ± 0.7	5.0 ± 0.8
eGFR (ml/min/1.73 m^2)	99.8 ± 17.5	87.7 ± 12.5*	45.5 ± 11.2**†

The baseline parameters of the normotensive and hypertensive subjects and chronic kidney disease patients (CKD) were determined at the time of the recruitment. SBP and DBP, systolic and diastolic blood pressure; HDL, high-density lipoprotein; eGFR, estimated glomerular filtration rate. Data are presented as means ± SD, *P<0.05 and **P<0.01 vs normotensive subjects, and †P<0.001 vs hypertensive subjects.

Table III-2. Hemodynamic and mechanical parameters

Parameters	Normotensive subjects	Hypertensive patients	CKD patients
Number of subjects	15	16	16
Right radial artery pressures			
SBP (mm Hg)	122 ± 56	125 ± 14*	127 ± 14*
DBP (mm Hg)	69 ± 8	77 ± 9*	74 ± 7
MBP (mm Hg)	83 ± 10	96 ± 11**	94 ± 9**
Estimated central pressures			
SBP (mmHg)	101 ± 13	117 ± 14*	118 ± 15**
DBP (mmHg)	70 ± 8	78 ± 9*	77 ± 8.2*
MBP (mmHg)	83 ± 10	96 ± 11**	94 ± 9**
Right common carotid artery pressures and mechanical properties			
SBP (mmHg)	102 ± 14	122 ± 16**	121 ± 16**
DBP (mmHg)	69 ± 8	77 ± 9*	76 ± 8*
MBP (mmHg)	83 ± 10	96 ± 11**	94 ± 9**
Internal diameter (mm)	5.36 ± 0.59	5.55 ± 0.75	5.94 ± 0.78
IMT (µm)	876 ± 132	861 ± 149	924 ± 134
Wall/Lumen	0.165 ± 0.033	0.159 ± 0.044	0.157 ± 0.027
WCSA (mm^2)	17.2 ± 13.5	17.3 ± 3.2	17.6 ± 14.9
Circumferential wall stress (KPa)	33.9 ± 4.8	41.7 ± 12*	40.4 ± 10
Distensibility ($kPa^{-1} \times 10^{-3}$)	37.1 ± 13	19.4 ± 17.5**	20.2 ± 9**

Table III-2. Hemodynamic and mechanical parameters (Cont.)

Parameters	Normotensive subjects	Hypertensive patients	CKD patients
Right common carotid artery pressures and mechanical properties			
Young elastic modulus (KPa)	217 ± 194	477 ± 347**	448 ± 260**
Stiffness (m/s)	5.47 ± 1.14	7.66 ± 1.86**	7.60 ± 1.95**
Aortic stiffness			
Carotid-femoral PWV (m/s)	7.9 ± 1.4	9.4 ± 1.74*	9.7 ± 2.2*

The hemodynamic and mechanical parameters of the normotensive and hypertensive subjects and chronic kidney disease patients (CKD) were determined at the time of the large artery evaluation. SBP, DBP and MBP, systolic, diastolic and mean blood pressure; IMT, intima media thickness; WCSA, wall cross-sectional area; PWV, pulse wave velocity. Data are presented as means ± SD, *P<0.05 and **P<0.01 vs normotensive subjects.

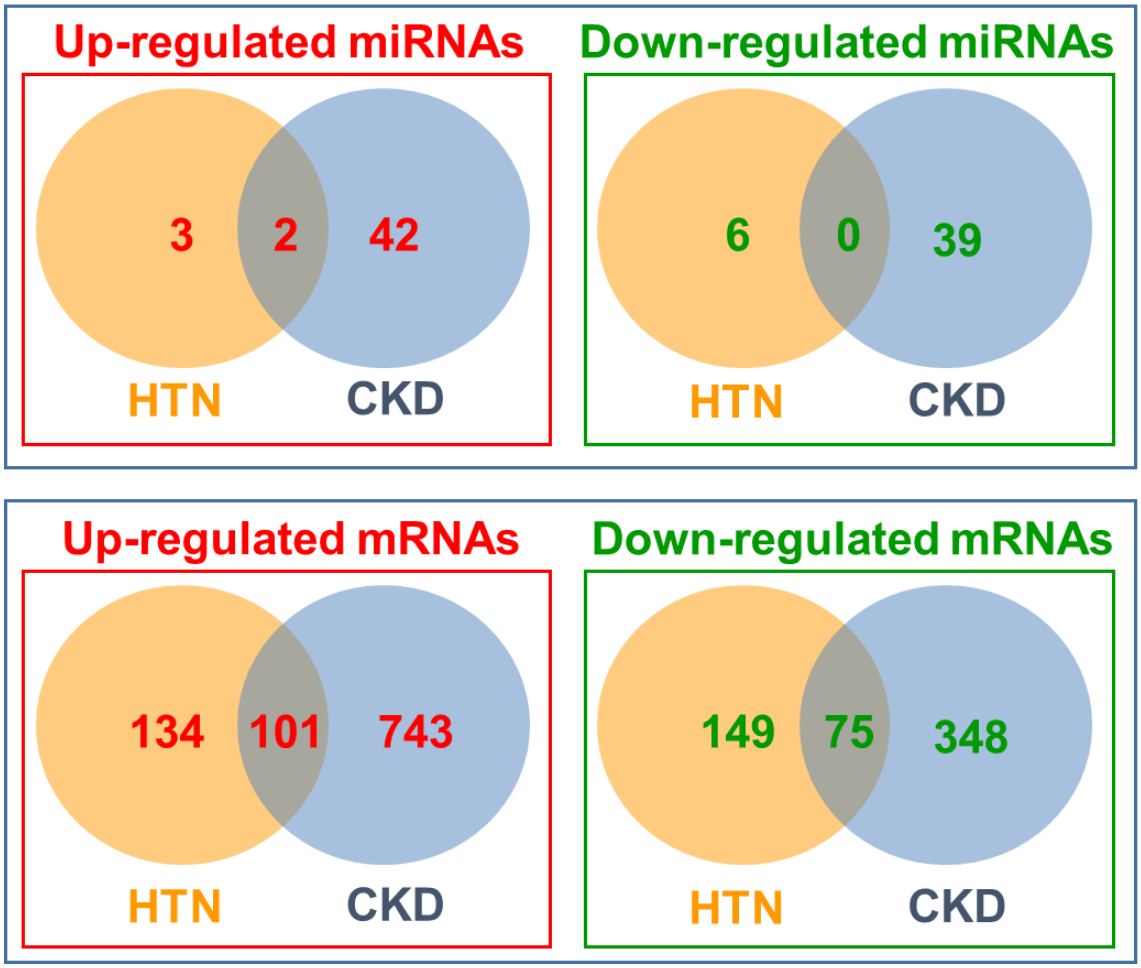

Figure III-1. Venn diagrams are presenting the number of differentially expressed miRNAs (upper panel) and differentially expressed mRNAs (lower panel) in small resistance arteries uniquely associated with the hypertensive (HTN), uniquely associated with the chronic kidney disease (CKD) patients and in both groups, compared to normotensive subjects ($P<0.05$).

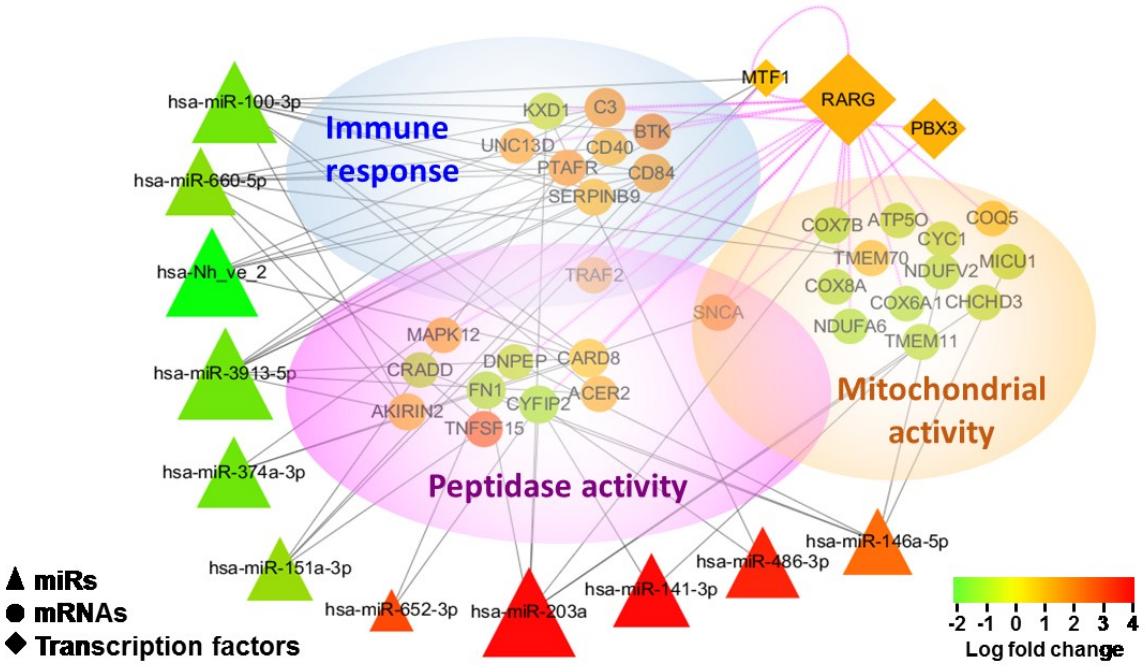

Figure III-2. The figure represents a molecular network integrating differentially expressed microRNA (miR) and gene data, the predicted interactions between miRs and mRNAs (black lines), transcription factors and genes (purple arrow lines), and top 3 enriched gene ontology (GO) terms in small arteries of hypertensive patients compared to normotensive subjects (q<0.01). The microRNA and transcription factor symbol sizes are proportional to the number of interaction with their targets. n = 15 for normotensive, 16 for hypertensive and 16 for CKD subjects.

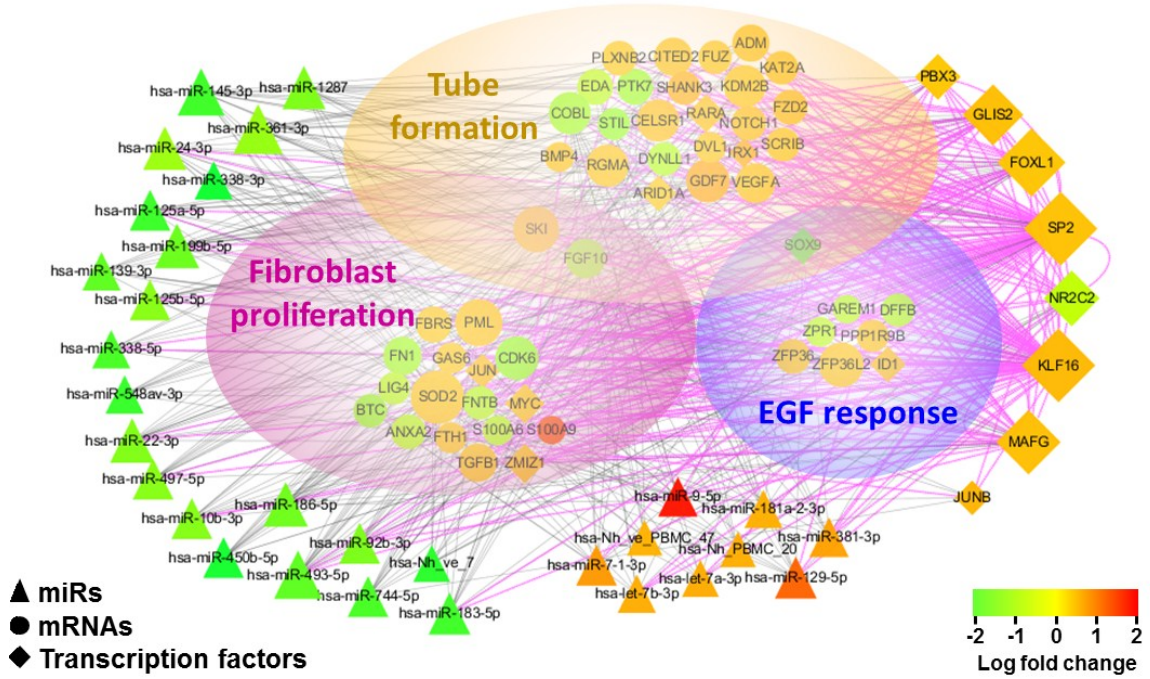

Figure III-3. The figure represents a molecular network integrating differentially expressed microRNA (miR) and gene data, the predicted interactions between miRs and mRNAs (black lines) and transcription factors and genes (purple arrow lines), and top 3 enriched gene ontology (GO) terms in small arteries of chronic kidney disease patients compared to normotensive subjects (q<0.001). The microRNA and transcription factor symbol sizes are proportional to the number of interaction with their targets. n = 15 for normotensive, 16 for hypertensive and 16 for CKD subjects.

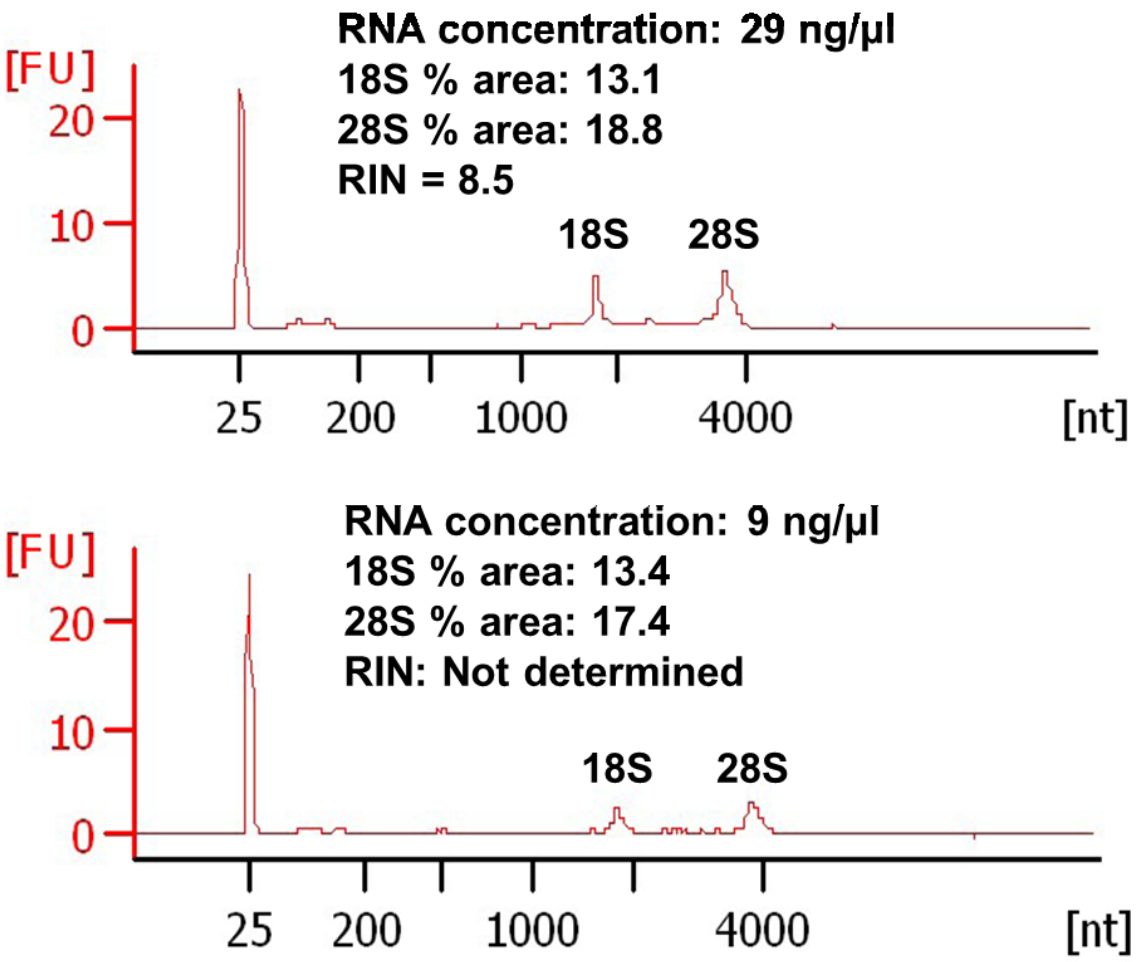

Figure III-4. **Determination of the quality of small artery RNA using an Agilent 2100 bioanalyzer.** Representative electrophoretic profiles for small artery RNA sample with high enough RNA concentration for detectable RIN of 8.5 (upper panel) and low RNA concentration that resulted in undetermined RIN (lower panel) are presented.

References

1. S. S. Lim, T. Vos, A. D. Flaxman, G. Danaei, K. Shibuya, H. Adair-Rohani, M. Amann, H. R. Anderson, K. G. Andrews, M. Aryee, C. Atkinson, L. J. Bacchus, A. N. Bahalim, K. Balakrishnan, J. Balmes, S. Barker-Collo, A. Baxter, M. L. Bell, J. D. Blore, F. Blyth, C. Bonner, G. Borges, R. Bourne, M. Boussinesq, M. Brauer, P. Brooks, N. G. Bruce, B. Brunekreef, C. Bryan-Hancock, C. Bucello, R. Buchbinder, F. Bull, R. T. Burnett, T. E. Byers, B. Calabria, J. Carapetis, E. Carnahan, Z. Chafe, F. Charlson, H. Chen, J. S. Chen, A. T. Cheng, J. C. Child, A. Cohen, K. E. Colson, B. C. Cowie, S. Darby, S. Darling, A. Davis, L. Degenhardt, F. Dentener, D. C. Des Jarlais, K. Devries, M. Dherani, E. L. Ding, E. R. Dorsey, T. Driscoll, K. Edmond, S. E. Ali, R. E. Engell, P. J. Erwin, S. Fahimi, G. Falder, F. Farzadfar, A. Ferrari, M. M. Finucane, S. Flaxman, F. G. Fowkes, G. Freedman, M. K. Freeman, E. Gakidou, S. Ghosh, E. Giovannucci, G. Gmel, K. Graham, R. Grainger, B. Grant, D. Gunnell, H. R. Gutierrez, W. Hall, H. W. Hoek, A. Hogan, H. D. Hosgood, 3rd, D. Hoy, H. Hu, B. J. Hubbell, S. J. Hutchings, S. E. Ibeanusi, G. L. Jacklyn, R. Jasrasaria, J. B. Jonas, H. Kan, J. A. Kanis, N. Kassebaum, N. Kawakami, Y. H. Khang, S. Khatibzadeh, J. P. Khoo, C. Kok, F. Laden, R. Lalloo, Q. Lan, T. Lathlean, J. L. Leasher, J. Leigh, Y. Li, J. K. Lin, S. E. Lipshultz, S. London, R. Lozano, Y. Lu, J. Mak, R. Malekzadeh, L. Mallinger, W. Marcenes, L. March, R. Marks, R. Martin, P. McGale, J. McGrath, S. Mehta, G. A. Mensah, T. R. Merriman, R. Micha, C. Michaud, V. Mishra, K. Mohd Hanafiah, A. A. Mokdad, L. Morawska, D. Mozaffarian, T. Murphy, M. Naghavi, B. Neal, P. K. Nelson, J. M. Nolla, R. Norman, C. Olives, S. B. Omer, J. Orchard, R. Osborne, B. Ostro, A. Page, K. D. Pandey, C. D. Parry, E. Passmore, J. Patra, N. Pearce, P. M. Pelizzari, M. Petzold, M. R. Phillips, D. Pope, C. A. Pope, 3rd, J. Powles, M. Rao, H. Razavi, E. A. Rehfuess, J. T. Rehm, B. Ritz, F. P. Rivara, T. Roberts, C. Robinson, J. A. Rodriguez-Portales, I. Romieu, R. Room, L. C. Rosenfeld, A. Roy, L. Rushton, J. A. Salomon, U. Sampson, L. Sanchez-Riera, E. Sanman, A. Sapkota, S. Seedat, P. Shi, K. Shield, R. Shivakoti, G. M. Singh, D. A. Sleet, E. Smith, K. R. Smith, N. J. Stapelberg, K. Steenland, H. Stockl, L. J. Stovner, K. Straif, L. Straney, G. D. Thurston, J. H. Tran, R. Van Dingenen, A. van Donkelaar, J. L. Veerman, L. Vijayakumar, R. Weintraub, M. M. Weissman, R. A. White, H. Whiteford,

S. T. Wiersma, J. D. Wilkinson, H. C. Williams, W. Williams, N. Wilson, A. D. Woolf, P. Yip, J. M. Zielinski, A. D. Lopez, C. J. Murray, M. Ezzati, M. A. AlMazroa, Z. A. Memish, A comparative risk assessment of burden of disease and injury attributable to 67 risk factors and risk factor clusters in 21 regions, 1990-2010: a systematic analysis for the Global Burden of Disease Study 2010. Lancet (London, England) 380, 2224-2260 (2012).

2. N. R. Hill, S. T. Fatoba, J. L. Oke, J. A. Hirst, C. A. O'Callaghan, D. S. Lasserson, F. D. Hobbs, Global Prevalence of Chronic Kidney Disease - A Systematic Review and Meta-Analysis. PloS one 11, e0158765 (2016).

3. M. V. Rao, Y. Qiu, C. Wang, G. Bakris, Hypertension and CKD: Kidney Early Evaluation Program (KEEP) and National Health and Nutrition Examination Survey (NHANES), 1999-2004. American journal of kidney diseases : the official journal of the National Kidney Foundation 51, S30-37 (2008).

4. E. L. Schiffrin, Remodeling of resistance arteries in essential hypertension and effects of antihypertensive treatment. American journal of hypertension 17, 1192-1200 (2004).

5. E. L. Schiffrin, Vascular remodeling in hypertension: mechanisms and treatment. Hypertension 59, 367-374 (2012).

6. H. D. Intengan, L. Y. Deng, J. S. Li, E. L. Schiffrin, Mechanics and composition of human subcutaneous resistance arteries in essential hypertension. Hypertension 33, 569-574 (1999).

7. G. M. London, A. P. Guerin, S. J. Marchais, F. Metivier, B. Pannier, H. Adda, Arterial media calcification in end-stage renal disease: impact on all-cause and cardiovascular mortality. Nephrology, dialysis, transplantation : official publication of the European Dialysis and Transplant Association - European Renal Association 18, 1731-1740 (2003).

8. M. L. Muiesan, M. Salvetti, C. Monteduro, C. Corbellini, D. Guelfi, D. Rizzoni, M. Castellano, E. Agabiti-Rosei, Flow-mediated dilatation of the brachial artery and left ventricular geometry in hypertensive patients. J Hypertens 19, 641-647 (2001).

9. J. B. Park, E. L. Schiffrin, Small artery remodeling is the most prevalent (earliest?) form of target organ damage in mild essential hypertension. J Hypertens 19, 921-930 (2001).

10. D. Poulikakos, L. Ross, A. Recio-Mayoral, D. Cole, J. Andoh, N. Chitalia, R. Sharma, J. Carlos Kaski, D. Banerjee, Left ventricular hypertrophy and endothelial dysfunction in chronic kidney disease. European heart journal cardiovascular Imaging 15, 56-61 (2014).

11. N. Luksha, L. Luksha, J. J. Carrero, F. Hammarqvist, P. Stenvinkel, K. Kublickiene, Impaired resistance artery function in patients with end-stage renal disease. Clinical science (London, England : 1979) 120, 525-536 (2011).

12. S. Laurent, P. Boutouyrie, R. Asmar, I. Gautier, B. Laloux, L. Guize, P. Ducimetiere, A. Benetos, Aortic stiffness is an independent predictor of all-cause and cardiovascular mortality in hypertensive patients. Hypertension 37, 1236-1241 (2001).

13. P. Boutouyrie, A. I. Tropeano, R. Asmar, I. Gautier, A. Benetos, P. Lacolley, S. Laurent, Aortic stiffness is an independent predictor of primary coronary events in hypertensive patients: a longitudinal study. Hypertension 39, 10-15 (2002).

14. L. He, G. J. Hannon, MicroRNAs: small RNAs with a big role in gene regulation. Nature reviews. Genetics 5, 522-531 (2004).

15. H. Guo, N. T. Ingolia, J. S. Weissman, D. P. Bartel, Mammalian microRNAs predominantly act to decrease target mRNA levels. Nature 466, 835-840 (2010).

16. W. Hu, J. Coller, What comes first: translational repression or mRNA degradation? The deepening mystery of microRNA function. Cell research 22, 1322-1324 (2012).

17. A. Leung, R. Natarajan, Noncoding RNAs in vascular disease. Current opinion in cardiology 29, 199-206 (2014).

18. S. P. R. Romaine, M. Tomaszewski, G. Condorelli, N. J. Samani, MicroRNAs in cardiovascular disease: an introduction for clinicians. Heart, (2015).

19. S. Heymans, M. F. Corsten, W. Verhesen, P. Carai, R. E. van Leeuwen, K. Custers, T. Peters, M. Hazebroek, L. Stoger, E. Wijnands, B. J. Janssen, E. E. Creemers,

Y. M. Pinto, D. Grimm, N. Schurmann, E. Vigorito, T. Thum, F. Stassen, X. Yin, M. Mayr, L. J. de Windt, E. Lutgens, K. Wouters, M. P. de Winther, S. Zacchigna, M. Giacca, M. van Bilsen, A. P. Papageorgiou, B. Schroen, Macrophage microRNA-155 promotes cardiac hypertrophy and failure. Circulation 128, 1420-1432 (2013).

20. K. H. Shi, H. Tao, J. J. Yang, J. X. Wu, S. S. Xu, H. Y. Zhan, Role of microRNAs in atrial fibrillation: new insights and perspectives. Cellular signalling 25, 2079-2084 (2013).

21. F. Lovren, Y. Pan, A. Quan, K. K. Singh, P. C. Shukla, N. Gupta, B. M. Steer, A. J. Ingram, M. Gupta, M. Al-Omran, H. Teoh, P. A. Marsden, S. Verma, MicroRNA-145 targeted therapy reduces atherosclerosis. Circulation 126, S81-90 (2012).

22. S. Li, J. Zhu, W. Zhang, Y. Chen, K. Zhang, L. M. Popescu, X. Ma, W. B. Lau, R. Rong, X. Yu, B. Wang, Y. Li, C. Xiao, M. Zhang, S. Wang, L. Yu, A. F. Chen, X. Yang, J. Cai, Signature microRNA expression profile of essential hypertension and its novel link to human cytomegalovirus infection. Circulation 124, 175-184 (2011).

23. M. Ulbing, A. H. Kirsch, B. Leber, S. Lemesch, J. Munzker, N. Schweighofer, D. Hofer, O. Trummer, A. R. Rosenkranz, H. Muller, K. Eller, V. Stadlbauer, B. Obermayer-Pietsch, MicroRNAs 223-3p and 93-5p in patients with chronic kidney disease before and after renal transplantation. Bone 95, 115-123 (2017).

24. I. Kocyigit, S. Taheri, E. F. Sener, E. Eroglu, F. Ozturk, A. Unal, K. Korkmaz, G. Zararsiz, M. H. Sipahioglu, Y. Ozkul, B. Tokgoz, O. Oymak, T. Ecder, J. Axelsson, Serum micro-rna profiles in patients with autosomal dominant polycystic kidney disease according to hypertension and renal function. BMC nephrology 18, 179 (2017).

25. A. Y. Nossent, J. L. Hansen, C. Doggen, P. H. Quax, S. P. Sheikh, F. R. Rosendaal, SNPs in microRNA binding sites in 3'-UTRs of RAAS genes influence arterial blood pressure and risk of myocardial infarction. American journal of hypertension 24, 999-1006 (2011).

26. B. Xiao, S. M. Gu, M. J. Li, J. Li, B. Tao, Y. Wang, Y. Wang, S. Zuo, Y. Shen, Y. Yu, D. Chen, G. Chen, D. Kong, J. Tang, Q. Liu, D. R. Chen, Y. Liu, S. Alberti, M. Dovizio, R. Landolfi, L. Mucci, P. Z. Miao, P. Gao, D. L. Zhu, J. Wang, B. Li, P.

Patrignani, Y. Yu, Rare SNP rs12731181 in the miR-590-3p Target Site of the Prostaglandin F2alpha Receptor Gene Confers Risk for Essential Hypertension in the Han Chinese Population. Arteriosclerosis, thrombosis, and vascular biology 35, 1687-1695 (2015).

27. A. S. Levey, J. P. Bosch, J. B. Lewis, T. Greene, N. Rogers, D. Roth, A more accurate method to estimate glomerular filtration rate from serum creatinine: a new prediction equation. Modification of Diet in Renal Disease Study Group. Ann Intern Med 130, 461-470 (1999).

28. M. Briet, E. Bozec, S. Laurent, C. Fassot, G. M. London, C. Jacquot, M. Froissart, P. Houillier, P. Boutouyrie, Arterial stiffness and enlargement in mild-to-moderate chronic kidney disease. Kidney international 69, 350-357 (2006).

29. M. Briet, G. Maruani, C. Collin, E. Bozec, C. Gauci, P. Boutouyrie, P. Houillier, S. Laurent, M. Froissart, Age-independent association between arterial and bone remodeling in mild-to-moderate chronic kidney disease. Nephrology, dialysis, transplantation : official publication of the European Dialysis and Transplant Association - European Renal Association 25, 191-197 (2010).

30. M. Briet, C. Collin, A. Karras, S. Laurent, E. Bozec, C. Jacquot, B. Stengel, P. Houillier, M. Froissart, P. Boutouyrie, Arterial remodeling associates with CKD progression. Journal of the American Society of Nephrology : JASN 22, 967-974 (2011).

31. C. H. Chen, E. Nevo, B. Fetics, P. H. Pak, F. C. Yin, W. L. Maughan, D. A. Kass, Estimation of central aortic pressure waveform by mathematical transformation of radial tonometry pressure. Validation of generalized transfer function. Circulation 95, 1827-1836 (1997).

32. P. Boutouyrie, C. Bussy, P. Lacolley, X. Girerd, B. Laloux, S. Laurent, Association between local pulse pressure, mean blood pressure, and large-artery remodeling. Circulation 100, 1387-1393 (1999).

33. A. I. Tropeano, P. Boutouyrie, B. Pannier, R. Joannides, E. Balkestein, S. Katsahian, B. Laloux, C. Thuillez, H. Struijker-Boudier, S. Laurent, Brachial pressure-

independent reduction in carotid stiffness after long-term angiotensin-converting enzyme inhibition in diabetic hypertensives. Hypertension 48, 80-86 (2006).

34. C. Bussy, P. Boutouyrie, P. Lacolley, P. Challande, S. Laurent, Intrinsic stiffness of the carotid arterial wall material in essential hypertensives. Hypertension 35, 1049-1054 (2000).

35. G. M. London, J. Blacher, B. Pannier, A. P. Guerin, S. J. Marchais, M. E. Safar, Arterial wave reflections and survival in end-stage renal failure. Hypertension 38, 434-438 (2001).

36. R. Asmar, A. Benetos, J. Topouchian, P. Laurent, B. Pannier, A. M. Brisac, R. Target, B. I. Levy, Assessment of arterial distensibility by automatic pulse wave velocity measurement. Validation and clinical application studies. Hypertension 26, 485-490 (1995).

37. L. M. Van Bortel, S. Laurent, P. Boutouyrie, P. Chowienczyk, J. K. Cruickshank, T. De Backer, J. Filipovsky, S. Huybrechts, F. U. Mattace-Raso, A. D. Protogerou, G. Schillaci, P. Segers, S. Vermeersch, T. Weber, S. Artery, S. European Society of Hypertension Working Group on Vascular, Function, A. European Network for Noninvasive Investigation of Large, Expert consensus document on the measurement of aortic stiffness in daily practice using carotid-femoral pulse wave velocity. J Hypertens 30, 445-448 (2012).

38. C. Savoia, R. M. Touyz, F. Amiri, E. L. Schiffrin, Selective mineralocorticoid receptor blocker eplerenone reduces resistance artery stiffness in hypertensive patients. Hypertension 51, 432-439 (2008).

39. E. L. Schiffrin, L. Y. Deng, P. Larochelle, Effects of a beta-blocker or a converting enzyme inhibitor on resistance arteries in essential hypertension. Hypertension 23, 83-91 (1994).

40. A. Dobin, C. A. Davis, F. Schlesinger, J. Drenkow, C. Zaleski, S. Jha, P. Batut, M. Chaisson, T. R. Gingeras, STAR: ultrafast universal RNA-seq aligner. Bioinformatics (Oxford, England) 29, 15-21 (2013).

41. S. Anders, P. T. Pyl, W. Huber, HTSeq--a Python framework to work with high-throughput sequencing data. Bioinformatics (Oxford, England) 31, 166-169 (2015).

42. M. R. Friedlander, S. D. Mackowiak, N. Li, W. Chen, N. Rajewsky, miRDeep2 accurately identifies known and hundreds of novel microRNA genes in seven animal clades. Nucleic acids research 40, 37-52 (2012).

43. M. D. Robinson, D. J. McCarthy, G. K. Smyth, edgeR: a Bioconductor package for differential expression analysis of digital gene expression data. Bioinformatics (Oxford, England) 26, 139-140 (2010).

44. V. Agarwal, G. W. Bell, J. W. Nam, D. P. Bartel, Predicting effective microRNA target sites in mammalian mRNAs. eLife 4, (2015).

45. C. E. Grant, T. L. Bailey, W. S. Noble, FIMO: scanning for occurrences of a given motif. Bioinformatics (Oxford, England) 27, 1017-1018 (2011).

46. P. Shannon, A. Markiel, O. Ozier, N. S. Baliga, J. T. Wang, D. Ramage, N. Amin, B. Schwikowski, T. Ideker, Cytoscape: a software environment for integrated models of biomolecular interaction networks. Genome research 13, 2498-2504 (2003).

47. G. Bindea, B. Mlecnik, H. Hackl, P. Charoentong, M. Tosolini, A. Kirilovsky, W. H. Fridman, F. Pages, Z. Trajanoski, J. Galon, ClueGO: a Cytoscape plug-in to decipher functionally grouped gene ontology and pathway annotation networks. Bioinformatics (Oxford, England) 25, 1091-1093 (2009).

48. G. M. Chen, A. J. Zheng, J. Cai, P. Han, H. B. Ji, L. L. Wang, microRNA-145-3p Inhibits Non-Small Cell Lung Cancer Cell Migration and Invasion by Targeting PDK1 via the mTOR Signaling Pathway. Journal of cellular biochemistry, (2017).

49. Y. Goto, A. Kurozumi, T. Arai, N. Nohata, S. Kojima, A. Okato, M. Kato, K. Yamazaki, Y. Ishida, Y. Naya, T. Ichikawa, N. Seki, Impact of novel miR-145-3p regulatory networks on survival in patients with castration-resistant prostate cancer. British journal of cancer, (2017).

50. Q. Yang, R. X. Yin, Y. J. Zhou, X. L. Cao, T. Guo, W. X. Chen, Association of polymorphisms in the MAFB gene and the risk of coronary artery disease and ischemic stroke: a case-control study. Lipids in health and disease 14, 79 (2015).

51. M. Wuttke, C. S. Wong, E. Wuhl, D. Epting, L. Luo, A. Hoppmann, A. Doyon, Y. Li, B. Sozeri, D. Thurn, M. Helmstadter, T. B. Huber, T. D. Blydt-Hansen, A. Kramer-Zucker, O. Mehls, A. Melk, U. Querfeld, S. L. Furth, B. A. Warady, F. Schaefer, A. Kottgen, Genetic loci associated with renal function measures and chronic kidney disease in children: the Pediatric Investigation for Genetic Factors Linked with Renal Progression Consortium. Nephrology, dialysis, transplantation : official publication of the European Dialysis and Transplant Association - European Renal Association 31, 262-269 (2016).

52. T. M. Kolb, J. Peabody, P. Baddoura, J. Fallica, J. R. Mock, B. D. Singer, F. R. D'Alessio, M. Damarla, R. L. Damico, P. M. Hassoun, Right Ventricular Angiogenesis is an Early Adaptive Response to Chronic Hypoxia-Induced Pulmonary Hypertension. Microcirculation (New York, N.Y. : 1994) 22, 724-736 (2015).

53. H. M. Cho, D. Y. Lee, H. Y. Kim, H. A. Lee, Y. M. Seok, I. K. Kim, Upregulation of the Na(+)-K(+)-2Cl(-) cotransporter 1 via histone modification in the aortas of angiotensin II-induced hypertensive rats. Hypertension research : official journal of the Japanese Society of Hypertension 35, 819-824 (2012).

54. C. Terao, K. Ohmura, Y. Kawaguchi, T. Nishimoto, A. Kawasaki, K. Takehara, H. Furukawa, Y. Kochi, Y. Ota, K. Ikari, S. Sato, S. Tohma, R. Yamada, K. Yamamoto, M. Kubo, H. Yamanaka, M. Kuwana, N. Tsuchiya, F. Matsuda, T. Mimori, PLD4 as a novel susceptibility gene for systemic sclerosis in a Japanese population. Arthritis and rheumatism 65, 472-480 (2013).

55. D. Pattanaik, M. Brown, A. E. Postlethwaite, Vascular involvement in systemic sclerosis (scleroderma). Journal of Inflammation Research 4, 105-125 (2011).

56. P. Perez-Pinera, J. R. Berenson, T. F. Deuel, Pleiotrophin, a multifunctional angiogenic factor: mechanisms and pathways in normal and pathological angiogenesis. Current opinion in hematology 15, 210-214 (2008).

57. D. Palmieri, M. Mura, S. Mambrini, D. Palombo, Effects of Pleiotrophin on endothelial and inflammatory cells: Pro-angiogenic and anti-inflammatory properties and potential role for vascular bio-prosthesis endothelialization. Advances in medical sciences 60, 287-293 (2015).

CHAPTER IV: Circulating ncRNA profiling in essential hypertension with or without CKD

Circulating let-7g-5p as potential biomarkers for vascular damage in chronic kidney disease

Olga Berillo[1*], Ku-Geng Huo[1*], Júlio C. Fraulob-Aquino[1], Chantal Richer[3], Marie Briet[1,5], Mark L. Lipman[1,2], Daniel Sinnett[3,4], Pierre Paradis[1], Ernesto L. Schiffrin[1,2]

[1]Vascular and Hypertension Research Unit, Lady Davis Institute for Medical Research, [2]Department of Medicine, Sir Mortimer B. Davis-Jewish General Hospital, McGill University,

[3]Division of Hematology-Oncology, Research Center, CHU Ste-Justine,

[4]Department of Pediatrics, Faculty of Medicine, Université de Montréal, Montréal, Canada;

[5]INSERM U1083, CNRS UMR 6214, Centre Hospitalier Universitaire d'Angers, Université d'Angers, Angers, France.

*These authors contributed equally

Disclosure:

This work was supported by the Canadian Institutes of Health Research (CIHR) grants MOP123465, a First Pilot Foundation Grant 143348, and a Discovery Grant from Servier France.

Abstract

Background: Chronic kidney disease (CKD) is a global health condition with a worldwide prevalence of 13.4% for stage 5 and 10.6% for stage 3-5. There is an epidemiological association between hypertension (HTN) and CKD. The prevalence of high blood pressure (BP) has been reported to be over 85% in stage 3 and over 90% in stage 4-5 CKD patients. Circulating cell-free small non-coding RNAs called microRNA (miRNA) have been shown to associate with different pathologies including cancer and cardiovascular disease, and accordingly possesses potential to serve as biomarkers with clinical application. We aimed to identify differentially expressed (DE) miRNAs that may be related to CKD.

Methods and Results: Normotensive, HTN (systolic BP > 135 mmHg or diastolic BP of 85-115 mmHg with BP) and CKD (estimated glomerular filtration rate (*eGFR*) < 60mL/min/m^2) subjects (n=15-16 per group) were studied. Platelet-free plasma was isolated by a 2-step centrifugation (1000x*g* followed by 10,000x*g*) from 6 ml total blood. Plasma miRNAs were extracted using the QIAamp Circulating Nucleic Acid Kit. cDNA libraries were prepared using the TruSeq Small RNA Library Prep Kit, and sequenced with the HiSeq 2500 platform. FastQC was used for quality control. Sequences were mapped by STAR to the hg38 genome and annotated by miRDeep2. DE miRNAs were identified using EdgeR. Six up-regulated and 3 down-regulated miRNAs were found to be uniquely associated with HTN, 2 up-regulated and 12 down-regulated miRNAs uniquely associated with CKD, and 3 down-regulated miRNAs were found in both groups (P<0.01 & q<0.1). Two down-regulated miRNAs in the HTN group, miR-26a-5p (r=-0.33, P<0.05) and miR-151a-5p (r=-0.33, P<0.05), correlated with SBP. One up-regulated miRNA in CKD group, let-7g-5p (r=0.31, P<0.05), correlated with *eGFR*.

Conclusion: DE platelet-free plasma miRNAs were identified in HTN and CKD patients. Some miRNAs may have the potential to serve as biomarkers in CKD.

Introduction

Hypertension and chronic kidney disease (CKD) are prevalent global health concerns that account for millions of deaths per year (1, 2). There is an epidemiological association between hypertension and CKD. The prevalence of high blood pressure has been reported to be over 85% in stage 3 and over 90% in stages 4-5 CKD patients in the Kidney Early Evaluation Program in 2000-2006 (3). Hypertension and CKD are both characterized by vascular damage that includes vascular remodeling (4, 5), stiffening (6, 7) and endothelial dysfunction (8-11).

microRNAs (miRNAs) are a class of small non-coding RNAs that regulate gene expression post-transcriptionally by binding to the 3' untranslated regions (UTRs) of their target mRNAs and leading to mRNA degradation and translational repression (12-14). Besides this canonical targeting machinery, a form of cell-free extracellular miRNAs in biological fluids such as circulating blood and urine has been shown to play a role in cell-cell communication. Circulating miRNAs were also reported to be associated with multiple pathologies including cancer and cardiovascular disease in the past few years, and therefore possess great value to serve as novel biomarkers for disease diagnosis and prognosis (15-17).

Abnormal circulating miRNA levels have been observed in essential hypertensive patients and CKD subjects. Li *et al*. used microarray to profile circulating miRNA in essential hypertensive patients and identified 27 differentially expressed (DE) miRNAs (18). However, the researchers in this study did not perform a high-speed centrifugation (10,000 X g) to remove platelets in the plasma. Their circulating miRNA profile therefore may likely come from platelets, as reported by Willeit *et al*. that platelet-rich plasma showed much higher miRNA levers than platelet-poor plasma (19). Recently, Ulbing *et al*. (20) used nanoString nCounter to identify DE circulating miRNAs associated with CKD. However, it is also noteworthy that nanaString nCounter is a medium-throughput profiling platform that limits the quantification to 800 known miRNAs.

In the present study, we profiled cell-free platelet-free circulating miRNAs using RNA deep sequencing to identify not only all known miRNAs, but also novel miRNAs that are associated with hypertension and CKD. Combined with vascular gene expression

profiling that we have previously performed in subcutaneous small resistance arteries from the same cohort of hypertensive patients with or without CKD and normotensive control subjects (Chapter III), we sought to identify circulating miRNAs that may be used as clinical biomarkers for vascular damage in hypertension and CKD.

Methods

Subject recruitment

The study protocol was approved by the Human Research Ethics Review Committee of the Jewish General Hospital, where the study was carried out. All the subjects included in the study provided written informed consent to participate.

A cohort of 15 normotensive subjects, 16 hypertensive patients and 16 hypertensive subjects with CKD were recruited in our previous study. Details of recruitment criteria have been previously described (Chapter III).

Biological sample collection

On the day of subject inclusion, blood and urine were sampled in the morning under fasting conditions. Blood was collected in BD Vacutainer EDTA or Vacutainer Plus serum tubes for blood biochemistry and urine analysis determined in the department of Diagnostic Medicine at the Jewish General Hospital according to routine methods. eGFR was determined by the Modification of Diet in Renal Disease formula (21). Blood samples on EDTA were centrifuged at 1,000 g for 15 min at 4°C to remove blood cells, followed by centrifugation at 10,000 g for 10 min at 4°C to remove platelets. Plasma was stored at -80°C until used for RNA extraction.

RNA extraction and small RNA library construction

Six ml plasma stored at -80°C was thawed, mixed thoroughly by inversion and centrifuged at 10,000 g at 4°C for 3 min to remove remaining debris. Circulating miRNAs was isolated from plasma with the QIAamp Circulating Nucleic Acid kit

(Qiagen, Venlo, Netherlands) using the miRNA extraction protocol for 3 ml of plasma with slight modifications. In brief, all reagents except for the washing and elution buffers were up-scaled 2 times. The quantity of small RNA and % of miRNA were assessed with an Agilent Small RNA kit using an Agilent 2100 bioanalyzer. RNA sample were separated into 2 parts: 4-20 ng for small RNA library preparation as previously described (Chapter III) and the remainder was reserved for real-rime quantitative reverse transcription polymerase chain reaction (RT-qPCR) validation of selected genes.

RNA sequencing and data analysis

Small RNA libraries were sequenced was with an Illumina HiSeq 2500 system following the manufacturer's protocol at the platform of Integrated Centre for Pediatric Clinical Genomics of the Research Center of the Sainte-Justine University Hospital. The miRNA sequencing was done in the 1 x 50 bp high-output mode.

Sequence data were first examined for base quality using FastQC (https://www.bioinformatics.babraham.ac.uk/projects/fastqc/). Sequences were mapped to the human genome hg38 with STAR (22). Small RNA sequences were mapped using the option *--outFilterMismatchNoverLmax 0.05* that allows a maximal mismatch ratio of 0.05 (no mismatch allowed for reads <20 nt and 1 mismatch allow per 20 nt). miRDeep2 was used for novel miRNA prediction, known and novel miRNA annotation and counting (23). EdgeR was used for differential expression analysis (24). A trimmed mean of M-values (TMM) method in the EdgeR protocol was used for sequence read normalization. Only genes with expression level ≥10 reads per million mapped reads in ≥14 samples (lowest subject # in any group) were analyzed.

DE circulating miRNA validation by RT-qPCR

Reversed transcription was done with 2 ng of the isolated RNA using the Qiagen miScript II RT Kit (Qiagen). qPCR was performed using the miScript Primer Assay with miScript SYBR Green PCR Kit (Qiagen) according to the manufacturer's protocol in an Applied Biosystems® 7500 Real-Time PCR System (ThermoFisher Scientific, Waltham,

MA). Primers were validated by PCR efficiency between 90% and 120% with single amplicon in the qPCR dissociation curves. Geometric mean of the 3 least variable miRNAs with at least 50 reads per million total mapped reads from the sequencing date was used for normalization.

Statistical analysis

Results are presented as means ± SD. Comparisons between multiple groups were analyzed by one-way analysis of variance (ANOVA) followed by a Student–Newman–Keuls *post-hoc* test or Kruskal-Wallis one-way ANOVA on ranks, as needed. For RNA sequencing data analysis, an ANOVA-like test in EdgeR based on generalized linear models was used for differential expression analysis. Differential expression was defined under a threshold of false discovery rate (FDR or q) <0.1. A Pearson correlation was performed between circulating DE miRNA expression and clinical parameters, as well as between circulating DE miRNA and vascular DE gene expression.

Results

Clinical characteristics and large artery evaluation

The demographic parameters and hemodynamic characteristics were presented in our previous study (Chapter III).

Platelet-free plasma small RNA profiling

Fifteen samples per group were used for the platelet-free plasma small RNA profiling. Total RNA was extracted successfully from 6 mL of platelet-free plasma in all the samples. However, the yield was very low. It was not possible to determine the RNA yield using a NanoDrop spectrophotometer. Since it has been described that circulating RNA are mostly small RNA, the quantity of small RNA was assessed with an Agilent Small RNA kit using an Agilent 2100 bioanalyzer. On average, 27.2 ng (5.5-99.0 ng) of small RNA was extracted from 6 mL of platelet-free plasma. Furthermore, the analysis of

the electrophoresis profiles revealed that the circulating small RNA was enriched in miRNAs (~36%). All the samples were used to construct the small and total RNA libraries.

An average of 13.6 million qualified single-end reads per sample was obtained in the small RNA sequencing data, of which 8.4% and 81.9% were mapped to a unique locus and multiple loci of the hg38 genome by STAR, respectively. It should be noted that one CKD RNA sample with low base quality (Q<20) and another CKD sample with low read counts (27 thousand qualified single-end reads) were excluded for further small RNA analyses.

We have Identified 6 up-regulated and 3 down-regulated miRNAs uniquely associated with the hypertensive group, 2 up-regulated and 12 down-regulated miRNAs uniquely associated with the CKD group and 3 down-regulated miRNAs in both groups (Fig. IV-1). Two down-regulated miRNAs in the hypertensive group, miR-26a-5p (r=-0.33, P<0.05) and miR-151a-5p (r=-0.33, P<0.05), were correlated with SBP. One up-regulated miRNA in CKD group, let-7g-5p, was correlated with eGFR (r=0.31, P<0.05).

DE miRNA validation by RT-qPCR

Comparing our results with those from a previous publication (20), we found 4 common DE miRNAs associated with CKD, namely let-7g-5p, miR-26a-5p, miR-191-5p and let-7b-5p. Next, we used RT-qPCR to validate the expression levels of these miRNAs. let-7g-5p, miR-191-5p and let-7b-5p showed a strong correlation between sequencing and qPCR results, whereas a moderate correlation was found for miR-26a-5p (Fig. IV-2).

Correlations between circulating DE miRNA and vascular DE gene expression

Among the 4 validated DE miRNAs, low circulating let-7g-5p levels has been previously linked to endothelial dysfunction in patients with lacunar infarction (25). *In vivo* and *in vitro* gain- and loss-of-function experiments showed that let-7g-5p targeted the endothelial dysfunction marker plasminogen activator inhibitor (*PAI-1*) and was able to reduce inflammation and vascular cell adhesion protein 1 (VCAM-1) secretion in

endothelial cells. Moreover, considering that let-7g-5p is the only circulating miRNA correlated with eGFR levels, this suggests a potential value of let-7g-5p to serve as a biomarker for vascular damage in CKD. We had previously performed gene expression profiling on subcutaneous small resistance arteries of the same subjects to identify DE genes associated with vascular damage in hypertension and CKD (Chapter III). Next, we looked at the correlations between vascular gene expression levels and circulating let-7g-5p expression levels. Among the top 10 correlated genes, 7 of them were also down-regulated in small resistance arteries in CKD patients, and 8 of them were correlated with at least 3 of the 4 validated DE circulating miRNAs (Table IV-1).

Discussion

In the present study, we have identified DE circulating miRNAs in essential hypertensive patients and in CKD patients. Comparing our results with those from a previous publication (20), we found 4 common CKD-associated miRNAs, among which let-7g-5p has been linked to endothelial dysfunction (25). let-7g-5p was down-regulated in CKD and was the only circulating miRNA correlated with eGFR levels. Moreover, out of the genes whose expression levels in small arteries were correlated with circulating let-7g-5p expression, the majority of the top correlated genes were also down-regulated in small arteries of CKD patients. The above findings suggest a potential link between circulating let-7g-5p and vascular damage in CKD.

Out of the top let-7g-5p-correlated genes, genome-wide association studies have reported the association between Unc-51 Like Kinase 4 (*ULK4*) and hypertension (26-28), as well as between Proprotein Convertase Subtilisin/Kexin Type 2 (*PCSK2*) and CKD (29), myocardial infarction (30) and type 2 diabetes (31). ST6 N-Acetylgalactosaminide Alpha-2,6-Sialyltransferase 2 (ST6GALNAC2) protein levels in peripheral blood mononuclear cells were shown to be a potential diagnostic biomarker for IgA nephropathy, an immune complex-mediated glomerulonephritis that causes damage to glomeruli and may lead to CKD (32). Ten-eleven translocation-2 (TET2), a DNA demethylation enzyme that oxidizes 5-methylcytosine (5-mC) to generate 5-hydroxymethylcytosine (5-hmC) and induce gene activation, has been shown to play a

master regulatory role in smooth muscle cell (SMC) differentiation. Promoters of SMC contractile genes displayed enrichment for 5-hmC and TET2 binding. The later were reduced on promoters of SMC dedifferentiated genes. Moreover, *TET2* overexpression was able to activate SMC gene expression in fibroblasts and induce contractile phenotype (33). *TET2* was predicted to be a target of let-7g-5p in our preliminary analysis. However, their relationship needs to be confirmed by future experiments.

The relationship between circulating let-7g-5p and correlated genes in small arteries is unclear. Cell-cell communication may be involved in the crosstalk between circulating miRNAs and vascular gene expression, and contribute to vascular damage in CKD. Further analyses and experiments will be required to investigate the underlying molecular mechanisms. It has been demonstrated that vesicle-associated circulating miRNAs released from immune cells can be incorporated by the co-cultured vascular endothelial cells, where they regulate expression of target genes (34, 35). One of the potential future experiments to investigate the communication between circulating let-7g-5p and vascular gene expression could be to co-culture extracellular let-7g-5p-secreting cells with endothelial cells in order to examine whether endothelial cells are able to take up the pre-labelled secreted let-7g-5p. The next step would be to measure the expression levels of potential let-7g-5p targets, the conserved correlated vascular genes and markers for endothelial function, vascular injury and inflammatory processes in the recipient endothelial cells. Considering that circulating let-7g-5p is down-regulated in CKD, it is of clinical interest to investigate the potential protective effect of systemic administration of vesicle-associated circulating let-7p-5p *in vivo*. However, *in vivo* miRNA delivery by current methods is still technically more difficult compared to *in vivo* miRNA inhibitor delivery. The former tends to induce stronger immunotoxicity and shows lower targeting efficacy (36). A throughout examination on specific and non-specific targeting effects, immunotoxicity and any potential abnormal phenotype should be conducted, if *in vivo* experiments are performed in animal models.

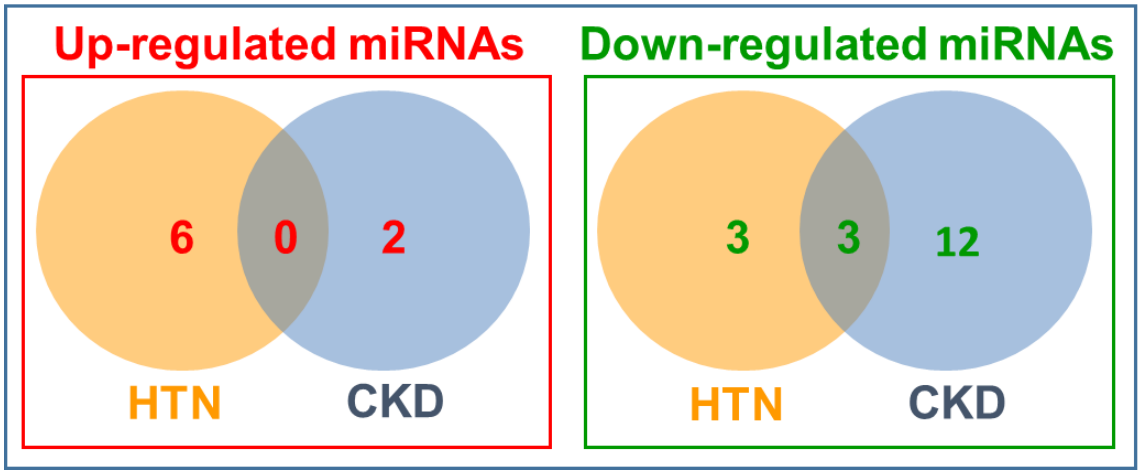

Figure IV-1. Venn diagrams represent the number of differentially expressed miRNAs in platelet-free plasma uniquely associated with the hypertensive subjects (HTN), uniquely associated with chronic kidney disease patients (CKD), compared to normotensive subjects (P<0.01 & q<0.1). n=15 for normotensive, 15 for hypertensive and 13 for CKD subjects.

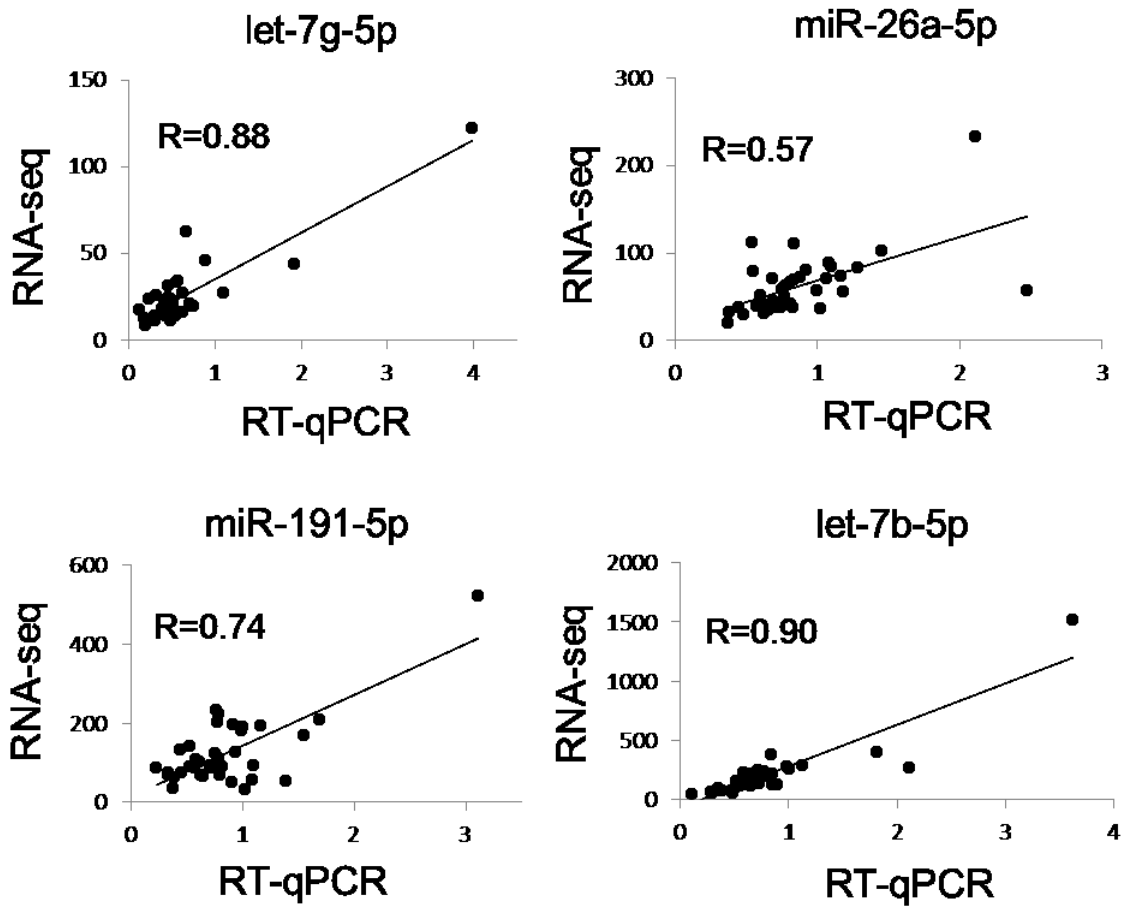

Figure IV-2. Correlations between RNA sequencing (RNA-seq) results and real-rime quantitative reverse transcription polymerase chain reaction (RT-qPCR) results on let-7g-5p, miR-26a-5p, miR-191-5p and let-7b-5p. n=36.

Table IV-1. Correlations between circulating DE miRNA and vascular gene expression.

Vascular genes	DE in small arteries		Correlations with circulating miRNAs							
			let-7g-5p		miR-26a-5p		miR-191-5p		let-7b-5p	
	FC	*P*	R	*P*	R	*P*	R	*P*	R	*P*
ULK4	0.87	*	0.62	***	0.40	**	0.43	**	0.37	*
ST6GALNAC2	0.62	**	0.59	***	0.38	*			0.50	***
TET2	0.92	*	0.56	***	0.34	*	0.43	**	0.40	**
S100A4	0.79	***	0.55	***	0.46	**	0.46	**	0.47	**
FDFT1	0.86	*	0.54	***	0.38	*	0.37	*	0.42	**
RDH10			0.53	***	0.46	**			0.58	***
PCSK2	0.69	*	0.52	***	0.47	**			0.53	***
COBL	0.87	**	0.51	***						
TGDS			0.50	***						
LINC00654			-0.50	***	-0.38	*	-0.33	*	-0.37	*

The top 10 let-7g-5p-correlated vascular genes are shown here. DE, differential expression. FC, fold change. n=42. * $P<0.05$. ** $P<0.01$. *** $P<0.001$.

References

1. S. S. Lim, T. Vos, A. D. Flaxman, G. Danaei, K. Shibuya, H. Adair-Rohani, M. Amann, H. R. Anderson, K. G. Andrews, M. Aryee, C. Atkinson, L. J. Bacchus, A. N. Bahalim, K. Balakrishnan, J. Balmes, S. Barker-Collo, A. Baxter, M. L. Bell, J. D. Blore, F. Blyth, C. Bonner, G. Borges, R. Bourne, M. Boussinesq, M. Brauer, P. Brooks, N. G. Bruce, B. Brunekreef, C. Bryan-Hancock, C. Bucello, R. Buchbinder, F. Bull, R. T. Burnett, T. E. Byers, B. Calabria, J. Carapetis, E. Carnahan, Z. Chafe, F. Charlson, H. Chen, J. S. Chen, A. T. Cheng, J. C. Child, A. Cohen, K. E. Colson, B. C. Cowie, S. Darby, S. Darling, A. Davis, L. Degenhardt, F. Dentener, D. C. Des Jarlais, K. Devries, M. Dherani, E. L. Ding, E. R. Dorsey, T. Driscoll, K. Edmond, S. E. Ali, R. E. Engell, P. J. Erwin, S. Fahimi, G. Falder, F. Farzadfar, A. Ferrari, M. M. Finucane, S. Flaxman, F. G. Fowkes, G. Freedman, M. K. Freeman, E. Gakidou, S. Ghosh, E. Giovannucci, G. Gmel, K. Graham, R. Grainger, B. Grant, D. Gunnell, H. R. Gutierrez, W. Hall, H. W. Hoek, A. Hogan, H. D. Hosgood, 3rd, D. Hoy, H. Hu, B. J. Hubbell, S. J. Hutchings, S. E. Ibeanusi, G. L. Jacklyn, R. Jasrasaria, J. B. Jonas, H. Kan, J. A. Kanis, N. Kassebaum, N. Kawakami, Y. H. Khang, S. Khatibzadeh, J. P. Khoo, C. Kok, F. Laden, R. Lalloo, Q. Lan, T. Lathlean, J. L. Leasher, J. Leigh, Y. Li, J. K. Lin, S. E. Lipshultz, S. London, R. Lozano, Y. Lu, J. Mak, R. Malekzadeh, L. Mallinger, W. Marcenes, L. March, R. Marks, R. Martin, P. McGale, J. McGrath, S. Mehta, G. A. Mensah, T. R. Merriman, R. Micha, C. Michaud, V. Mishra, K. Mohd Hanafiah, A. A. Mokdad, L. Morawska, D. Mozaffarian, T. Murphy, M. Naghavi, B. Neal, P. K. Nelson, J. M. Nolla, R. Norman, C. Olives, S. B. Omer, J. Orchard, R. Osborne, B. Ostro, A. Page, K. D. Pandey, C. D. Parry, E. Passmore, J. Patra, N. Pearce, P. M. Pelizzari, M. Petzold, M. R. Phillips, D. Pope, C. A. Pope, 3rd, J. Powles, M. Rao, H. Razavi, E. A. Rehfuess, J. T. Rehm, B. Ritz, F. P. Rivara, T. Roberts, C. Robinson, J. A. Rodriguez-Portales, I. Romieu, R. Room, L. C. Rosenfeld, A. Roy, L. Rushton, J. A. Salomon, U. Sampson, L. Sanchez-Riera, E. Sanman, A. Sapkota, S. Seedat, P. Shi, K. Shield, R. Shivakoti, G. M. Singh, D. A. Sleet, E. Smith, K. R. Smith, N. J. Stapelberg, K. Steenland, H. Stockl, L. J. Stovner, K. Straif, L. Straney, G. D. Thurston, J. H. Tran, R. Van Dingenen, A. van Donkelaar, J. L. Veerman, L. Vijayakumar, R. Weintraub, M. M. Weissman, R. A. White, H. Whiteford, S. T. Wiersma, J. D. Wilkinson, H. C. Williams, W. Williams, N. Wilson, A. D. Woolf, P.

Yip, J. M. Zielinski, A. D. Lopez, C. J. Murray, M. Ezzati, M. A. AlMazroa, Z. A. Memish, A comparative risk assessment of burden of disease and injury attributable to 67 risk factors and risk factor clusters in 21 regions, 1990-2010: a systematic analysis for the Global Burden of Disease Study 2010. Lancet (London, England) 380, 2224-2260 (2012).

2. N. R. Hill, S. T. Fatoba, J. L. Oke, J. A. Hirst, C. A. O'Callaghan, D. S. Lasserson, F. D. Hobbs, Global Prevalence of Chronic Kidney Disease - A Systematic Review and Meta-Analysis. PloS one 11, e0158765 (2016).

3. M. V. Rao, Y. Qiu, C. Wang, G. Bakris, Hypertension and CKD: Kidney Early Evaluation Program (KEEP) and National Health and Nutrition Examination Survey (NHANES), 1999-2004. American journal of kidney diseases : the official journal of the National Kidney Foundation 51, S30-37 (2008).

4. E. L. Schiffrin, Remodeling of resistance arteries in essential hypertension and effects of antihypertensive treatment. American journal of hypertension 17, 1192-1200 (2004).

5. E. L. Schiffrin, Vascular remodeling in hypertension: mechanisms and treatment. Hypertension 59, 367-374 (2012).

6. H. D. Intengan, L. Y. Deng, J. S. Li, E. L. Schiffrin, Mechanics and composition of human subcutaneous resistance arteries in essential hypertension. Hypertension 33, 569-574 (1999).

7. G. M. London, A. P. Guerin, S. J. Marchais, F. Metivier, B. Pannier, H. Adda, Arterial media calcification in end-stage renal disease: impact on all-cause and cardiovascular mortality. Nephrology, dialysis, transplantation : official publication of the European Dialysis and Transplant Association - European Renal Association 18, 1731-1740 (2003).

8. D. Poulikakos, L. Ross, A. Recio-Mayoral, D. Cole, J. Andoh, N. Chitalia, R. Sharma, J. Carlos Kaski, D. Banerjee, Left ventricular hypertrophy and endothelial dysfunction in chronic kidney disease. European heart journal cardiovascular Imaging 15, 56-61 (2014).

9. M. L. Muiesan, M. Salvetti, C. Monteduro, C. Corbellini, D. Guelfi, D. Rizzoni, M. Castellano, E. Agabiti-Rosei, Flow-mediated dilatation of the brachial artery and left ventricular geometry in hypertensive patients. J Hypertens 19, 641-647 (2001).

10. J. B. Park, E. L. Schiffrin, Small artery remodeling is the most prevalent (earliest?) form of target organ damage in mild essential hypertension. J Hypertens 19, 921-930 (2001).

11. N. Luksha, L. Luksha, J. J. Carrero, F. Hammarqvist, P. Stenvinkel, K. Kublickiene, Impaired resistance artery function in patients with end-stage renal disease. Clinical science (London, England : 1979) 120, 525-536 (2011).

12. L. He, G. J. Hannon, MicroRNAs: small RNAs with a big role in gene regulation. Nature reviews. Genetics 5, 522-531 (2004).

13. H. Guo, N. T. Ingolia, J. S. Weissman, D. P. Bartel, Mammalian microRNAs predominantly act to decrease target mRNA levels. Nature 466, 835-840 (2010).

14. W. Hu, J. Coller, What comes first: translational repression or mRNA degradation? The deepening mystery of microRNA function. Cell research 22, 1322-1324 (2012).

15. H. Schwarzenbach, N. Nishida, G. A. Calin, K. Pantel, Clinical relevance of circulating cell-free microRNAs in cancer. Nature reviews. Clinical oncology 11, 145-156 (2014).

16. P. Qi, X. Y. Zhou, X. Du, Circulating long non-coding RNAs in cancer: current status and future perspectives. Molecular cancer 15, 39 (2016).

17. J. Viereck, T. Thum, Circulating Noncoding RNAs as Biomarkers of Cardiovascular Disease and Injury. Circulation research 120, 381-399 (2017).

18. S. Li, J. Zhu, W. Zhang, Y. Chen, K. Zhang, L. M. Popescu, X. Ma, W. B. Lau, R. Rong, X. Yu, B. Wang, Y. Li, C. Xiao, M. Zhang, S. Wang, L. Yu, A. F. Chen, X. Yang, J. Cai, Signature microRNA expression profile of essential hypertension and its novel link to human cytomegalovirus infection. Circulation 124, 175-184 (2011).

19. P. Willeit, A. Zampetaki, K. Dudek, D. Kaudewitz, A. King, N. S. Kirkby, R. Crosby-Nwaobi, M. Prokopi, I. Drozdov, S. R. Langley, S. Sivaprasad, H. S. Markus, J.

A. Mitchell, T. D. Warner, S. Kiechl, M. Mayr, Circulating microRNAs as novel biomarkers for platelet activation. Circulation research 112, 595-600 (2013).

20. M. Ulbing, A. H. Kirsch, B. Leber, S. Lemesch, J. Munzker, N. Schweighofer, D. Hofer, O. Trummer, A. R. Rosenkranz, H. Muller, K. Eller, V. Stadlbauer, B. Obermayer-Pietsch, MicroRNAs 223-3p and 93-5p in patients with chronic kidney disease before and after renal transplantation. Bone 95, 115-123 (2017).

21. A. S. Levey, J. P. Bosch, J. B. Lewis, T. Greene, N. Rogers, D. Roth, A more accurate method to estimate glomerular filtration rate from serum creatinine: a new prediction equation. Modification of Diet in Renal Disease Study Group. Ann Intern Med 130, 461-470 (1999).

22. A. Dobin, C. A. Davis, F. Schlesinger, J. Drenkow, C. Zaleski, S. Jha, P. Batut, M. Chaisson, T. R. Gingeras, STAR: ultrafast universal RNA-seq aligner. Bioinformatics (Oxford, England) 29, 15-21 (2013).

23. M. R. Friedlander, S. D. Mackowiak, N. Li, W. Chen, N. Rajewsky, miRDeep2 accurately identifies known and hundreds of novel microRNA genes in seven animal clades. Nucleic acids research 40, 37-52 (2012).

24. M. D. Robinson, D. J. McCarthy, G. K. Smyth, edgeR: a Bioconductor package for differential expression analysis of digital gene expression data. Bioinformatics (Oxford, England) 26, 139-140 (2010).

25. Y. C. Liao, Y. S. Wang, Y. C. Guo, W. L. Lin, M. H. Chang, S. H. Juo, Let-7g improves multiple endothelial functions through targeting transforming growth factor-beta and SIRT-1 signaling. Journal of the American College of Cardiology 63, 1685-1694 (2014).

26. D. Levy, G. B. Ehret, K. Rice, G. C. Verwoert, L. J. Launer, A. Dehghan, N. L. Glazer, A. C. Morrison, A. D. Johnson, T. Aspelund, Y. Aulchenko, T. Lumley, A. Kottgen, R. S. Vasan, F. Rivadeneira, G. Eiriksdottir, X. Guo, D. E. Arking, G. F. Mitchell, F. U. Mattace-Raso, A. V. Smith, K. Taylor, R. B. Scharpf, S. J. Hwang, E. J. Sijbrands, J. Bis, T. B. Harris, S. K. Ganesh, C. J. O'Donnell, A. Hofman, J. I. Rotter, J. Coresh, E. J. Benjamin, A. G. Uitterlinden, G. Heiss, C. S. Fox, J. C. Witteman, E.

Boerwinkle, T. J. Wang, V. Gudnason, M. G. Larson, A. Chakravarti, B. M. Psaty, C. M. van Duijn, Genome-wide association study of blood pressure and hypertension. Nature genetics 41, 677-687 (2009).

27. G. B. Ehret, P. B. Munroe, K. M. Rice, M. Bochud, A. D. Johnson, D. I. Chasman, A. V. Smith, M. D. Tobin, G. C. Verwoert, S. J. Hwang, V. Pihur, P. Vollenweider, P. F. O'Reilly, N. Amin, J. L. Bragg-Gresham, A. Teumer, N. L. Glazer, L. Launer, J. H. Zhao, Y. Aulchenko, S. Heath, S. Sober, A. Parsa, J. Luan, P. Arora, A. Dehghan, F. Zhang, G. Lucas, A. A. Hicks, A. U. Jackson, J. F. Peden, T. Tanaka, S. H. Wild, I. Rudan, W. Igl, Y. Milaneschi, A. N. Parker, C. Fava, J. C. Chambers, E. R. Fox, M. Kumari, M. J. Go, P. van der Harst, W. H. Kao, M. Sjogren, D. G. Vinay, M. Alexander, Y. Tabara, S. Shaw-Hawkins, P. H. Whincup, Y. Liu, G. Shi, J. Kuusisto, B. Tayo, M. Seielstad, X. Sim, K. D. Nguyen, T. Lehtimaki, G. Matullo, Y. Wu, T. R. Gaunt, N. C. Onland-Moret, M. N. Cooper, C. G. Platou, E. Org, R. Hardy, S. Dahgam, J. Palmen, V. Vitart, P. S. Braund, T. Kuznetsova, C. S. Uiterwaal, A. Adeyemo, W. Palmas, H. Campbell, B. Ludwig, M. Tomaszewski, I. Tzoulaki, N. D. Palmer, T. Aspelund, M. Garcia, Y. P. Chang, J. R. O'Connell, N. I. Steinle, D. E. Grobbee, D. E. Arking, S. L. Kardia, A. C. Morrison, D. Hernandez, S. Najjar, W. L. McArdle, D. Hadley, M. J. Brown, J. M. Connell, A. D. Hingorani, I. N. Day, D. A. Lawlor, J. P. Beilby, R. W. Lawrence, R. Clarke, J. C. Hopewell, H. Ongen, A. W. Dreisbach, Y. Li, J. H. Young, J. C. Bis, M. Kahonen, J. Viikari, L. S. Adair, N. R. Lee, M. H. Chen, M. Olden, C. Pattaro, J. A. Bolton, A. Kottgen, S. Bergmann, V. Mooser, N. Chaturvedi, T. M. Frayling, M. Islam, T. H. Jafar, J. Erdmann, S. R. Kulkarni, S. R. Bornstein, J. Grassler, L. Groop, B. F. Voight, J. Kettunen, P. Howard, A. Taylor, S. Guarrera, F. Ricceri, V. Emilsson, A. Plump, I. Barroso, K. T. Khaw, A. B. Weder, S. C. Hunt, Y. V. Sun, R. N. Bergman, F. S. Collins, L. L. Bonnycastle, L. J. Scott, H. M. Stringham, L. Peltonen, M. Perola, E. Vartiainen, S. M. Brand, J. A. Staessen, T. J. Wang, P. R. Burton, M. Soler Artigas, Y. Dong, H. Snieder, X. Wang, H. Zhu, K. K. Lohman, M. E. Rudock, S. R. Heckbert, N. L. Smith, K. L. Wiggins, A. Doumatey, D. Shriner, G. Veldre, M. Viigimaa, S. Kinra, D. Prabhakaran, V. Tripathy, C. D. Langefeld, A. Rosengren, D. S. Thelle, A. M. Corsi, A. Singleton, T. Forrester, G. Hilton, C. A. McKenzie, T. Salako, N. Iwai, Y. Kita, T. Ogihara, T. Ohkubo, T. Okamura, H. Ueshima, S. Umemura, S. Eyheramendy, T. Meitinger, H. E. Wichmann,

Y. S. Cho, H. L. Kim, J. Y. Lee, J. Scott, J. S. Sehmi, W. Zhang, B. Hedblad, P. Nilsson, G. D. Smith, A. Wong, N. Narisu, A. Stancakova, L. J. Raffel, J. Yao, S. Kathiresan, C. J. O'Donnell, S. M. Schwartz, M. A. Ikram, W. T. Longstreth, Jr., T. H. Mosley, S. Seshadri, N. R. Shrine, L. V. Wain, M. A. Morken, A. J. Swift, J. Laitinen, I. Prokopenko, P. Zitting, J. A. Cooper, S. E. Humphries, J. Danesh, A. Rasheed, A. Goel, A. Hamsten, H. Watkins, S. J. Bakker, W. H. van Gilst, C. S. Janipalli, K. R. Mani, C. S. Yajnik, A. Hofman, F. U. Mattace-Raso, B. A. Oostra, A. Demirkan, A. Isaacs, F. Rivadeneira, E. G. Lakatta, M. Orru, A. Scuteri, M. Ala-Korpela, A. J. Kangas, L. P. Lyytikainen, P. Soininen, T. Tukiainen, P. Wurtz, R. T. Ong, M. Dorr, H. K. Kroemer, U. Volker, H. Volzke, P. Galan, S. Hercberg, M. Lathrop, D. Zelenika, P. Deloukas, M. Mangino, T. D. Spector, G. Zhai, J. F. Meschia, M. A. Nalls, P. Sharma, J. Terzic, M. V. Kumar, M. Denniff, E. Zukowska-Szczechowska, L. E. Wagenknecht, F. G. Fowkes, F. J. Charchar, P. E. Schwarz, C. Hayward, X. Guo, C. Rotimi, M. L. Bots, E. Brand, N. J. Samani, O. Polasek, P. J. Talmud, F. Nyberg, D. Kuh, M. Laan, K. Hveem, L. J. Palmer, Y. T. van der Schouw, J. P. Casas, K. L. Mohlke, P. Vineis, O. Raitakari, S. K. Ganesh, T. Y. Wong, E. S. Tai, R. S. Cooper, M. Laakso, D. C. Rao, T. B. Harris, R. W. Morris, A. F. Dominiczak, M. Kivimaki, M. G. Marmot, T. Miki, D. Saleheen, G. R. Chandak, J. Coresh, G. Navis, V. Salomaa, B. G. Han, X. Zhu, J. S. Kooner, O. Melander, P. M. Ridker, S. Bandinelli, U. B. Gyllensten, A. F. Wright, J. F. Wilson, L. Ferrucci, M. Farrall, J. Tuomilehto, P. P. Pramstaller, R. Elosua, N. Soranzo, E. J. Sijbrands, D. Altshuler, R. J. Loos, A. R. Shuldiner, C. Gieger, P. Meneton, A. G. Uitterlinden, N. J. Wareham, V. Gudnason, J. I. Rotter, R. Rettig, M. Uda, D. P. Strachan, J. C. Witteman, A. L. Hartikainen, J. S. Beckmann, E. Boerwinkle, R. S. Vasan, M. Boehnke, M. G. Larson, M. R. Jarvelin, B. M. Psaty, G. R. Abecasis, A. Chakravarti, P. Elliott, C. M. van Duijn, C. Newton-Cheh, D. Levy, M. J. Caulfield, T. Johnson, Genetic variants in novel pathways influence blood pressure and cardiovascular disease risk. Nature 478, 103-109 (2011).

28. A. S. Datta, Y. Zhang, L. Zhang, S. Biswas, Association of rare haplotypes on ULK4 and MAP4 genes with hypertension. BMC proceedings 10, 363-369 (2016).

29. T. Yoshida, K. Kato, K. Yokoi, M. Oguri, S. Watanabe, N. Metoki, H. Yoshida, K. Satoh, Y. Aoyagi, Y. Nozawa, Y. Yamada, Association of gene polymorphisms with

chronic kidney disease in Japanese individuals. International journal of molecular medicine 24, 539-547 (2009).

30. T. Fujimaki, K. Kato, K. Yokoi, M. Oguri, T. Yoshida, S. Watanabe, N. Metoki, H. Yoshida, K. Satoh, Y. Aoyagi, Y. Nozawa, G. Kimura, Y. Yamada, Association of genetic variants in SEMA3F, CLEC16A, LAMA3, and PCSK2 with myocardial infarction in Japanese individuals. Atherosclerosis 210, 468-473 (2010).

31. T. J. Chang, Y. F. Chiu, W. H. Sheu, K. C. Shih, C. M. Hwu, T. Quertermous, Y. S. Jou, S. S. Kuo, Y. C. Chang, L. M. Chuang, Genetic polymorphisms of PCSK2 are associated with glucose homeostasis and progression to type 2 diabetes in a Chinese population. Scientific reports 5, 14380 (2015).

32. Y. X. Xie, L. Y. He, X. Chen, X. F. Peng, M. Y. Ye, Y. J. Zhao, W. Z. Yan, C. Liu, J. Shao, Y. M. Peng, Potential diagnostic biomarkers for IgA nephropathy: a comparative study pre- and post-tonsillectomy. International urology and nephrology 48, 1855-1861 (2016).

33. R. Liu, Y. Jin, W. H. Tang, L. Qin, X. Zhang, G. Tellides, J. Hwa, J. Yu, K. A. Martin, Ten-eleven translocation-2 (TET2) is a master regulator of smooth muscle cell plasticity. Circulation 128, 2047-2057 (2013).

34. Y. Zhang, D. Liu, X. Chen, J. Li, L. Li, Z. Bian, F. Sun, J. Lu, Y. Yin, X. Cai, Q. Sun, K. Wang, Y. Ba, Q. Wang, D. Wang, J. Yang, P. Liu, T. Xu, Q. Yan, J. Zhang, K. Zen, C. Y. Zhang, Secreted monocytic miR-150 enhances targeted endothelial cell migration. Molecular cell 39, 133-144 (2010).

35. T. Umezu, K. Ohyashiki, M. Kuroda, J. H. Ohyashiki, Leukemia cell to endothelial cell communication via exosomal miRNAs. Oncogene 32, 2747-2755 (2013).

36. Y. Chen, D. Y. Gao, L. Huang, In vivo delivery of miRNAs for cancer therapy: challenges and strategies. Advanced drug delivery reviews 81, 128-141 (2015).

CHAPTER V: Discussion

9. miRNAs and vascular damage in hypertension and CKD

In the first and second studies, we investigated the role of miRNAs in vascular injury using an Ang II-induced hypertension mouse model and hypertensive patients with or without CKD. It has been suggested that small artery remodeling may be the earliest manifestation of target-organ damage in hypertension (*68*). In these 2 studies, we focused on miRNA profiling in small resistance arteries. Combined with total RNA profiling, it allowed us to study not only the differentially expressed miRNAs and mRNAs associated with small artery injury, but also their interplay in molecular networks.

This approach led us to the identification of key miRNAs in the Delta-like homolog 1-Type III iodothyronine deiodinase (*Dlk1-Dio3*) region that are associated with Ang II-induced vascular damage and hypertension. Among those *Dlk1-Dio3* miRNAs, miR-431-5p acts as a key regulators in the pathophysiological molecular networks of vascular damage, by mediating expression of *Ehf*, Collagen Type I Alpha 1 Chain (*Col1a1*), miR-382, and potentially other ECM genes and *Dlk1-Dio3* miRNAs. Our translational approach combines human and mouse studies that allow us to identify a conserved miRNA, namely miR-145-3p, that is associated with vascular damage involving RAAS activation.

9.1 *Dlk1-Dio3* region

The *Dlk1-Dio3* region is a conserved region flanked by the *Dlk1* gene and the *Dio3* gene, located on chromosome 12qF1 in mouse and chromosome 14q32 in human. The protein-coding genes in this region are highly conserved across species, whereas the miRNAs are conserved only in mammals (*295*). Not only do different genes in this region have different degrees of conservation, they also possess different expression patterns between the paternal and maternal alleles. The *Dlk1-Dio3* region is an imprinted region, in which *Dlk1,* Retrotransposon Gag Like 1 (*Rtl1*), *Dio3* are only paternally expressed, whereas the miRNA cluster, the *SNORD* mall nucleolar RNA cluster (in the human but not the

mouse genome), the Maternally Expressed Gene family (*MEG3* and *MEG8* in human and *Meg3* in mouse) are only maternally expressed (*296, 297*).

The miRNA cluster in the *DLK1-DIO3* region is the largest known mammalian miRNA cluster comprised of 2 sub-clusters. The larger one contains 43 and 41 currently identified miRNAs in the human genome and mouse genome, respectively. In the smaller sub-cluster, there are 11 and 20 known miRNAs in the human genome and mouse genome, respectively (*298, 299*).

9.1.1 DLK1-DIO3 miRNAs in cell proliferation and migration

Dysregulation of *DLK1-DIO3* miRNAs has been shown to associate with cell proliferation and migration in multiple pathologies (*300, 301*), as well as with survival in liver (*302*), lung (*301*) and ovarian (*303*) cancers. Nossent *et al*. demonstrated that miR-487b is up-regulated in the aorta of Ang II-infused rats. miR-487b targets Insulin Receptor Substrate 1 (*IRS1*), which plays an important role in cell proliferation and vascular remodeling via insulin signaling pathways (*304*). miR-541 was shown to be up-regulated in proliferative vascular SMCs induced by Platelet-Derived Growth Factor-BB (PDGF-BB) or fetal bovine serum (FBS). miR-541 mimic transfection was able to induce vascular SMC proliferation by targeting transcription factor Interferon Regulatory Factor 7 (*IRF7*) (*305*), which has been demonstrated to inhibit vascular SMC proliferation and neointima formation (*306*). miR-411 was reported to promote lung cancer cell proliferation by targeting tumor suppressor gene Forkhead Box O1 (*FOXO1*) (*307*). Nadal *et al*. demonstrated that increased miR-411 expression is associated with metastatic relapse and poor survival in lung cancer. They also found that miR-411 expression is correlated with epithelial–mesenchymal transition (EMT) gene expression, and miR-411 knockdown inhibits cell migration in lung cancer cell lines (*301*). miR-495, which was up-regulated in breast cancer, was shown to promote cancer cell invasion and proliferation by targeting Cadherin 1 (*CDH1*), a key player in EMT and cell-cell adhesion during cancer cell invasion, and Protein Regulated In Development And DNA Damage Response 1 (*REDD1*), an mTOR signaling inhibitor (*308*). miR-370 and miR-376a on the other hand, displayed suppressive effect on cell proliferation and migration. Ning *et al*.

showed that miR-370 inhibits gastric cancer cell proliferation and migration by targeting *EGFR (309)*. Zheng *et al.* demonstrated that miR-376a inhibits cell proliferation and promotes apoptosis in liver cancer cell lines by targeting Phosphoinositide-3-Kinase Regulatory Subunit 1 (*PIK3R1*) (*310*).

9.1.2 DLK1-DIO3 region in cardiovascular disease

Risk SNPs associated with coronary artery disease (*311*) and type I diabetes (*312*) were identified in the *DLK1-DIO3* region in large-scale GWASs. Wu *et al*. revealed linkage evidence for hypertension, systolic BP and diastolic BP at the 14q32.2 region, which corresponds to the *DLK1-DIO3* region that contains the smaller miRNA cluster (*313*). Wezel *et al*. used a reverse target prediction strategy to predict miRNAs that target atherosclerosis-related genes and found an enrichment of *DLK1-DIO3* miRNAs. They demonstrated that miR-494 levels are higher in unstable human carotid artery atherosclerotic plaques than in stable ones; miR-494 knockdown by gene silencing oligonucleotides reduces atherosclerotic lesion formation and stabilized atherosclerotic plaques in carotid arteries (*314*). Aavik *et al*. also found an association between atherosclerosis and increased expression of *DLK1-DIO3* miRNAs including miR-127, miR-136, miR-410, miR-431-5p, miR-432 and miR-433 (*315*). Up-regulation of *Dlk1-Dio3* miRNAs was observed during neovascularization process in a mouse hindlimb ischemia (HLI) model (*298*). Thirteen and 39 *Dlk1-Dio3* miRNAs were found up-regulated 24 hours and 72 hours after HLI, respectively. Knockdown of miR-329, miR-487b, miR-494, and miR-495 by gene silencing oligonucleotides increased neovascularization and blood flow recovery after HLI. The authors also demonstrated that miR-329 targets Toll Like Receptor 4 (*Tlr4*), Vascular Endothelial Growth Factor A (*Vegfa*), Myocyte Enhancer Factor 2A (*Mef2a*) and Fibroblast Growth Factor Receptor 2 (*Fgfr2*), whereas miR-494 targets *Tlr4*, *Fgfr2* and ADP Ribosylation Factor 6 (*Arf6*).

9.1.3 DNA methylation in DLK1-DIO3 miRNA expression

As an imprinted region, the *Dlk1-Dio3* region has different gene expression patterns between the paternal and maternal alleles. This means that DNA methylation plays a critical regulatory role mediating gene expression in this region. Global activation of *DLK1-DIO3* miRNAs has been implicated in lung cancer (*301, 307, 316*). Molina-Pinelo *et al*. observed DNA hypomethylation in the *DLK1-DIO3* miRNA region, which may explain the global activation of *DLK1-DIO3* miRNA expression in lung cancer. Inverse correlations were also found between DNA methylation levels and expression levels of randomly selected genes in the *DLK1-DIO3* region (*297*). Similarly, Dai *et al*. revealed that 11 out of the 17 up-regulated miRNAs in a mouse lupus model are located in the *Dlk1-Dio3* region, which is accompanied by DNA hypomethylation; DNA demethylation treatment by 5-aza-2'-deoxycitydine is able to activate expression of selected *Dlk1-Dio3* miRNAs including miR-154, miR-127, miR-379, miR-382, miR-433, and miR-300 in lymphocyte mitogen Con A-activated splenocytes (*317*). Up-regulation of atherosclerosis-*DLK1-DIO3* miRNAs observed by Aavik *et al*. was also accompanied by DNA hypomethylation (*315*).

Considering that 14-day Ang II infusion induced a global up-regulation of *Dlk1-Dio3* miRNAs in mesenteric arteries, this effect may be attributable to a common upstream activator. DNA demethylation is one of the mechanisms that lead to gene activation in imprinted regions. Ten-Eleven Translocation proteins (TETs) have been shown to play a critical role in DNA demethylation at CpG islands in mammals by oxidizing 5-methylcytosine to generate 5-hydroxymethylcytosine. Double-knockdown or double-knockout of *Tet1* and *Tet2* has been demonstrated to increase DNA methylation in imprinted gene regions and suppress imprinted gene expression (*318-320*). Similar results were shown in *Tet1* (*321*) and *Tet3* (*322*) knockout. It is noteworthy that *Tet1* and *Tet3* were also up-regulated upon 14 days of Ang II infusion in our results. However, whether Ang II infusion changes DNA methylation pattern in the *Dlk1-Dio3* region, and whether *Tet1* and *Tet3* play a role in DNA demethlyation in the *Dlk1-Dio3* region causing miRNA activation are still unclear. To address these questions, bisulfite sequencing would be required to examine potential changes of DNA methylation pattern at the CpG islands of the *Dlk1-Dio3* region by Ang II infusion, and by *Tet1* or *Tet3* gain- or loss-of-function

experiments. The next step is to determine whether *Tet1* or *Tet3* gain- or loss-of-function alone is sufficient to change *Dlk1-Dio3* miRNA expression levels.

9.2 miR-431-5p and Ets homologous factor (Ehf)

Another potential mechanism that may cause a global up-regulation of *Dlk1-Dio3* miRNAs is the sharing of a common adjacent cis-regulatory region or presence of a common TF binding site in their promoter regions. We extracted the differentially expressed TFs that were predicted to regulate expression of 9 *Dlk1-Dio3* miRNAs which were correlated with BP (Figure V-1). There are 4 TFs that target at least 6 out of 9 BP-correlated *Dlk1-Dio3* miRNAs. Among those 4 TFs, EHF was also correlated with BP. With our candidate miRNA selection criteria, we had chosen miR-431-5p for further functional studies. EHF, which may regulate miR-431-5p expression, was also predicted to be a downstream target of miR-431-5p. Moreover, the miR-431-5p binding site on the *Ehf* 3' UTR is highly conserved between mouse and human. We therefore focused on the study of the role of the miR-431-5p-*Ehf* pair in Ang II-induced vascular injury and hypertension.

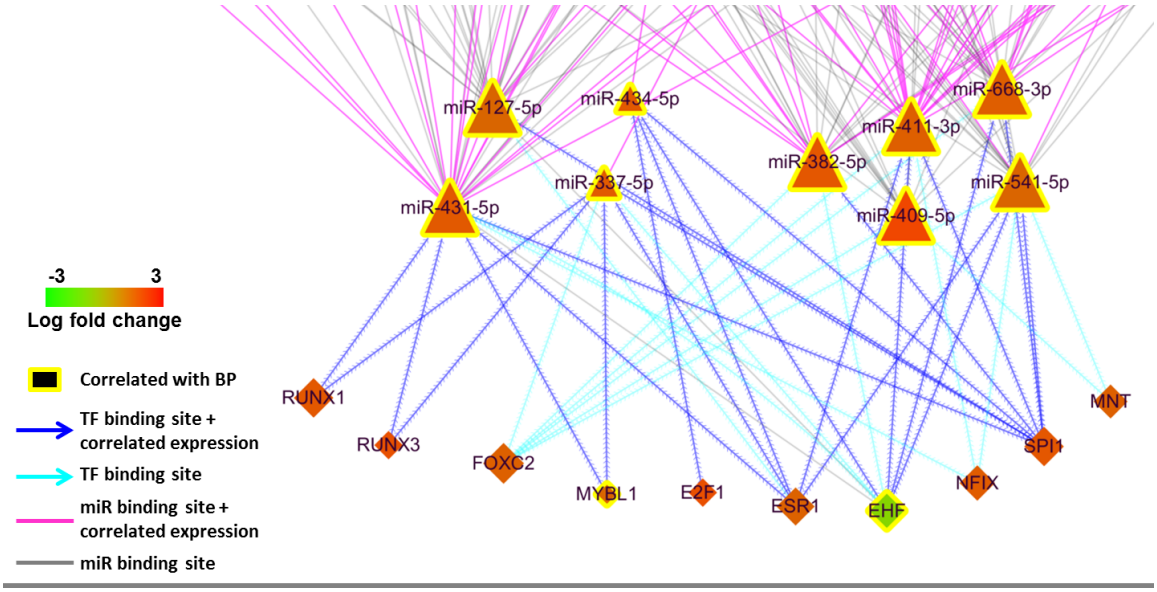

Figure V-1. Interactions between differentially expressed TFs and differentially expressed *Dlk1-Dio3* miRNAs.

9.2.1 miR-431-5p

miR-431-5p has been previously shown to play a role in skeletal muscle differentiation, regeneration and dystrophy. Aged myoblasts exhibited reduced miR-431-5p levels. Transfection of miR-431-5p mimics promoted differentiation and improved regenerative capacity in aged myoblasts by targeting SMAD Family Member 4 (*Smad4*), which inhibited myogenic differentiation (*323*). Overexpression of Paired Box 7 (*Pax-7*) has been shown to down-regulate expression of the MyoD family of transcription factors, leading to myogenesis inhibition in mouse skeletal muscle stem cells, whereas *Pax-7* knockdown by siRNAs promoted myogenesis (*324*). Wu *et al*. demonstrated that miR-431-5p targets *Pax-7* in mouse skeletal muscle stem cells, inducing myogenic differentiation and accelerating muscle regeneration after injury; overexpression of miR-431-5p reduces muscular dystrophy in *mdx* mice (*325*). Myostatin (MSTN) is a member of the transforming growth factor-β (TGF-β) superfamily that negatively regulates skeletal muscle growth. Knockout of *Mstn* up-regulates miR-431-5p via the Ras-Mek-Erk signaling pathway. Overexpression of miR-431-5p was able to abrogate MSTN-induced suppression of skeletal muscle cell differentiation (*326*).

miR-431-5p has also been shown to regulate neuron outgrowth and regeneration. Mutation in the Survival of Motor Neuron 1 (*SMN1*) is associated with neurodegeneration, leading to loss of spinal motor neurons in spinal muscular atrophy (*327*). Knockdown of *Smn1* by small hairpin RNAs (shRNAs) was demonstrated to increase miR-431-5p levels and impair motor neuron viability and outgrowth. miR-431-5p was found to regulate motor neuron outgrowth by targeting chondrolectin (*Chodl*) (*328*). Wu *et al*. showed that sciatic nerve crush-induced injury activates miR-431-5p expression in nerve cells; transfection of miR-431-5p mimics promotes post-injury neuron regeneration by targeting Kringle Containing Transmembrane Protein 1 (*Kremen1*), which is an antagonist of Wnt/beta-catenin signaling and a negative regulator of neuron outgrowth (*329*).

9.2.1 EHF

EHF is an ETS family TF that has been shown to act as either a transcriptional activator or a transcriptional repressor in epithelial cells. Albino *et al*. demonstrated that knockdown of *EHF* by shRNAs induces stem-like and tumor-like features such as increased EMT, the ability to propagate and form tumors, as well as metastatic properties in prostate epithelial cells; re-expression of *EHF* inhibits those stem-like and tumor-like features, and reduces cell migration and proliferation by regulating expression of genes involved in EMT and stemness such as G Protein Subunit Gamma 11 (*GNG11*), Vimentin (*VIM*), Cadherin 1 (*CDH1*), Forkhead Box A1 (*FOXA1*), *COL1A1* and Fibrillin 1 (*FBN1*) (*330*). However, other groups have observed an opposite role of EHF on tumor cells (*331, 332*). Taniue *et al*. found that that EHF is required for colon tumor cell survival via activating RuvB Like AAA ATPase 1 (RUVBL1) expression, which allows tumor cells to avoid p53-induced apoptosis (*331*). Park *et al*. found that *EHF* is down-regulated by DNA damage-induced senescence in prostate and breast cancer cells; knockdown of *EHF* by siRNAs inhibited cell proliferation, induced premature cellular senescence and decreased telomerase activity (*332*). Fossum *et al*. demonstrated that overexpression and knockdown of *EHF* in airway epithelial cells by expression vectors and siRNAs, respectively, altered expression of gene associated with response to wounding, maintenance of barrier function and inflammation; *EHF* knockdown was accompanied by a slower rate of wound repair (*333, 334*).

9.2.3 The interaction between miR-431-5p and Ehf in Ang II-induced vascular injury and hypertension

Although miR-431-5p has been implicated in differentiation and proliferation of skeletal muscle cells and motor neurons, its role in SMCs has not been studied before. We demonstrated for the first time that miR-431-5p targets *Ehf* in vascular SMCs, leading to activation of *Col1a1* and miR-382-5p expression. Human EHF has already been shown to negatively regulate *COL1A1* expression in prostate cancer cells and inhibit cell migration and proliferation (*330*). Increased type I collagen deposition is one of the main mechanisms of vascular remodeling and stiffening (*27-29*). Periadventitial delivery to

mouse carotid arteries of R1R2, a peptide that inhibits type I collagen deposition by interfering with the binding of fibronectin to collagen, using pluronic gel was reported to efficiently decrease carotid artery type I collagen deposition and reduce flow-induced vascular remodeling and inflammation. *In vitro* treatment of R1R2 inhibited cell proliferation and migration, and as well decreased *VCAM-1* and *ICAM-1* expression in SMCs (*335*). However, considering that R1R2 has never been used *in vivo* in any other published study and that potential side effects were not stated, whether it possesses therapeutic value remain to be elucidated. Our study demonstrated that miR-431-5p inhibition could be an alternative approach to inhibit collagen deposition via EHF. It is noteworthy the R1R2 was shown to reduce vascular remodeling in carotid arteries whereas we showed that miR-431-5p inhibitors reduces vascular stiffening in mesenteric arteries. Whether miR-431-5p inhibition affects large artery stiffening is unclear as the latter was not investigated in our study. Another target of EHF reported in our study is miR-382-5p, which has been shown to control hematopoietic stem cell differentiation by targeting the cell differentiation-associated transcriptional repressor MAX Dimerization Protein 1 (*MXD1*) (*336*), as well as to inhibit tumor progression and metastasis by targeting the EMT-associated TF Y box-binding protein 1 (*YB-1*) (*337*) and tumor suppressor gene SET Domain-Containing Protein 8 (*SETD8*) (*338*). However, the role of miR-382-5p on the vascular cell phenotype or hypertension has not been previously investigated. Deeper analysis on the potential targets of miR-382-5p as well as functional gain- and loss-of-function experiments will be required to examine whether miR-382-5p plays a role in vascular injury. As a TF, EHF is expected to mediate expression of other genes. According to the gene ontology (GO) enrichment analysis, the EHF targets in our DE genes are enriched in genes involved in ECM, developmental processes, growth factor signaling, responses to wounding, ossification, peptidase activity, cell proliferation and protein transport. This result is partially consistent with what Fossum *et al*. found in airway epithelial cells (*333, 334*). Although expression of other predicted targets of EHF, namely Biglycan (*Bgn*), fibronectin 1 (*Fn1*) and connective tissue growth factor (*Ctgf*), were not affected by siEHF treatment in human vascular SMCs, nor in mouse mesenteric arteries by miR-431-5p inhibitor injection, future experiments should be conducted to examine the effect of miR-431-5p inhibitors on other miR-431-5p targets and Ehf targets.

9.3 miR-145-3p

Comparing the human and mouse vascular miRNA profiling results, there is only one common miRNA, namely miR-145-3p, associated with vascular injury in both Ang II-induced hypertension and human hypertension associated with CKD. Its opposite strand, miR-145-5p, inhibits vascular SMC proliferation and differentiation by targeting different TFs (*239*). Knockout of miR-145-5p caused structural changes in the SMC layers of the vessels, compromised vascular contractility and significantly reduced BP (*240-242*). However, miR-145-3p has only been implicated in migration and proliferation of cancer cells but not SMCs (*339, 340*). miR-145-5p and miR-145-3p originate from the same pre-miRNA. According to the canonical miRNA biogenesis pathway, they are co-expressed by the genome and therefore co-regulated during transcription. When one is dysregulated, the other should be as well. In fact, in the mouse mesenteric artery miRNA sequencing profile, miR-145-5p was also down-regulated by 7 days of Ang II infusion like miR-145-3p. However, miR-145-5p did not pass the 1.5-fold-change threshold that we set to define differential expression. Although both miR-145-5p and miR-145-3p have been shown to inhibit cell migration and proliferation, they have completely different seed sequences and therefore target different genes. We focused on miR-145-3p because it reached statistical significance in both the human and the mouse studies.

We have demonstrated *in vitro* by gain- and loss-of-function experiments that miR-145-3p down-regulates Insulin Like Growth Factor 1 (*Igf1*), *Fn1* and Follistatin Like 1 (*Fstl1*) in mouse vascular SMCs. (Data are not presented in this thesis.) Luciferase assays are currently being conducted to confirm whether miR-145-3p targets these genes in the canonical machinery. *Igf1*, *Fn1* and *Fstl1*, which were all up-regulated by Ang II infusion, have been associated with vascular growth and remodeling. Sun *et al*. showed that SMC-specific *Igf1* knockout or IGF1R inhibition by OSI-906 attenuates small artery remodeling in hypoxia-induced pulmonary hypertension (*341*). IGF1 also plays a role in brain vessel growth. Systemic IGF1 administration promotes angiogenesis, whereas systemic blockade of IGF1 by antibodies inhibits injury-induced angiogenesis in the brain (*342*). As one of the major ECM components in the media of the artery, fibronectin

is a critical determinant of vascular stiffness. Increased fibronectin deposition has been shown to contribute to vascular remodeling and stiffening (*27-29*). Chiang *et al*. demonstrated that *in vivo* periadventitial administration of the fibronectin blocker pUR4 attenuates ligation-induce vascular remodeling and decreases ICAM-1 and VCAM-1 in carotid arteries, whereas *in vitro* pUR4 treatment in vascular SMCs inhibits cell proliferation (*343*). *Fstl1* is required for SMC growth and differentiation in pulmonary arteries (*344*) and has been shown to regulate pulmonary vasculature development via the BMP/Smad signaling pathway (*345*).

It is noteworthy that the 7-day Ang II-induced down-regulation of miR-145-3p is no longer found in the 14-day Ang II group while *Igf1*, *Fn1* and *Fstl1* are up-regulated by both 7-day and 14-day Ang II infusion. It is well known that the gene-gene interaction network is characterized by a high degree of complexity and robustness, which means that in most cases genes are not regulated by a single factor. miR-145-3p is not expected to be the sole mediator for *Igf1*, *Fn1* and *Fstl1* expression. Up-regulation of *Igf1*, *Fn1* and *Fstl1* observed in the 14-day Ang II group could be attributed to other miRNAs or TFs.

10. Circulating miRNAs in hypertension and CKD

In the third study, we performed small RNA sequencing in plasma to study circulating miRNAs associated with essential hypertension and CKD, as well as with vascular injury in these conditions. The differential expression of 4 miRNAs, namely let-7g-5p, miR-26a-5p, miR-191-5p and let-7b-5p, were also observed by another research group (*215*), and were validated by us using RT-qPCR. Among all the differentially expressed circulating miRNAs, let-7g-5p was the only one whose expression was correlated with eGFR. Combined with the vascular RNA profiling results from the same cohort of human subjects, we have identified genes whose expression in small arteries was correlated with circulating let-7g-5p levels. The majority of the top correlated genes were also dys-regulated in small arteries of CKD patients. This suggests a potential link between circulating let-7g-5p and abnormal vascular gene expression in CKD.

10.1 let-7g-5p

Low circulating let-7g-5p levels have been associated with endothelial dysfunction in subjects who have had lacunar infarcts. *In vivo* and *in vitro* gain- and loss-of-function experiments showed that let-7g-5p targets the endothelial dysfunction marker Plasminogen Activator Inhibitor (*PAI-1*) and is able to reduce inflammation and VCAM-1 secretion in endothelial cells (*346*). Activation or overexpression of Oxidized Low Density Lipoprotein Receptor 1 (OLR1) has been reported to induce vascular SMC proliferation, vascular remodeling and atherosclerosis (*347, 348*). Liu *et al*. demonstrated that let-7g-5p targets *OLR1* and inhibits OLR1-induced vascular SMC proliferation. Systemic *in vivo* let-7g-5p administration down-regulated *OLR1* in the aorta, and attenuated high-fat diet-induced vascular growth and atherosclerotic lesions in Apolipoprotein E (*apoE*) knockout mice (*349*). Let-7g-5p was also shown to prevent PDGF-induced vascular SMC status switch from contractile to synthetic phenotype by targeting PDGF Subunit B (*PDGFB*) and Mitogen-Activated Protein Kinase Kinase Kinase 1 (*MEKK1*) involved in the PDGF/MEKK1/ERK/KLF4 signaling pathway. *In vivo* overexpression of let-7g-5p by lentivirus caused up-regulation of let-7g-5p in the aorta and decreased atherosclerotic plaques in *apoE* knockout mice (*350*).

10.2 Circulating miRNAs and vascular damage

A few studies have demonstrated communication between extracellular miRNAs and vascular cells *in vitro*, in which endothelial cell- or immune cell-originated vesicle-associated miRNAs were taken up by co-cultured endothelial cells where they mediated gene expression (*184-186*). However, it is still unclear whether circulating miRNAs can be incorporated into vascular cells and target gene expression *in vivo*. Chao *et al*. observed a decrease of circulating miR-125b in adenine-induced CKD rats as well as an inverse correlation between circulating miR-125b levels and the severity of vascular calcification in CKD patients. They were also able to use circulating miR-125b levels in a stepwise multivariate logistic regression model to predict vascular calcification

progression in the same cohort of patients after a 2-year follow-up, as well as in another independent cohort of patients (*351*).

Although circulating let-7g-5p was shown by us to correlate with vascular damage-associated genes in CKD, whether it regulates gene expression in the vasculature and plays a role in vascular damage remains to be elucidated. It is also unclear which tissues circulating let-7g-5p originates from or what causes its down-regulation in CKD. Injection of pre-labeled vesicle-associated let-7g-5p could be used to detect which tissues will take up let-7g-5p and whether expression of target genes is mediated by the miRNA. The origin of endogenous circulating let-7g-5p, however, is more difficult to determine. Considering that circulating let-7g-5p may be associated with vascular damage in CKD, renal vascular endothelial cells could be a potential source. Knockdown of let-7g-5p specifically in candidate tissues or cell types can be conducted to examine whether endogenous circulating let-7g-5p levels are altered. Regardless of the unknown upstream regulators and its potential downstream effect on vascular cells, circulating let-7g-5p still has potential value to serve as biomarker of vascular injury in CKD.

11. Limitations and challenges

There are limitations to our studies as well as challenges that we encountered during data analysis. In the first study, we identified miR-431-5p and its target *Ehf* as key regulators in Ang II-induced vascular damage and hypertension. Intravenous injection of miR-431-5p inhibitors caused up-regulation of *Ehf* and down-regulation of miR-431-5p, miR-382-5p and *Col1a1* in mouse mesenteric arteries. We selected *Ehf* as a miR-431-5p target, and *Col1a1* and miR-382-5p as EHF targets for functional studies based on our candidate approach criteria. However, miR-431-5p and EHF are expected to mediate expression of many other genes that we did not investigate. Intravenous delivery of miR-431-5p inhibitors is expected to cause a systemic knockdown of miR-431-5p elsewhere than only in mesenteric arteries, therefore affecting expression of its targets in other tissues. Although we did not observe weight changes in heart, kidneys, liver or spleen, future

experiments will be required to examine potential toxicity and off-target effects in different tissues and organs.

The design of our miRNA profiling project was directed toward identifying conserved key miRNA regulators in vascular damage in essential hypertension with or without CKD by conducting a multi-model study using different rodent hypertension models as well as hypertensive and CKD patients. The Ang II-infused mouse was the first rodent hypertensive model that we used in combination with the human study to identify conserved vascular damage-associated miRNAs that are involved in RAAS activation. However, the expression levels of both candidate key regulators that we identified in the first study, namely miR-431-5p and *Ehf*, were too low in the human small artery expression profiles to allow statistical analysis. It is possible that miR-431-5p and *Ehf* levels are lower in human arteries than in mouse arteries, or lower in subcutaneous arteries than in mesenteric arteries. As a result, we were not able to demonstrate whether miR-431-5p and *Ehf* are involved in vascular damage in human hypertension and CKD. Nevertheless, miRNAs or transcriptional factors with low expression levels can have large regulatory effect on gene expression. A more sensitive measurement approach such as deeper RNA sequencing or RT-qPCR with pre-amplification will be required in future studies conducted on human small arteries.

Combining the mouse and human studies led us to the identification of miR-145-3p, which was down-regulated in both Ang II-associated and CKD-associated vascular damage. However, no common miR-145-3p target was found in the differentially expressed genes in both studies. The validation of miR-145-3p targets in mouse and human vessels, as well as investigation whether miR-145-3p plays a role in vascular damage, are ongoing. It is important to point out again that the gene-gene interaction network is complex and robust. The expression of miR-145-3p targets is not expected to be regulated solely by miR-145-3p. Other regulators that are differentially expressed between the Ang II-infused mouse model and CKD patients may explain the difference in miR-145-3p target expression between two studies. This remains a challenge for candidate miR-145-3p target selection and future experimental design.

We have also encountered challenges in data analysis when we had to set the threshold to define differential expression. In the first study, we used a threshold of 1.5-fold change with false discovery rate (FDR) < 0.05. In the second study, we used a threshold of *P* value < 0.05. In the third study, we used a threshold of FDR < 0.1. The purpose of applying FDR using the Benjamini–Hochberg test was to correct for multiple comparisons and achieve a lower type I error (false positive). However, when using an FDR < 0.05 in the second and third studies, only very few differentially expressed miRNAs were identified. This may be attributable to the well-known high genetic heterogeneity in humans compared to the inbred mice we used in the first study. We therefore applied a less stringent threshold in the human studies. Although a correction for multiple comparisons lowers a type I error, it at the same time increases a type II error (false negative) and may hinder us from finding true positive vascular damage-associated miRNAs. In order to better analyze the data, we adopted an optimized approach to use uncorrected *P* values or higher FDR in the differential expression analysis combined with RT-qPCR validation to minimize both type I and type II errors, followed by correlation analysis between clinical parameters and gene expression levels to identify key vascular damage-associated miRNAs in hypertension and CKD.

12. Perspectives

Despite a variety of anti-hypertensive drug of different classes available in the market and often used in combination, a significant proportion of the population of hypertensive patients (33% in Canada and 50% in the USA, much higher percent elsewhere) have uncontrolled BP (*293*). Current treatments for CKD are barely able to delay disease progression (*294*). There is no cure for hypertension or CKD but there is growing demand for better treatment. Small artery damage has been suggested to be the earliest manifestation of target-organ damage in hypertension (*68*) and is tightly associated with CKD (*85, 86, 97, 98*). Tissue miRNAs possess the potential to become master regulators in cardiovascular disease development (*201-203*), whereas circulating miRNAs are being demonstrated to be valuable biomarkers for disease diagnosis and prognosis (*283, 285,*

286, 351). Our studies not only shed light onto the pathophysiological molecular networks involved in vascular damage in hypertension and CKD, but also provide potential important candidate miRNA regulators that may be utilized as therapeutic targets as well as candidate circulating miRNAs that may be used as biomarkers for vascular damage in hypertension and CKD.

References

1. K. T. Mills, J. D. Bundy, T. N. Kelly, J. E. Reed, P. M. Kearney, K. Reynolds, J. Chen, J. He, Global Disparities of Hypertension Prevalence and Control: A Systematic Analysis of Population-Based Studies From 90 Countries. *Circulation* **134**, 441-450 (2016).

2. D. Mozaffarian, E. J. Benjamin, A. S. Go, D. K. Arnett, M. J. Blaha, M. Cushman, S. de Ferranti, J. P. Despres, H. J. Fullerton, V. J. Howard, M. D. Huffman, S. E. Judd, B. M. Kissela, D. T. Lackland, J. H. Lichtman, L. D. Lisabeth, S. Liu, R. H. Mackey, D. B. Matchar, D. K. McGuire, E. R. Mohler, 3rd, C. S. Moy, P. Muntner, M. E. Mussolino, K. Nasir, R. W. Neumar, G. Nichol, L. Palaniappan, D. K. Pandey, M. J. Reeves, C. J. Rodriguez, P. D. Sorlie, J. Stein, A. Towfighi, T. N. Turan, S. S. Virani, J. Z. Willey, D. Woo, R. W. Yeh, M. B. Turner, Heart disease and stroke statistics--2015 update: a report from the American Heart Association. *Circulation* **131**, e29-322 (2015).

3. P. A. Heidenreich, J. G. Trogdon, O. A. Khavjou, J. Butler, K. Dracup, M. D. Ezekowitz, E. A. Finkelstein, Y. Hong, S. C. Johnston, A. Khera, D. M. Lloyd-Jones, S. A. Nelson, G. Nichol, D. Orenstein, P. W. Wilson, Y. J. Woo, Forecasting the future of cardiovascular disease in the United States: a policy statement from the American Heart Association. *Circulation* **123**, 933-944 (2011).

4. S. S. Lim, T. Vos, A. D. Flaxman, G. Danaei, K. Shibuya, H. Adair-Rohani, M. Amann, H. R. Anderson, K. G. Andrews, M. Aryee, C. Atkinson, L. J. Bacchus, A. N. Bahalim, K. Balakrishnan, J. Balmes, S. Barker-Collo, A. Baxter, M. L. Bell, J. D. Blore, F. Blyth, C. Bonner, G. Borges, R. Bourne, M. Boussinesq, M. Brauer, P. Brooks, N. G. Bruce, B. Brunekreef, C. Bryan-Hancock, C. Bucello, R. Buchbinder, F. Bull, R. T. Burnett, T. E. Byers, B. Calabria, J. Carapetis, E. Carnahan, Z. Chafe, F. Charlson, H. Chen, J. S. Chen, A. T. Cheng, J. C. Child, A. Cohen, K. E. Colson, B. C. Cowie, S. Darby, S. Darling, A. Davis, L. Degenhardt, F. Dentener, D. C. Des Jarlais, K. Devries, M. Dherani, E. L. Ding, E. R. Dorsey,

T. Driscoll, K. Edmond, S. E. Ali, R. E. Engell, P. J. Erwin, S. Fahimi, G. Falder, F. Farzadfar, A. Ferrari, M. M. Finucane, S. Flaxman, F. G. Fowkes, G. Freedman, M. K. Freeman, E. Gakidou, S. Ghosh, E. Giovannucci, G. Gmel, K. Graham, R. Grainger, B. Grant, D. Gunnell, H. R. Gutierrez, W. Hall, H. W. Hoek, A. Hogan, H. D. Hosgood, 3rd, D. Hoy, H. Hu, B. J. Hubbell, S. J. Hutchings, S. E. Ibeanusi, G. L. Jacklyn, R. Jasrasaria, J. B. Jonas, H. Kan, J. A. Kanis, N. Kassebaum, N. Kawakami, Y. H. Khang, S. Khatibzadeh, J. P. Khoo, C. Kok, F. Laden, R. Lalloo, Q. Lan, T. Lathlean, J. L. Leasher, J. Leigh, Y. Li, J. K. Lin, S. E. Lipshultz, S. London, R. Lozano, Y. Lu, J. Mak, R. Malekzadeh, L. Mallinger, W. Marcenes, L. March, R. Marks, R. Martin, P. McGale, J. McGrath, S. Mehta, G. A. Mensah, T. R. Merriman, R. Micha, C. Michaud, V. Mishra, K. Mohd Hanafiah, A. A. Mokdad, L. Morawska, D. Mozaffarian, T. Murphy, M. Naghavi, B. Neal, P. K. Nelson, J. M. Nolla, R. Norman, C. Olives, S. B. Omer, J. Orchard, R. Osborne, B. Ostro, A. Page, K. D. Pandey, C. D. Parry, E. Passmore, J. Patra, N. Pearce, P. M. Pelizzari, M. Petzold, M. R. Phillips, D. Pope, C. A. Pope, 3rd, J. Powles, M. Rao, H. Razavi, E. A. Rehfuess, J. T. Rehm, B. Ritz, F. P. Rivara, T. Roberts, C. Robinson, J. A. Rodriguez-Portales, I. Romieu, R. Room, L. C. Rosenfeld, A. Roy, L. Rushton, J. A. Salomon, U. Sampson, L. Sanchez-Riera, E. Sanman, A. Sapkota, S. Seedat, P. Shi, K. Shield, R. Shivakoti, G. M. Singh, D. A. Sleet, E. Smith, K. R. Smith, N. J. Stapelberg, K. Steenland, H. Stockl, L. J. Stovner, K. Straif, L. Straney, G. D. Thurston, J. H. Tran, R. Van Dingenen, A. van Donkelaar, J. L. Veerman, L. Vijayakumar, R. Weintraub, M. M. Weissman, R. A. White, H. Whiteford, S. T. Wiersma, J. D. Wilkinson, H. C. Williams, W. Williams, N. Wilson, A. D. Woolf, P. Yip, J. M. Zielinski, A. D. Lopez, C. J. Murray, M. Ezzati, M. A. AlMazroa, Z. A. Memish, A comparative risk assessment of burden of disease and injury attributable to 67 risk factors and risk factor clusters in 21 regions, 1990-2010: a systematic analysis for the Global Burden of Disease Study 2010. *Lancet (London, England)* **380**, 2224-2260 (2012).

5. A. A. Leung, K. Nerenberg, S. S. Daskalopoulou, K. McBrien, K. B. Zarnke, K. Dasgupta, L. Cloutier, M. Gelfer, M. Lamarre-Cliche, A. Milot, P. Bolli, G. Tremblay, D. McLean, S. W. Tobe, M. Ruzicka, K. D. Burns, M. Vallee, G. V.

Prasad, M. Lebel, R. D. Feldman, P. Selby, A. Pipe, E. L. Schiffrin, P. A. McFarlane, P. Oh, R. A. Hegele, M. Khara, T. W. Wilson, S. B. Penner, E. Burgess, R. J. Herman, S. L. Bacon, S. W. Rabkin, R. E. Gilbert, T. S. Campbell, S. Grover, G. Honos, P. Lindsay, M. D. Hill, S. B. Coutts, G. Gubitz, N. R. Campbell, G. W. Moe, J. G. Howlett, J. M. Boulanger, A. Prebtani, P. Larochelle, L. A. Leiter, C. Jones, R. I. Ogilvie, V. Woo, J. Kaczorowski, L. Trudeau, R. J. Petrella, S. Hiremath, D. Drouin, K. L. Lavoie, P. Hamet, G. Fodor, J. C. Gregoire, R. Lewanczuk, G. K. Dresser, M. Sharma, D. Reid, S. A. Lear, G. Moullec, M. Gupta, L. A. Magee, A. G. Logan, K. C. Harris, J. Dionne, A. Fournier, G. Benoit, J. Feber, L. Poirier, R. S. Padwal, D. M. Rabi, Hypertension Canada's 2016 Canadian Hypertension Education Program Guidelines for Blood Pressure Measurement, Diagnosis, Assessment of Risk, Prevention, and Treatment of Hypertension. *The Canadian journal of cardiology* **32**, 569-588 (2016).

6. O. A. Carretero, S. Oparil, Essential hypertension. Part I: definition and etiology. *Circulation* **101**, 329-335 (2000).

7. H. M. Wadei, S. C. Textor, The role of the kidney in regulating arterial blood pressure. *Nature reviews. Nephrology* **8**, 602-609 (2012).

8. J. L. Osborn, Relation between sodium intake, renal function, and the regulation of arterial pressure. *Hypertension (Dallas, Tex. : 1979)* **17**, I91-96 (1991).

9. S. Udani, I. Lazich, G. L. Bakris, Epidemiology of hypertensive kidney disease. *Nature reviews. Nephrology* **7**, 11-21 (2011).

10. G. Remuzzi, N. Perico, M. Macia, P. Ruggenenti, The role of renin-angiotensin-aldosterone system in the progression of chronic kidney disease. *Kidney international. Supplement*, S57-65 (2005).

11. T. K. Ma, K. K. Kam, B. P. Yan, Y. Y. Lam, Renin-angiotensin-aldosterone system blockade for cardiovascular diseases: current status. *British journal of pharmacology* **160**, 1273-1292 (2010).

12. J. P. Casas, W. Chua, S. Loukogeorgakis, P. Vallance, L. Smeeth, A. D. Hingorani, R. J. MacAllister, Effect of inhibitors of the renin-angiotensin system

and other antihypertensive drugs on renal outcomes: systematic review and meta-analysis. *Lancet (London, England)* **366**, 2026-2033 (2005).

13. D. Zhao, D. M. Seth, L. G. Navar, Enhanced distal nephron sodium reabsorption in chronic angiotensin II-infused mice. *Hypertension (Dallas, Tex. : 1979)* **54**, 120-126 (2009).

14. J. E. Hall, A. C. Guyton, M. J. Smith, Jr., T. G. Coleman, Blood pressure and renal function during chronic changes in sodium intake: role of angiotensin. *The American journal of physiology* **239**, F271-280 (1980).

15. J. M. Wyss, S. H. Carlson, The role of the central nervous system in hypertension. *Current hypertension reports* **1**, 246-253 (1999).

16. M. P. Schlaich, P. A. Sobotka, H. Krum, R. Whitbourn, A. Walton, M. D. Esler, Renal Denervation as a Therapeutic Approach for Hypertension. *Novel Implications for an Old Concept* **54**, 1195-1201 (2009).

17. G. F. DiBona, The Sympathetic Nervous System and Hypertension. *Recent Developments* **43**, 147-150 (2004).

18. M. C. Zimmerman, E. Lazartigues, R. V. Sharma, R. L. Davisson, Hypertension caused by angiotensin II infusion involves increased superoxide production in the central nervous system. *Circulation research* **95**, 210-216 (2004).

19. M. C. Zimmerman, E. Lazartigues, J. A. Lang, P. Sinnayah, I. M. Ahmad, D. R. Spitz, R. L. Davisson, Superoxide mediates the actions of angiotensin II in the central nervous system. *Circulation research* **91**, 1038-1045 (2002).

20. T. Kahan, L. Bergfeldt, Left ventricular hypertrophy in hypertension: its arrhythmogenic potential. *Heart (British Cardiac Society)* **91**, 250-256 (2005).

21. E. D. Frohlich, An updated concept for left ventricular hypertrophy risk in hypertension. *The Ochsner journal* **9**, 181-190 (2009).

22. M. P. Schlaich, D. M. Kaye, E. Lambert, M. Sommerville, F. Socratous, M. D. Esler, Relation between cardiac sympathetic activity and hypertensive left ventricular hypertrophy. *Circulation* **108**, 560-565 (2003).

23. J. Sadoshima, S. Izumo, Molecular characterization of angiotensin II--induced hypertrophy of cardiac myocytes and hyperplasia of cardiac fibroblasts. Critical role of the AT1 receptor subtype. *Circulation research* **73**, 413-423 (1993).

24. R. B. Devereux, B. Dahlof, E. Gerdts, K. Boman, M. S. Nieminen, V. Papademetriou, J. Rokkedal, K. E. Harris, J. M. Edelman, K. Wachtell, Regression of hypertensive left ventricular hypertrophy by losartan compared with atenolol: the Losartan Intervention for Endpoint Reduction in Hypertension (LIFE) trial. *Circulation* **110**, 1456-1462 (2004).

25. R. E. Schmieder, P. Martus, A. Klingbeil, Reversal of left ventricular hypertrophy in essential hypertension. A meta-analysis of randomized double-blind studies. *Jama* **275**, 1507-1513 (1996).

26. E. L. Schiffrin, Remodeling of resistance arteries in essential hypertension and effects of antihypertensive treatment. *American journal of hypertension* **17**, 1192-1200 (2004).

27. H. D. Intengan, L. Y. Deng, J. S. Li, E. L. Schiffrin, Mechanics and composition of human subcutaneous resistance arteries in essential hypertension. *Hypertension (Dallas, Tex. : 1979)* **33**, 569-574 (1999).

28. H. D. Intengan, G. Thibault, J. S. Li, E. L. Schiffrin, Resistance artery mechanics, structure, and extracellular components in spontaneously hypertensive rats : effects of angiotensin receptor antagonism and converting enzyme inhibition. *Circulation* **100**, 2267-2275 (1999).

29. E. L. Schiffrin, Vascular remodeling in hypertension: mechanisms and treatment. *Hypertension (Dallas, Tex. : 1979)* **59**, 367-374 (2012).

30. G. F. Mitchell, Effects of central arterial aging on the structure and function of the peripheral vasculature: implications for end-organ damage. *Journal of applied physiology (Bethesda, Md. : 1985)* **105**, 1652-1660 (2008).

31. G. F. Mitchell, H. Parise, E. J. Benjamin, M. G. Larson, M. J. Keyes, J. A. Vita, R. S. Vasan, D. Levy, Changes in arterial stiffness and wave reflection with

advancing age in healthy men and women: the Framingham Heart Study. *Hypertension (Dallas, Tex. : 1979)* **43**, 1239-1245 (2004).

32. H. Tomiyama, A. Yamashina, Non-invasive vascular function tests: their pathophysiological background and clinical application. *Circulation journal : official journal of the Japanese Circulation Society* **74**, 24-33 (2010).

33. T. Barhoumi, D. A. Kasal, M. W. Li, L. Shbat, P. Laurant, M. F. Neves, P. Paradis, E. L. Schiffrin, T regulatory lymphocytes prevent angiotensin II-induced hypertension and vascular injury. *Hypertension (Dallas, Tex. : 1979)* **57**, 469-476 (2011).

34. A. Caillon, M. O. Mian, J. C. Fraulob-Aquino, K. G. Huo, T. Barhoumi, S. Ouerd, P. R. Sinnaeve, P. Paradis, E. L. Schiffrin, Gamma Delta T Cells Mediate Angiotensin II-Induced Hypertension and Vascular Injury. *Circulation*, (2017).

35. E. L. Schiffrin, R. M. Touyz, From bedside to bench to bedside: role of renin-angiotensin-aldosterone system in remodeling of resistance arteries in hypertension. *American journal of physiology. Heart and circulatory physiology* **287**, H435-446 (2004).

36. C. Newton-Cheh, T. Johnson, V. Gateva, M. D. Tobin, M. Bochud, L. Coin, S. S. Najjar, J. H. Zhao, S. C. Heath, S. Eyheramendy, K. Papadakis, B. F. Voight, L. J. Scott, F. Zhang, M. Farrall, T. Tanaka, C. Wallace, J. C. Chambers, K. T. Khaw, P. Nilsson, P. van der Harst, S. Polidoro, D. E. Grobbee, N. C. Onland-Moret, M. L. Bots, L. V. Wain, K. S. Elliott, A. Teumer, J. Luan, G. Lucas, J. Kuusisto, P. R. Burton, D. Hadley, W. L. McArdle, M. Brown, A. Dominiczak, S. J. Newhouse, N. J. Samani, J. Webster, E. Zeggini, J. S. Beckmann, S. Bergmann, N. Lim, K. Song, P. Vollenweider, G. Waeber, D. M. Waterworth, X. Yuan, L. Groop, M. Orho-Melander, A. Allione, A. Di Gregorio, S. Guarrera, S. Panico, F. Ricceri, V. Romanazzi, C. Sacerdote, P. Vineis, I. Barroso, M. S. Sandhu, R. N. Luben, G. J. Crawford, P. Jousilahti, M. Perola, M. Boehnke, L. L. Bonnycastle, F. S. Collins, A. U. Jackson, K. L. Mohlke, H. M. Stringham, T. T. Valle, C. J. Willer, R. N. Bergman, M. A. Morken, A. Doring, C. Gieger, T. Illig, T. Meitinger, E. Org, A. Pfeufer, H. E. Wichmann, S. Kathiresan, J. Marrugat, C. J. O'Donnell, S. M.

Schwartz, D. S. Siscovick, I. Subirana, N. B. Freimer, A. L. Hartikainen, M. I. McCarthy, P. F. O'Reilly, L. Peltonen, A. Pouta, P. E. de Jong, H. Snieder, W. H. van Gilst, R. Clarke, A. Goel, A. Hamsten, J. F. Peden, U. Seedorf, A. C. Syvanen, G. Tognoni, E. G. Lakatta, S. Sanna, P. Scheet, D. Schlessinger, A. Scuteri, M. Dorr, F. Ernst, S. B. Felix, G. Homuth, R. Lorbeer, T. Reffelmann, R. Rettig, U. Volker, P. Galan, I. G. Gut, S. Hercberg, G. M. Lathrop, D. Zelenika, P. Deloukas, N. Soranzo, F. M. Williams, G. Zhai, V. Salomaa, M. Laakso, R. Elosua, N. G. Forouhi, H. Volzke, C. S. Uiterwaal, Y. T. van der Schouw, M. E. Numans, G. Matullo, G. Navis, G. Berglund, S. A. Bingham, J. S. Kooner, J. M. Connell, S. Bandinelli, L. Ferrucci, H. Watkins, T. D. Spector, J. Tuomilehto, D. Altshuler, D. P. Strachan, M. Laan, P. Meneton, N. J. Wareham, M. Uda, M. R. Jarvelin, V. Mooser, O. Melander, R. J. Loos, P. Elliott, G. R. Abecasis, M. Caulfield, P. B. Munroe, Genome-wide association study identifies eight loci associated with blood pressure. *Nature genetics* **41**, 666-676 (2009).

37. D. Levy, G. B. Ehret, K. Rice, G. C. Verwoert, L. J. Launer, A. Dehghan, N. L. Glazer, A. C. Morrison, A. D. Johnson, T. Aspelund, Y. Aulchenko, T. Lumley, A. Kottgen, R. S. Vasan, F. Rivadeneira, G. Eiriksdottir, X. Guo, D. E. Arking, G. F. Mitchell, F. U. Mattace-Raso, A. V. Smith, K. Taylor, R. B. Scharpf, S. J. Hwang, E. J. Sijbrands, J. Bis, T. B. Harris, S. K. Ganesh, C. J. O'Donnell, A. Hofman, J. I. Rotter, J. Coresh, E. J. Benjamin, A. G. Uitterlinden, G. Heiss, C. S. Fox, J. C. Witteman, E. Boerwinkle, T. J. Wang, V. Gudnason, M. G. Larson, A. Chakravarti, B. M. Psaty, C. M. van Duijn, Genome-wide association study of blood pressure and hypertension. *Nature genetics* **41**, 677-687 (2009).

38. G. B. Ehret, P. B. Munroe, K. M. Rice, M. Bochud, A. D. Johnson, D. I. Chasman, A. V. Smith, M. D. Tobin, G. C. Verwoert, S. J. Hwang, V. Pihur, P. Vollenweider, P. F. O'Reilly, N. Amin, J. L. Bragg-Gresham, A. Teumer, N. L. Glazer, L. Launer, J. H. Zhao, Y. Aulchenko, S. Heath, S. Sober, A. Parsa, J. Luan, P. Arora, A. Dehghan, F. Zhang, G. Lucas, A. A. Hicks, A. U. Jackson, J. F. Peden, T. Tanaka, S. H. Wild, I. Rudan, W. Igl, Y. Milaneschi, A. N. Parker, C. Fava, J. C. Chambers, E. R. Fox, M. Kumari, M. J. Go, P. van der Harst, W. H. Kao, M. Sjogren, D. G. Vinay, M. Alexander, Y. Tabara, S. Shaw-Hawkins, P. H.

Whincup, Y. Liu, G. Shi, J. Kuusisto, B. Tayo, M. Seielstad, X. Sim, K. D. Nguyen, T. Lehtimaki, G. Matullo, Y. Wu, T. R. Gaunt, N. C. Onland-Moret, M. N. Cooper, C. G. Platou, E. Org, R. Hardy, S. Dahgam, J. Palmen, V. Vitart, P. S. Braund, T. Kuznetsova, C. S. Uiterwaal, A. Adeyemo, W. Palmas, H. Campbell, B. Ludwig, M. Tomaszewski, I. Tzoulaki, N. D. Palmer, T. Aspelund, M. Garcia, Y. P. Chang, J. R. O'Connell, N. I. Steinle, D. E. Grobbee, D. E. Arking, S. L. Kardia, A. C. Morrison, D. Hernandez, S. Najjar, W. L. McArdle, D. Hadley, M. J. Brown, J. M. Connell, A. D. Hingorani, I. N. Day, D. A. Lawlor, J. P. Beilby, R. W. Lawrence, R. Clarke, J. C. Hopewell, H. Ongen, A. W. Dreisbach, Y. Li, J. H. Young, J. C. Bis, M. Kahonen, J. Viikari, L. S. Adair, N. R. Lee, M. H. Chen, M. Olden, C. Pattaro, J. A. Bolton, A. Kottgen, S. Bergmann, V. Mooser, N. Chaturvedi, T. M. Frayling, M. Islam, T. H. Jafar, J. Erdmann, S. R. Kulkarni, S. R. Bornstein, J. Grassler, L. Groop, B. F. Voight, J. Kettunen, P. Howard, A. Taylor, S. Guarrera, F. Ricceri, V. Emilsson, A. Plump, I. Barroso, K. T. Khaw, A. B. Weder, S. C. Hunt, Y. V. Sun, R. N. Bergman, F. S. Collins, L. L. Bonnycastle, L. J. Scott, H. M. Stringham, L. Peltonen, M. Perola, E. Vartiainen, S. M. Brand, J. A. Staessen, T. J. Wang, P. R. Burton, M. Soler Artigas, Y. Dong, H. Snieder, X. Wang, H. Zhu, K. K. Lohman, M. E. Rudock, S. R. Heckbert, N. L. Smith, K. L. Wiggins, A. Doumatey, D. Shriner, G. Veldre, M. Viigimaa, S. Kinra, D. Prabhakaran, V. Tripathy, C. D. Langefeld, A. Rosengren, D. S. Thelle, A. M. Corsi, A. Singleton, T. Forrester, G. Hilton, C. A. McKenzie, T. Salako, N. Iwai, Y. Kita, T. Ogihara, T. Ohkubo, T. Okamura, H. Ueshima, S. Umemura, S. Eyheramendy, T. Meitinger, H. E. Wichmann, Y. S. Cho, H. L. Kim, J. Y. Lee, J. Scott, J. S. Sehmi, W. Zhang, B. Hedblad, P. Nilsson, G. D. Smith, A. Wong, N. Narisu, A. Stancakova, L. J. Raffel, J. Yao, S. Kathiresan, C. J. O'Donnell, S. M. Schwartz, M. A. Ikram, W. T. Longstreth, Jr., T. H. Mosley, S. Seshadri, N. R. Shrine, L. V. Wain, M. A. Morken, A. J. Swift, J. Laitinen, I. Prokopenko, P. Zitting, J. A. Cooper, S. E. Humphries, J. Danesh, A. Rasheed, A. Goel, A. Hamsten, H. Watkins, S. J. Bakker, W. H. van Gilst, C. S. Janipalli, K. R. Mani, C. S. Yajnik, A. Hofman, F. U. Mattace-Raso, B. A. Oostra, A. Demirkan, A. Isaacs, F. Rivadeneira, E. G. Lakatta, M. Orru, A. Scuteri, M. Ala-Korpela, A. J.

Kangas, L. P. Lyytikainen, P. Soininen, T. Tukiainen, P. Wurtz, R. T. Ong, M. Dorr, H. K. Kroemer, U. Volker, H. Volzke, P. Galan, S. Hercberg, M. Lathrop, D. Zelenika, P. Deloukas, M. Mangino, T. D. Spector, G. Zhai, J. F. Meschia, M. A. Nalls, P. Sharma, J. Terzic, M. V. Kumar, M. Denniff, E. Zukowska-Szczechowska, L. E. Wagenknecht, F. G. Fowkes, F. J. Charchar, P. E. Schwarz, C. Hayward, X. Guo, C. Rotimi, M. L. Bots, E. Brand, N. J. Samani, O. Polasek, P. J. Talmud, F. Nyberg, D. Kuh, M. Laan, K. Hveem, L. J. Palmer, Y. T. van der Schouw, J. P. Casas, K. L. Mohlke, P. Vineis, O. Raitakari, S. K. Ganesh, T. Y. Wong, E. S. Tai, R. S. Cooper, M. Laakso, D. C. Rao, T. B. Harris, R. W. Morris, A. F. Dominiczak, M. Kivimaki, M. G. Marmot, T. Miki, D. Saleheen, G. R. Chandak, J. Coresh, G. Navis, V. Salomaa, B. G. Han, X. Zhu, J. S. Kooner, O. Melander, P. M. Ridker, S. Bandinelli, U. B. Gyllensten, A. F. Wright, J. F. Wilson, L. Ferrucci, M. Farrall, J. Tuomilehto, P. P. Pramstaller, R. Elosua, N. Soranzo, E. J. Sijbrands, D. Altshuler, R. J. Loos, A. R. Shuldiner, C. Gieger, P. Meneton, A. G. Uitterlinden, N. J. Wareham, V. Gudnason, J. I. Rotter, R. Rettig, M. Uda, D. P. Strachan, J. C. Witteman, A. L. Hartikainen, J. S. Beckmann, E. Boerwinkle, R. S. Vasan, M. Boehnke, M. G. Larson, M. R. Jarvelin, B. M. Psaty, G. R. Abecasis, A. Chakravarti, P. Elliott, C. M. van Duijn, C. Newton-Cheh, D. Levy, M. J. Caulfield, T. Johnson, Genetic variants in novel pathways influence blood pressure and cardiovascular disease risk. *Nature* **478**, 103-109 (2011).

39. T. Huan, T. Esko, M. J. Peters, L. C. Pilling, K. Schramm, C. Schurmann, B. H. Chen, C. Liu, R. Joehanes, A. D. Johnson, C. Yao, S. X. Ying, P. Courchesne, L. Milani, N. Raghavachari, R. Wang, P. Liu, E. Reinmaa, A. Dehghan, A. Hofman, A. G. Uitterlinden, D. G. Hernandez, S. Bandinelli, A. Singleton, D. Melzer, A. Metspalu, M. Carstensen, H. Grallert, C. Herder, T. Meitinger, A. Peters, M. Roden, M. Waldenberger, M. Dorr, S. B. Felix, T. Zeller, R. Vasan, C. J. O'Donnell, P. J. Munson, X. Yang, H. Prokisch, U. Volker, J. B. van Meurs, L. Ferrucci, D. Levy, A meta-analysis of gene expression signatures of blood pressure and hypertension. *PLoS genetics* **11**, e1005035 (2015).

40. A. Y. Nossent, J. L. Hansen, C. Doggen, P. H. Quax, S. P. Sheikh, F. R. Rosendaal, SNPs in microRNA binding sites in 3'-UTRs of RAAS genes

influence arterial blood pressure and risk of myocardial infarction. *American journal of hypertension* **24**, 999-1006 (2011).

41. N. Kato, M. Loh, F. Takeuchi, N. Verweij, X. Wang, W. Zhang, T. N. Kelly, D. Saleheen, B. Lehne, I. Mateo Leach, A. W. Drong, J. Abbott, S. Wahl, S. T. Tan, W. R. Scott, G. Campanella, M. Chadeau-Hyam, U. Afzal, T. S. Ahluwalia, M. J. Bonder, P. Chen, A. Dehghan, T. L. Edwards, T. Esko, M. J. Go, S. E. Harris, J. Hartiala, S. Kasela, A. Kasturiratne, C. C. Khor, M. E. Kleber, H. Li, Z. Y. Mok, M. Nakatochi, N. S. Sapari, R. Saxena, A. F. Stewart, L. Stolk, Y. Tabara, A. L. Teh, Y. Wu, J. Y. Wu, Y. Zhang, I. Aits, A. Da Silva Couto Alves, S. Das, R. Dorajoo, J. C. Hopewell, Y. K. Kim, R. W. Koivula, J. Luan, L. P. Lyytikainen, Q. N. Nguyen, M. A. Pereira, I. Postmus, O. T. Raitakari, M. Scannell Bryan, R. A. Scott, R. Sorice, V. Tragante, M. Traglia, J. White, K. Yamamoto, Y. Zhang, L. S. Adair, A. Ahmed, K. Akiyama, R. Asif, T. Aung, I. Barroso, A. Bjonnes, T. R. Braun, H. Cai, L. C. Chang, C. H. Chen, C. Y. Cheng, Y. S. Chong, R. Collins, R. Courtney, G. Davies, G. Delgado, L. D. Do, P. A. Doevendans, R. T. Gansevoort, Y. T. Gao, T. B. Grammer, N. Grarup, J. Grewal, D. Gu, G. S. Wander, A. L. Hartikainen, S. L. Hazen, J. He, C. K. Heng, J. E. Hixson, A. Hofman, C. Hsu, W. Huang, L. L. Husemoen, J. Y. Hwang, S. Ichihara, M. Igase, M. Isono, J. M. Justesen, T. Katsuya, M. G. Kibriya, Y. J. Kim, M. Kishimoto, W. P. Koh, K. Kohara, M. Kumari, K. Kwek, N. R. Lee, J. Lee, J. Liao, W. Lieb, D. C. Liewald, T. Matsubara, Y. Matsushita, T. Meitinger, E. Mihailov, L. Milani, R. Mills, N. Mononen, M. Muller-Nurasyid, T. Nabika, E. Nakashima, H. K. Ng, K. Nikus, T. Nutile, T. Ohkubo, K. Ohnaka, S. Parish, L. Paternoster, H. Peng, A. Peters, S. T. Pham, M. J. Pinidiyapathirage, M. Rahman, H. Rakugi, O. Rolandsson, M. A. Rozario, D. Ruggiero, C. F. Sala, R. Sarju, K. Shimokawa, H. Snieder, T. Sparso, W. Spiering, J. M. Starr, D. J. Stott, D. O. Stram, T. Sugiyama, S. Szymczak, W. H. Tang, L. Tong, S. Trompet, V. Turjanmaa, H. Ueshima, A. G. Uitterlinden, S. Umemura, M. Vaarasmaki, R. M. van Dam, W. H. van Gilst, D. J. van Veldhuisen, J. S. Viikari, M. Waldenberger, Y. Wang, A. Wang, R. Wilson, T. Y. Wong, Y. B. Xiang, S. Yamaguchi, X. Ye, R. D. Young, T. L. Young, J. M. Yuan, X. Zhou, F. W. Asselbergs, M. Ciullo, R. Clarke, P. Deloukas, A. Franke, P. W.

Franks, S. Franks, Y. Friedlander, M. D. Gross, Z. Guo, T. Hansen, M. R. Jarvelin, T. Jorgensen, J. W. Jukema, M. Kahonen, H. Kajio, M. Kivimaki, J. Y. Lee, T. Lehtimaki, A. Linneberg, T. Miki, O. Pedersen, N. J. Samani, T. I. Sorensen, R. Takayanagi, D. Toniolo, H. Ahsan, H. Allayee, Y. T. Chen, J. Danesh, I. J. Deary, O. H. Franco, L. Franke, B. T. Heijman, J. D. Holbrook, A. Isaacs, B. J. Kim, X. Lin, J. Liu, W. Marz, A. Metspalu, K. L. Mohlke, D. K. Sanghera, X. O. Shu, J. B. van Meurs, E. Vithana, A. R. Wickremasinghe, C. Wijmenga, B. H. Wolffenbuttel, M. Yokota, W. Zheng, D. Zhu, P. Vineis, S. A. Kyrtopoulos, J. C. Kleinjans, M. I. McCarthy, R. Soong, C. Gieger, J. Scott, Y. Y. Teo, J. He, P. Elliott, E. S. Tai, P. van der Harst, J. S. Kooner, J. C. Chambers, Trans-ancestry genome-wide association study identifies 12 genetic loci influencing blood pressure and implicates a role for DNA methylation. *Nature genetics* **47**, 1282-1293 (2015).

42. T. G. Pickering, The effects of environmental and lifestyle factors on blood pressure and the intermediary role of the sympathetic nervous system. *Journal of human hypertension* **11 Suppl 1**, S9-18 (1997).

43. S. Rahman, H. Hu, E. McNeely, S. M. Rahman, N. Krieger, P. Waterman, J. Peters, C. Harris, C. H. Harris, D. Prothrow-Stith, B. K. Gibbs, P. C. Brown, G. Johnson, A. Burgess, R. D. Gragg, Social and Environmental Risk Factors for Hypertension in African Americans. *Florida public health review* **5**, 64-72 (2008).

44. M. V. Rao, Y. Qiu, C. Wang, G. Bakris, Hypertension and CKD: Kidney Early Evaluation Program (KEEP) and National Health and Nutrition Examination Survey (NHANES), 1999-2004. *American journal of kidney diseases : the official journal of the National Kidney Foundation* **51**, S30-37 (2008).

45. M. Briet, K. D. Burns, Chronic kidney disease and vascular remodelling: molecular mechanisms and clinical implications. *Clinical science (London, England : 1979)* **123**, 399-416 (2012).

46. M. Frimodt-Moller, A. L. Kamper, S. Strandgaard, S. Kreiner, A. H. Nielsen, Beneficial effects on arterial stiffness and pulse-wave reflection of combined

enalapril and candesartan in chronic kidney disease--a randomized trial. *PloS one* **7**, e41757 (2012).

47. S. Lopez-Giacoman, M. Madero, Biomarkers in chronic kidney disease, from kidney function to kidney damage. *World journal of nephrology* **4**, 57-73 (2015).

48. H. Schwarzenbach, N. Nishida, G. A. Calin, K. Pantel, Clinical relevance of circulating cell-free microRNAs in cancer. *Nature reviews. Clinical oncology* **11**, 145-156 (2014).

49. E. E. Creemers, A. J. Tijsen, Y. M. Pinto, Circulating microRNAs: novel biomarkers and extracellular communicators in cardiovascular disease? *Circulation research* **110**, 483-495 (2012).

50. J. Y. Li, T. Y. Yong, M. Z. Michael, J. M. Gleadle, Review: The role of microRNAs in kidney disease. *Nephrology (Carlton, Vic.)* **15**, 599-608 (2010).

51. B. Brigant, V. Metzinger-Le Meuth, Z. A. Massy, N. McKay, S. Liabeuf, M. Pelletier, M. Sallée, E. M'Baya-Moutoula, P. Paul, T. B. Drueke, S. Burtey, L. Metzinger, Serum microRNAs are altered in various stages of chronic kidney disease: a preliminary study. *Clinical Kidney Journal* **10**, 30-37 (2017).

52. J. Maroski, B. J. Vorderwulbecke, K. Fiedorowicz, L. Da Silva-Azevedo, G. Siegel, A. Marki, A. R. Pries, A. Zakrzewicz, Shear stress increases endothelial hyaluronan synthase 2 and hyaluronan synthesis especially in regard to an atheroprotective flow profile. *Experimental physiology* **96**, 977-986 (2011).

53. J. Yang, J. W. Clark, R. M. Bryan, C. S. Robertson, Mathematical modeling of the nitric oxide/cGMP pathway in the vascular smooth muscle cell. *American Journal of Physiology - Heart and Circulatory Physiology* **289**, H886-H897 (2005).

54. D. D. Heistad, M. L. Marcus, G. E. Larsen, M. L. Armstrong, Role of vasa vasorum in nourishment of the aortic wall. *The American journal of physiology* **240**, H781-787 (1981).

55. D. D. Gutterman, Adventitia-dependent influences on vascular function. *The American journal of physiology* **277**, H1265-1272 (1999).

56. G. Li, S. J. Chen, S. Oparil, Y. F. Chen, J. A. Thompson, Direct in vivo evidence demonstrating neointimal migration of adventitial fibroblasts after balloon injury of rat carotid arteries. *Circulation* **101**, 1362-1365 (2000).

57. M. W. Majesky, X. R. Dong, V. Hoglund, W. M. Mahoney, G. Daum, The Adventitia. *A Dynamic Interface Containing Resident Progenitor Cells* **31**, 1530-1539 (2011).

58. M. J. Haurani, P. J. Pagano, Adventitial fibroblast reactive oxygen species as autacrine and paracrine mediators of remodeling: bellwether for vascular disease? *Cardiovascular research* **75**, 679-689 (2007).

59. M. E. Safar, X. Girerd, S. Laurent, Structural changes of large conduit arteries in hypertension. *Journal of hypertension* **14**, 545-555 (1996).

60. H. D. Intengan, E. L. Schiffrin, Structure and mechanical properties of resistance arteries in hypertension: role of adhesion molecules and extracellular matrix determinants. *Hypertension (Dallas, Tex. : 1979)* **36**, 312-318 (2000).

61. P. Brassard, F. Amiri, E. L. Schiffrin, Combined angiotensin II type 1 and type 2 receptor blockade on vascular remodeling and matrix metalloproteinases in resistance arteries. *Hypertension (Dallas, Tex. : 1979)* **46**, 598-606 (2005).

62. E. N. Bakker, E. T. van der Meulen, B. M. van den Berg, V. Everts, J. A. Spaan, E. VanBavel, Inward remodeling follows chronic vasoconstriction in isolated resistance arteries. *Journal of vascular research* **39**, 12-20 (2002).

63. F. A. Yaghini, C. Y. Song, E. N. Lavrentyev, H. U. Ghafoor, X. R. Fang, A. M. Estes, W. B. Campbell, K. U. Malik, Angiotensin II-induced vascular smooth muscle cell migration and growth are mediated by cytochrome P450 1B1-dependent superoxide generation. *Hypertension (Dallas, Tex. : 1979)* **55**, 1461-1467 (2010).

64. G. H. Gibbons, R. E. Pratt, V. J. Dzau, Vascular smooth muscle cell hypertrophy vs. hyperplasia. Autocrine transforming growth factor-beta 1 expression determines growth response to angiotensin II. *The Journal of clinical investigation* **90**, 456-461 (1992).

65. T. Yamada, M. Horiuchi, V. J. Dzau, Angiotensin II type 2 receptor mediates programmed cell death. *Proceedings of the National Academy of Sciences of the United States of America* **93**, 156-160 (1996).

66. B. S. Tea, S. Der Sarkissian, R. M. Touyz, P. Hamet, D. deBlois, Proapoptotic and growth-inhibitory role of angiotensin II type 2 receptor in vascular smooth muscle cells of spontaneously hypertensive rats in vivo. *Hypertension (Dallas, Tex. : 1979)* **35**, 1069-1073 (2000).

67. L. V. d'Uscio, M. Barton, S. Shaw, P. Moreau, T. F. Luscher, Structure and function of small arteries in salt-induced hypertension: effects of chronic endothelin-subtype-A-receptor blockade. *Hypertension (Dallas, Tex. : 1979)* **30**, 905-911 (1997).

68. J. B. Park, E. L. Schiffrin, Small artery remodeling is the most prevalent (earliest?) form of target organ damage in mild essential hypertension. *Journal of hypertension* **19**, 921-930 (2001).

69. M. E. Safar, P. Laurent, Pulse pressure and arterial stiffness in rats: comparison with humans. *American journal of physiology. Heart and circulatory physiology* **285**, H1363-1369 (2003).

70. F. Kum, J. Karalliedde, Critical appraisal of the differential effects of antihypertensive agents on arterial stiffness. *Integrated blood pressure control* **3**, 63-71 (2010).

71. A. Rehman, A. Leibowitz, N. Yamamoto, Y. Rautureau, P. Paradis, E. L. Schiffrin, Angiotensin type 2 receptor agonist compound 21 reduces vascular injury and myocardial fibrosis in stroke-prone spontaneously hypertensive rats. *Hypertension (Dallas, Tex. : 1979)* **59**, 291-299 (2012).

72. C. M. Ford, S. Li, J. G. Pickering, Angiotensin II stimulates collagen synthesis in human vascular smooth muscle cells. Involvement of the AT(1) receptor, transforming growth factor-beta, and tyrosine phosphorylation. *Arteriosclerosis, thrombosis, and vascular biology* **19**, 1843-1851 (1999).

73. B. G. Sharifi, D. W. LaFleur, C. J. Pirola, J. S. Forrester, J. A. Fagin, Angiotensin II regulates tenascin gene expression in vascular smooth muscle cells. *The Journal of biological chemistry* **267**, 23910-23915 (1992).

74. I. Tokimitsu, H. Kato, H. Wachi, S. Tajima, Elastin synthesis is inhibited by angiotensin II but not by platelet-derived growth factor in arterial smooth muscle cells. *Biochimica et biophysica acta* **1207**, 68-73 (1994).

75. Q. Pu, M. F. Neves, A. Virdis, R. M. Touyz, E. L. Schiffrin, Endothelin antagonism on aldosterone-induced oxidative stress and vascular remodeling. *Hypertension (Dallas, Tex. : 1979)* **42**, 49-55 (2003).

76. V. Fontana, P. S. Silva, R. F. Gerlach, J. E. Tanus-Santos, Circulating matrix metalloproteinases and their inhibitors in hypertension. *Clinica chimica acta; international journal of clinical chemistry* **413**, 656-662 (2012).

77. M. Wang, S. H. Kim, R. E. Monticone, E. G. Lakatta, Matrix metalloproteinases promote arterial remodeling in aging, hypertension, and atherosclerosis. *Hypertension (Dallas, Tex. : 1979)* **65**, 698-703 (2015).

78. C. Wang, X. Qian, X. Sun, Q. Chang, Angiotensin II increases matrix metalloproteinase 2 expression in human aortic smooth muscle cells via AT1R and ERK1/2. *Experimental biology and medicine (Maywood, N.J.)* **240**, 1564-1571 (2015).

79. T. Tang, P. G. Wilson, J. C. Thompson, C. Nelson, M. H. Yoder, L. R. Tannock, Prevention of TGFbeta induction attenuates angII-stimulated vascular biglycan and atherosclerosis in Ldlr-/- mice. *Journal of lipid research* **54**, 2255-2264 (2013).

80. M. A. Sardo, G. Mandraffino, S. Riggio, A. D'Ascola, A. Alibrandi, C. Saitta, E. Imbalzano, M. Castaldo, M. Cinquegrani, A. Saitta, Effects of the angiotensin II receptor blocker losartan on the monocyte expression of biglycan in hypertensive patients. *Clinical and experimental pharmacology & physiology* **37**, 933-938 (2010).

81. P. Finckenberg, K. Inkinen, J. Ahonen, S. Merasto, M. Louhelainen, H. Vapaatalo, D. Muller, D. Ganten, F. Luft, E. Mervaala, Angiotensin II induces connective tissue growth factor gene expression via calcineurin-dependent pathways. *The American journal of pathology* **163**, 355-366 (2003).

82. M. Ruperez, M. Ruiz-Ortega, V. Esteban, O. Lorenzo, S. Mezzano, J. J. Plaza, J. Egido, Angiotensin II increases connective tissue growth factor in the kidney. *The American journal of pathology* **163**, 1937-1947 (2003).

83. S. Laurent, M. Briet, P. Boutouyrie, Large and small artery cross-talk and recent morbidity-mortality trials in hypertension. *Hypertension (Dallas, Tex. : 1979)* **54**, 388-392 (2009).

84. M. Briet, E. L. Schiffrin, Treatment of arterial remodeling in essential hypertension. *Current hypertension reports* **15**, 3-9 (2013).

85. L. S. Ibels, A. C. Alfrey, W. E. Huffer, P. W. Craswell, J. T. Anderson, R. Weil, 3rd, Arterial calcification and pathology in uremic patients undergoing dialysis. *The American journal of medicine* **66**, 790-796 (1979).

86. G. M. London, A. P. Guerin, S. J. Marchais, F. Metivier, B. Pannier, H. Adda, Arterial media calcification in end-stage renal disease: impact on all-cause and cardiovascular mortality. *Nephrology, dialysis, transplantation : official publication of the European Dialysis and Transplant Association - European Renal Association* **18**, 1731-1740 (2003).

87. M. J. Budoff, D. J. Rader, M. P. Reilly, E. R. Mohler, 3rd, J. Lash, W. Yang, L. Rosen, M. Glenn, V. Teal, H. I. Feldman, Relationship of estimated GFR and coronary artery calcification in the CRIC (Chronic Renal Insufficiency Cohort) Study. *American journal of kidney diseases : the official journal of the National Kidney Foundation* **58**, 519-526 (2011).

88. H. Shimokawa, K. Satoh, Vascular Function. *Arteriosclerosis, thrombosis, and vascular biology* **34**, 2359-2362 (2014).

89. B. J. Ballermann, A. Dardik, E. Eng, A. Liu, Shear stress and the endothelium. *Kidney international. Supplement* **67**, S100-108 (1998).

90. E. Gkaliagkousi, E. Gavriilaki, A. Triantafyllou, S. Douma, Clinical Significance of Endothelial Dysfunction in Essential Hypertension. *Current hypertension reports* **17**, 85 (2015).

91. R. P. Brandes, Endothelial dysfunction and hypertension. *Hypertension (Dallas, Tex. : 1979)* **64**, 924-928 (2014).

92. E. Gkaliagkousi, S. Douma, C. Zamboulis, A. Ferro, Nitric oxide dysfunction in vascular endothelium and platelets: role in essential hypertension. *Journal of hypertension* **27**, 2310-2320 (2009).

93. N. Kuzkaya, N. Weissmann, D. G. Harrison, S. Dikalov, Interactions of peroxynitrite, tetrahydrobiopterin, ascorbic acid, and thiols: implications for uncoupling endothelial nitric-oxide synthase. *The Journal of biological chemistry* **278**, 22546-22554 (2003).

94. T. Maruhashi, J. Soga, N. Fujimura, N. Idei, S. Mikami, Y. Iwamoto, M. Kajikawa, T. Matsumoto, T. Hidaka, Y. Kihara, K. Chayama, K. Noma, A. Nakashima, C. Goto, H. Tomiyama, B. Takase, A. Yamashina, Y. Higashi, Relationship between flow-mediated vasodilation and cardiovascular risk factors in a large community-based study. *Heart (British Cardiac Society)* **99**, 1837-1842 (2013).

95. M. L. Muiesan, M. Salvetti, C. Monteduro, C. Corbellini, D. Guelfi, D. Rizzoni, M. Castellano, E. Agabiti-Rosei, Flow-mediated dilatation of the brachial artery and left ventricular geometry in hypertensive patients. *Journal of hypertension* **19**, 641-647 (2001).

96. D. Poulikakos, L. Ross, A. Recio-Mayoral, D. Cole, J. Andoh, N. Chitalia, R. Sharma, J. Carlos Kaski, D. Banerjee, Left ventricular hypertrophy and endothelial dysfunction in chronic kidney disease. *European heart journal cardiovascular Imaging* **15**, 56-61 (2014).

97. S. T. Morris, J. J. McMurray, A. Spiers, A. G. Jardine, Impaired endothelial function in isolated human uremic resistance arteries. *Kidney international* **60**, 1077-1082 (2001).

98. N. Luksha, L. Luksha, J. J. Carrero, F. Hammarqvist, P. Stenvinkel, K. Kublickiene, Impaired resistance artery function in patients with end-stage renal disease. *Clinical science (London, England : 1979)* **120**, 525-536 (2011).

99. Q. Pu, P. Brassard, D. M. Javeshghani, M. Iglarz, R. L. Webb, F. Amiri, E. L. Schiffrin, Effects of combined AT1 receptor antagonist/NEP inhibitor on vascular remodeling and cardiac fibrosis in SHRSP. *Journal of hypertension* **26**, 322-333 (2008).

100. R. M. Touyz, E. L. Schiffrin, Signal transduction mechanisms mediating the physiological and pathophysiological actions of angiotensin II in vascular smooth muscle cells. *Pharmacological reviews* **52**, 639-672 (2000).

101. P. K. Mehta, K. K. Griendling, Angiotensin II cell signaling: physiological and pathological effects in the cardiovascular system. *American journal of physiology. Cell physiology* **292**, C82-97 (2007).

102. R. M. Touyz, X. H. Wu, E. L. Schiffrin, Src modulates Ang II-mediated Ca2+ signaling in human vascular smooth muscle cells. *American journal of hypertension* **12**, 8A-8A (1999).

103. G. A. Vallega, M. L. Canessa, B. C. Berk, T. A. Brock, R. W. Alexander, Vascular smooth muscle Na+-H+ exchanger kinetics and its activation by angiotensin II. *The American journal of physiology* **254**, C751-758 (1988).

104. K. K. Griendling, D. Sorescu, M. Ushio-Fukai, NAD(P)H oxidase: role in cardiovascular biology and disease. *Circulation research* **86**, 494-501 (2000).

105. S. Rajagopalan, S. Kurz, T. Munzel, M. Tarpey, B. A. Freeman, K. K. Griendling, D. G. Harrison, Angiotensin II-mediated hypertension in the rat increases vascular superoxide production via membrane NADH/NADPH oxidase activation. Contribution to alterations of vasomotor tone. *The Journal of clinical investigation* **97**, 1916-1923 (1996).

106. S. Papaiahgari, Q. Zhang, S. R. Kleeberger, H. Y. Cho, S. P. Reddy, Hyperoxia stimulates an Nrf2-ARE transcriptional response via ROS-EGFR-PI3K-Akt/ERK

MAP kinase signaling in pulmonary epithelial cells. *Antioxidants & redox signaling* **8**, 43-52 (2006).

107. C. K. Sen, L. Packer, Antioxidant and redox regulation of gene transcription. *FASEB journal : official publication of the Federation of American Societies for Experimental Biology* **10**, 709-720 (1996).

108. R. Aikawa, I. Komuro, T. Yamazaki, Y. Zou, S. Kudoh, M. Tanaka, I. Shiojima, Y. Hiroi, Y. Yazaki, Oxidative stress activates extracellular signal-regulated kinases through Src and Ras in cultured cardiac myocytes of neonatal rats. *The Journal of clinical investigation* **100**, 1813-1821 (1997).

109. M. Ruiz-Ortega, O. Lorenzo, M. Ruperez, S. Konig, B. Wittig, J. Egido, Angiotensin II activates nuclear transcription factor kappaB through AT(1) and AT(2) in vascular smooth muscle cells: molecular mechanisms. *Circulation research* **86**, 1266-1272 (2000).

110. P. G. Frank, M. P. Lisanti, ICAM-1: role in inflammation and in the regulation of vascular permeability. *American journal of physiology. Heart and circulatory physiology* **295**, H926-H927 (2008).

111. M. M. Billah, Phospholipase D and cell signaling. *Current opinion in immunology* **5**, 114-123 (1993).

112. M. M. Muthalif, I. F. Benter, N. Karzoun, S. Fatima, J. Harper, M. R. Uddin, K. U. Malik, 20-Hydroxyeicosatetraenoic acid mediates calcium/calmodulin-dependent protein kinase II-induced mitogen-activated protein kinase activation in vascular smooth muscle cells. *Proceedings of the National Academy of Sciences of the United States of America* **95**, 12701-12706 (1998).

113. K. K. Griendling, P. Delafontaine, S. E. Rittenhouse, M. A. Gimbrone, Jr., R. W. Alexander, Correlation of receptor sequestration with sustained diacylglycerol accumulation in angiotensin II-stimulated cultured vascular smooth muscle cells. *The Journal of biological chemistry* **262**, 14555-14562 (1987).

114. T. Inuzuka, Y. Fujioka, M. Tsuda, M. Fujioka, A. O. Satoh, K. Horiuchi, S. Nishide, A. Nanbo, S. Tanaka, Y. Ohba, Attenuation of ligand-induced activation

of angiotensin II type 1 receptor signaling by the type 2 receptor via protein kinase C. *Scientific reports* **6**, 21613 (2016).

115. M. Oppermann, N. J. Freedman, R. W. Alexander, R. J. Lefkowitz, Phosphorylation of the type 1A angiotensin II receptor by G protein-coupled receptor kinases and protein kinase C. *The Journal of biological chemistry* **271**, 13266-13272 (1996).

116. L. Hunyady, M. Bor, T. Balla, K. J. Catt, Identification of a cytoplasmic Ser-Thr-Leu motif that determines agonist-induced internalization of the AT1 angiotensin receptor. *The Journal of biological chemistry* **269**, 31378-31382 (1994).

117. A. Fatica, I. Bozzoni, Long non-coding RNAs: new players in cell differentiation and development. *Nature reviews. Genetics* **15**, 7-21 (2014).

118. H. Guo, N. T. Ingolia, J. S. Weissman, D. P. Bartel, Mammalian microRNAs predominantly act to decrease target mRNA levels. *Nature* **466**, 835-840 (2010).

119. W. Hu, J. Coller, What comes first: translational repression or mRNA degradation? The deepening mystery of microRNA function. *Cell research* **22**, 1322-1324 (2012).

120. J. Krol, I. Loedige, W. Filipowicz, The widespread regulation of microRNA biogenesis, function and decay. *Nature reviews. Genetics* **11**, 597-610 (2010).

121. W. Sun, Y. S. Julie Li, H. D. Huang, J. Y. Shyy, S. Chien, microRNA: a master regulator of cellular processes for bioengineering systems. *Annual review of biomedical engineering* **12**, 1-27 (2010).

122. D. S. Schwarz, G. Hutvagner, T. Du, Z. Xu, N. Aronin, P. D. Zamore, Asymmetry in the assembly of the RNAi enzyme complex. *Cell* **115**, 199-208 (2003).

123. A. Khvorova, A. Reynolds, S. D. Jayasena, Functional siRNAs and miRNAs exhibit strand bias. *Cell* **115**, 209-216 (2003).

124. P. Brodersen, O. Voinnet, Revisiting the principles of microRNA target recognition and mode of action. *Nature reviews. Molecular cell biology* **10**, 141-148 (2009).

125. A. Grimson, K. K. Farh, W. K. Johnston, P. Garrett-Engele, L. P. Lim, D. P. Bartel, MicroRNA targeting specificity in mammals: determinants beyond seed pairing. *Molecular cell* **27**, 91-105 (2007).

126. R. C. Friedman, K. K. Farh, C. B. Burge, D. P. Bartel, Most mammalian mRNAs are conserved targets of microRNAs. *Genome research* **19**, 92-105 (2009).

127. J. Brennecke, A. Stark, R. B. Russell, S. M. Cohen, Principles of microRNA-target recognition. *PLoS biology* **3**, e85 (2005).

128. K. Wang, F. Liu, L. Y. Zhou, B. Long, S. M. Yuan, Y. Wang, C. Y. Liu, T. Sun, X. J. Zhang, P. F. Li, The long noncoding RNA CHRF regulates cardiac hypertrophy by targeting miR-489. *Circulation research* **114**, 1377-1388 (2014).

129. S. Bagga, J. Bracht, S. Hunter, K. Massirer, J. Holtz, R. Eachus, A. E. Pasquinelli, Regulation by let-7 and lin-4 miRNAs results in target mRNA degradation. *Cell* **122**, 553-563 (2005).

130. T. W. Nilsen, Mechanisms of microRNA-mediated gene regulation in animal cells. *Trends in genetics : TIG* **23**, 243-249 (2007).

131. D. T. Humphreys, B. J. Westman, D. I. Martin, T. Preiss, MicroRNAs control translation initiation by inhibiting eukaryotic initiation factor 4E/cap and poly(A) tail function. *Proceedings of the National Academy of Sciences of the United States of America* **102**, 16961-16966 (2005).

132. M. Wakiyama, K. Takimoto, O. Ohara, S. Yokoyama, Let-7 microRNA-mediated mRNA deadenylation and translational repression in a mammalian cell-free system. *Genes & development* **21**, 1857-1862 (2007).

133. G. Mathonnet, M. R. Fabian, Y. V. Svitkin, A. Parsyan, L. Huck, T. Murata, S. Biffo, W. C. Merrick, E. Darzynkiewicz, R. S. Pillai, W. Filipowicz, T. F. Duchaine, N. Sonenberg, MicroRNA inhibition of translation initiation in vitro by targeting the cap-binding complex eIF4F. *Science (New York, N.Y.)* **317**, 1764-1767 (2007).

134. C. L. Jopling, M. Yi, A. M. Lancaster, S. M. Lemon, P. Sarnow, Modulation of hepatitis C virus RNA abundance by a liver-specific MicroRNA. *Science (New York, N.Y.)* **309**, 1577-1581 (2005).

135. H. L. Janssen, H. W. Reesink, E. J. Lawitz, S. Zeuzem, M. Rodriguez-Torres, K. Patel, A. J. van der Meer, A. K. Patick, A. Chen, Y. Zhou, R. Persson, B. D. King, S. Kauppinen, A. A. Levin, M. R. Hodges, Treatment of HCV infection by targeting microRNA. *The New England journal of medicine* **368**, 1685-1694 (2013).

136. J. R. Lytle, T. A. Yario, J. A. Steitz, Target mRNAs are repressed as efficiently by microRNA-binding sites in the 5' UTR as in the 3' UTR. *Proceedings of the National Academy of Sciences of the United States of America* **104**, 9667-9672 (2007).

137. Z. Fang, N. Rajewsky, The impact of miRNA target sites in coding sequences and in 3'UTRs. *PloS one* **6**, e18067 (2011).

138. H. W. Hwang, E. A. Wentzel, J. T. Mendell, A hexanucleotide element directs microRNA nuclear import. *Science (New York, N.Y.)* **315**, 97-100 (2007).

139. R. F. Place, L. C. Li, D. Pookot, E. J. Noonan, R. Dahiya, MicroRNA-373 induces expression of genes with complementary promoter sequences. *Proceedings of the National Academy of Sciences of the United States of America* **105**, 1608-1613 (2008).

140. S. T. Younger, D. R. Corey, Transcriptional gene silencing in mammalian cells by miRNA mimics that target gene promoters. *Nucleic acids research* **39**, 5682-5691 (2011).

141. R. A. Boon, K. Iekushi, S. Lechner, T. Seeger, A. Fischer, S. Heydt, D. Kaluza, K. Treguer, G. Carmona, A. Bonauer, A. J. Horrevoets, N. Didier, Z. Girmatsion, P. Biliczki, J. R. Ehrlich, H. A. Katus, O. J. Muller, M. Potente, A. M. Zeiher, H. Hermeking, S. Dimmeler, MicroRNA-34a regulates cardiac ageing and function. *Nature* **495**, 107-110 (2013).

142. A. Bonauer, G. Carmona, M. Iwasaki, M. Mione, M. Koyanagi, A. Fischer, J. Burchfield, H. Fox, C. Doebele, K. Ohtani, E. Chavakis, M. Potente, M. Tjwa, C. Urbich, A. M. Zeiher, S. Dimmeler, MicroRNA-92a controls angiogenesis and functional recovery of ischemic tissues in mice. *Science (New York, N.Y.)* **324**, 1710-1713 (2009).

143. M. S. Beg, A. J. Brenner, J. Sachdev, M. Borad, Y. K. Kang, J. Stoudemire, S. Smith, A. G. Bader, S. Kim, D. S. Hong, Phase I study of MRX34, a liposomal miR-34a mimic, administered twice weekly in patients with advanced solid tumors. *Investigational new drugs* **35**, 180-188 (2017).

144. A. Care, D. Catalucci, F. Felicetti, D. Bonci, A. Addario, P. Gallo, M. L. Bang, P. Segnalini, Y. Gu, N. D. Dalton, L. Elia, M. V. Latronico, M. Hoydal, C. Autore, M. A. Russo, G. W. Dorn, 2nd, O. Ellingsen, P. Ruiz-Lozano, K. L. Peterson, C. M. Croce, C. Peschle, G. Condorelli, MicroRNA-133 controls cardiac hypertrophy. *Nature medicine* **13**, 613-618 (2007).

145. D. Torella, C. Iaconetti, D. Catalucci, G. M. Ellison, A. Leone, C. D. Waring, A. Bochicchio, C. Vicinanza, I. Aquila, A. Curcio, G. Condorelli, C. Indolfi, MicroRNA-133 controls vascular smooth muscle cell phenotypic switch in vitro and vascular remodeling in vivo. *Circulation research* **109**, 880-893 (2011).

146. S. Kasar, E. Salerno, Y. Yuan, C. Underbayev, D. Vollenweider, M. F. Laurindo, H. Fernandes, D. Bonci, A. Addario, F. Mazzella, E. Raveche, Systemic in vivo lentiviral delivery of miR-15a/16 reduces malignancy in the NZB de novo mouse model of chronic lymphocytic leukemia. *Genes and immunity* **13**, 109-119 (2012).

147. Y. Chen, D. Y. Gao, L. Huang, In vivo delivery of miRNAs for cancer therapy: challenges and strategies. *Advanced drug delivery reviews* **81**, 128-141 (2015).

148. H. Y. Jin, A. Gonzalez-Martin, A. V. Miletic, M. Lai, S. Knight, M. Sabouri-Ghomi, S. R. Head, M. S. Macauley, R. C. Rickert, C. Xiao, Transfection of microRNA Mimics Should Be Used with Caution. *Frontiers in Genetics* **6**, (2015).

149. S. Geisler, J. Coller, RNA in unexpected places: long non-coding RNA functions in diverse cellular contexts. *Nature reviews. Molecular cell biology* **14**, 699-712 (2013).

150. M. C. Tsai, R. C. Spitale, H. Y. Chang, Long intergenic non-coding RNAs – New links in cancer progression. *Cancer research* **71**, 3-7 (2011).

151. P. Qi, X. Du, The long non-coding RNAs, a new cancer diagnostic and therapeutic gold mine. *Modern pathology : an official journal of the United States and Canadian Academy of Pathology, Inc* **26**, 155-165 (2013).

152. J. T. Lee, M. S. Bartolomei, X-inactivation, imprinting, and long noncoding RNAs in health and disease. *Cell* **152**, 1308-1323 (2013).

153. M. Cesana, D. Cacchiarelli, I. Legnini, T. Santini, O. Sthandier, M. Chinappi, A. Tramontano, I. Bozzoni, A long noncoding RNA controls muscle differentiation by functioning as a competing endogenous RNA. *Cell* **147**, 358-369 (2011).

154. L. L. Chen, The biogenesis and emerging roles of circular RNAs. *Nature reviews. Molecular cell biology* **17**, 205-211 (2016).

155. S. Qu, X. Yang, X. Li, J. Wang, Y. Gao, R. Shang, W. Sun, K. Dou, H. Li, Circular RNA: A new star of noncoding RNAs. *Cancer letters* **365**, 141-148 (2015).

156. S. Memczak, M. Jens, A. Elefsinioti, F. Torti, J. Krueger, A. Rybak, L. Maier, S. D. Mackowiak, L. H. Gregersen, M. Munschauer, A. Loewer, U. Ziebold, M. Landthaler, C. Kocks, F. le Noble, N. Rajewsky, Circular RNAs are a large class of animal RNAs with regulatory potency. *Nature* **495**, 333-338 (2013).

157. T. B. Hansen, T. I. Jensen, B. H. Clausen, J. B. Bramsen, B. Finsen, C. K. Damgaard, J. Kjems, Natural RNA circles function as efficient microRNA sponges. *Nature* **495**, 384-388 (2013).

158. F. Li, L. Zhang, W. Li, J. Deng, J. Zheng, M. An, J. Lu, Y. Zhou, Circular RNA ITCH has inhibitory effect on ESCC by suppressing the Wnt/beta-catenin pathway. *Oncotarget* **6**, 6001-6013 (2015).

159. V. Pelechano, L. M. Steinmetz, Gene regulation by antisense transcription. *Nature reviews. Genetics* **14**, 880-893 (2013).

160. D. Stazic, D. Lindell, C. Steglich, Antisense RNA protects mRNA from RNase E degradation by RNA–RNA duplex formation during phage infection. *Nucleic acids research* **39**, 4890-4899 (2011).

161. M. A. Faghihi, F. Modarresi, A. M. Khalil, D. E. Wood, B. G. Sahagan, T. E. Morgan, C. E. Finch, G. St Laurent, 3rd, P. J. Kenny, C. Wahlestedt, Expression of a noncoding RNA is elevated in Alzheimer's disease and drives rapid feed-forward regulation of beta-secretase. *Nature medicine* **14**, 723-730 (2008).

162. M. A. Faghihi, M. Zhang, J. Huang, F. Modarresi, M. P. Van der Brug, M. A. Nalls, M. R. Cookson, G. St-Laurent, 3rd, C. Wahlestedt, Evidence for natural antisense transcript-mediated inhibition of microRNA function. *Genome biology* **11**, R56 (2010).

163. C. Carrieri, L. Cimatti, M. Biagioli, A. Beugnet, S. Zucchelli, S. Fedele, E. Pesce, I. Ferrer, L. Collavin, C. Santoro, A. R. Forrest, P. Carninci, S. Biffo, E. Stupka, S. Gustincich, Long non-coding antisense RNA controls Uchl1 translation through an embedded SINEB2 repeat. *Nature* **491**, 454-457 (2012).

164. F. Darfeuille, C. Unoson, J. Vogel, E. G. Wagner, An antisense RNA inhibits translation by competing with standby ribosomes. *Molecular cell* **26**, 381-392 (2007).

165. A. J. Mighell, N. R. Smith, P. A. Robinson, A. F. Markham, Vertebrate pseudogenes. *FEBS letters* **468**, 109-114 (2000).

166. R. C. Pink, K. Wicks, D. P. Caley, E. K. Punch, L. Jacobs, D. R. Francisco Carter, Pseudogenes: Pseudo-functional or key regulators in health and disease? *Rna* **17**, 792-798 (2011).

167. S. Aparicio, K. Hawker, A. Cottage, Y. Mikawa, L. Zuo, B. Venkatesh, E. Chen, R. Krumlauf, S. Brenner, Organization of the Fugu rubripes Hox clusters: evidence for continuing evolution of vertebrate Hox complexes. *Nature genetics* **16**, 79-83 (1997).

168. A. Meyer, Hox gene variation and evolution. *Nature* **391**, 225, 227-228 (1998).

169. L. Poliseno, L. Salmena, J. Zhang, B. Carver, W. J. Haveman, P. P. Pandolfi, A coding-independent function of gene and pseudogene mRNAs regulates tumour biology. *Nature* **465**, 1033-1038 (2010).

170. N. A. Rapicavoli, K. Qu, J. Zhang, M. Mikhail, R. M. Laberge, H. Y. Chang, A mammalian pseudogene lncRNA at the interface of inflammation and anti-inflammatory therapeutics. *eLife* **2**, e00762 (2013).

171. A. A. Bazzini, T. G. Johnstone, R. Christiano, S. D. Mackowiak, B. Obermayer, E. S. Fleming, C. E. Vejnar, M. T. Lee, N. Rajewsky, T. C. Walther, A. J. Giraldez, Identification of small ORFs in vertebrates using ribosome footprinting and evolutionary conservation. *The EMBO journal* **33**, 981-993 (2014).

172. V. Olexiouk, J. Crappe, S. Verbruggen, K. Verhegen, L. Martens, G. Menschaert, sORFs.org: a repository of small ORFs identified by ribosome profiling. *Nucleic acids research* **44**, D324-329 (2016).

173. C. Y. Chen, P. Sarnow, Initiation of protein synthesis by the eukaryotic translational apparatus on circular RNAs. *Science (New York, N.Y.)* **268**, 415-417 (1995).

174. D. M. Anderson, K. M. Anderson, C. L. Chang, C. A. Makarewich, B. R. Nelson, J. R. McAnally, P. Kasaragod, J. M. Shelton, J. Liou, R. Bassel-Duby, E. N. Olson, A micropeptide encoded by a putative long noncoding RNA regulates muscle performance. *Cell* **160**, 595-606 (2015).

175. T. Kondo, S. Plaza, J. Zanet, E. Benrabah, P. Valenti, Y. Hashimoto, S. Kobayashi, F. Payre, Y. Kageyama, Small peptides switch the transcriptional activity of Shavenbaby during Drosophila embryogenesis. *Science (New York, N.Y.)* **329**, 336-339 (2010).

176. S. Djebali, C. A. Davis, A. Merkel, A. Dobin, T. Lassmann, A. Mortazavi, A. Tanzer, J. Lagarde, W. Lin, F. Schlesinger, C. Xue, G. K. Marinov, J. Khatun, B. A. Williams, C. Zaleski, J. Rozowsky, M. Roder, F. Kokocinski, R. F. Abdelhamid, T. Alioto, I. Antoshechkin, M. T. Baer, N. S. Bar, P. Batut, K. Bell,

I. Bell, S. Chakrabortty, X. Chen, J. Chrast, J. Curado, T. Derrien, J. Drenkow, E. Dumais, J. Dumais, R. Duttagupta, E. Falconnet, M. Fastuca, K. Fejes-Toth, P. Ferreira, S. Foissac, M. J. Fullwood, H. Gao, D. Gonzalez, A. Gordon, H. Gunawardena, C. Howald, S. Jha, R. Johnson, P. Kapranov, B. King, C. Kingswood, O. J. Luo, E. Park, K. Persaud, J. B. Preall, P. Ribeca, B. Risk, D. Robyr, M. Sammeth, L. Schaffer, L. H. See, A. Shahab, J. Skancke, A. M. Suzuki, H. Takahashi, H. Tilgner, D. Trout, N. Walters, H. Wang, J. Wrobel, Y. Yu, X. Ruan, Y. Hayashizaki, J. Harrow, M. Gerstein, T. Hubbard, A. Reymond, S. E. Antonarakis, G. Hannon, M. C. Giddings, Y. Ruan, B. Wold, P. Carninci, R. Guigo, T. R. Gingeras, Landscape of transcription in human cells. *Nature* **489**, 101-108 (2012).

177. A. M. Khalil, M. Guttman, M. Huarte, M. Garber, A. Raj, D. Rivea Morales, K. Thomas, A. Presser, B. E. Bernstein, A. van Oudenaarden, A. Regev, E. S. Lander, J. L. Rinn, Many human large intergenic noncoding RNAs associate with chromatin-modifying complexes and affect gene expression. *Proceedings of the National Academy of Sciences of the United States of America* **106**, 11667-11672 (2009).

178. T. Hung, Y. Wang, M. F. Lin, A. K. Koegel, Y. Kotake, G. D. Grant, H. M. Horlings, N. Shah, C. Umbricht, P. Wang, Y. Wang, B. Kong, A. Langerod, A. L. Borresen-Dale, S. K. Kim, M. van de Vijver, S. Sukumar, M. L. Whitfield, M. Kellis, Y. Xiong, D. J. Wong, H. Y. Chang, Extensive and coordinated transcription of noncoding RNAs within cell-cycle promoters. *Nature genetics* **43**, 621-629 (2011).

179. T. M. Wheeler, A. J. Leger, S. K. Pandey, A. R. MacLeod, M. Nakamori, S. H. Cheng, B. M. Wentworth, C. F. Bennett, C. A. Thornton, Targeting nuclear RNA for in vivo correction of myotonic dystrophy. *Nature* **488**, 111-115 (2012).

180. C. H. Li, Y. Chen, Targeting long non-coding RNAs in cancers: progress and prospects. *The international journal of biochemistry & cell biology* **45**, 1895-1910 (2013).

181. S. Grasedieck, A. Sorrentino, C. Langer, C. Buske, H. Dohner, D. Mertens, F. Kuchenbauer, Circulating microRNAs in hematological diseases: principles, challenges, and perspectives. *Blood* **121**, 4977-4984 (2013).

182. K. C. Vickers, B. T. Palmisano, B. M. Shoucri, R. D. Shamburek, A. T. Remaley, MicroRNAs are transported in plasma and delivered to recipient cells by high-density lipoproteins. *Nature cell biology* **13**, 423-433 (2011).

183. P. Qi, X. Y. Zhou, X. Du, Circulating long non-coding RNAs in cancer: current status and future perspectives. *Molecular cancer* **15**, 39 (2016).

184. Y. Zhang, D. Liu, X. Chen, J. Li, L. Li, Z. Bian, F. Sun, J. Lu, Y. Yin, X. Cai, Q. Sun, K. Wang, Y. Ba, Q. Wang, D. Wang, J. Yang, P. Liu, T. Xu, Q. Yan, J. Zhang, K. Zen, C. Y. Zhang, Secreted monocytic miR-150 enhances targeted endothelial cell migration. *Molecular cell* **39**, 133-144 (2010).

185. T. Umezu, K. Ohyashiki, M. Kuroda, J. H. Ohyashiki, Leukemia cell to endothelial cell communication via exosomal miRNAs. *Oncogene* **32**, 2747-2755 (2013).

186. A. Zernecke, K. Bidzhekov, H. Noels, E. Shagdarsuren, L. Gan, B. Denecke, M. Hristov, T. Koppel, M. N. Jahantigh, E. Lutgens, S. Wang, E. N. Olson, A. Schober, C. Weber, Delivery of microRNA-126 by apoptotic bodies induces CXCL12-dependent vascular protection. *Science signaling* **2**, ra81 (2009).

187. T. Arita, D. Ichikawa, H. Konishi, S. Komatsu, A. Shiozaki, K. Shoda, T. Kawaguchi, S. Hirajima, H. Nagata, T. Kubota, H. Fujiwara, K. Okamoto, E. Otsuji, Circulating long non-coding RNAs in plasma of patients with gastric cancer. *Anticancer research* **33**, 3185-3193 (2013).

188. J. Viereck, T. Thum, Circulating Noncoding RNAs as Biomarkers of Cardiovascular Disease and Injury. *Circulation research* **120**, 381-399 (2017).

189. P. S. Mitchell, R. K. Parkin, E. M. Kroh, B. R. Fritz, S. K. Wyman, E. L. Pogosova-Agadjanyan, A. Peterson, J. Noteboom, K. C. O'Briant, A. Allen, D. W. Lin, N. Urban, C. W. Drescher, B. S. Knudsen, D. L. Stirewalt, R. Gentleman, R. L. Vessella, P. S. Nelson, D. B. Martin, M. Tewari, Circulating microRNAs as

stable blood-based markers for cancer detection. *Proceedings of the National Academy of Sciences of the United States of America* **105**, 10513-10518 (2008).

190. X. Chen, Y. Ba, L. Ma, X. Cai, Y. Yin, K. Wang, J. Guo, Y. Zhang, J. Chen, X. Guo, Q. Li, X. Li, W. Wang, Y. Zhang, J. Wang, X. Jiang, Y. Xiang, C. Xu, P. Zheng, J. Zhang, R. Li, H. Zhang, X. Shang, T. Gong, G. Ning, J. Wang, K. Zen, J. Zhang, C. Y. Zhang, Characterization of microRNAs in serum: a novel class of biomarkers for diagnosis of cancer and other diseases. *Cell research* **18**, 997-1006 (2008).

191. J. D. Arroyo, J. R. Chevillet, E. M. Kroh, I. K. Ruf, C. C. Pritchard, D. F. Gibson, P. S. Mitchell, C. F. Bennett, E. L. Pogosova-Agadjanyan, D. L. Stirewalt, J. F. Tait, M. Tewari, Argonaute2 complexes carry a population of circulating microRNAs independent of vesicles in human plasma. *Proceedings of the National Academy of Sciences of the United States of America* **108**, 5003-5008 (2011).

192. Q. Li, Y. Shao, X. Zhang, T. Zheng, M. Miao, L. Qin, B. Wang, G. Ye, B. Xiao, J. Guo, Plasma long noncoding RNA protected by exosomes as a potential stable biomarker for gastric cancer. *Tumour biology : the journal of the International Society for Oncodevelopmental Biology and Medicine* **36**, 2007-2012 (2015).

193. L. Dong, P. Qi, M. D. Xu, S. J. Ni, D. Huang, Q. H. Xu, W. W. Weng, C. Tan, W. Q. Sheng, X. Y. Zhou, X. Du, Circulating CUDR, LSINCT-5 and PTENP1 long noncoding RNAs in sera distinguish patients with gastric cancer from healthy controls. *International journal of cancer* **137**, 1128-1135 (2015).

194. J. Jarry, D. Schadendorf, C. Greenwood, A. Spatz, L. C. van Kempen, The validity of circulating microRNAs in oncology: five years of challenges and contradictions. *Molecular oncology* **8**, 819-829 (2014).

195. E. M. Kroh, R. K. Parkin, P. S. Mitchell, M. Tewari, Analysis of circulating microRNA biomarkers in plasma and serum using quantitative reverse transcription-PCR (qRT-PCR). *Methods (San Diego, Calif.)* **50**, 298-301 (2010).

196. M. B. Kirschner, S. C. Kao, J. J. Edelman, N. J. Armstrong, M. P. Vallely, N. van Zandwijk, G. Reid, Haemolysis during sample preparation alters microRNA content of plasma. *PloS one* **6**, e24145 (2011).

197. P. Willeit, A. Zampetaki, K. Dudek, D. Kaudewitz, A. King, N. S. Kirkby, R. Crosby-Nwaobi, M. Prokopi, I. Drozdov, S. R. Langley, S. Sivaprasad, H. S. Markus, J. A. Mitchell, T. D. Warner, S. Kiechl, M. Mayr, Circulating microRNAs as novel biomarkers for platelet activation. *Circulation research* **112**, 595-600 (2013).

198. M. Xiang, Y. Zeng, R. Yang, H. Xu, Z. Chen, J. Zhong, H. Xie, Y. Xu, X. Zeng, U6 is not a suitable endogenous control for the quantification of circulating microRNAs. *Biochemical and biophysical research communications* **454**, 210-214 (2014).

199. F. Benz, C. Roderburg, D. Vargas Cardenas, M. Vucur, J. Gautheron, A. Koch, H. Zimmermann, J. Janssen, L. Nieuwenhuijsen, M. Luedde, N. Frey, F. Tacke, C. Trautwein, T. Luedde, U6 is unsuitable for normalization of serum miRNA levels in patients with sepsis or liver fibrosis. *Experimental & molecular medicine* **45**, e42 (2013).

200. J. Vandesompele, K. De Preter, F. Pattyn, B. Poppe, N. Van Roy, A. De Paepe, F. Speleman, Accurate normalization of real-time quantitative RT-PCR data by geometric averaging of multiple internal control genes. *Genome biology* **3**, RESEARCH0034 (2002).

201. S. Uchida, S. Dimmeler, Long Noncoding RNAs in Cardiovascular Diseases. *Circulation research* **116**, 737-750 (2015).

202. A. Leung, R. Natarajan, Noncoding RNAs in vascular disease. *Current opinion in cardiology* **29**, 199-206 (2014).

203. S. P. R. Romaine, M. Tomaszewski, G. Condorelli, N. J. Samani, MicroRNAs in cardiovascular disease: an introduction for clinicians. *Heart (British Cardiac Society)*, (2015).

204. Y. Zhao, J. F. Ransom, A. Li, V. Vedantham, M. von Drehle, A. N. Muth, T. Tsuchihashi, M. T. McManus, R. J. Schwartz, D. Srivastava, Dysregulation of cardiogenesis, cardiac conduction, and cell cycle in mice lacking miRNA-1-2. *Cell* **129**, 303-317 (2007).

205. S. Heymans, M. F. Corsten, W. Verhesen, P. Carai, R. E. van Leeuwen, K. Custers, T. Peters, M. Hazebroek, L. Stoger, E. Wijnands, B. J. Janssen, E. E. Creemers, Y. M. Pinto, D. Grimm, N. Schurmann, E. Vigorito, T. Thum, F. Stassen, X. Yin, M. Mayr, L. J. de Windt, E. Lutgens, K. Wouters, M. P. de Winther, S. Zacchigna, M. Giacca, M. van Bilsen, A. P. Papageorgiou, B. Schroen, Macrophage microRNA-155 promotes cardiac hypertrophy and failure. *Circulation* **128**, 1420-1432 (2013).

206. J. Ganesan, D. Ramanujam, Y. Sassi, A. Ahles, C. Jentzsch, S. Werfel, S. Leierseder, X. Loyer, M. Giacca, L. Zentilin, T. Thum, B. Laggerbauer, S. Engelhardt, MiR-378 controls cardiac hypertrophy by combined repression of mitogen-activated protein kinase pathway factors. *Circulation* **127**, 2097-2106 (2013).

207. K. H. Shi, H. Tao, J. J. Yang, J. X. Wu, S. S. Xu, H. Y. Zhan, Role of microRNAs in atrial fibrillation: new insights and perspectives. *Cellular signalling* **25**, 2079-2084 (2013).

208. Y. Lu, Y. Zhang, N. Wang, Z. Pan, X. Gao, F. Zhang, Y. Zhang, H. Shan, X. Luo, Y. Bai, L. Sun, W. Song, C. Xu, Z. Wang, B. Yang, MicroRNA-328 contributes to adverse electrical remodeling in atrial fibrillation. *Circulation* **122**, 2378-2387 (2010).

209. D. S. Karolina, S. Tavintharan, A. Armugam, S. Sepramaniam, S. L. Pek, M. T. Wong, S. C. Lim, C. F. Sum, K. Jeyaseelan, Circulating miRNA profiles in patients with metabolic syndrome. *The Journal of clinical endocrinology and metabolism* **97**, E2271-2276 (2012).

210. T. Zhang, C. Lv, L. Li, S. Chen, S. Liu, C. Wang, B. Su, Plasma miR-126 is a potential biomarker for early prediction of type 2 diabetes mellitus in susceptible individuals. *BioMed research international* **2013**, 761617 (2013).

211. A. Schober, M. Nazari-Jahantigh, Y. Wei, K. Bidzhekov, F. Gremse, J. Grommes, R. T. Megens, K. Heyll, H. Noels, M. Hristov, S. Wang, F. Kiessling, E. N. Olson, C. Weber, MicroRNA-126-5p promotes endothelial proliferation and limits atherosclerosis by suppressing Dlk1. *Nature medicine* **20**, 368-376 (2014).

212. F. Lovren, Y. Pan, A. Quan, K. K. Singh, P. C. Shukla, N. Gupta, B. M. Steer, A. J. Ingram, M. Gupta, M. Al-Omran, H. Teoh, P. A. Marsden, S. Verma, MicroRNA-145 targeted therapy reduces atherosclerosis. *Circulation* **126**, S81-90 (2012).

213. F. Z. Marques, A. E. Campain, M. Tomaszewski, E. Zukowska-Szczechowska, Y. H. Yang, F. J. Charchar, B. J. Morris, Gene expression profiling reveals renin mRNA overexpression in human hypertensive kidneys and a role for microRNAs. *Hypertension (Dallas, Tex. : 1979)* **58**, 1093-1098 (2011).

214. S. Li, J. Zhu, W. Zhang, Y. Chen, K. Zhang, L. M. Popescu, X. Ma, W. B. Lau, R. Rong, X. Yu, B. Wang, Y. Li, C. Xiao, M. Zhang, S. Wang, L. Yu, A. F. Chen, X. Yang, J. Cai, Signature microRNA expression profile of essential hypertension and its novel link to human cytomegalovirus infection. *Circulation* **124**, 175-184 (2011).

215. M. Ulbing, A. H. Kirsch, B. Leber, S. Lemesch, J. Munzker, N. Schweighofer, D. Hofer, O. Trummer, A. R. Rosenkranz, H. Muller, K. Eller, V. Stadlbauer, B. Obermayer-Pietsch, MicroRNAs 223-3p and 93-5p in patients with chronic kidney disease before and after renal transplantation. *Bone* **95**, 115-123 (2017).

216. N. X. Chen, K. Kiattisunthorn, K. D. O'Neill, X. Chen, R. N. Moorthi, V. H. Gattone, 2nd, M. R. Allen, S. M. Moe, Decreased microRNA is involved in the vascular remodeling abnormalities in chronic kidney disease (CKD). *PloS one* **8**, e64558 (2013).

217. N. Ishii, K. Ozaki, H. Sato, H. Mizuno, S. Saito, A. Takahashi, Y. Miyamoto, S. Ikegawa, N. Kamatani, M. Hori, S. Saito, Y. Nakamura, T. Tanaka, Identification of a novel non-coding RNA, MIAT, that confers risk of myocardial infarction. *Journal of human genetics* **51**, 1087-1099 (2006).

218. N. J. Samani, J. Erdmann, A. S. Hall, C. Hengstenberg, M. Mangino, B. Mayer, R. J. Dixon, T. Meitinger, P. Braund, H. E. Wichmann, J. H. Barrett, I. R. Konig, S. E. Stevens, S. Szymczak, D. A. Tregouet, M. M. Iles, F. Pahlke, H. Pollard, W. Lieb, F. Cambien, M. Fischer, W. Ouwehand, S. Blankenberg, A. J. Balmforth, A. Baessler, S. G. Ball, T. M. Strom, I. Braenne, C. Gieger, P. Deloukas, M. D. Tobin, A. Ziegler, J. R. Thompson, H. Schunkert, Genomewide association analysis of coronary artery disease. *The New England journal of medicine* **357**, 443-453 (2007).

219. A. Helgadottir, G. Thorleifsson, A. Manolescu, S. Gretarsdottir, T. Blondal, A. Jonasdottir, A. Jonasdottir, A. Sigurdsson, A. Baker, A. Palsson, G. Masson, D. F. Gudbjartsson, K. P. Magnusson, K. Andersen, A. I. Levey, V. M. Backman, S. Matthiasdottir, T. Jonsdottir, S. Palsson, H. Einarsdottir, S. Gunnarsdottir, A. Gylfason, V. Vaccarino, W. C. Hooper, M. P. Reilly, C. B. Granger, H. Austin, D. J. Rader, S. H. Shah, A. A. Quyyumi, J. R. Gulcher, G. Thorgeirsson, U. Thorsteinsdottir, A. Kong, K. Stefansson, A common variant on chromosome 9p21 affects the risk of myocardial infarction. *Science (New York, N.Y.)* **316**, 1491-1493 (2007).

220. S. Dechamethakun, M. Muramatsu, Long noncoding RNA variations in cardiometabolic diseases. *Journal of human genetics* **62**, 97-104 (2017).

221. A. Congrains, K. Kamide, R. Oguro, O. Yasuda, K. Miyata, E. Yamamoto, T. Kawai, H. Kusunoki, H. Yamamoto, Y. Takeya, K. Yamamoto, M. Onishi, K. Sugimoto, T. Katsuya, N. Awata, K. Ikebe, Y. Gondo, Y. Oike, M. Ohishi, H. Rakugi, Genetic variants at the 9p21 locus contribute to atherosclerosis through modulation of ANRIL and CDKN2A/B. *Atherosclerosis* **220**, 449-455 (2012).

222. H. M. Broadbent, J. F. Peden, S. Lorkowski, A. Goel, H. Ongen, F. Green, R. Clarke, R. Collins, M. G. Franzosi, G. Tognoni, U. Seedorf, S. Rust, P. Eriksson,

A. Hamsten, M. Farrall, H. Watkins, Susceptibility to coronary artery disease and diabetes is encoded by distinct, tightly linked SNPs in the ANRIL locus on chromosome 9p. *Human molecular genetics* **17**, 806-814 (2008).

223. B. Xiao, S. M. Gu, M. J. Li, J. Li, B. Tao, Y. Wang, Y. Wang, S. Zuo, Y. Shen, Y. Yu, D. Chen, G. Chen, D. Kong, J. Tang, Q. Liu, D. R. Chen, Y. Liu, S. Alberti, M. Dovizio, R. Landolfi, L. Mucci, P. Z. Miao, P. Gao, D. L. Zhu, J. Wang, B. Li, P. Patrignani, Y. Yu, Rare SNP rs12731181 in the miR-590-3p Target Site of the Prostaglandin F2alpha Receptor Gene Confers Risk for Essential Hypertension in the Han Chinese Population. *Arteriosclerosis, thrombosis, and vascular biology* **35**, 1687-1695 (2015).

224. S. Yang, Y. Gao, G. Liu, J. Li, K. Shi, B. Du, D. Si, P. Yang, The human ATF1 rs11169571 polymorphism increases essential hypertension risk through modifying miRNA binding. *FEBS letters* **589**, 2087-2093 (2015).

225. T. V. Eskildsen, P. L. Jeppesen, M. Schneider, A. Y. Nossent, M. B. Sandberg, P. B. Hansen, C. H. Jensen, M. L. Hansen, N. Marcussen, L. M. Rasmussen, P. Bie, D. C. Andersen, S. P. Sheikh, Angiotensin II regulates microRNA-132/-212 in hypertensive rats and humans. *International journal of molecular sciences* **14**, 11190-11207 (2013).

226. P. L. Jeppesen, G. L. Christensen, M. Schneider, A. Y. Nossent, H. B. Jensen, D. C. Andersen, T. Eskildsen, S. Gammeltoft, J. L. Hansen, S. P. Sheikh, Angiotensin II type 1 receptor signalling regulates microRNA differentially in cardiac fibroblasts and myocytes. *British journal of pharmacology* **164**, 394-404 (2011).

227. W. Jin, M. A. Reddy, Z. Chen, S. Putta, L. Lanting, M. Kato, J. T. Park, M. Chandra, C. Wang, R. K. Tangirala, R. Natarajan, Small RNA sequencing reveals microRNAs that modulate angiotensin II effects in vascular smooth muscle cells. *The Journal of biological chemistry* **287**, 15672-15683 (2012).

228. H. Zhao, J. Dupont, S. Yakar, M. Karas, D. LeRoith, PTEN inhibits cell proliferation and induces apoptosis by downregulating cell surface IGF-IR expression in prostate cancer cells. *Oncogene* **23**, 786-794 (2004).

229. G. Y. Oudit, Z. Kassiri, J. Zhou, Q. C. Liu, P. P. Liu, P. H. Backx, F. Dawood, M. A. Crackower, J. W. Scholey, J. M. Penninger, Loss of PTEN attenuates the development of pathological hypertrophy and heart failure in response to biomechanical stress. *Cardiovascular research* **78**, 505-514 (2008).

230. G. Schwartzbauer, J. Robbins, The Tumor Suppressor Gene PTEN Can Regulate Cardiac Hypertrophy and Survival. *Journal of Biological Chemistry* **276**, 35786-35793 (2001).

231. K. Gopalakrishnan, S. Kumarasamy, B. Mell, B. Joe, Genome-wide identification of long noncoding RNAs in rat models of cardiovascular and renal disease. *Hypertension (Dallas, Tex. : 1979)* **65**, 200-210 (2015).

232. A. Leung, C. Trac, W. Jin, L. Lanting, A. Akbany, P. Saetrom, D. E. Schones, R. Natarajan, Novel long noncoding RNAs are regulated by angiotensin II in vascular smooth muscle cells. *Circulation research* **113**, 266-278 (2013).

233. J. Y. Chu, S. Sims-Lucas, D. S. Bushnell, A. J. Bodnar, J. A. Kreidberg, J. Ho, Dicer function is required in the metanephric mesenchyme for early kidney development. *American journal of physiology. Renal physiology* **306**, F764-772 (2014).

234. Q. Wei, K. Bhatt, H. Z. He, Q. S. Mi, V. H. Haase, Z. Dong, Targeted deletion of Dicer from proximal tubules protects against renal ischemia-reperfusion injury. *Journal of the American Society of Nephrology : JASN* **21**, 756-761 (2010).

235. C. S. Neal, M. Z. Michael, L. K. Pimlott, T. Y. Yong, J. Y. Li, J. M. Gleadle, Circulating microRNA expression is reduced in chronic kidney disease. *Nephrology, dialysis, transplantation : official publication of the European Dialysis and Transplant Association - European Renal Association* **26**, 3794-3802 (2011).

236. Y.-C. Shi, Y.-T. Chen, C.-F. Lai, C.-H. Lin, J. Gu, K.-W. Chuang, Y.-T. Lee, K.-C. Yang, Abstract 12938: Circulating Long Noncoding RNAs Predicts Adverse Cardiovascular Outcomes in Patients With End-Stage Renal Disease. *Circulation* **134**, A12938-A12938 (2016).

237. S. Albinsson, Y. Suarez, A. Skoura, S. Offermanns, J. M. Miano, W. C. Sessa, MicroRNAs are necessary for vascular smooth muscle growth, differentiation, and function. *Arteriosclerosis, thrombosis, and vascular biology* **30**, 1118-1126 (2010).

238. Y. Pan, L. Balazs, G. Tigyi, J. Yue, Conditional deletion of Dicer in vascular smooth muscle cells leads to the developmental delay and embryonic mortality. *Biochemical and biophysical research communications* **408**, 369-374 (2011).

239. K. R. Cordes, N. T. Sheehy, M. P. White, E. C. Berry, S. U. Morton, A. N. Muth, T. H. Lee, J. M. Miano, K. N. Ivey, D. Srivastava, miR-145 and miR-143 regulate smooth muscle cell fate and plasticity. *Nature* **460**, 705-710 (2009).

240. L. Elia, M. Quintavalle, J. Zhang, R. Contu, L. Cossu, M. V. Latronico, K. L. Peterson, C. Indolfi, D. Catalucci, J. Chen, S. A. Courtneidge, G. Condorelli, The knockout of miR-143 and -145 alters smooth muscle cell maintenance and vascular homeostasis in mice: correlates with human disease. *Cell death and differentiation* **16**, 1590-1598 (2009).

241. T. Boettger, N. Beetz, S. Kostin, J. Schneider, M. Kruger, L. Hein, T. Braun, Acquisition of the contractile phenotype by murine arterial smooth muscle cells depends on the Mir143/145 gene cluster. *The Journal of clinical investigation* **119**, 2634-2647 (2009).

242. M. Xin, E. M. Small, L. B. Sutherland, X. Qi, J. McAnally, C. F. Plato, J. A. Richardson, R. Bassel-Duby, E. N. Olson, MicroRNAs miR-143 and miR-145 modulate cytoskeletal dynamics and responsiveness of smooth muscle cells to injury. *Genes & development* **23**, 2166-2178 (2009).

243. P. Li, N. Zhu, B. Yi, N. Wang, M. Chen, X. You, X. Zhao, C. C. Solomides, Y. Qin, J. Sun, MicroRNA-663 regulates human vascular smooth muscle cell

phenotypic switch and vascular neointimal formation. *Circulation research* **113**, 1117-1127 (2013).

244. N. C. Mackenzie, K. A. Staines, D. Zhu, P. Genever, V. E. Macrae, miRNA-221 and miRNA-222 synergistically function to promote vascular calcification. *Cell biochemistry and function* **32**, 209-216 (2014).

245. Y. Suarez, C. Fernandez-Hernando, J. S. Pober, W. C. Sessa, Dicer dependent microRNAs regulate gene expression and functions in human endothelial cells. *Circulation research* **100**, 1164-1173 (2007).

246. A. Kuehbacher, C. Urbich, A. M. Zeiher, S. Dimmeler, Role of Dicer and Drosha for endothelial microRNA expression and angiogenesis. *Circulation research* **101**, 59-68 (2007).

247. S. Wang, A. B. Aurora, B. A. Johnson, X. Qi, J. McAnally, J. A. Hill, J. A. Richardson, R. Bassel-Duby, E. N. Olson, The endothelial-specific microRNA miR-126 governs vascular integrity and angiogenesis. *Developmental cell* **15**, 261-271 (2008).

248. J. E. Fish, M. M. Santoro, S. U. Morton, S. Yu, R. F. Yeh, J. D. Wythe, K. N. Ivey, B. G. Bruneau, D. Y. Stainier, D. Srivastava, miR-126 regulates angiogenic signaling and vascular integrity. *Developmental cell* **15**, 272-284 (2008).

249. L. Poliseno, A. Tuccoli, L. Mariani, M. Evangelista, L. Citti, K. Woods, A. Mercatanti, S. Hammond, G. Rainaldi, MicroRNAs modulate the angiogenic properties of HUVECs. *Blood* **108**, 3068-3071 (2006).

250. C. Iaconetti, A. Polimeni, S. Sorrentino, J. Sabatino, G. Pironti, G. Esposito, A. Curcio, C. Indolfi, Inhibition of miR-92a increases endothelial proliferation and migration in vitro as well as reduces neointimal proliferation in vivo after vascular injury. *Basic research in cardiology* **107**, 296 (2012).

251. L. Zhang, D. Huang, Q. Wang, D. Shen, Y. Wang, B. Chen, J. Zhang, L. Gai, MiR-132 inhibits expression of SIRT1 and induces pro-inflammatory processes of vascular endothelial inflammation through blockade of the SREBP-1c metabolic pathway. *Cardiovascular drugs and therapy* **28**, 303-311 (2014).

252. E. Hergenreider, S. Heydt, K. Treguer, T. Boettger, A. J. Horrevoets, A. M. Zeiher, M. P. Scheffer, A. S. Frangakis, X. Yin, M. Mayr, T. Braun, C. Urbich, R. A. Boon, S. Dimmeler, Atheroprotective communication between endothelial cells and smooth muscle cells through miRNAs. *Nature cell biology* **14**, 249-256 (2012).

253. P. Dentelli, A. Rosso, F. Orso, C. Olgasi, D. Taverna, M. F. Brizzi, microRNA-222 controls neovascularization by regulating signal transducer and activator of transcription 5A expression. *Arteriosclerosis, thrombosis, and vascular biology* **30**, 1562-1568 (2010).

254. Y. Minami, M. Satoh, C. Maesawa, Y. Takahashi, T. Tabuchi, T. Itoh, M. Nakamura, Effect of atorvastatin on microRNA 221 / 222 expression in endothelial progenitor cells obtained from patients with coronary artery disease. *European journal of clinical investigation* **39**, 359-367 (2009).

255. Y. Fang, C. Shi, E. Manduchi, M. Civelek, P. F. Davies, MicroRNA-10a regulation of proinflammatory phenotype in athero-susceptible endothelium in vivo and in vitro. *Proceedings of the National Academy of Sciences of the United States of America* **107**, 13450-13455 (2010).

256. M. Nazari-Jahantigh, Y. Wei, H. Noels, S. Akhtar, Z. Zhou, R. R. Koenen, K. Heyll, F. Gremse, F. Kiessling, J. Grommes, C. Weber, A. Schober, MicroRNA-155 promotes atherosclerosis by repressing Bcl6 in macrophages. *The Journal of clinical investigation* **122**, 4190-4202 (2012).

257. A. Courboulin, R. Paulin, N. J. Giguere, N. Saksouk, T. Perreault, J. Meloche, E. R. Paquet, S. Biardel, S. Provencher, J. Cote, M. J. Simard, S. Bonnet, Role for miR-204 in human pulmonary arterial hypertension. *The Journal of experimental medicine* **208**, 535-548 (2011).

258. B. N. Davis, A. C. Hilyard, G. Lagna, A. Hata, SMAD proteins control DROSHA-mediated microRNA maturation. *Nature* **454**, 56-61 (2008).

259. P. Caruso, M. R. MacLean, R. Khanin, J. McClure, E. Soon, M. Southgate, R. A. MacDonald, J. A. Greig, K. E. Robertson, R. Masson, L. Denby, Y. Dempsie, L.

Long, N. W. Morrell, A. H. Baker, Dynamic changes in lung microRNA profiles during the development of pulmonary hypertension due to chronic hypoxia and monocrotaline. *Arteriosclerosis, thrombosis, and vascular biology* **30**, 716-723 (2010).

260. P. Caruso, Y. Dempsie, H. C. Stevens, R. A. McDonald, L. Long, R. Lu, K. White, K. M. Mair, J. D. McClure, M. Southwood, P. Upton, M. Xin, E. van Rooij, E. N. Olson, N. W. Morrell, M. R. MacLean, A. H. Baker, A role for miR-145 in pulmonary arterial hypertension: evidence from mouse models and patient samples. *Circulation research* **111**, 290-300 (2012).

261. T. Bertero, Y. Lu, S. Annis, A. Hale, B. Bhat, R. Saggar, R. Saggar, W. D. Wallace, D. J. Ross, S. O. Vargas, B. B. Graham, R. Kumar, S. M. Black, S. Fratz, J. R. Fineman, J. D. West, K. J. Haley, A. B. Waxman, B. N. Chau, K. A. Cottrill, S. Y. Chan, Systems-level regulation of microRNA networks by miR-130/301 promotes pulmonary hypertension. *The Journal of clinical investigation* **124**, 3514-3528 (2014).

262. G. Wu, J. Cai, Y. Han, J. Chen, Z. P. Huang, C. Chen, Y. Cai, H. Huang, Y. Yang, Y. Liu, Z. Xu, D. He, X. Zhang, X. Hu, L. Pinello, D. Zhong, F. He, G. C. Yuan, D. Z. Wang, C. Zeng, LincRNA-p21 regulates neointima formation, vascular smooth muscle cell proliferation, apoptosis, and atherosclerosis by enhancing p53 activity. *Circulation* **130**, 1452-1465 (2014).

263. M. D. Ballantyne, K. Pinel, R. Dakin, A. T. Vesey, L. Diver, R. Mackenzie, R. Garcia, P. Welsh, N. Sattar, G. Hamilton, N. Joshi, M. R. Dweck, J. M. Miano, M. W. McBride, D. E. Newby, R. A. McDonald, A. H. Baker, Smooth Muscle Enriched Long Noncoding RNA (SMILR) Regulates Cell Proliferation. *Circulation* **133**, 2050-2065 (2016).

264. X. Zhou, X. Han, A. Wittfeldt, J. Sun, C. Liu, X. Wang, L. M. Gan, H. Cao, Z. Liang, Long non-coding RNA ANRIL regulates inflammatory responses as a novel component of NF-kappaB pathway. *RNA biology* **13**, 98-108 (2016).

265. K. M. Michalik, X. You, Y. Manavski, A. Doddaballapur, M. Zornig, T. Braun, D. John, Y. Ponomareva, W. Chen, S. Uchida, R. A. Boon, S. Dimmeler, Long noncoding RNA MALAT1 regulates endothelial cell function and vessel growth. *Circulation research* **114**, 1389-1397 (2014).

266. M. Bilban, L. K. Buehler, S. Head, G. Desoye, V. Quaranta, Defining signal thresholds in DNA microarrays: exemplary application for invasive cancer. *BMC genomics* **3**, 19 (2002).

267. G. K. Geiss, R. E. Bumgarner, B. Birditt, T. Dahl, N. Dowidar, D. L. Dunaway, H. P. Fell, S. Ferree, R. D. George, T. Grogan, J. J. James, M. Maysuria, J. D. Mitton, P. Oliveri, J. L. Osborn, T. Peng, A. L. Ratcliffe, P. J. Webster, E. H. Davidson, L. Hood, K. Dimitrov, Direct multiplexed measurement of gene expression with color-coded probe pairs. *Nature biotechnology* **26**, 317-325 (2008).

268. B. Langmead, C. Trapnell, M. Pop, S. L. Salzberg, Ultrafast and memory-efficient alignment of short DNA sequences to the human genome. *Genome biology* **10**, R25 (2009).

269. B. Langmead, S. L. Salzberg, Fast gapped-read alignment with Bowtie 2. *Nature methods* **9**, 357-359 (2012).

270. C. Trapnell, A. Roberts, L. Goff, G. Pertea, D. Kim, D. R. Kelley, H. Pimentel, S. L. Salzberg, J. L. Rinn, L. Pachter, Differential gene and transcript expression analysis of RNA-seq experiments with TopHat and Cufflinks. *Nature protocols* **7**, 562-578 (2012).

271. C. Trapnell, L. Pachter, S. L. Salzberg, TopHat: discovering splice junctions with RNA-Seq. *Bioinformatics (Oxford, England)* **25**, 1105-1111 (2009).

272. D. Kim, G. Pertea, C. Trapnell, H. Pimentel, R. Kelley, S. L. Salzberg, TopHat2: accurate alignment of transcriptomes in the presence of insertions, deletions and gene fusions. *Genome biology* **14**, R36 (2013).

273. C. Trapnell, B. A. Williams, G. Pertea, A. Mortazavi, G. Kwan, M. J. van Baren, S. L. Salzberg, B. J. Wold, L. Pachter, Transcript assembly and quantification by

RNA-Seq reveals unannotated transcripts and isoform switching during cell differentiation. *Nature biotechnology* **28**, 511-515 (2010).

274. A. Dobin, C. A. Davis, F. Schlesinger, J. Drenkow, C. Zaleski, S. Jha, P. Batut, M. Chaisson, T. R. Gingeras, STAR: ultrafast universal RNA-seq aligner. *Bioinformatics (Oxford, England)* **29**, 15-21 (2013).

275. S. Anders, P. T. Pyl, W. Huber, HTSeq--a Python framework to work with high-throughput sequencing data. *Bioinformatics (Oxford, England)* **31**, 166-169 (2015).

276. M. D. Robinson, D. J. McCarthy, G. K. Smyth, edgeR: a Bioconductor package for differential expression analysis of digital gene expression data. *Bioinformatics (Oxford, England)* **26**, 139-140 (2010).

277. M. R. Friedlander, S. D. Mackowiak, N. Li, W. Chen, N. Rajewsky, miRDeep2 accurately identifies known and hundreds of novel microRNA genes in seven animal clades. *Nucleic acids research* **40**, 37-52 (2012).

278. Y. Gao, J. Wang, F. Zhao, CIRI: an efficient and unbiased algorithm for de novo circular RNA identification. *Genome biology* **16**, 4 (2015).

279. V. Agarwal, G. W. Bell, J. W. Nam, D. P. Bartel, Predicting effective microRNA target sites in mammalian mRNAs. *eLife* **4**, (2015).

280. M. Rehmsmeier, P. Steffen, M. Hochsmann, R. Giegerich, Fast and effective prediction of microRNA/target duplexes. *Rna* **10**, 1507-1517 (2004).

281. D. Betel, A. Koppal, P. Agius, C. Sander, C. Leslie, Comprehensive modeling of microRNA targets predicts functional non-conserved and non-canonical sites. *Genome biology* **11**, R90 (2010).

282. H. Liu, D. Yue, Y. Chen, S. J. Gao, Y. Huang, Improving performance of mammalian microRNA target prediction. *BMC bioinformatics* **11**, 476 (2010).

283. K. Wu, L. Li, S. Li, Circulating microRNA-21 as a biomarker for the detection of various carcinomas: an updated meta-analysis based on 36 studies. *Tumour*

biology : the journal of the International Society for Oncodevelopmental Biology and Medicine **36**, 1973-1981 (2015).

284. Y. Wang, X. Gao, F. Wei, X. Zhang, J. Yu, H. Zhao, Q. Sun, F. Yan, C. Yan, H. Li, X. Ren, Diagnostic and prognostic value of circulating miR-21 for cancer: a systematic review and meta-analysis. *Gene* **533**, 389-397 (2014).

285. Y. D'Alessandra, P. Devanna, F. Limana, S. Straino, A. Di Carlo, P. G. Brambilla, M. Rubino, M. C. Carena, L. Spazzafumo, M. De Simone, B. Micheli, P. Biglioli, F. Achilli, F. Martelli, S. Maggiolini, G. Marenzi, G. Pompilio, M. C. Capogrossi, Circulating microRNAs are new and sensitive biomarkers of myocardial infarction. *European heart journal* **31**, 2765-2773 (2010).

286. C. Widera, S. K. Gupta, J. M. Lorenzen, C. Bang, J. Bauersachs, K. Bethmann, T. Kempf, K. C. Wollert, T. Thum, Diagnostic and prognostic impact of six circulating microRNAs in acute coronary syndrome. *Journal of molecular and cellular cardiology* **51**, 872-875 (2011).

287. R. Kumarswamy, C. Bauters, I. Volkmann, F. Maury, J. Fetisch, A. Holzmann, G. Lemesle, P. de Groote, F. Pinet, T. Thum, Circulating long noncoding RNA, LIPCAR, predicts survival in patients with heart failure. *Circulation research* **114**, 1569-1575 (2014).

288. X. J. Lin, Y. Chong, Z. W. Guo, C. Xie, X. J. Yang, Q. Zhang, S. P. Li, Y. Xiong, Y. Yuan, J. Min, W. H. Jia, Y. Jie, M. S. Chen, M. X. Chen, J. H. Fang, C. Zeng, Y. Zhang, R. P. Guo, Y. Wu, G. Lin, L. Zheng, S. M. Zhuang, A serum microRNA classifier for early detection of hepatocellular carcinoma: a multicentre, retrospective, longitudinal biomarker identification study with a nested case-control study. *The Lancet. Oncology* **16**, 804-815 (2015).

289. H. C. Kuo, K. S. Hsieh, M. Ming-Huey Guo, K. P. Weng, L. P. Ger, W. C. Chan, S. C. Li, Next-generation sequencing identifies micro-RNA-based biomarker panel for Kawasaki disease. *The Journal of allergy and clinical immunology* **138**, 1227-1230 (2016).

290. K. W. Witwer, Circulating microRNA biomarker studies: pitfalls and potential solutions. *Clinical chemistry* **61**, 56-63 (2015).

291. R. E. Lanford, E. S. Hildebrandt-Eriksen, A. Petri, R. Persson, M. Lindow, M. E. Munk, S. Kauppinen, H. Orum, Therapeutic silencing of microRNA-122 in primates with chronic hepatitis C virus infection. *Science (New York, N.Y.)* **327**, 198-201 (2010).

292. K. J. Rayner, C. C. Esau, F. N. Hussain, A. L. McDaniel, S. M. Marshall, J. M. van Gils, T. D. Ray, F. J. Sheedy, L. Goedeke, X. Liu, O. G. Khatsenko, V. Kaimal, C. J. Lees, C. Fernandez-Hernando, E. A. Fisher, R. E. Temel, K. J. Moore, Inhibition of miR-33a/b in non-human primates raises plasma HDL and lowers VLDL triglycerides. *Nature* **478**, 404-407 (2011).

293. S. Oparil, R. E. Schmieder, New approaches in the treatment of hypertension. *Circulation research* **116**, 1074-1095 (2015).

294. M. D. Breyer, K. Susztak, The next generation of therapeutics for chronic kidney disease. *Nature reviews. Drug discovery* **15**, 568-588 (2016).

295. L. Liu, G. Z. Luo, W. Yang, X. Zhao, Q. Zheng, Z. Lv, W. Li, H. J. Wu, L. Wang, X. J. Wang, Q. Zhou, Activation of the imprinted Dlk1-Dio3 region correlates with pluripotency levels of mouse stem cells. *The Journal of biological chemistry* **285**, 19483-19490 (2010).

296. E. Gardiner, N. J. Beveridge, J. Q. Wu, V. Carr, R. J. Scott, P. A. Tooney, M. J. Cairns, Imprinted DLK1-DIO3 region of 14q32 defines a schizophrenia-associated miRNA signature in peripheral blood mononuclear cells. *Molecular psychiatry* **17**, 827-840 (2012).

297. S. Molina-Pinelo, A. Salinas, N. Moreno-Mata, I. Ferrer, R. Suarez, E. Andres-Leon, M. Rodriguez-Paredes, J. Gutekunst, E. Jantus-Lewintre, C. Camps, A. Carnero, L. Paz-Ares, Impact of DLK1-DIO3 imprinted cluster hypomethylation in smoker patients with lung cancer. *Oncotarget*, (2016).

298. S. M. Welten, A. J. Bastiaansen, R. C. de Jong, M. R. de Vries, E. A. Peters, M. C. Boonstra, S. P. Sheikh, N. La Monica, E. R. Kandimalla, P. H. Quax, A. Y.

Nossent, Inhibition of 14q32 MicroRNAs miR-329, miR-487b, miR-494, and miR-495 increases neovascularization and blood flow recovery after ischemia. *Circulation research* **115**, 696-708 (2014).

299. S. M. Welten, E. A. Goossens, P. H. Quax, A. Y. Nossent, The multifactorial nature of microRNAs in vascular remodelling. *Cardiovascular research* **110**, 6-22 (2016).

300. L. Benetatos, E. Hatzimichael, E. Londin, G. Vartholomatos, P. Loher, I. Rigoutsos, E. Briasoulis, The microRNAs within the DLK1-DIO3 genomic region: involvement in disease pathogenesis. *Cellular and molecular life sciences : CMLS* **70**, 795-814 (2013).

301. E. Nadal, J. Zhong, J. Lin, R. M. Reddy, N. Ramnath, M. B. Orringer, A. C. Chang, D. G. Beer, G. Chen, A MicroRNA cluster at 14q32 drives aggressive lung adenocarcinoma. *Clinical cancer research : an official journal of the American Association for Cancer Research* **20**, 3107-3117 (2014).

302. J. M. Luk, J. Burchard, C. Zhang, A. M. Liu, K. F. Wong, F. H. Shek, N. P. Lee, S. T. Fan, R. T. Poon, I. Ivanovska, U. Philippar, M. A. Cleary, C. A. Buser, P. M. Shaw, C. N. Lee, D. G. Tenen, H. Dai, M. Mao, DLK1-DIO3 genomic imprinted microRNA cluster at 14q32.2 defines a stemlike subtype of hepatocellular carcinoma associated with poor survival. *The Journal of biological chemistry* **286**, 30706-30713 (2011).

303. K. K. Shih, L. X. Qin, E. J. Tanner, Q. Zhou, M. Bisogna, F. Dao, N. Olvera, A. Viale, R. R. Barakat, D. A. Levine, A microRNA survival signature (MiSS) for advanced ovarian cancer. *Gynecologic oncology* **121**, 444-450 (2011).

304. A. Y. Nossent, T. V. Eskildsen, L. B. Andersen, P. Bie, H. Bronnum, M. Schneider, D. C. Andersen, S. M. Welten, P. L. Jeppesen, J. F. Hamming, J. L. Hansen, P. H. Quax, S. P. Sheikh, The 14q32 microRNA-487b targets the antiapoptotic insulin receptor substrate 1 in hypertension-induced remodeling of the aorta. *Annals of surgery* **258**, 743-751; discussion 752-743 (2013).

305. F. Yang, Z. Xu, S. Duan, M. Luo, MicroRNA-541 promotes the proliferation of vascular smooth muscle cells by targeting IRF7. *American journal of translational research* **8**, 506-515 (2016).

306. L. Huang, S. M. Zhang, P. Zhang, X. J. Zhang, L. H. Zhu, K. Chen, L. Gao, Y. Zhang, X. J. Kong, S. Tian, X. D. Zhang, H. Li, Interferon regulatory factor 7 protects against vascular smooth muscle cell proliferation and neointima formation. *Journal of the American Heart Association* **3**, e001309 (2014).

307. Z. Zhao, L. Qin, S. Li, miR-411 contributes the cell proliferation of lung cancer by targeting FOXO1. *Tumour biology : the journal of the International Society for Oncodevelopmental Biology and Medicine* **37**, 5551-5560 (2016).

308. W. W. Hwang-Verslues, P. H. Chang, P. C. Wei, C. Y. Yang, C. K. Huang, W. H. Kuo, J. Y. Shew, K. J. Chang, E. Y. Lee, W. H. Lee, miR-495 is upregulated by E12/E47 in breast cancer stem cells, and promotes oncogenesis and hypoxia resistance via downregulation of E-cadherin and REDD1. *Oncogene* **30**, 2463-2474 (2011).

309. T. Ning, H. Zhang, X. Wang, S. Li, L. Zhang, T. Deng, L. Zhou, R. Liu, X. Wang, M. Bai, S. Ge, H. Li, D. Huang, G. Ying, Y. Ba, miR-370 regulates cell proliferation and migration by targeting EGFR in gastric cancer. *Oncology reports* **38**, 384-392 (2017).

310. Y. Zheng, L. Yin, H. Chen, S. Yang, C. Pan, S. Lu, M. Miao, B. Jiao, miR-376a suppresses proliferation and induces apoptosis in hepatocellular carcinoma. *FEBS letters* **586**, 2396-2403 (2012).

311. H. Schunkert, I. R. Konig, S. Kathiresan, M. P. Reilly, T. L. Assimes, H. Holm, M. Preuss, A. F. Stewart, M. Barbalic, C. Gieger, D. Absher, Z. Aherrahrou, H. Allayee, D. Altshuler, S. S. Anand, K. Andersen, J. L. Anderson, D. Ardissino, S. G. Ball, A. J. Balmforth, T. A. Barnes, D. M. Becker, L. C. Becker, K. Berger, J. C. Bis, S. M. Boekholdt, E. Boerwinkle, P. S. Braund, M. J. Brown, M. S. Burnett, I. Buysschaert, J. F. Carlquist, L. Chen, S. Cichon, V. Codd, R. W. Davies, G. Dedoussis, A. Dehghan, S. Demissie, J. M. Devaney, P. Diemert, R. Do, A.

Doering, S. Eifert, N. E. Mokhtari, S. G. Ellis, R. Elosua, J. C. Engert, S. E. Epstein, U. de Faire, M. Fischer, A. R. Folsom, J. Freyer, B. Gigante, D. Girelli, S. Gretarsdottir, V. Gudnason, J. R. Gulcher, E. Halperin, N. Hammond, S. L. Hazen, A. Hofman, B. D. Horne, T. Illig, C. Iribarren, G. T. Jones, J. W. Jukema, M. A. Kaiser, L. M. Kaplan, J. J. Kastelein, K. T. Khaw, J. W. Knowles, G. Kolovou, A. Kong, R. Laaksonen, D. Lambrechts, K. Leander, G. Lettre, M. Li, W. Lieb, C. Loley, A. J. Lotery, P. M. Mannucci, S. Maouche, N. Martinelli, P. P. McKeown, C. Meisinger, T. Meitinger, O. Melander, P. A. Merlini, V. Mooser, T. Morgan, T. W. Muhleisen, J. B. Muhlestein, T. Munzel, K. Musunuru, J. Nahrstaedt, C. P. Nelson, M. M. Nothen, O. Olivieri, R. S. Patel, C. C. Patterson, A. Peters, F. Peyvandi, L. Qu, A. A. Quyyumi, D. J. Rader, L. S. Rallidis, C. Rice, F. R. Rosendaal, D. Rubin, V. Salomaa, M. L. Sampietro, M. S. Sandhu, E. Schadt, A. Schafer, A. Schillert, S. Schreiber, J. Schrezenmeir, S. M. Schwartz, D. S. Siscovick, M. Sivananthan, S. Sivapalaratnam, A. Smith, T. B. Smith, J. D. Snoep, N. Soranzo, J. A. Spertus, K. Stark, K. Stirrups, M. Stoll, W. H. Tang, S. Tennstedt, G. Thorgeirsson, G. Thorleifsson, M. Tomaszewski, A. G. Uitterlinden, A. M. van Rij, B. F. Voight, N. J. Wareham, G. A. Wells, H. E. Wichmann, P. S. Wild, C. Willenborg, J. C. Witteman, B. J. Wright, S. Ye, T. Zeller, A. Ziegler, F. Cambien, A. H. Goodall, L. A. Cupples, T. Quertermous, W. Marz, C. Hengstenberg, S. Blankenberg, W. H. Ouwehand, A. S. Hall, P. Deloukas, J. R. Thompson, K. Stefansson, R. Roberts, U. Thorsteinsdottir, C. J. O'Donnell, R. McPherson, J. Erdmann, N. J. Samani, Large-scale association analysis identifies 13 new susceptibility loci for coronary artery disease. *Nature genetics* **43**, 333-338 (2011).

312. C. Wallace, D. J. Smyth, M. Maisuria-Armer, N. M. Walker, J. A. Todd, D. G. Clayton, The imprinted DLK1-MEG3 gene region on chromosome 14q32.2 alters susceptibility to type 1 diabetes. *Nature genetics* **42**, 68-71 (2010).

313. X. Wu, D. Kan, M. Province, T. Quertermous, D. C. Rao, C. Chang, T. H. Mosley, D. Curb, E. Boerwinkle, R. S. Cooper, An updated meta-analysis of genome scans for hypertension and blood pressure in the NHLBI Family Blood Pressure Program (FBPP). *American journal of hypertension* **19**, 122-127 (2006).

314. A. Wezel, S. M. Welten, W. Razawy, H. M. Lagraauw, M. R. de Vries, E. A. Goossens, M. C. Boonstra, J. F. Hamming, E. R. Kandimalla, J. Kuiper, P. H. Quax, A. Y. Nossent, I. Bot, Inhibition of MicroRNA-494 Reduces Carotid Artery Atherosclerotic Lesion Development and Increases Plaque Stability. *Annals of surgery* **262**, 841-847; discussion 847-848 (2015).

315. E. Aavik, H. Lumivuori, O. Leppanen, T. Wirth, S. K. Hakkinen, J. H. Brasen, U. Beschorner, T. Zeller, M. Braspenning, W. van Criekinge, K. Makinen, S. Yla-Herttuala, Global DNA methylation analysis of human atherosclerotic plaques reveals extensive genomic hypomethylation and reactivation at imprinted locus 14q32 involving induction of a miRNA cluster. *European heart journal* **36**, 993-1000 (2015).

316. P. N. Valdmanis, B. Roy-Chaudhuri, H. K. Kim, L. C. Sayles, Y. Zheng, C. H. Chuang, D. R. Caswell, K. Chu, Y. Zhang, M. M. Winslow, E. A. Sweet-Cordero, M. A. Kay, Upregulation of the microRNA cluster at the Dlk1-Dio3 locus in lung adenocarcinoma. *Oncogene* **34**, 94-103 (2015).

317. R. Dai, R. Lu, S. A. Ahmed, The Upregulation of Genomic Imprinted DLK1-Dio3 miRNAs in Murine Lupus Is Associated with Global DNA Hypomethylation. *PloS one* **11**, e0153509 (2016).

318. M. M. Dawlaty, A. Breiling, T. Le, G. Raddatz, M. I. Barrasa, A. W. Cheng, Q. Gao, B. E. Powell, Z. Li, M. Xu, K. F. Faull, F. Lyko, R. Jaenisch, Combined deficiency of Tet1 and Tet2 causes epigenetic abnormalities but is compatible with postnatal development. *Developmental cell* **24**, 310-323 (2013).

319. J. A. Hackett, R. Sengupta, J. J. Zylicz, K. Murakami, C. Lee, T. A. Down, M. A. Surani, Germline DNA demethylation dynamics and imprint erasure through 5-hydroxymethylcytosine. *Science (New York, N.Y.)* **339**, 448-452 (2013).

320. F. M. Piccolo, H. Bagci, K. E. Brown, D. Landeira, J. Soza-Ried, A. Feytout, D. Mooijman, P. Hajkova, H. G. Leitch, T. Tada, S. Kriaucionis, M. M. Dawlaty, R. Jaenisch, M. Merkenschlager, A. G. Fisher, Different roles for Tet1 and Tet2

proteins in reprogramming-mediated erasure of imprints induced by EGC fusion. *Molecular cell* **49**, 1023-1033 (2013).

321. S. Yamaguchi, L. Shen, Y. Liu, D. Sendler, Y. Zhang, Role of Tet1 in erasure of genomic imprinting. *Nature* **504**, 460-464 (2013).

322. T. P. Gu, F. Guo, H. Yang, H. P. Wu, G. F. Xu, W. Liu, Z. G. Xie, L. Shi, X. He, S. G. Jin, K. Iqbal, Y. G. Shi, Z. Deng, P. E. Szabo, G. P. Pfeifer, J. Li, G. L. Xu, The role of Tet3 DNA dioxygenase in epigenetic reprogramming by oocytes. *Nature* **477**, 606-610 (2011).

323. K. P. Lee, Y. J. Shin, A. C. Panda, K. Abdelmohsen, J. Y. Kim, S. M. Lee, Y. J. Bahn, J. Y. Choi, E. S. Kwon, S. J. Baek, S. Y. Kim, M. Gorospe, K. S. Kwon, miR-431 promotes differentiation and regeneration of old skeletal muscle by targeting Smad4. *Genes & development* **29**, 1605-1617 (2015).

324. H. C. Olguin, B. B. Olwin, Pax-7 up-regulation inhibits myogenesis and cell cycle progression in satellite cells: a potential mechanism for self-renewal. *Developmental biology* **275**, 375-388 (2004).

325. R. Wu, H. Li, L. Zhai, X. Zou, J. Meng, R. Zhong, C. Li, H. Wang, Y. Zhang, D. Zhu, MicroRNA-431 accelerates muscle regeneration and ameliorates muscular dystrophy by targeting Pax7 in mice. *Nature communications* **6**, 7713 (2015).

326. R. Wu, H. Li, T. Li, Y. Zhang, D. Zhu, Myostatin regulates miR-431 expression via the Ras-Mek-Erk signaling pathway. *Biochemical and biophysical research communications* **461**, 224-229 (2015).

327. S. Lefebvre, L. Burglen, S. Reboullet, O. Clermont, P. Burlet, L. Viollet, B. Benichou, C. Cruaud, P. Millasseau, M. Zeviani, et al., Identification and characterization of a spinal muscular atrophy-determining gene. *Cell* **80**, 155-165 (1995).

328. M. H. Wertz, K. Winden, P. Neveu, S. Y. Ng, E. Ercan, M. Sahin, Cell-type-specific miR-431 dysregulation in a motor neuron model of spinal muscular atrophy. *Human molecular genetics* **25**, 2168-2181 (2016).

329. D. Wu, A. K. Murashov, MicroRNA-431 regulates axon regeneration in mature sensory neurons by targeting the Wnt antagonist Kremen1. *Frontiers in molecular neuroscience* **6**, 35 (2013).

330. D. Albino, N. Longoni, L. Curti, M. Mello-Grand, S. Pinton, G. Civenni, G. Thalmann, G. D'Ambrosio, M. Sarti, F. Sessa, G. Chiorino, C. V. Catapano, G. M. Carbone, ESE3/EHF controls epithelial cell differentiation and its loss leads to prostate tumors with mesenchymal and stem-like features. *Cancer research* **72**, 2889-2900 (2012).

331. K. Taniue, T. Oda, T. Hayashi, M. Okuno, T. Akiyama, A member of the ETS family, EHF, and the ATPase RUVBL1 inhibit p53-mediated apoptosis. *EMBO reports* **12**, 682-689 (2011).

332. C. Park, I. Lee, W. K. Kang, Influence of small interfering RNA corresponding to ets homologous factor on senescence-associated modulation of prostate carcinogenesis. *Molecular cancer therapeutics* **5**, 3191-3196 (2006).

333. S. L. Fossum, M. J. Mutolo, R. Yang, H. Dang, W. K. O'Neal, M. R. Knowles, S. H. Leir, A. Harris, Ets homologous factor regulates pathways controlling response to injury in airway epithelial cells. *Nucleic acids research* **42**, 13588-13598 (2014).

334. S. L. Fossum, M. J. Mutolo, A. Tugores, S. Ghosh, S. H. Randell, L. C. Jones, S. H. Leir, A. Harris, Ets homologous factor (EHF) has critical roles in epithelial dysfunction in airway disease. *The Journal of biological chemistry* **292**, 10938-10949 (2017).

335. T. H. Lee, J. Sottile, H. Y. Chiang, Collagen inhibitory peptide R1R2 mediates vascular remodeling by decreasing inflammation and smooth muscle cell activation. *PloS one* **10**, e0117356 (2015).

336. R. Zini, C. Rossi, R. Norfo, V. Pennucci, G. Barbieri, S. Ruberti, S. Rontauroli, S. Salati, E. Bianchi, R. Manfredini, miR-382-5p Controls Hematopoietic Stem Cell Differentiation Through the Downregulation of MXD1. *Stem cells and development* **25**, 1433-1443 (2016).

337. M. Xu, H. Jin, C. X. Xu, B. Sun, Z. G. Song, W. Z. Bi, Y. Wang, miR-382 inhibits osteosarcoma metastasis and relapse by targeting Y box-binding protein 1. *Molecular therapy : the journal of the American Society of Gene Therapy* **23**, 89-98 (2015).

338. T. Chen, H. Ren, A. Thakur, T. Yang, Y. Li, S. Zhang, T. Wang, M. Chen, miR-382 inhibits tumor progression by targeting SETD8 in non-small cell lung cancer. *Biomedicine & pharmacotherapy = Biomedecine & pharmacotherapie* **86**, 248-253 (2017).

339. G. M. Chen, A. J. Zheng, J. Cai, P. Han, H. B. Ji, L. L. Wang, microRNA-145-3p Inhibits Non-Small Cell Lung Cancer Cell Migration and Invasion by Targeting PDK1 via the mTOR Signaling Pathway. *Journal of cellular biochemistry*, (2017).

340. Y. Goto, A. Kurozumi, T. Arai, N. Nohata, S. Kojima, A. Okato, M. Kato, K. Yamazaki, Y. Ishida, Y. Naya, T. Ichikawa, N. Seki, Impact of novel miR-145-3p regulatory networks on survival in patients with castration-resistant prostate cancer. *British journal of cancer* **117**, 409-420 (2017).

341. M. Sun, R. Ramchandran, J. Chen, Q. Yang, J. U. Raj, Smooth Muscle Insulin-Like Growth Factor-1 Mediates Hypoxia-Induced Pulmonary Hypertension in Neonatal Mice. *American journal of respiratory cell and molecular biology* **55**, 779-791 (2016).

342. C. Lopez-Lopez, D. LeRoith, I. Torres-Aleman, Insulin-like growth factor I is required for vessel remodeling in the adult brain. *Proceedings of the National Academy of Sciences of the United States of America* **101**, 9833-9838 (2004).

343. H. Y. Chiang, V. A. Korshunov, A. Serour, F. Shi, J. Sottile, Fibronectin is an important regulator of flow-induced vascular remodeling. *Arteriosclerosis, thrombosis, and vascular biology* **29**, 1074-1079 (2009).

344. X. Liu, Y. Liu, X. Li, J. Zhao, Y. Geng, W. Ning, Follistatin like-1 (Fstl1) is required for the normal formation of lung airway and vascular smooth muscle at birth. *PloS one* **12**, e0177899 (2017).

345. N. P. Tania, H. Maarsingh, T. B. IS, A. Mattiotti, S. Prakash, W. Timens, Q. D. Gunst, L. J. Jimenez-Borreguero, M. Schmidt, M. J. B. van den Hoff, R. Gosens, Endothelial follistatin-like-1 regulates the postnatal development of the pulmonary vasculature by modulating BMP/Smad signaling. *Pulmonary circulation* **7**, 219-231 (2017).

346. Y. C. Liao, Y. S. Wang, Y. C. Guo, W. L. Lin, M. H. Chang, S. H. Juo, Let-7g improves multiple endothelial functions through targeting transforming growth factor-beta and SIRT-1 signaling. *Journal of the American College of Cardiology* **63**, 1685-1694 (2014).

347. Z. Ding, S. Liu, B. Yang, Y. Fan, X. Deng, Effect of oxidized low-density lipoprotein concentration polarization on human smooth muscle cells' proliferation, cycle, apoptosis and oxidized low-density lipoprotein uptake. *Journal of the Royal Society, Interface* **9**, 1233-1240 (2012).

348. Z. Ding, X. Wang, L. Schnackenberg, M. Khaidakov, S. Liu, S. Singla, Y. Dai, J. L. Mehta, Regulation of autophagy and apoptosis in response to ox-LDL in vascular smooth muscle cells, and the modulatory effects of the microRNA hsa-let-7 g. *International journal of cardiology* **168**, 1378-1385 (2013).

349. M. Liu, G. Tao, Q. Liu, K. Liu, X. Yang, MicroRNA let-7g alleviates atherosclerosis via the targeting of LOX-1 in vitro and in vivo. *International journal of molecular medicine* **40**, 57-64 (2017).

350. T. M. Wang, K. C. Chen, P. Y. Hsu, H. F. Lin, Y. S. Wang, C. Y. Chen, Y. C. Liao, S. H. Juo, microRNA let-7g suppresses PDGF-induced conversion of vascular smooth muscle cell into the synthetic phenotype. *Journal of cellular and molecular medicine*, (2017).

351. C. T. Chao, Y. P. Liu, S. F. Su, H. Y. Yeh, H. Y. Chen, P. J. Lee, W. J. Chen, Y. M. Lee, J. W. Huang, C. K. Chiang, K. Y. Hung, H. W. Chen, Circulating MicroRNA-125b Predicts the Presence and Progression of Uremic Vascular Calcification. *Arteriosclerosis, thrombosis, and vascular biology* **37**, 1402-1414 (2017).